Catalytic Enantioselective Synthesis of Oxindoles and Benzofuranones bearing a Quaternary Stereocenter and Reactions of Palladium Bisphosphine Complexes Relevant to Catalytic C-C Bond Formation

by

Ivory Derrick Hills

B.S., Chemistry
University of North Carolina — Chapel Hill, 1999

Submitted to the Department of Chemistry
In Partial Fulfillment of the Requirements
For the Degree of

DOCTOR OF PHILOSOPHY
IN ORGANIC CHEMISTRY

at the

Massachusetts Institute of Technology
[September 2004]
August 2004

Signature of Author_____
Department of Chemistry
August 12, 2004

Certified by_____
Gregory C. Fu
Thesis Supervisor

Accepted by_____
Robert W. Field
Chairman, Departmental Committee on Graduate Studies

This doctoral thesis has been examined by a committee of the Department of Chemistry as follows:

Professor Stephen L. Buchwald_____
Chairman

Professor Gregory C. Fu_____
Thesis Supervisor

Professor Rick L. Danheiser_____

To Chrissy, my best friend

Catalytic Enantioselective Synthesis of Oxindoles and Benzofuranones bearing a Quaternary Stereocenter

and

Reactions of Palladium Bisphosphine Complexes Relevant to Catalytic C-C Bond Formation

by

Ivory D. Hills

Submitted to the Department of Chemistry on August 12, 2004
In Partial Fulfillment of the Requirements For the Degree of
Doctor of Philosophy in Organic Chemistry

ABSTRACT

In Part I the development of a new method for the construction of oxindoles and benzofuranones bearing quaternary stereocenters is discussed. A planar-chiral PPY derivative catalyzes the *O*-to-*C* acyl group migration (Black rearrangement) in a highly efficient and enantioselective manner. The utility of this method is further demonstrated by the formal total synthesis of the natural product aplysin.

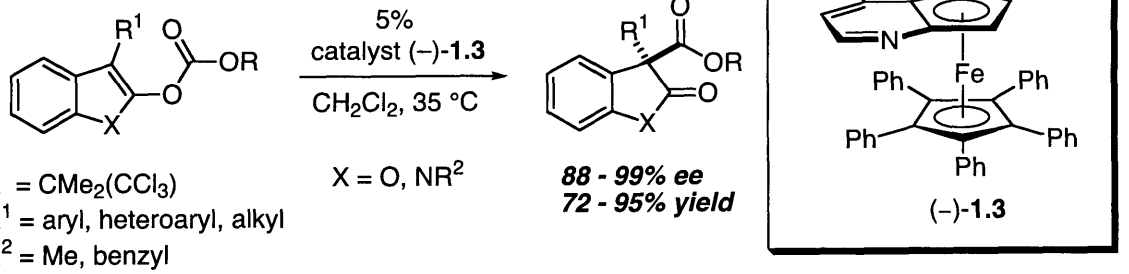

In Part II reactivity of bisphosphine palladium-complexes is discussed. It is shown that the oxidative addition of bisphosphine palladium-complexes bearing P(t-Bu_2)Me occurs through an S_N2-type mechanism. This discovery allows us rationalize the difference in catalytic activity between Pd(P(*t*-Bu_2)Me)$_2$ and Pd(P(*t*-Bu_2)Et)$_2$ for the cross-coupling of alkyl electrophiles.

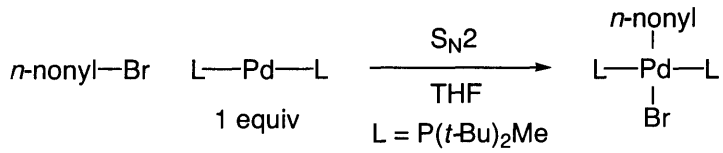

- $\Delta G^{\ddagger}$ = 20.8 kcal/mol (20 °C); $\Delta H^{\ddagger}$ = 2.4 kcal/mol; $\Delta S^{\ddagger}$ = –63 eu
- added phosphine does not affect the rate

Solvent	Less Polar << More Polar
Leaving Group	Fluoride << Chloride < Tosylate < Bromide << Iodide
Substrate Branching	α << β < γ < straight chain

Slower Reaction → Faster Reaction

The reductive elimination of H-X from bisphosphine palladium-hydride complexes is also discussed. The discovery that (P(*t*-$Bu)_3)_2$PdHCl undergoes facile reductive elimination in the presence of Cy_2NMe, while ($PCy_3)_2$PdHCl does not, is explained using X-ray crystal structures. These reactivity patterns may help to explain why Pd(P(*t*-$Bu)_3)_2$ is a much better catalyst than Pd($PCy_3)_2$ for the Heck coupling of aryl chlorides.

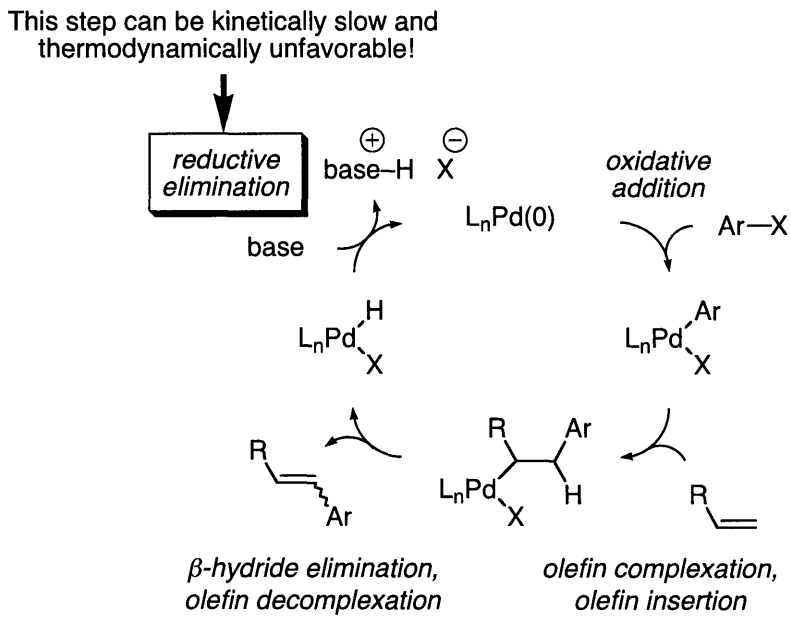

Finally, Part III describes preliminary work on a palladium-hydride catalyzed isomerization of allylic alcohols as well as initial attempts to study the mechanism of nickel-catalyzed cross-couplings of secondary alkyl-electrophiles.

Portions of this document have appeared in the following publications:

Hills, I. D.; Fu, G. C. "Elucidating Reactivity Differences in Palladium-Catalyzed Processes: The Chemistry of Palladium Hydrides" *J. Am. Chem. Soc.* Accepted for publication.

Hills, I. D.; Netherton, M. R.; Fu, G. C. "Toward in Improved Understanding of the Unusual Reactivity of Pd(0)/Trialkylphosphine Catalysts in Cross-Couplings of Alkyl Electrophiles: Quantifying the Factors That Determine the Rate of Oxidative Addition" *Angew. Chem. Int. Ed.* **2003**, *42*, 5749-5752.

Hills, I. D.; Fu, G. C. "Catalytic Enantioselective Synthesis of Oxindoles and Benzofuranones that Bear a Quaternary Stereocenter" *Angew. Chem. Int. Ed.* **2003**, *42*, 3921-3924.

Kirchhoff, J. H.; Netherton, M. R.; Hills, I. D.; Fu, G. C. "Boronic Acids: New Coupling Partners in Room-Temperature Suzuki Reactions of Alkyl Bromides. Crystallographic Characterization of an Oxidative-Addition Adduct Generated Under Remarkably Mild Conditions" *J. Am. Chem. Soc.* **2002**, *124*, 13662-13663.

ACKNOWLEGMENTS

I have many people to thank for helping me get to this point in my life. First I would like to thank all of the great teachers I had in high school. I would also like to express my gratitude for Professors Joseph Templeton, Maurice Brookhart, and Lee Pedersen, mentors who showed me that research could be lots of fun. I would also like to mention the support that I've received from the MIT Organic Faculty. Specifically, I learned a tremendous amount as a first-year student in Prof. Barbara Imperiali's tutorial class and in Prof. Tim Jamison's advanced organic class. These two great teachers helped prepare me for the latter parts of my graduate career. I would also like to thank Profs. Steve Buchwald and Tim Swager for many encouraging words and enlightening discussions concerning my future. I consider myself fortunate to be in the midst of a faculty that is committed to both educating students and performing excellent research.

Of course it would have been difficult to conduct any research without the support of a group. I've had many co-workers over the years and would like to mention, by name, some the excellent scientists I've had the privilege of working with: Dr. Craig Ruble, Dr. Michael Lo, Dr. Brian Hodous, Dr. Beata Tao, Dr. Shih-Yuan Liu, Dr. Matthew Netherton, Dr. Wayne Tang, Mr. Jianrong (Steve) Zhou, Mr. Jon Wilson and of course Professor Ryo Shintani.

I would also like to thank the group members who took time out of their busy schedules and help proofread this thesis: Jon, Wade, Steve, Kevin, Sheryl, Dave, and Christian.

I've been lucky enough to have a supportive family, which helped me through the tough times. This used to be exclusively the Hills family, which consisted of my parents and brother. Then I got married and somehow it was extended to the Adams, Kopp, Rosso, and Schultz families. All of these people have been tremendously caring over the years and they have my everlasting gratitude.

I've made some great friends in graduate school, including Johann, Ryo, Martin and Liu. I'm grateful that we've been able to help each other through the tough times. We've also had the opportunity to share many happy moments, and I expect the future to hold more of the same.

Finally, I should mention my advisor, Prof. Greg Fu, and my wife, Chrissy Kopp, the two most important people in helping me to get to this point in my life. Greg has helped me in immeasurable ways, simply by expecting me to do my best. He's the best role model I could have, and I'm eternally grateful for his guidance. Chrissy has also been supportive in more ways than I can describe here; however, I should mention she's been a great friend by encouraging me when my advisor was pushing me to do my best, which can be rather stressful to say the least. Thanks to both of you.

TABLE OF CONTENTS

Abbreviations

BP	bathophenantroline
bpy	2,2'-bipyridine
cod	cyclooctadiene
DMA	N,N-dimethylacetamide
DMAP	4-(dimethylamine)pyridine
DMF	N,N-dimethylformamide
DMSO	dimethylsulfoxide
eq	equation
equiv	equivalent(s)
GC	gas chromatography
HPLC	high performance liquid chromatography
HRMS	high resolution mass spectrometry
PPY	4-pyrrolidinopyridine
r.t.	room temperature
THF	tetrahydrofuran

Part I

Enantioselective Synthesis Catalyzed by a Planar-Chiral Heterocycle

Chapter 1

Synthesis of Oxindoles and Benzofuranones Bearing a Quaternary Stereocenter

A. Introduction

Heterocycles represent a vitally important class of molecules, which manifest themselves in both natural products and synthetic molecules with therapeutic properties.[1] In particular, molecules derived from aromatic-fused heterocycles such as oxindoles and benzofuranones have proven to be popular synthetic targets due to their interesting structure and biological activity.[2] Several of these natural products bear quaternary stereocenters, such as diazonamide A,[3,4] gelsemine,[5] and aplysin[6] (Figure 1.1). Recent advances have been made in the development of methods capable of constructing these stereocenters.[7,8,9]

---

[1] For reviews on the synthesis of natural and unnatural heterocycles and their biological relevance, see: (a) Deiters, A.; Martin, S. F. *Chem. Rev.* **2004**, *104*, 2199-2238. (b) Wijtmans, R.; Vink, M. K. S.; Schoemaker, H. E.; Van Delft, F. L.; Blaauw, R. H.; Rutjes, F. P. J. T. *Synthesis* **2004**, 641-662. (c) Royer, J.; Bonin, M.; Micouin, L. *Chem. Rev.* **2004**, *104*, 2311-2352. (d) Fürstner, A. *Angew. Chem. Int. Ed.* **2003**, *42*, 3582-3603.

[2] For reviews on recent syntheses of oxindole-derived natural products, see: (a) Lin, H.; Danishefsky, S. J. *Angew. Chem. Int. Ed.* **2003**, *42*, 36-51. (b) Green, L.; Chauder, B.; Snieckus, V. *J. Heterocycl. Chem.* **1999**, *36*, 1453-1468. (c) Brossi, A.; Pei, X.-F.; Greig, N. H. *Aust. J. Chem.* **1996**, *49*, 171-181.

[3] The structure of diazonamide A has undergone revision. For details, see: (a) Ritter, T.; Carreira, E. M. *Angew. Chem. Int. Ed.* **2002**, *41*, 2489-2495. (b) Li, J.; Jeong, S.; Esser, L.; Harran, P. G. *Angew. Chem. Int. Ed.* **2001**, *40*, 4765-4769. (c) Li, J.; Burgett, A. W. G.; Esser, L.; Amezcua, C.; Harran, P. G. *Angew. Chem. Int. Ed.* **2001**, *40*, 4770-4773.

[4] For total syntheses of diazonamide A, see: (a) Burgett, A. W. G.; Li, Q.; Wei, Q.; Harran, P. G. *Angew. Chem. Int. Ed.* **2003**, *42*, 4961-4966. (b) Nicolaou, K. C.; Rao, P. B.; Hao, J.; Reddy, M. V.; Rassias, G.; Huang, X.; Chen, D. Y.-K.; Snyder, S. A. *Angew. Chem. Int. Ed.* **2003**, *42*, 1753-1758. (c) Nicolaou, K. C.; Bella, M.; Chen. D. Y.-K.; Huang, X.; Ling, T.; Snyder, S. A. *Angew. Chem. Int. Ed.* **2002**, *41*, 3495-3499.

[5] For total syntheses of gelsemine, see: (a) Ng, F. W.; Lin, H.; Danishefsky, S. J. *J. Am. Chem. Soc.* **2002**, *124*, 9812-9824. (b) Yokoshima, S.; Tokuyama, H.; Fukuyama, T. *Angew. Chem. Int. Ed.* **2000**, *39*, 4073-4075. (c) Madin, A.; O'Donnell, C. J.; Oh, T.; Old, D. W.; Overman, L. E.; Sharpe, M. J. *Angew. Chem. Int. Ed.* **1999**, *38*, 2934-2936. (d) Fukuyama, T.; Liu, G. *J. Am. Chem. Soc.* **1996**, *118*, 7426-7427. (e) Newcombe, N. J.; Ya, F.; Vijn, R. J.; Hiemstra, H.; Speckamp, W. N. *J. Chem. Soc., Chem. Commun.* **1994**, 767-768.

[6] For the most recent synthesis of aplysin, see: Srikrishna, A.; Babu, N. C. *Tetrahedron Lett.* **2001**, *42*, 4913-4914. For an overview of the aplysin family of natural products, see: Harrowven, D. C.; Lucas, M. C.; Howes, P. D. *Tetrahedron* **2001**, *57*, 791-804, and references therein.

[7] For an excellent example of the Heck reaction used in the formation of quaternary stereocenters, see: Matsuura, T.; Overman, L. E.; Poon, D. J. *J. Am. Chem. Soc.* **1998**, *120*, 6500-6503.

[8] Recently, Carreira has developed a ring expansion strategy and applied it to the synthesis of spirooxindoles. For details, see: (a) Meyers, C.; Carreira, E. M. *Angew. Chem. Int. Ed.* **2003**, *42*, 694-696. (b) Lerchner, A.; Carreira, E. M. *J. Am. Chem. Soc.* **2002**, *124*, 14826-14827.

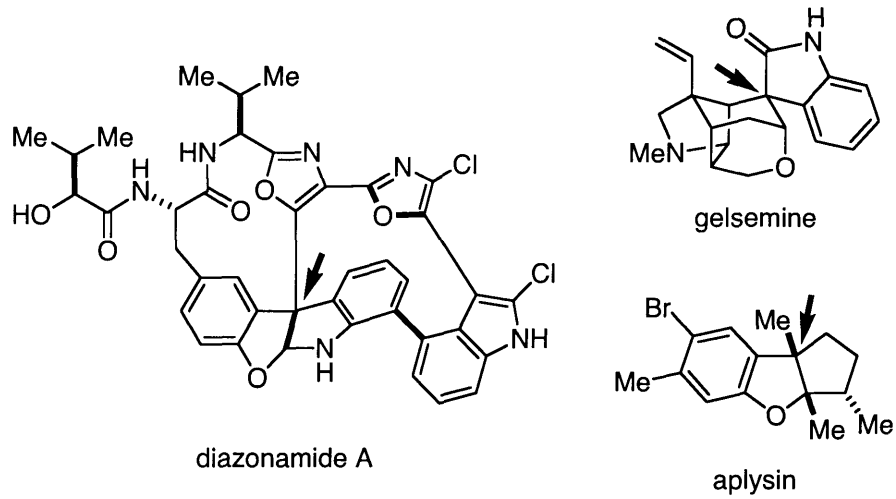

Figure 1.1. Oxindole- and benzofuranone-derived natural products bearing quaternary stereocenters.

Overman and co-workers have developed an intramolecular enantioselective Heck reaction, and have successfully applied this method to natural product synthesis (Figure 1.2).[7] Thus, an aryl iodide can undergo a palladium-catalyzed Heck cyclization to furnish an oxindole core bearing a quaternary stereocenter, which can be further elaborated to either physovenine or physostigmine.

[9] For reviews on the catalytic enantioselective construction of quaternary centers, see: (a) Douglas, C. J.; Overman, L. E. *Proc. Natl. Acad. Sci. U.S.A.* **2004**, *101*, 5363-5367. (b) Christoffers, J.; Baro, A. *Angew. Chem. Int. Ed.* **2003**, *42*, 1688-1690. (c) Christoffers, J.; Mann, A. *Angew. Chem. Int. Ed.* **2001**, *40*, 4591-4597. (d) Corey, E. J.; Guzman-Perez, A. *Angew. Chem. Int. Ed.* **1998**, *37*, 388-401.

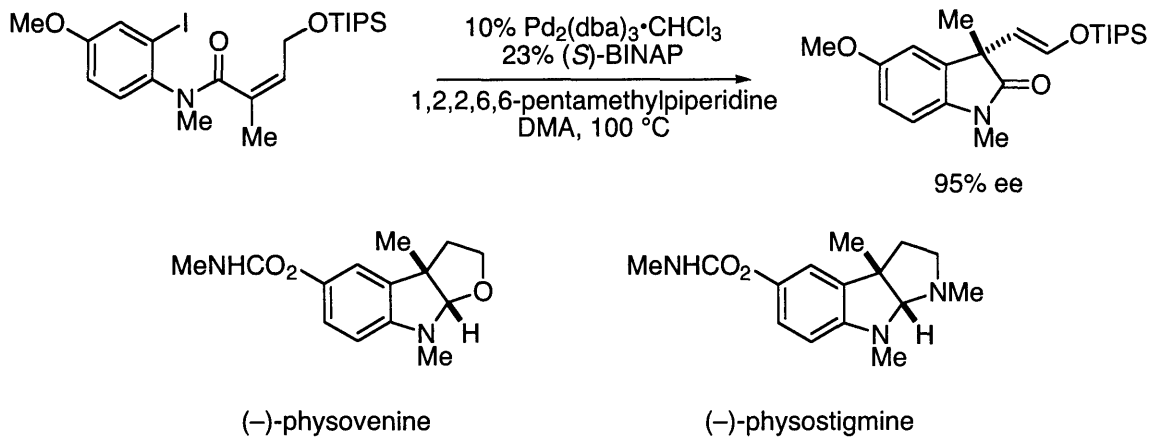

Figure 1.2. Use of an enantioselective Heck reaction by Overman and co-workers to synthesize a key intermediate in the synthesis of physovenine and physostigmine.

Another interesting example of the construction of a quaternary stereocenter on a heterocyclic core is the catalytic diastereoselective ring-expansion protocol developed by Carreira and co-workers.[8] The MgI_2-catalyzed diastereoselective ring expansion between a spiro[cyclopropane-1,3′-oxindole] and an aldimine furnishes a spiro[oxindole-3,3′-pyrrolidine] (Figure 1.3). Carreira has shown that subsequent coupling with a proline derivative allows resolution of the enantiomers, and ultimately the synthesis of (–)-spirotryprostatin B.

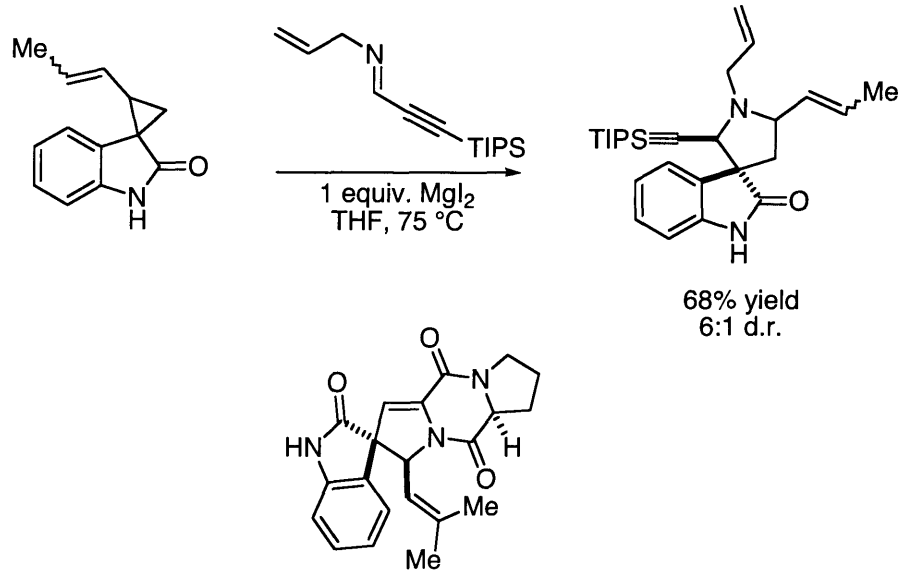

Figure 1.3. Use of a diastereoselective ring-expansion strategy by Carreira and co-workers to synthesize a key intermediate in the synthesis of spirotryprostatin B.

The methods of Overman and Carreira are examples of methods capable of the synthesis of quaternary stereocenters on an oxindole framework;[10] however, in general, efficient catalytic enantioselective synthesis of these stereocenters remains a challenge in organic chemistry.

In 1986 Black reported that 4-dimethylaminopyridine (DMAP)[11] catalyzes the rearrangement of *O*-acylated benzofuranones to their *C*-acylated isomers (eq 1.1).[12] Although this method furnishes racemic products, the transformation is excellent for the efficient assembly of quaternary stereocenters on this

[10] For other examples, see: (a) Lee, S.; Hartwig, J. F. *J. Org. Chem.* **2001**, *66*, 3402-3415. (b) Onishi, T.; Sebahar, P. R.; Williams, R. M. *Org. Lett.* **2003**, *5*, 3135-3137.
[11] For examples of applications of DMAP in organic synthesis, see: (a) Murugan, R.; Scriven, E. F. V. *Aldrichimica Acta* **2003**, *36*, 21-27. (b) Hoefle, G.; Steglich, W. *Synthesis* **1972**, 619-621.
[12] (a) Black, T. H.; Arrivo, S. M.; Schumm, J. S.; Knobeloch, J. M. *J. Org. Chem.* **1987**, *52*, 5425-5430. (b) Black, T. H.; Arrivo, S. M.; Schumm, J. S.; Knobeloch, J. M. *J. Chem. Soc., Chem. Commun.* **1986**, 1524-1525.

heterocyclic core,[13] which is confirmed by attempts to develop diastereoselective versions for use in complex natural product synthesis. For example, in studies directed toward the synthesis of the incorrect structure initially assigned to diazonamide A, Vedejs performed a diastereoselective rearrangement employing DMAP and a chiral auxiliary (eq 1.2).[14] Although an advance in the formation of this key stereocenter, only relatively low levels of diastereoselectivity could be achieved (d.r. = 3:1). Clearly an efficient catalytic enantioselective variant of the Black rearrangement would have synthetic utility.

Black Rearrangment

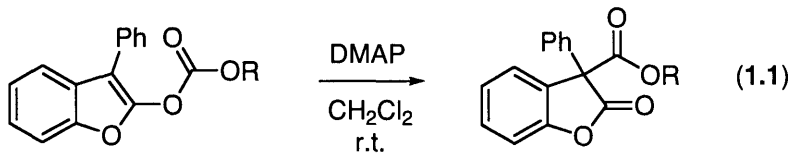

(1.1)

R = Me, Et, *n*-Pr, *n*-Bu, *sec*-Bu
Bn, Ph, Allyl, Vinyl

64% - 96% yield

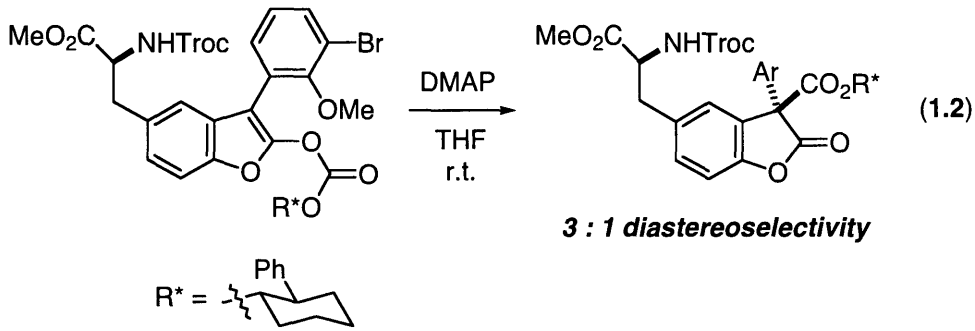

(1.2)

3 : 1 diastereoselectivity

In recent years, our group has been interested in the development of methods employing a family of planar-chiral derivatives of DMAP and PPY

[13] Moody has used a non-asymmetric Black rearrangement in studies directed toward the originally assigned incorrect structure of diazonamide A. For details, see: Moody, C. J.; Doyle, K. J.; Elliott, M. C.; Mowlem, T. J. *J. Chem. Soc., Perkin Trans. 1* **1997**, 2413-2419.
[14] Vedejs, E.; Wang, J. *Org. Lett.* **2000**, *2*, 1031-1032.

(PPY = 4-(pyrrolidino)pyridine; e.g., **1.1-1.4**).[15,16] In the context of enantioselective C-C bond formation through acylation, we have explored the rearrangement of *O*-acylated azlactones[17] and the acylation of latent enolates (e.g., silyl ketene acetals[18] and silyl ketene imines[19]). In view of the potential significance of the reaction products, we decided to explore the use of the planar-chiral catalysts in an asymmetric variant of the Black rearrangement of *O*-acylated oxindoles and benzofuranones.[20]

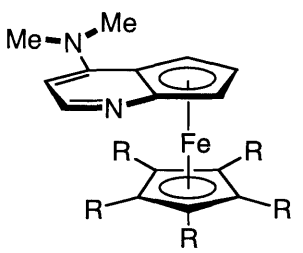

DMAP-derived

R = Ph: (–)-**1.1**
Me: (–)-**1.2**

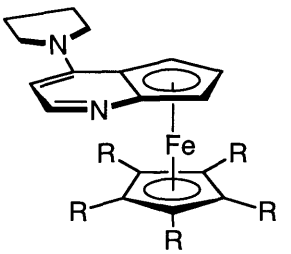

PPY-derived

R = Ph: (–)-**1.3**
Me: (–)-**1.4**

[15] For an overview, see: (a) Fu, G. C. *Acc. Chem. Res.* **2004**, ASAP. (b) Fu, G. C. *Acc. Chem. Res.* **2000**, *33*, 412-420.
[16] For examples of other chiral DMAP derivatives, see: Spivey, A. C.; Maddaford, A.; Redgrave, A. *J. Org. Prep. Proced. Int.* **2000**, *32*, 333-365.
[17] Ruble, J. C.; Fu, G. C. *J. Am. Chem. Soc.* **1998**, *120*, 11532-11533.
[18] Mermerian, A. H.; Fu, G. C. *J. Am. Chem. Soc.* **2003**, *125*, 4050-4051.
[19] Mermerian, A. H.; Fu, G. C. Manuscript in preparation.
[20] Vedejs has studied the catalytic enantioselective rearrangement of *O*-acylated azlactones, oxindoles and benzofuranones. For details, see: Shaw, S. A.; Aleman, P.; Vedejs, E. *J. Am. Chem. Soc.* **2003**, *125*, 13368-13369.

B. Results and Discussion

An early study of the catalytic enantioselective rearrangement of *O*-acylated benzofuranones gave modest results (eq 1.3),[21] but, we were optimistic that further optimization was possible. Due to the greater prevalence and importance of oxindole-derived products in the literature, we turned our focus to optimizing the rearrangement of *O*-acylated oxindoles to furnish their *C*-acylated isomers.

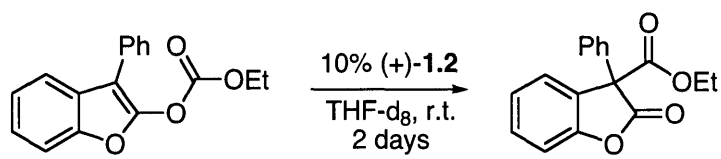

(1.3)

56% ee

Initial screens of catalyst, solvent, and temperature established a system capable of rearranging *O*-acylated oxindoles with modest levels of enantioselectivity (eq 1.4).

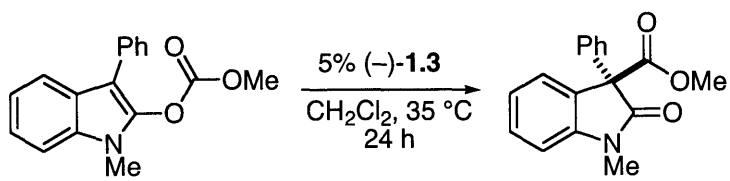

(1.4)

58% ee

We reasoned that the bulk of the rearranged acyl group might have an influence on the outcome of the reaction. Thus, we synthesized derivatives of our model substrate and tested them under our standard conditions (Table 1.1).

[21] Initial studies were performed by Dr. J. C. Ruble. For details, see: Ruble, J. C. Development of Asymmetric Catalysts Based on Planar-Chiral π-Complexes of Nitrogen Heterocycles with Iron. Ph.D. Thesis, Massachusetts Institute of Technology, Cambridge, MA, June 1999.

We were gratified to discover that, upon increasing the steric bulk of the acyl group (Me → Et), an increase in enantioselectivities could be realized (entries 1 and 2, 58→63% ee). Unfortunately, attempts to achieve an additional increase in ee by using a *t*-butyl group were stymied by a lack of reactivity (entry 3). We believed that the reactivity of the substrate could be improved by enhancing the electrophilicity of the acyl group; therefore, we employed an electron deficient *t*-butyl analogue, a 2,2,2-trichloro-1,1-dimethylethyl (trichloro-*t*-butyl) group.[22] Use of the trichloro-*t*-butyl group allowed access to the 3,3-disubstituted oxindole with an excellent level of enantioselectivity (entry 4, 98% ee).

Table 1.1. Effect of the acyl group on the enantioselectivity of O-to-C rearrangements.

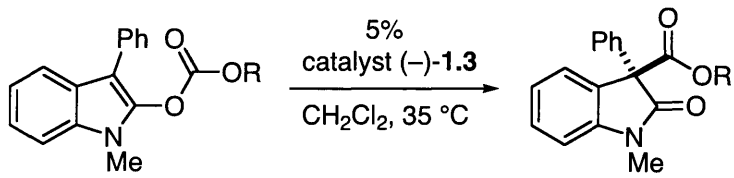

entry	R	% ee[a]
1	Me	58
2	Et	63
3	*t*-Bu	–[b]
4	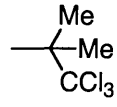	98

[a] The data are an average of two runs.
[b] No rearrangement was observed.

With these conditions established, we next examined the scope of this rearrangement. Employing the trichloro-*t*-butoxycarbonyl substituent as the

[22] 2,2,2-Trichloro-1,1-dimethyl chloroformate is commercially available. The trichloro-*tert*-butoxycarbonyl group has been employed in kinetic resolutions of secondary alcohols by an *N*-acylated chiral derivative of DMAP. For details, see: Vedejs, E.; Chen, X. *J. Am. Chem. Soc.* **1996**, *118*, 1809-1810.

migrating group, catalyst **1.3** can effect highly enantioselective rearrangements for a diverse array of substrates (Table 1.2).[23,24] The reaction proceeds well with either an aromatic or heteroaromatic group in the 3-position (entries 1 and 2). Alkyl substitutents, such as benzyl and methyl, require higher catalyst loading due to a slower rate of reaction; however, the desired products can still be obtained in excellent ee with good yields (entries 3 and 4). Remote substituents, such as a 5-iodo group, have no negative impact on the outcome of the reaction (entry 5). Finally, use of an *N*-benzyl group gives results comparable to those obtained with an *N*-methyl group (compare entries 1 and 6).

Table 1.2. Catalytic enantioselective rearrangement of oxindole derivatives.

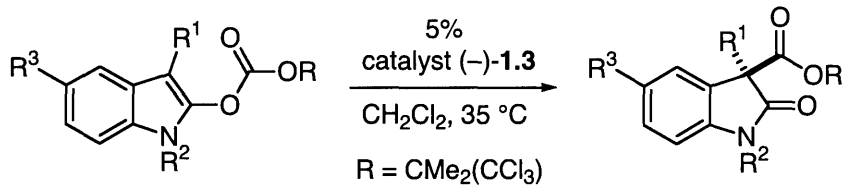

entry	R^1	R^2	R^3	% ee[a]	isolated yield (%)[a]
1	Ph	Me	H	99	91
2	2-thienyl	Me	H	95	81
3[b]	benzyl	Me	H	94	82
4[b]	Me	Me	H	93	72
5	Ph	Me	I	98	94
6	Ph	Bn	H	98	88

[a] The data are an average of two runs. [b]10% catalyst was used.

We next chose to determine if our optimized conditions for the rearrangement of *O*-acylated oxindoles could be extended to *O*-acylated

[23] The slight difference in enantiomeric excess between Table 1.1, entry 4 and Table 1.2, entry 1 is due to the difference in the scale of the reactions. See the experimental for additional details.
[24] The absolute stereochemistry of the product of Table 1.2, entry 3 was determined by X-ray crystallography (see experimental); the other configurations were assigned by analogy.

benzofuranones. We were pleased to discover that our standard conditions can furnish highly enantio-enriched benzofuranones bearing quaternary stereocenters (Table 1.3). Aromatic-substituted substrates (entry 1) furnish products with excellent ee, while alkyl substituents also provide satisfactory results (entries 2 and 3).

Table 1.3. Catalytic enantioselective rearrangements of benzofuranone derivatives.

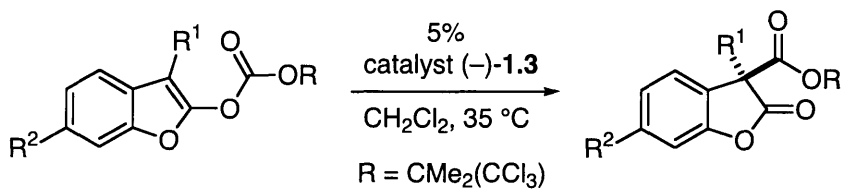

entry	R^1	R^2	% ee	isolated yield (%)
1	Ph	H	97	81
2	Bn	H	88	95
3[a]	Me	Me	90	93

[a] This reaction was run at –12 °C with 10% catalyst.

Of particular interest is the 3,6-dimethyl-substituted benzofuranone (Table 1.3, entry 3). We have used a racemic mixture of the benzofuranone product to complete an unoptimized formal total synthesis of aplysin (Scheme 1.1). Thus, benzofuranone **1.5** undergoes olefination with Petasis' reagent[25] to furnish enol ether **1.6**.[26] Subsequent reduction of the remaining ester with $LiAlH_4$ furnishes primary alcohol **1.7** in excellent yield, which can then be transformed to the alkyl

[25] For examples of the olefination of esters with titanium reagents, see: Hartley, R. C.; McKiernan, G. J. *J. Chem. Soc., Perkin Trans. 1* **2002**, 2763-2793.
[26] Olefination of **1.5** proceeds with only modest selectivity, and after initial workup a 78:22 mixture of mono-olefinated **1.6** and di-olefinated product is obtained in 54% yield. After additional purification by silica chromatography, **1.6** can be isolated in 32% yield. See experimental for details.

iodide, **1.8**, using PPh_3, I_2, and imidazole.[27,28] Finally, metal-halogen exchange[29] followed by quenching with allyl bromide furnishes butenyl-substituted benzofuranone, **1.9**, which has been demonstrated to be a competent intermediate in the synthesis of aplysin.[30]

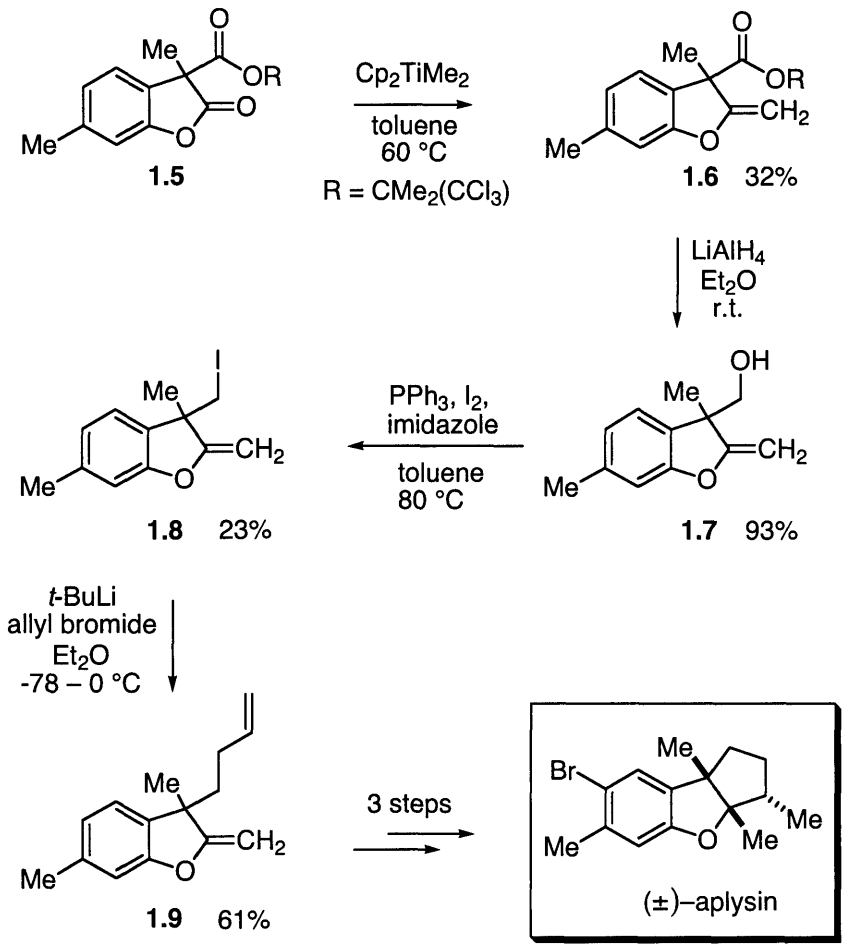

Scheme 1.1. Outline of a formal synthesis of (±)aplysin.

[27] For examples of the formation of alkyl iodides from sterically encumbered primary alcohols, see: (a) Lange, G. L.; Gottardo, C.; Merica, A. *J. Org. Chem.* **1999**, *64*, 6738-6744. (b) Rydon, H. H. *Org. Synth.* **1971**, *51*, 44-47.

[28] The iodination of **1.7** occurs with unusually low yield. This may be due, in part, to the presence of an electron-rich enol ether functional group, which may undergo undesired side-reactions with the combination of PPh_3/I_2.

[29] Bailey, W. F.; Nurmi, T. T.; Patricia, J. J.; Wang, W. *J. Am. Chem. Soc.* **1987**, *109*, 2442-2448.

[30] Harrowven, D. C.; Lucas, M. C.; Howes, P. D. *Tetrahedron* **2001**, *57*, 791-804.

While developing rearrangement reactions catalyzed by **1.3**, we monitored a remarkable color change in the reaction mixture when we employed *O*-acylated benzofuranones as substrates.[31] During initial studies on the non-asymmetric variant of this rearrangement, Black also observed an unusual change in reaction color; upon combination of a colorless solution of DMAP with a colorless solution of *O*-acylated benzofuranone, the mixture became a deep-blue color, which persisted for the duration of the reaction.[32] Black postulated that the rearrangement occurs through the mechanism illustrated in Scheme 1.2,[33] and that an intermediate ion-pair, **1.10**, was responsible for the deep-blue color; however, he did not provide spectroscopic evidence for this intermediate.[34]

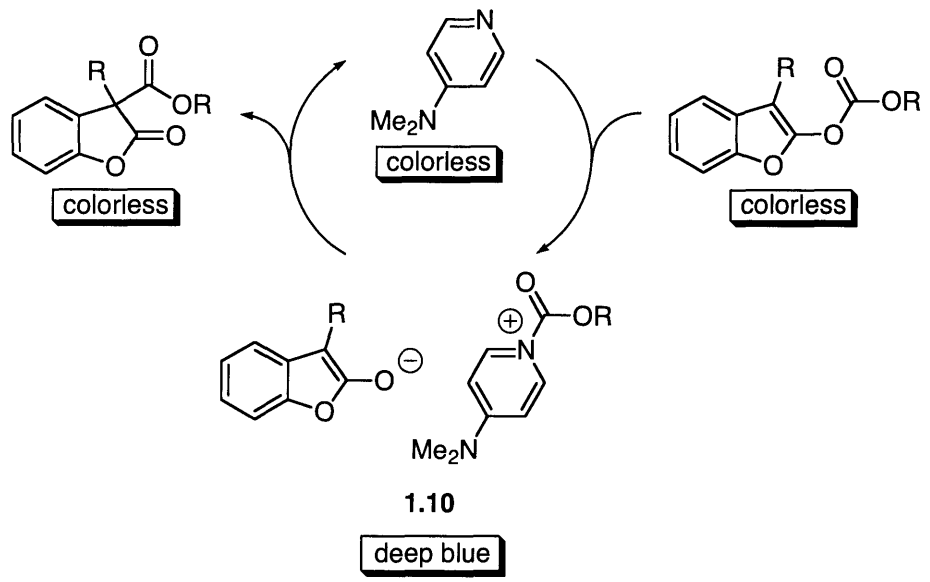

Scheme 1.2. Proposed mechanism for DMAP-catalyzed rearrangements of *O*-acylated benzofuranones.

---

[31] The catalyst **1.3** is a red-purple color when dissolved in CH_2Cl_2, but when combined with an *O*-acylated benzofuranone the color rapidly changes to deep green.
[32] Black, T. H.; Arrivo, S. M.; Schumm, J. S.; Knobeloch, J. M. *J. Org. Chem.* **1987**, *52*, 5425-5430.
[33] This mechanism is consistent with typical pathways proposed for catalysis by nitrogen-based nucleophiles. For further discussions, see: Eboka, C. J.; Connors, K. A. *J. Pharm. Sci.* **1983**, *72*, 366-369.
[34] For additional examples of colored ion-pair charge-transfer complexes involving pyridinium, see: (a) Zhu, D.; Kochi, J. K. *Organometallics* **1999**, *18*, 161-172. (b) Nagamura, T. *Pure Appl. Chem.* **1996**, *68*, 1449-1454.

We reasoned that it is likely that our planar-chiral nucleophilic catalyst promotes the rearrangement of *O*-acylated benzofuranones through a path similar to that outlined in Scheme 1.2. Thus, we postulated that the change in reaction color from red-purple (catalyst in the absence of substrate) to deep green (catalyst in the presence of substrate) is a result of the formation of an intermediate ion-pair (the *N*-acylated catalyst and an enolate). We are able to support this hypothesis with experiments that show a shift in the ^{1}H NMR resonances of **1.3** when the complex is combined with *O*-acylated benzofuranone, which is consistent with the ion-pair being the resting state of the catalytic cycle (Figure 1.4, **A** and **B**). However, in contrast to this result, rearrangements of *O*-acylated oxindoles catalyzed by **1.3** do not occur with a color change, and the ^{1}H NMR spectrum of this combination do not show any significant changes in the shifts associated with **1.3**, which is consistent with free catalyst and substrate being the resting state of this system (Figure 1.4, **B** and **C**). In addition to the ^{1}H NMR data, we have been able to acquire a low-resolution X-ray crystal structure of the ion pair implicated in our catalytic cycle (Figure 1.5). These data are consistent with the **1.3**-catalyzed rearrangement of *O*-acylated benzofuranones occurring through a mechanism similar to that proposed by Black (Scheme 1.2).

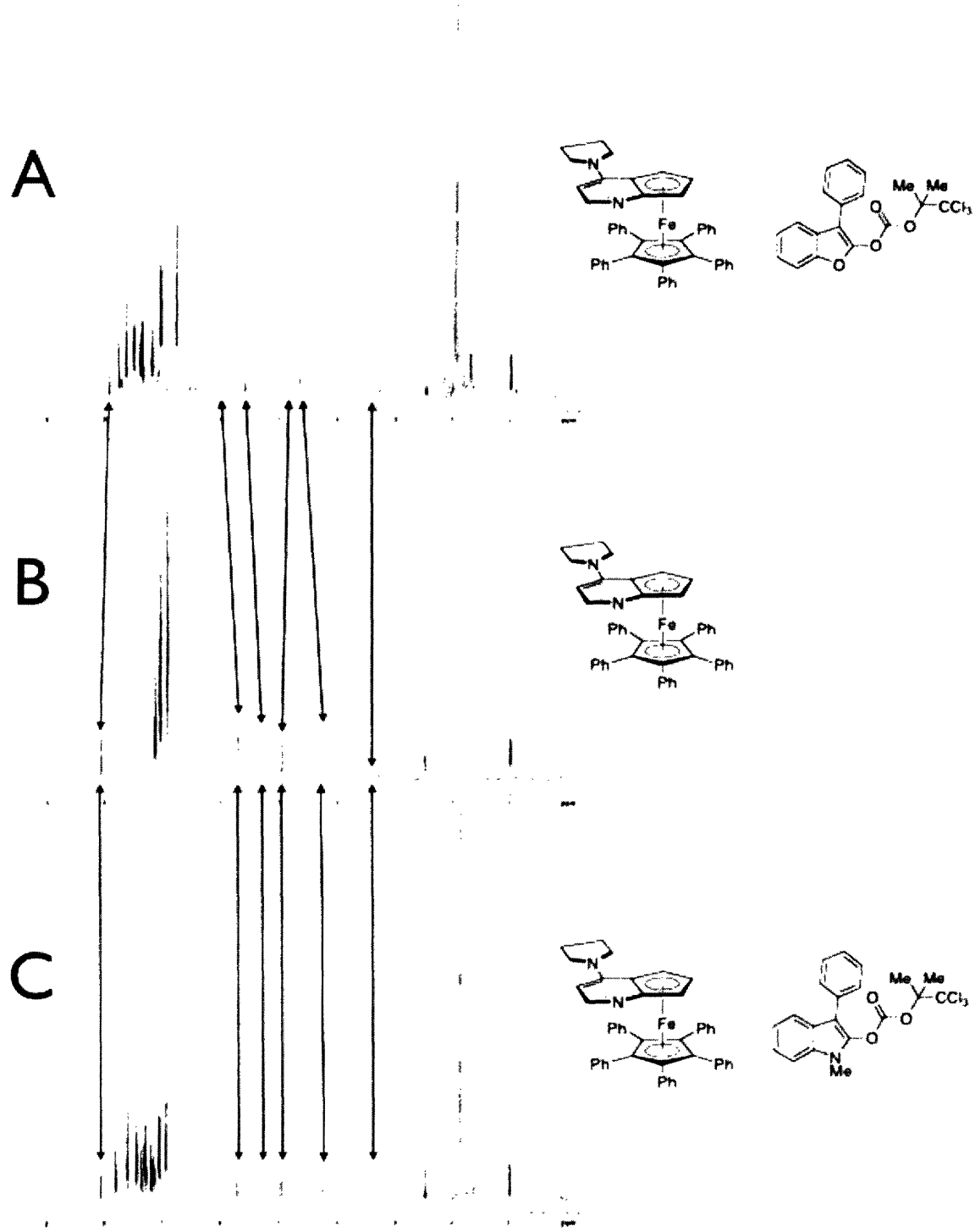

Figure 1.4. ^{1}H NMR spectra of **A**: catalyst + *O*-acylated benzofuranone; **B**: free catalys; **C**: catalyst + *O*-acylated oxindole.

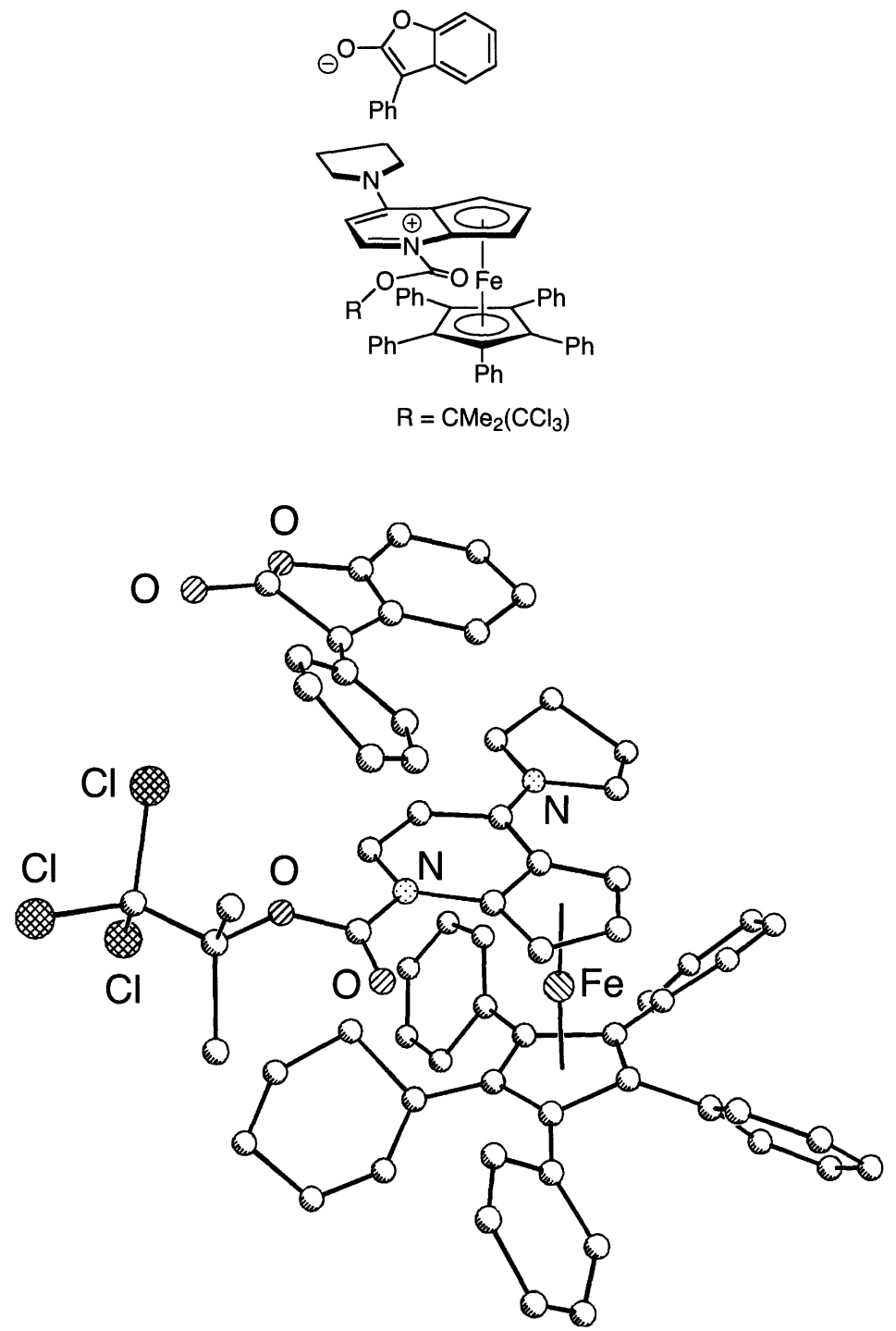

Figure 1.5. X-ray crystal structure of an ion pair derived from catalyst **1.3** and an *O*-acylated benzofuranone.

C. Conclusions

We have described the development of a catalytic enantioselective rearrangement of *O*-acylated oxindoles and benzofuranones to their *C*-acylated isomers (Black rearrangement). This transformation proceeds in both good enantioselectivities and yields for aryl, heteroaryl, and alkyl substituents, furnishing 3,3-disubstituted oxindoles and benzofuranones, which may be valuable intermediates in natural product synthesis (eq 1.5). The utility of these products has been demonstrated by conducting a formal total synthesis of aplysin. We have also gathered evidence (reaction color, ^{1}H NMR, X-ray crystallography) that suggests this transformation takes place through an *N*-acylated catalyst intermediate, similar to that proposed by Black. In view of the importance of oxindoles and benzofuranones bearing a quaternary stereocenter in the 3-position, we believe that this method may provide a powerful tool for asymmetric synthesis.

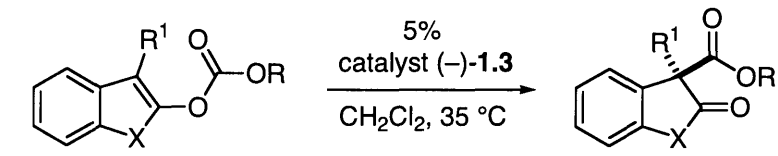

(**1.5**)

R = $CMe_2(CCl_3)$
R^1 = aryl, heteroaryl, alkyl
R^2 = Me, benzyl

X = O, NR^2

88 - 99% ee
72 - 95% yield

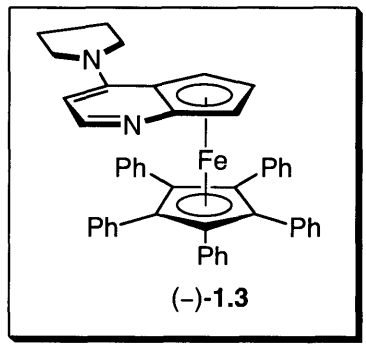

(–)-**1.3**

D. Experimental

I. General

All reactions were carried out under an atmosphere of nitrogen or argon in oven-dried glassware with magnetic stirring, unless otherwise indicated. THF and CH_2Cl_2 were purified by passage through a neutral alumina column. All other reagents were used as received from commercial sources: NEt_3 (EM Science), methyl chloroformate (Aldrich), ethyl chloroformate (Avocado), di-*tert*-butyl dicarbonate (Avocado), 2,2,2-trichloro-1,1-dimethylethyl chloroformate (Aldrich), NaH (Aldrich), isatin (Avocado), *N*-methylisatin (Avocado), 5-iodoisatin (Alfa), MeMgCl (Aldrich), PhMgBr (Aldrich), benzylmagnesium chloride (Aldrich), thiophen-2-yl-magnesium bromide (Aldrich), benzyl bromide (Alfa Aesar), $SnCl_2$ (Alfa), and DMF (Aldrich). Cp_2TiMe_2 was prepared according to a known procedure.[35]

Catalyst (–)-**1.3**,[36] 3-phenyl-3*H*-benzofuran-2-one,[37] 3-benzyl-3*H*-benzofuran-2-one,[38] and 3,6-dimethyl-3*H*-benzofuran-2-one[39] were prepared by literature methods.

---

[35] Payack, J. F.; Hughes, D. L.; Cai, D.; Cottrell, I. F.; Verhoeven, T. R. *Org. Prep. Proced. Int.* **1995**, *27*, 707-709.
[36] Tao, B.; Ruble, J. C.; Hoic, D. A.; Fu, G. C. *J. Am. Chem. Soc.* **1999**, *121*, 5091-5092.
[37] Padwa, A.; Dehm, D.; Oine, T.; Lee, G. A. *J. Am. Chem. Soc.* **1975**, *97*, 1837-1845.
[38] (a) Degnan, A. P.; Meyers, A. I. *J. Am. Chem. Soc.* **1999**, *121*, 2762-2769. (b) Yamazaki, J.; Watanabe, T.; Tanaka, K. *Tetrahedron: Asymmetry* **2001**, *12*, 669-675.
[39] Piccolo, O.; Filippini, L.; Tinucci, L.; Valoti, E.; Citterio, A. *J. Chem. Res., Synop.* **1985**, 258-259.

II. Synthesis of Oxindoles

The yields have not been optimized.

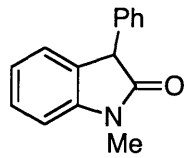

General Procedure. 1-Methyl-3-phenyl-1,3-dihydro-indol-2-one. A flask containing *N*-methylisatin (1.0 equiv, 3.0 g, 19 mmol) was sealed with a septum and flushed with argon. THF (80 mL) was added to give a 0.24 M solution, which was then cooled to –78 °C. Next, PhMgBr (3.0 M solution in Et_2O; 1.1 equiv, 6.8 mL, 20 mmol) was added to the reaction mixture, which was stirred at –78 °C for 1 h and then warmed to room temperature and stirred for 24 h. The reaction was quenched with aq NH_4Cl, and the product was extracted with CH_2Cl_2. The organic layer was washed with aq NaCl, dried with $MgSO_4$, and then concentrated to afford a yellow oil.

The oil was dissolved in 90 mL of AcOH/HCl (15/1), and then $SnCl_2$ (2 equiv, 7.1 g, 37 mmol) was added. The reaction mixture was stirred at 80 °C for 90 min and then cooled to room temperature and diluted with water. The product was extracted with Et_2O. The organic layer was washed with aq NaOH, dried with $MgSO_4$, and then concentrated to afford a fluffy yellow solid. Purification by column chromatography (70% hexanes/30% Et_2O) furnished a pale-yellow solid in 29% overall yield (1.20 g).

CAS registry number: 3335-97-5. ^1H NMR (500 MHz, $CDCl_3$) δ 3.26 (s, 3H), 4.62 (s, 1H), 6.91 (d, 1H, J = 7.5 Hz), 7.07 (t, 1H, J = 7.5 Hz), 7.18 (d, 1H, J = 7.5 Hz),

7.21 (d, 2H, J = 7.5 Hz), 7.29 (m, 1H), 7.34 (m, 3H). ^{13}C NMR (500 MHz, $CDCl_3$) δ 26.6, 52.2, 108.3, 122.9, 125.2, 127.7, 128.59, 128.60, 129.00, 129.04, 136.8, 144.7, 176.1.

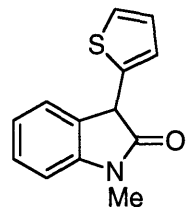

1-Methyl-3-thiophen-2-yl-1,3-dihydro-indol-2-one. The general procedure was followed: *N*-methylisatin (2.0 g, 12 mmol), thiophen-2-yl-magnesium bromide (1.0 M in THF; 14 mL, 14 mmol), 65 mL of AcOH/HCl (15/1), and $SnCl_2$ (4.6 g, 24 mmol). The product was purified by column chromatography (80% hexanes/20% Et_2O), which furnished a yellow oil in 62% yield (1.76 g). ^1H NMR (500 MHz, $CDCl_3$) δ 3.24 (s, 3H), 4.85 (s, 1H), 6.90 (d, 1H, J = 7.5 Hz), 6.99 (m, 1H), 7.03 (m, 1H), 7.11 (t, 1H, J = 7.5 Hz), 7.23 (d, 1H, J = 5.0 Hz), 7.35 (d, 2H, J = 8.0 Hz). ^{13}C NMR (500 MHz, $CDCl_3$) δ 26.6, 47.0, 108.4, 122.8, 125.1, 125.2, 126.0, 127.0, 128.0, 128.8, 137.9, 144.1, 174.6. FTIR (thin film) 1715, 1612, 1493, 1469, 1345, 1086 cm^{-1}. HRMS (ESI) calcd for $C_{13}H_{11}NNaOS$ ($M+Na^+$) 252.0454, found 252.0454.

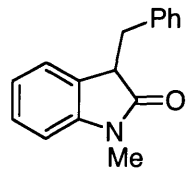

1-Methyl-3-benzyl-1,3-dihydro-indol-2-one. The general procedure was followed: *N*-methylisatin (3.0 g, 19 mmol), benzylmagnesium chloride (2.0 M in THF; 10 mL, 20 mmol), 90 mL of AcOH/HCl (15/1), and $SnCl_2$ (7.1 g, 37 mmol). The product was purified by column chromatography (80% hexanes/20% Et_2O), which furnished a pale-yellow solid in 34% yield (1.55 g).

CAS registry number: 3335-85-1. ^1H NMR (500 MHz, $CDCl_3$) δ 2.86 (dd, 1H, J = 13.5, 9.5 Hz), 3.11 (s, 3H), 3.49 (dd, 1H, J = 13.5, 4.5 Hz), 3.67 (dd, 1H, J = 9.0, 4.5 Hz), 6.73 (dd, 2H, J = 11.5, 8.0 Hz), 6.90 (t, 1H, J = 7.5 Hz), 7.15 (d, 2H, J = 8.0 Hz), 7.21 (m, 4H). ^{13}C NMR (500 MHz, $CDCl_3$) δ 26.0, 36.7, 46.9, 107.8, 121.9, 124.4, 126.5, 127.9, 128.19, 128.23, 129.3, 137.9, 144.1, 176.8.

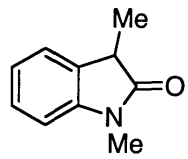

1,3-Dimethyl-1,3-dihydro-indol-2-one. The general procedure was followed: N-methylisatin (2.5 g, 16 mmol), MeMgCl (3.0 M in THF; 5.7 mL, 17 mmol), 60 mL of AcOH/HCl (15/1), and $SnCl_2$ (4.4 g, 23 mmol). The product was purified by column chromatography (80% hexanes/20% Et_2O), which furnished a yellow oil in 53% yield (1.31 g).

CAS registry number: 24438-17-3. ^{1}H NMR (500 MHz, $CDCl_3$) δ 1.46 (d, 3H, J = 7.5 Hz), 3.18 (s, 3H), 3.40 (q, 1H, J = 7.5 Hz), 6.81 (d, 1H, J = 7.5 Hz), 7.04 (t, 1H, J = 7.0 Hz), 7.22 (d, 1H, J = 7.0 Hz), 7.26 (t, 1H, J = 8.0 Hz). ^{13}C NMR (500 MHz, $CDCl_3$) δ 15.4, 26.2, 40.6, 108.0, 122.4, 123.5, 127.9, 130.7, 144.0, 178.7.

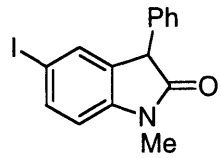

1-Methyl-3-phenyl-5-iodo-1,3-dihydro-indol-2-one. The general procedure was followed: *N*-methyl-5-iodoisatin (2.0 g, 7.0 mmol), PhMgBr (1.0 M in THF; 8.4 mL, 8.4 mmol), 35 mL of AcOH/HCl (15/1), and $SnCl_2$ (2.7 g, 14 mmol). The reaction mixture was cooled, and the desired product crystallized from the mixture. The isolated crystals were washed with Et_2O to furnish a white solid in 58% yield (1.45 g).

^{1}H NMR (500 MHz, $CDCl_3$) δ 3.24 (s, 3H), 4.60 (s, 1H), 6.69 (d, 1H, J = 8.0 Hz), 7.19 (d, 2H, J = 7.5 Hz), 7.34 (m, 3H), 7.45 (s, 1H), 7.65 (d, 1H, J = 7.5 Hz). ^{13}C NMR (500 MHz, $CDCl_3$) δ 26.6, 51.9, 85.3, 110.3, 127.9, 128.5, 129.1, 131.3, 133.7, 136.0, 137.4, 144.3, 175.3. FTIR (thin film) 1700, 1597, 1488, 1338, 1098 cm^{-1}. mp 180-183 °C.HRMS (ESI) calcd for $C_{15}H_{12}INO$ ($M+H^+$) 350.0036, found 350.0031.

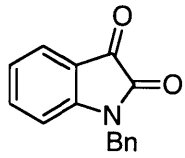

***N*-Benzylisatin**. In a glovebox, NaH (590 mg, 24 mmol) was added to a solution of isatin (3.0 g, 20 mmol) in DMF (40 mL). The reaction mixture was stirred at room temperature for 30 min, and then the flask was sealed with a septum and removed from the glovebox. Benzyl bromide (4.2 g, 24 mmol) was added, and the reaction mixture was stirred at room temperature for 20 h. The reaction was then quenched by careful addition of water, and the product was extracted into Et_2O. The organic layer was washed with aq NaCl, dried with Na_2SO_4, and concentrated, yielding 4.5 g of an orange crystalline solid (92% yield).

CAS registry number: 1217-89-6. ^{1}H NMR (500 MHz, $CDCl_3$) δ 4.95 (s, 2H), 6.78 (d, 1H, J = 8.0 Hz), 7.10 (t, 1H, J = 7.3 Hz), 7.35 (m, 5H), 7.49 (dt, 1H, J = 8.0, 1.5 Hz), 7.63 (dd, 1H, J = 7.5, 1.4 Hz).

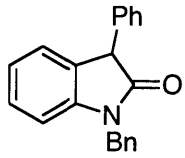

1-Benzyl-3-phenyl-1,3-dihydro-indol-2-one. The general procedure was followed: *N*-benzylisatin (2.5 g, 11 mmol), PhMgBr (1.0 M in THF; 13 mL, 13 mmol), 70 mL of AcOH/HCl (15/1), and $SnCl_2$ (4.0 g, 21 mmol). The product was purified by column chromatography (80% hexanes/20% Et_2O), which furnished a pale-yellow solid in 65% yield (2.08 g).

CAS registry number: 3335-95-3. ^{1}H NMR (500 MHz, $CDCl_3$) δ 4.78 (s, 1H), 4.96 (d, 1H, J = 15.6 Hz), 5.08 (d, 1H, J = 15.6 Hz), 6.89 (d, 1H, J = 7.0 Hz), 7.09 (m, 1H), 7.32 (m, 12H). ^{13}C NMR (500 MHz, $CDCl_3$) δ 43.8, 52.0, 109.2, 122.7, 125.0, 127.3, 127.5, 127.6, 128.3, 128.4, 128.7, 128.8, 128.9, 135.9, 136.7, 143.5, 176.0.

III. Synthesis of Enol Carbonates (Tables 1-3)

The enol carbonates were synthesized according to the general procedure of Black.[40] The yields have not been optimized.

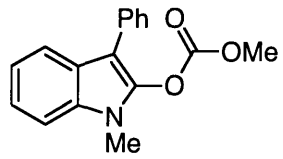

General Procedure. Carbonic acid methyl ester 1-methyl-3-phenyl-1*H*-indol-2-yl ester (Table 1.1, entry 1). NaH (39 mg, 1.6 mmol) was added to a THF solution (5.0 mL) of 1-methyl-3-phenyl-1,3-dihydro-indol-2-one (300 mg, 1.4 mmol), and the resulting mixture was stirred at room temperature for 30 min. Then, methyl chloroformate (0.13 mL, 1.6 mmol) was added, and the reaction mixture was stirred at 35 °C for 24 h. The reaction was then quenched with water, and the product was extracted into Et_2O. The organic layer was washed with brine, dried with Na_2SO_4, and concentrated. The product was purified by column chromatography (80% hexanes/20% Et_2O), which furnished 300 mg (79%) of a white solid.

^{1}H NMR (500 MHz, $CDCl_3$) δ 3.65 (s, 3H), 3.87 (s, 3H), 7.27 (m, 1H), 7.35 (m, 3H), 7.52 (t, 2H, J = 7.7 Hz), 7.70 (d, 2H, J = 7.5 Hz), 7.91 (d, 1H, J = 7.9 Hz). ^{13}C NMR (500 MHz, $CDCl_3$) δ 28.4, 56.4, 103.1, 109.4, 119.7, 120.7, 122.3, 124.7, 126.3, 128.4, 128.9, 132.7, 133.1, 138.9, 153.1. FTIR (thin film) 1776, 1242, 1478, 1435 cm^{-1}. mp 102–105 °C. HRMS (ESI) calcd for $C_{17}H_{16}NO_3$ ($M+H^+$) 282.1125, found 282.1128.

[40] Black, T. H.; Arrivo, S. M.; Schumm, J. S.; Knobeloch, J. M. *J. Org. Chem.* **1987**, *52*, 5425-5430.

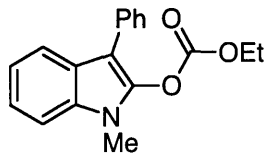

Carbonic acid ethyl ester 1-methyl-3-phenyl-1H-indol-2-yl ester (Table 1.1, entry 2). The general procedure was followed: NaH (48 mg, 2.0 mmol), 1-methyl-3-phenyl-1,3-dihydro-indol-2-one (400 mg, 1.8 mmol), and ethyl chloroformate (0.19 mL, 2.0 mmol). The product was purified by column chromatography (80% hexanes/20% Et_2O), which furnished 410 mg (77%) of a pale-yellow oil.

^{1}H NMR (500 MHz, $CDCl_3$) δ 1.38 (t, 3H, J = 7.2 Hz), 3.73 (s, 3H), 4.36 (q, 2H, J = 7.2 Hz), 7.30 (m, 1H), 7.39 (m, 3H), 7.55 (t, 2H, J = 7.7 Hz), 7.72 (d, 2H, J = 8.0 Hz), 7.93 (d, 1H, J = 7.9 Hz). ^{13}C NMR (500 MHz, $CDCl_3$) δ 14.2, 28.5, 66.1, 103.1, 109.4, 119.7, 120.7, 122.2, 124.8, 126.2, 128.4, 128.9, 132.8, 133.2, 139.1, 152.4. FTIR (thin film) 1773, 1477, 1368, 1231 cm^{-1}. HRMS (ESI) calcd for $C_{18}H_{17}NNaO_3$ ($M+Na^+$) 318.1100, found 318.1096.

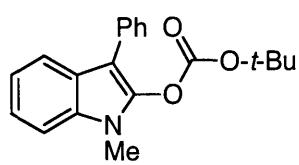

Carbonic acid *tert*-butyl ester 1-methyl-3-phenyl-1*H*-indol-2-yl ester (Table 1.1, entry 3). The general procedure was followed: NaH (48 mg, 2.0 mmol), 1-methyl-3-phenyl-1,3-dihydro-indol-2-one (400 mg, 1.8 mmol), and di-*t*-butyl dicarbonate (440 mg, 2.0 mmol). The product was purified by column

chromatography (90% hexanes/10% Et_2O), which furnished 530 mg (90%) of a white solid.

^1H NMR (500 MHz, $CDCl_3$) δ 1.46 (s, 9H), 3.68 (s, 3H), 7.19 (m, 1H), 7.28 (m, 3H), 7.45 (m, 2H), 7.60 (m, 2H), 7.82 (m, 1H). ^{13}C NMR (500 MHz, $CDCl_3$) δ 27.6, 28.5, 85.2, 103.1, 109.4, 119.7, 120.6, 122.0, 125.0, 126.2, 128.5, 128.9, 132.8, 133.5, 139.4, 150.4. FTIR (thin film) 1767, 1245, 1135 cm^{-1}. mp 105–108 °C. HRMS (ESI) calcd for $C_{20}H_{21}NNaO_3$ ($M+Na^+$) 346.1413, found 346.1407.

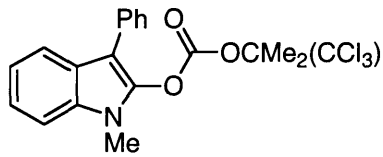

Carbonic acid 1-methyl-3-phenyl-1*H*-indol-2-yl ester 2,2,2-trichloro-1,1,-dimethyl-ethyl ester (Table 1.1, entry 4 and Table 1.2, entry 1). The general procedure was followed: NaH (83 mg, 3.5 mmol), 1-methyl-3-phenyl-1,3-dihydro-indol-2-one (700 mg, 3.1 mmol), and 2,2,2-trichloro-1,1-dimethylethyl chloroformate (830 mg, 3.5 mmol). The product was purified by column chromatography (90% hexanes/10% Et_2O), which furnished 960 mg (72%) of a white solid.

^1H NMR (500 MHz, $CDCl_3$) δ 1.90 (s, 6H), 3.73 (s, 3H), 7.26 (m, 1H), 7.35 (m, 3H), 7.50 (t, 2H, J = 7.3 Hz), 7.69 (d, 2H, J = 7.4 Hz), 7.90 (d, 1H, J = 7.6 Hz). ^{13}C NMR (500 MHz, $CDCl_3$) δ 21.0, 28.5, 91.8, 103.0, 104.9, 109.5, 119.8, 120.8, 122.3, 124.7, 126.3, 128.3, 128.9, 132.8, 133.2, 139.0, 149.4. FTIR (thin film) 1781, 1240, 1211,

1136 cm^{-1}. mp 106–108 °C. HRMS (ESI) calcd for $C_{20}H_{18}Cl_3NNaO_3$ ($M+Na^+$) 448.0244, found 448.0263.

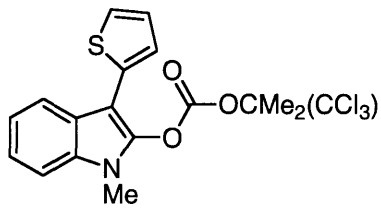

Carbonic acid 1-methyl-3-thiophen-2-yl-1*H*-indol-2-yl ester 2,2,2-trichloro-1,1-dimethyl-ethyl ester (Table 1.2, entry 2). The general procedure was followed: NaH (200 mg, 8.2 mmol), 1-methyl-3-thiophen-2-yl-1,3-dihydro-indol-2-one (1.7 g, 7.4 mmol), and 2,2,2-trichloro-1,1-dimethylethyl chloroformate (2.0 g, 8.2 mmol). The product was purified by column chromatography (90% hexanes/10% Et_2O), which furnished 920 mg (29%) of a pale-yellow solid. ^1H NMR (500 MHz, $CDCl_3$) δ 1.98 (s, 6H), 3.70 (s, 3H), 7.15 (m, 1H), 7.28 (m, 2H), 7.34 (m, 3H), 7.99 (d, 1H, J = 7.8 Hz). ^{13}C NMR (500 MHz, $CDCl_3$) δ 21.2, 28.6, 92.2, 97.7, 104.8, 109.5, 120.2, 121.1, 122.6, 123.1, 123.5, 124.1, 127.4, 132.7, 132.8, 138.9, 149.2. FTIR (thin film) 1781, 1621, 1588, 1240, 1211, 1127 cm^{-1}. mp 104–107 °C. HRMS (ESI) calcd for $C_{18}H_{17}Cl_3NO_3S$ ($M+H^+$) 431.9989, found 431.9989.

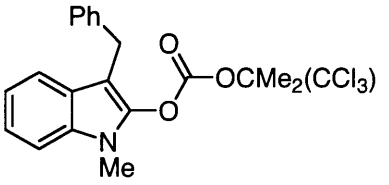

Carbonic acid 3-benzyl-1-methyl-1*H*-indol-2-yl ester 2,2,2-trichloro-1,1-dimethyl-ethyl ester (Table 1.2, entry 3). The general procedure was followed: NaH (75 mg, 3.1 mmol), 1-methyl-3-benzyl-1,3-dihydro-indol-2-one (680 mg, 2.9 mmol), and 2,2,2-trichloro-1,1-dimethylethyl chloroformate (750 g ,3.1 mmol). The product was purified by column chromatography (80% hexanes/20% Et_2O), which furnished 670 mg (53%) of a pale-yellow solid.

^{1}H NMR (500 MHz, $CDCl_3$) δ 1.98 (s, 6H), 3.65 (s, 3H), 4.09 (s, 2H), 7.13 (t, 1H, J = 7.3 Hz), 7.21 (t, 1H, J = 7.7 Hz), 7.30 (m, 6H), 7.49 (d, 1H, J = 7.9 Hz). ^{13}C NMR (500 MHz, $CDCl_3$) δ 21.1, 21.4, 28.5, 29.3, 91.7, 100.2, 109.2, 119.4, 119.9, 121.9, 125.9, 126.1, 128.5, 128.7, 132.8, 139.5, 140.5, 149.8. FTIR (thin film) 1776, 1473, 1244, 1209, 1145 cm^{-1}. mp 126–132 °C. HRMS (ESI) calcd for $C_{21}H_{21}Cl_3NO_3$ ($M+H^+$) 440.0582, found 440.0570.

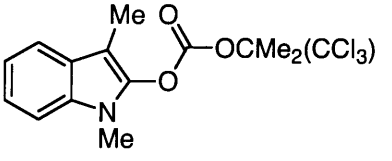

Carbonic acid 1,3-dimethyl-1*H*-indol-2-yl ester 2,2,2-trichloro-1,1-dimethyl-ethyl ester (Table 1.2, entry 4). The general procedure was followed: NaH (290 mg, 12 mmol), 1,3-dimethyl-1,3-dihydro-indol-2-one (1.3 g, 8.1 mmol), and 2,2,2-trichloro-1,1-dimethylethyl chloroformate (2.9 g, 12 mmol). The product was

purified by column chromatography (90% hexanes/10% Et_2O), which furnished 1.47 g (50%) of a white solid.

^1H NMR (500 MHz, $CDCl_3$) δ 2.09 (s, 6H), 2.27 (s, 3H), 3.65 (s, 3H), 7.20 (m, 1H), 7.29 (m, 2H), 7.59 (d, 1H, J = 7.7 Hz). ^{13}C NMR (500 MHz, $CDCl_3$) δ 7.5, 21.3, 28.4, 91.7, 96.6, 109.0, 119.0, 119.6, 121.8, 126.5, 132.8, 133.3, 139.1, 149.8. FTIR (thin film) 1776, 1472, 1243, 1146 cm^{-1}. mp 78–81 °C. HRMS (ESI) calcd for $C_{15}H_{16}Cl_3NNaO_3$ ($M+Na^+$) 386.0088, found 386.0088.

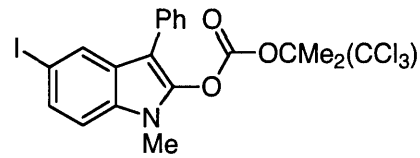

Carbonic acid 1-methyl-3-phenyl-5-iodo-1*H*-indol-2-yl ester 2,2,2-trichloro-1,1,-dimethyl-ethyl ester (Table 1.2, entry 5). The general procedure was followed: NaH (71 mg, 3.0 mmol), 1-methyl-3-phenyl-5-iodo-1,3-dihydro-indol-2-one (940 mg, 2.7 mmol), and 2,2,2-trichloro-1,1-dimethylethyl chloroformate (710 mg, 3.0 mmol). The product was purified by column chromatography (80% hexanes/20% Et_2O), which furnished 1.02 g (70%) of a white solid.

^1H NMR (500 MHz, $CDCl_3$) δ 1.85 (s, 6H), 3.68 (s, 3H), 7.11 (d, 1H, J = 8.7 Hz), 7.31 (t, 1H, J = 7.5 Hz), 7.46 (t, 2H, J = 7.6 Hz), 7.57 (m, 3H), 8.13 (s, 1H). ^{13}C NMR (500 MHz, $CDCl_3$) δ 21.0, 28.7, 84.3, 92.1, 102.7, 111.5, 126.7, 127.1, 128.3, 128.4, 129.1, 130.68, 130.74, 131.9, 132.4, 139.3, 149.1. FTIR (thin film) 1778, 1613, 1469, 1240, 1210, 1132 cm^{-1}. mp 157–160 °C. HRMS (ESI) calcd for $C_{20}H_{17}Cl_3INNaO_3$ ($M+Na^+$) 573.9211, found 573.9206.

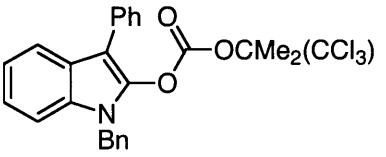

Carbonic acid 1-benzyl-3-phenyl-1*H*-indol-2-yl ester 2,2,2-trichloro-1,1-dimethyl-ethyl ester (Table 1.2, entry 6). The general procedure was followed: NaH (150 mg, 6.3 mmol), 1-benzyl-3-phenyl-1,3-dihydro-indol-2-one (1.7 g, 5.7 mmol), and 2,2,2-trichloro-1,1-dimethylethyl chloroformate (1.5 g, 6.3 mmol). The product was purified by crystallization (90% hexanes/10% Et_2O), which furnished 810 mg (27%) of white crystals.

^{1}H NMR (500 MHz, $CDCl_3$) δ 1.79 (s, 6H), 5.31 (s, 2H), 7.27 (m, 9H), 7.44 (t, 2H, J = 7.5 Hz), 7.66 (d, 2H, J = 7.4 Hz), 7.87 (d, 1H, J = 7.6 Hz). ^{13}C NMR (500 MHz, $CDCl_3$) δ 20.9, 46.3, 91.7, 103.7, 110.0, 119.9, 121.0, 122.5, 125.0, 126.4, 127.1, 127.9, 128.3, 128.9, 129.0, 130.8, 132.5, 133.1, 136.8, 138.9, 149.0. FTIR (thin film) 1785, 1464, 1241, 1206, 1150 cm^{-1}. mp 123–126 °C. HRMS (ESI) calcd for $C_{26}H_{22}Cl_3NNaO_3$ ($M+Na^+$) 524.0557, found 524.0540.

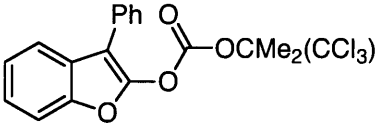

Carbonic acid 3-phenyl-benzofuran-2-yl ester 2,2,2-trichloro-1,1-dimethyl-ethyl ester (Table 1.3, entry 1). The general procedure was followed: NaH (210 mg, 8.6 mmol), 3-phenyl-3*H*-benzofuran-2-one (1.5 g, 7.1 mmol), and 2,2,2-trichloro-1,1-dimethylethyl chloroformate (2.1 g, 8.6 mmol). The product was purified by

column chromatography (90% hexanes/10% Et_2O), which furnished 1.39 g (47%) of a white solid.

^1H NMR (500 MHz, $CDCl_3$) δ 1.85 (s, 6H), 7.26 (m, 3H), 7.40 (m, 3H), 7.55 (d, 2H, J = 7.7 Hz), 7.66 (d, 1H, J = 7.5 Hz). ^{13}C NMR (500 MHz, $CDCl_3$) δ 21.2, 21.5, 92.4, 104.8, 111.5, 120.5, 123.8, 124.8, 127.6, 127.8, 128.2, 129.1, 130.2, 148.5, 149.0, 149.9. FTIR (thin film) 1789, 1643, 1453, 1241, 1199, 1144. cm^{-1}. mp 94–100 °C. HRMS (ESI) calcd for $C_{19}H_{15}Cl_3NaO_4$ ($M+Na^+$) 434.9928, found 434.9925.

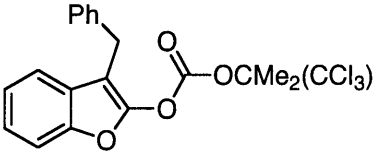

Carbonic acid 3-benzyl-benzofuran-2-yl ester 2,2,2-trichloro-1,1-dimethyl-ethyl ester (Table 1.3, entry 2). A modified general procedure was followed: NEt_3 (0.91 mL, 5.4 mmol), 3-benzyl-3*H*-benzofuran-2-one (810 mg, 3.6 mmol), and 2,2,2-trichloro-1,1-dimethylethyl chloroformate (950 mg, 3.9 mmol). The product was purified by column chromatography (95% hexanes/5% Et_2O), which furnished 1.23 g (82%) of a white solid.

^1H NMR (500 MHz, $CDCl_3$) δ 2.00 (s, 6H), 3.99 (s, 2H), 7.19 (t, 1H, J = 7.6 Hz), 7.24 (m, 1H), 7.28 (d, 1H, J = 7.3 Hz), 7.31 (m, 5H), 7.43 (d, 1H, J = 8.2 Hz). ^{13}C NMR (500 MHz, $CDCl_3$) δ 21.2, 28.7, 92.3, 102.1, 111.3, 120.1, 123.2, 124.4, 126.7, 128.6, 128.7, 128.8, 130.7, 138.4, 148.8, 149.7, 149.9. FTIR (thin film) 1786, 1655, 1454,

1241, 1205, 1144 cm^{-1}. mp 92–95 °C. HRMS (ESI) calcd for $C_{20}H_{17}Cl_3NaO_4$ ($M+Na^+$) 449.0084, found 449.0080.

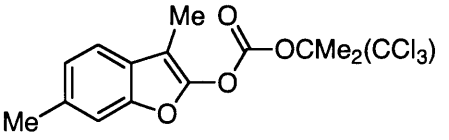

Carbonic acid 3,6-dimethyl-benzofuran-2-yl ester 2,2,2-trichloro-1,1-dimethyl-ethyl ester (Table 1.3, entry 3). A modified general procedure was followed: NEt_3 (0.61 mL, 4.4 mmol), 3,6-dimethyl-3*H*-benzofuran-2-one (470 mg, 2.9 mmol), and 2,2,2-trichloro-1,1-dimethylethyl chloroformate (770 mg, 3.2 mmol). The product was purified by column chromatography (97% hexanes/3% Et_2O), which furnished 970 mg (91%) of a white solid.

^1H NMR (500 MHz, $CDCl_3$) δ 2.04 (s, 6H), 2.13 (s, 3H), 2.47, (s, 3H), 7.08 (d, 1H, J = 7.0 Hz), 7.20 (s, 1H), 7.34 (d, 1H, J = 7.5 Hz). ^{13}C NMR (500 MHz, $CDCl_3$) δ 6.8, 12.5, 21.2, 21.9, 92.1, 98.6, 111.4, 119.1, 124.4. 127.0, 134.5, 148.7, 149.0, 150.0. FTIR (thin film) 1780, 1243, 1201, 1152, 1123, 807 cm^{-1}. mp 86–93 °C. HRMS (ESI) calcd for $C_{15}H_{15}Cl_3NaO_4$ ($M+Na^+$) 386.9928 , found 386.9938.

IV. Catalytic Enantioselective Rearrangements (Tables 1-3)

General procedure: In the air, the substrate (1.00 equiv) and catalyst (–)-**1** (0.050 equiv) were added to a vial that contained a stir bar. The vial was sealed with a septum, and the vial was purged with argon. Next, CH_2Cl_2 (the volume required for [substrate] = 1.0 M) was added to the vial via syringe, and the reaction mixture was heated at 35 °C for 48 h. The reaction mixture was then applied directly to a silica-gel column for purification by flash chromatography (typically, ~85% of the catalyst was recovered).

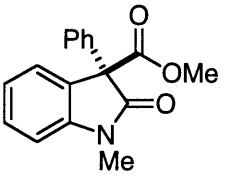

(*R*)-(–)-1-Methyl-2-oxo-3-phenyl-2,3-dihydro-1*H*-indole-3-carboxylic acid methyl ester (Table 1.1, entry 1). The general procedure was followed: enol carbonate (28 mg, 0.10 mmol), catalyst (–)-**1** (3.4 mg, 0.0050 mmol), and CH_2Cl_2 (0.10 mL). The product was isolated by column chromatography (60% hexanes/40% Et_2O) as a white solid (22.6 mg; 80% yield). HPLC analysis: 58% ee [Daicel CHIRALPAK OD column; solvent system: 2% isopropanol/98% hexanes; 1.0 mL/min; retention times: 25.8 min (major), 27.6 min (minor)]. $[\alpha]^{20}_D = -21.2$ ($c = 0.10$, CH_2Cl_2).

A second run was performed on the same scale, and the product was isolated in 77% yield and 58% ee.

^{1}H NMR (500 MHz, $CDCl_3$) δ 3.24 (s, 3H), 3.76 (s, 3H), 6.94 (d, 1H, J = 7.5 Hz), 7.18 (t, 1H, J = 7.0 Hz), 7.34 (m, 5H), 7.43 (t, 1H, J = 8.0 Hz), 7.47 (d, 1H, J = 7.0 Hz). ^{13}C NMR (500 MHz, $CDCl_3$) δ 27.0, 53.6, 64.1, 108.9, 123.2, 126.2, 127.0, 128.1, 128.5, 128.8, 129.9, 136.0, 144.5, 169.9, 172.9. FTIR (thin film) 1752, 1722, 1609, 1151 cm^{-1}. mp 92–97 °C. HRMS (ESI) calcd for $C_{17}H_{15}NNaO_3$ ($M+Na^+$) 304.0944, found 304.0952.

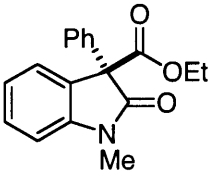

(*R*)-(–)-1-Methyl-2-oxo-3-phenyl-2,3,-dihydro-1*H*-indole-3-carboxylic acid ethyl ester (Table 1.1, entry 2). The general procedure was followed: enol carbonate (30 mg, 0.10 mmol), catalyst (–)-**1** (3.4 mg, 0.0050 mmol), and CH_2Cl_2 (0.10 mL). The product was isolated by column chromatography (60% hexanes/40% Et_2O) as a light-yellow solid (25.0 mg; 85% yield). HPLC analysis: 64% ee [Daicel CHIRALPAK OD column; solvent system: 5% isopropanol/95% hexanes; 1.0 mL/min; retention times: 13.9 min (major), 15.5 min (minor)]. $[\alpha]^{20}_D$ = –249.4 (c = 1.14, CH_2Cl_2).

A second run was performed on the same scale, and the product was isolated in 78% yield and 63% ee.

^{1}H NMR (500 MHz, $CDCl_3$) δ 1.21 (t, 3H, J = 7.0 Hz), 3.24 (s, 3H), 4.23 (m, 2H), 6.94 (d, 1H, J = 8.0 Hz), 7.17 (t, 1H, J = 7.5 Hz), 7.34 (m, 5H), 7.43 (t, 1H, J = 7.0

Hz), 7.48 (d, 1H, J = 7.5 Hz). ^{13}C NMR (500 MHz, $CDCl_3$) δ 14.1, 26.9, 62.5, 108.8, 123.1, 126.1, 127.2, 128.0, 128.4, 128.7, 129.8, 130.8, 136.1, 144.6, 169.3, 173.0. FTIR (thin film) 1719, 1609, 1471, 1222, 1024 cm^{-1}. mp 85–90 °C. HRMS (ESI) calcd for $C_{18}H_{17}NNaO_3$ ($M+Na^+$) 318.1100, found 318.1094.

Table 1.1, entry 3. The general procedure was followed: enol carbonate (32 mg, 0.10 mmol), catalyst (–)-**1** (3.4 mg, 0.0050 mmol), and CH_2Cl_2 (0.10 mL). The reaction did not produce any desired product, and the enol carbonate was re-isolated by column chromatography (60% hexanes/40% Et_2O) as a white solid (80% recovery).

A second run was performed on the same scale, and the starting material was re-isolated with 90% recovery.

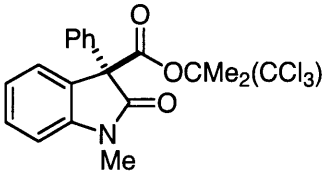

(*R*)-(–)-1-Methyl-2-oxo-3-phenyl-2,3-dihydro-1*H*-indole-3-carboxylic acid 2,2,2-trichloro-1,1-dimethyl-ethyl ester (Table 1.1, entry 4). The general procedure was followed: enol carbonate (43 mg, 0.10 mmol), catalyst (–)-**1** (3.4 mg, 0.0050 mmol), and CH_2Cl_2 (0.10 mL). The product was isolated by column chromatography (60% hexanes/40% Et_2O) as a colorless oil (32.7 mg; 77% yield). HPLC analysis: 99% ee [Daicel CHIRALPAK OD column; solvent system: 10%

isopropanol/90% hexanes; 1.0 mL/min; retention times: 6.6 min (major), 7.9 min (minor)]. $[\alpha]^{20}_{D} = -334.5$ (c = 1.19, CH_2Cl_2).

A second run was performed on the same scale, and the product was isolated in 86% yield and 98% ee.

^{1}H NMR (500 MHz, $CDCl_3$) δ 1.76 (s, 3H), 1.92 (s, 3H), 3.23 (s, 3H), 6.93 (d, 1H, J = 7.5 Hz), 7.17 (t, 1H, J = 7.5 Hz), 7.34 (m, 3H), 7.41 (t, 1H, J = 8.0 Hz), 7.44 (m, 2H), 7.50 (d, 1H, J = 7.5 Hz). ^{13}C NMR (500 MHz, $CDCl_3$) δ 20.8, 21.5, 26.9, 64.9, 90.3, 109.0, 123.0, 124.9, 125.9, 126.8, 128.43, 128.46, 128.6, 129.9, 134.7, 145.0, 166.9, 172.5. FTIR (thin film) 1746, 1720, 1238 cm^{-1}. HRMS (ESI) calcd for $C_{20}H_{18}Cl_3NNaO_3$ ($M+Na^+$) 448.0244, found 448.0231.

(*R*)-(–)-1-Methyl-2-oxo-3-phenyl-2,3-dihydro-1*H*-indole-3-carboxylic acid 2,2,2-trichloro-1,1-dimethyl-ethyl ester (Table 1.2, entry 1). The general procedure was followed: enol carbonate (110 mg, 0.25 mmol), catalyst (–)-**1** (8.6 mg, 0.013 mmol), and CH_2Cl_2 (0.25 mL). The product was isolated by column chromatography (60% hexanes/40% Et_2O) as a white solid (100 mg; 94% yield). HPLC analysis: 99% ee [Daicel CHIRALPAK OD column; solvent system: 2% isopropanol/98% hexanes; 1.0 mL/min; retention times: 25.8 min (major), 27.6 min (minor)]. $[\alpha]^{20}_{D} = -21.2$ (c = 0.10, CH_2Cl_2).

A second run was performed on the same scale, and the product was isolated in 88% yield and 99% ee.

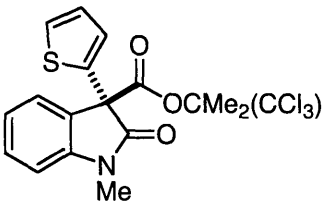

(*S*)-(–)-1-Methyl-2-oxo-3-thiophen-2-yl-2,3-dihydro-1*H*-indole-3-carboxylic acid 2,2,2-trichloro-1,1-dimethyl-ethyl ester (Table 1.2, entry 2). The general procedure was followed: enol carbonate (110 mg, 0.25 mmol), catalyst (–)-**1** (8.6 mg, 0.013 mmol), and CH_2Cl_2 (0.25 mL). The product was isolated by column chromatography (80% hexanes/20% Et_2O) as a colorless oil (88 mg; 81% yield). HPLC analysis: 96% ee [Daicel CHIRALPAK OD column; solvent system: 5% isopropanol/95% hexanes; 1.0 mL/min; retention times: 11.1 min (minor), 12.0 min (major)]. $[\alpha]^{20}_D = -22.7$ (c = 1.05, CH_2Cl_2).

A second run was performed on the same scale, and the product was isolated in 81% yield and 95% ee.

^{1}H NMR (500 MHz, $CDCl_3$) δ 1.74 (s, 3H), 1.89 (s, 3H), 3.25 (s, 3H), 6.91 (d, 1H, J = 7.5 Hz), 7.00 (dd, 1H, J = 5.0, 3.5 Hz), 7.15 (t, 1H, J = 6.5 Hz), 7.21 (dd, 1H, J = 3.5, 1.0 Hz), 7.31 (d, 1H, J = 5.5 Hz), 7.40 (t, 1H, J = 8.0 Hz), 7.56 (d, 1H, J = 7.0Hz). ^{13}C NMR (500 MHz, $CDCl_3$) δ 20.8, 21.4, 27.0, 61.6, 90.4, 105.4, 109.0, 123.1, 124.9, 126.5, 126.8, 127.5, 127.8, 130.1, 136.4, 144.5, 165.8, 171.7. FTIR (thin film) 1754, 1722, 1609, 1151 cm^{-1}. HRMS (ESI) calcd for $C_{18}H_{17}Cl_3NO_3S$ ($M+H^+$) 431.9989, found 431.9989.

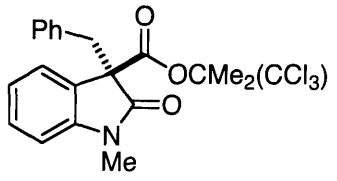

(*R*)-(–)-3-Benzyl-1-methyl-2-oxo-2,3-dihydro-1*H*-indole-3-carboxylic acid 2,2,2-trichloro-1,1-dimethyl-ethyl ester (Table 1.2, entry 3). The general procedure was followed: enol carbonate (110 mg, 0.25 mmol), catalyst (–)-**1** (17 mg, 0.025 mmol), and CH_2Cl_2 (0.25 mL). The product was isolated by column chromatography (80% hexanes/20% Et_2O) as a white solid (90 mg; 82% yield). HPLC analysis: 94% ee [Daicel CHIRALPAK OD column; solvent system: 10% isopropanol/90% hexanes; 1.0 mL/min; retention times: 5.6 min (major), 6.7 min (minor)]. $[\alpha]^{20}_D = -11.1$ (c = 1.07, CH_2Cl_2).

A second run was performed on the same scale, and the product was isolated in 83% yield and 94% ee.

^{1}H NMR (500 MHz, $CDCl_3$) δ 1.78 (s, 3H), 1.90 (s, 3H), 2.98 (s, 3H), 3.54 (d, 1H, J = 13.5 Hz), 3.61 (d, 1H, J = 13.5 Hz), 6.59 (d, 1H, J = 8.0 Hz), 6.91 (m, 2H), 7.03 (m, 4H), 7.21 (t, 1H, J = 8.0 Hz), 7.36 (d, 1H, J = 7.5 Hz). ^{13}C NMR (500 MHz, $CDCl_3$) δ 21.0, 21.4, 26.3, 38.4, 62.0, 76.0, 89.9, 105.7, 108.4, 122.6, 123.6, 127.2, 127.8, 129.3, 130.1, 134.6, 144.6, 166.9, 173.1. FTIR (thin film) 1750, 1717, 1610, 1153 cm^{-1}. mp 127–131 °C. HRMS (ESI) calcd for $C_{21}H_{21}Cl_3NO_3$ ($M+H^+$) 440.0582, found 440.0599.

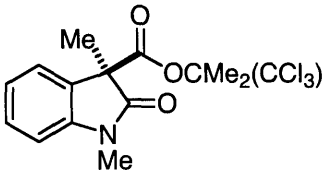

(*R*)-(–)-1,3-Dimethyl-2-oxo-2,3-dihydro-1*H*-indole-3-carboxylic acid 2,2,2-trichloro-1,1-dimethyl-ethyl ester (Table 1.2, entry 4). The general procedure was followed: enol carbonate (91 mg, 0.25 mmol), catalyst (–)-**1** (17 mg, 0.025 mmol), and CH_2Cl_2 (0.25 mL). The product was isolated by column chromatography (80% hexanes/20% Et_2O) as a white solid (65 mg; 72% yield). HPLC analysis: 93% ee [Daicel CHIRALPAK OD column; solvent system: 10% isopropanol/90% hexanes; 1.0 mL/min; retention times: 5.2 min (major), 5.9 min (minor)]. $[\alpha]^{20}_D = -8.6$ (c = 1.05, CH_2Cl_2).

A second run was performed on the same scale, and the product was isolated in 72% yield and 93% ee.

^{1}H NMR (500 MHz, $CDCl_3$) δ 1.67 (s, 3H), 1.71 (s, 3H), 1.85 (s, 3H), 3.24 (s, 3H), 6.86 (d, 1H, J = 8.0 Hz), 7.06 (t, 1H, J = 7.5 Hz), 7.26 (d, 1H, J = 7.5 Hz), 7.31 (t, 1H, J = 8.3 Hz). ^{13}C NMR (500 MHz, $CDCl_3$) δ 18.5, 20.9, 21.3, 26.7, 56.2, 89.7, 99.9, 108.6, 122.8, 123.0, 129.3, 130.0, 144.3, 167.4, 174.8. FTIR (thin film) 1752, 1722, 1611, 1494, 1376, 1160 cm^{-1}. mp 73–76 °C. HRMS (ESI) calcd for $C_{15}H_{16}Cl_3NNaO_3$ ($M+Na^+$) 386.0088, found 386.0100.

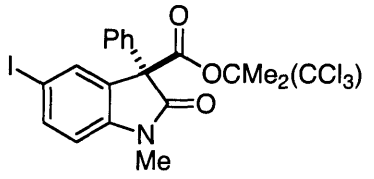

(*R*)-(–)-1-Methyl-2-oxo-3-phenyl-5-iodo-2,3-dihydro-1*H*-indole-3-carboxylic acid 2,2,2-trichloro-1,1-dimethyl-ethyl ester (Table 1.2, entry 5). The general procedure was followed: enol carbonate (140 mg, 0.25 mmol), catalyst (–)-**1** (8.6 mg, 0.013 mmol), and CH_2Cl_2 (0.25 mL). The product was isolated by column chromatography (80% hexanes/20% Et_2O) as a white foamy solid (132 mg; 95% yield). HPLC analysis: 98% ee [Daicel CHIRALPAK OD column; solvent system: 10% isopropanol/90% hexanes; 1.0 mL/min; retention times: 7.6 min (major), 9.0 min (minor)]. $[\alpha]^{20}_D$ = –24.5 (c = 1.05, CH_2Cl_2).

A second run was performed on the same scale, and the product was isolated in 92% yield and 98% ee.

^{1}H NMR (500 MHz, $CDCl_3$) δ 1.81 (s, 3H), 1.90 (s, 3H), 3.19 (s, 3H), 6.71 (d, 1H, J = 7.5 Hz), 7.37 (m, 5H), 7.73 (d, 1H, J = 7.5 Hz), 7.86 (s, 1H),. ^{13}C NMR (500 MHz, $CDCl_3$) δ 20.8, 21.4, 26.9, 64.5, 85.0, 90.6, 105.4, 110.9, 128.0, 128.6, 128.7, 128.8, 134.2, 134.7, 138.6, 144.5, 166.0, 171.6. FTIR (thin film) 1754, 1724, 1602, 1487, 1149 cm^{-1}. mp 60–67 °C. HRMS (ESI) calcd for $C_{20}H_{17}Cl_3INNaO_3$ ($M+Na^+$) 573.9211, found 573.9237.

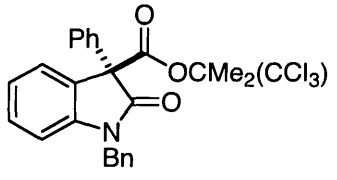

(*R*)-(–)-1-Benzyl-2-oxo-3-phenyl-2,3-dihydro-1*H*-indole-3-carboxylic acid 2,2,2-trichloro-1,1-dimethyl-ethyl ester (Table 1.2, entry 6). The general procedure was followed: enol carbonate (130 mg, 0.25 mmol), catalyst (–)-**1** (8.6 mg, 0.013 mmol), and CH_2Cl_2 (0.25 mL). The product was isolated by column chromatography (80% hexanes/20% Et_2O) as a white foamy solid (115 mg; 91% yield). HPLC analysis: 98% ee [Daicel CHIRALPAK OD column; solvent system: 1% isopropanol/99% hexanes; 1.0 mL/min; retention times: 6.6 min (major), 7.9 min (minor)]. $[\alpha]^{20}_D = -171.3$ (c = 1.13, CH_2Cl_2).

A second run was performed on the same scale, and the product was isolated in 84% yield and 97% ee.

^{1}H NMR (500 MHz, $CDCl_3$) δ 1.85 (s, 3H), 1.94 (s, 3H), 4.85 (d, 1H, J = 16.0 Hz), 5.03 (d, 1H, J = 16.0 Hz), 6.80 (d, 1H, J = 8.0 Hz), 7.14 (t, 1H, J = 7.0 Hz), 7.29 (m, 6H), 7.38 (m, 3H), 7.47 (m, 2H), 7.55 (d, 1H, J = 7.5Hz). ^{13}C NMR (500 MHz, $CDCl_3$) δ 20.9, 21.5, 44.5, 64.9, 90.5, 105.5, 110.0, 123.0, 126.0, 126.7, 127.4, 127.8, 128.3, 128.4, 128.7, 129.0, 129.8, 135.2, 135.5, 144.0, 167.0, 172.6. FTIR (thin film) 1750, 1720, 1609, 1150 cm^{-1}. mp 56–60 °C. HRMS (ESI) calcd for $C_{26}H_{22}Cl_3NNaO_3$ ($M+Na^+$) 524.0557, found 524.0567.

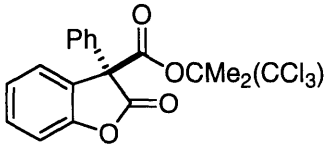

(*R*)-(–)-2-Oxo-3-phenyl-2,3-dihydro-benzofuran-3-carboxylic acid 2,2,2-trichloro-1,1-dimethyl-ethyl ester (Table 1.3, entry 1). The general procedure was followed: enol carbonate (100 mg, 0.25 mmol), catalyst (–)-**1** (8.6 mg, 0.013

mmol), and CH_2Cl_2 (0.25 mL). The product was isolated by column chromatography (80% hexanes/20% Et_2O) as a white solid (84 mg; 81% yield). HPLC analysis: 97% ee [Daicel CHIRALPAK OD column; solvent system: 10% isopropanol/90% hexanes; 1.0 mL/min; retention times: 5.6 min (minor), 6.4 min (major)]. $[\alpha]^{20}_D = -12.0$ (c = 1.00, CH_2Cl_2).

A second run was performed on the same scale, and the product was isolated in 81% yield and 96% ee.

^1H NMR (500 MHz, $CDCl_3$) δ 1.82 (s, 3H), 1.93 (s, 3H), 7.24 (d, 1H, J = 8.0 Hz), 7.30 (t, 1H, J = 7.5 Hz), 7.41 (m, 5H), 7.47 (t, 1H, J = 7.8 Hz), 7.60 (d, 1H J = 7.5 Hz). ^{13}C NMR (500 MHz, $CDCl_3$) δ 20.9, 21.5, 63.5, 91.1, 105.2, 111.6, 124.8, 125.2, 126.5, 127.9, 129.0, 129.1, 130.9, 133.8, 154.1, 165.4, 171.2. FTIR (thin film) 1822, 1759, 1464, 1149 cm^{-1}. mp 90–94 °C. HRMS (ESI) calcd for $C_{19}H_{15}Cl_3NaO_4$ ($M+Na^+$) 434.9928, found 434.9907.

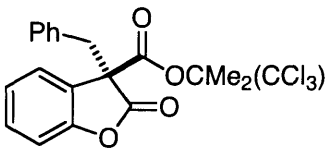

(*R*)-(–)-3-Benzyl-2-oxo-2,3-dihydro-benzofuran-3-carboxylic acid 2,2,2-trichloro-1,1-dimethyl-ethyl ester (Table 1.3, entry 2). The general procedure was followed: enol carbonate (110 mg, 0.25 mmol), catalyst (–)-**1** (8.6 mg, 0.013 mmol), and CH_2Cl_2 (0.25 mL). The product was isolated by column chromatography (80% hexanes/20% Et_2O) as a white solid (101 mg; 95% yield). HPLC analysis: 88% ee [Daicel CHIRALPAK OD column; solvent system: 2%

isopropanol/98% hexanes; 1.0 mL/min; retention times: 7.3 min (minor), 8.3 min (major)]. $[\alpha]^{20}_{D} = -7.6$ (c = 0.90, CH_2Cl_2).

A second run was performed on the same scale, and the product was isolated in 94% yield and 89% ee.

^{1}H NMR (500 MHz, $CDCl_3$) δ 1.84 (s, 3H), 1.93 (s, 3H), 3.62 (s, 2H), 6.93 (m, 3H), 7.10 (m, 3H), 7.18 (t, 1H, J = 7.5 Hz), 7.27 (t, 1H, J = 7.0 Hz), 7.41 (d, 1H, J = 7.0 Hz). ^{13}C NMR (500 MHz, $CDCl_3$) δ 21.1, 21.4, 39.6, 61.3, 90.9, 105.3, 111.2, 124.2, 124.4, 125.8, 127.5, 128.4, 130.2, 130.3, 133.5, 153.8, 165.4, 172.3. FTIR (thin film) 1808, 1752, 1463, 1240, 1150 cm^{-1}. mp 113–116 °C. HRMS (ESI) calcd for $C_{20}H_{17}Cl_3NaO_4$ ($M+Na^+$) 449.0084, found 449.0067.

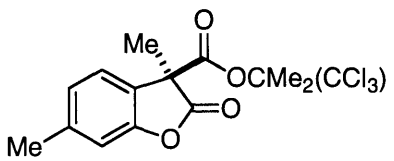

(*R*)-3,6-Dimethyl-2-oxo-2,3-dihydro-benzofuran-3-carboxylic acid 2,2,2-trichloro-1,1-dimethyl-ethyl ester (Table 1.3, entry 3). A modified general procedure was followed: enol carbonate (107 mg, 0.29 mmol), catalyst (–)-**1** (20 mg, 0.029 mmol), and CH_2Cl_2 (0.29 mL). The reaction was conducted at –12 °C for 19 h. The product was isolated by column chromatography (95% hexanes/5% Et_2O) as a white solid (99 mg; 93% yield). HPLC analysis: 90% ee [Daicel CHIRALPAK OJ column; solvent system: 3% isopropanol/97% hexanes; 1.0 mL/min; retention times: 5.9 min (major), 6.6 min (minor)].

^{1}H NMR (500 MHz, $CDCl_3$) δ 1.76 (s, 3H), 1.78 (s, 3H), 1.88 (s, 3H), 2.39 (s, 3H), 6.98 (m, 2H), 7.19 (d, 1H, J = 8 Hz). ^{13}C NMR (500 MHz, $CDCl_3$) δ 20.0, 21.1, 21.4, 22.0, 55.0, 90.6, 105.4, 111.9, 123.0, 125.4, 140.9, 153.7, 166.2, 174.2, 206.0. FTIR (thin film) 1814, 1753, 1263, 1156, 1036, 792 cm^{-1}. mp 109–116 °C. HRMS (ESI) calcd for $C_{15}H_{15}Cl_3NaO_4$ ($M+Na^+$) 386.9928, found 386.9933.

V. Formal Total Synthesis of Aplysin (Scheme 1.1)

The yields are unoptimized and only partial characterization data was obtained.

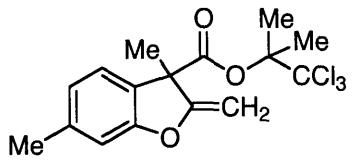

3,6-Dimethyl-2-methylene-2,3-dihydro-benzofuran-3-carboxylic acid 2,2,2-trichloro-1,1-dimethyl-ethyl ester (Scheme 1.1, compound 1.6). To a round-bottomed flask with stirbar was added 1.02 g of benzofuranone **1.5**. The flask was evacuated and back-filled with argon three times and then was wrapped in foil in order to perform the reaction in the dark. Next, 56.0 mL of a 0.1 M solution of Cp_2TiMe_2 was added to the flask and the reaction was stirred at 58 °C for 43 hours. The reaction was cooled to room temperature and diluted with approximately 50 mL of hexanes. The resulting mixture was then filtered through a silica plug with liberal hexanes washings. The solvent was removed by rotary evaporation to furnish a yellow-orange oil. The product was isolated by column chromatography (100% hexanes → 99% hexanes : 1% Et_2O) as a yellow oil (546 mg; 54% yield). Analysis of this product by ^1H NMR showed a mixture between compound **1.6** and an impurity assigned as structure **1.11** (78:22). Additional purification by column chromatography (100% hexanes → 99% hexanes : 1% Et_2O) allowed isolation of a mixture that was mostly (~95%) **1.6** as a yellow oil (324 mg; 32% yield).

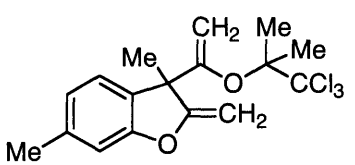

1.11

^{1}H NMR (500 MHz, $CDCl_3$) δ 1.74 (s, 3H), 1.86 (s, 3H), 1.89 (s, 3H), 2.35 (s, 3H), 4.51 (d, 1H, J = 3 Hz), 4.84 (d, 1H, J = 3 Hz), 6.77 (s, 1H), 6.82 (d, 1H, J = 8 Hz), 7.17 (d, 1H, J = 7.5 Hz). ^{13}C NMR (500 MHz, $CDCl_3$) δ 21.13, 21.15, 21.8, 25.4, 55.0, 86.4, 89.6, 110.4, 110.5, 123.0, 123.1, 123.5, 123.6, 126.7, 139.9, 165.3. FTIR (thin film) 1742, 1688, 1619, 1211, 1124, 962 cm^{-1}.

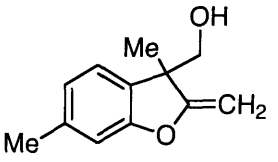

(3,6-Dimethyl-2-methylene-2,3-dihydro-benzofuran-3-yl)-methanol (Scheme 1.1, compound 1.7). To a round-bottomed flask with stir bar was added a solution of benzofuran **1.6** (615mg, 1.69 mmol) dissolved in 15 mL of dry Et_2O. Next, $LiAlH_4$ (129 mg, 3.38 mmol) was added and the reaction mixture was stirred for 5 minutes. The reaction was quenched with ~2 mL of water then dried over Na_2SO_4. The mixture was filtered through an acrodisk to remove the solids and the solvent of the filtrate was removed my rotary evaporation. The product was isolated by column chromatography (70% hexanes : 30% Et_2O) as a colorless oil (300 mg; 93% yield).

^{1}H NMR (500 MHz, C_6D_6) δ 1.21 (s, 3H), 2.02 (s, 3H), 3.29 (m, 2H), 4.05 (d, 1H, J = 2.5 Hz), 4.74 (d, 1H, J = 2 Hz), 6.60 (d, 1H, J = 7.5 Hz), 6.65 (s, 1H), 6.84 (d, 1H, J = 7.5 Hz). ^{13}C NMR (500 MHz, C_6D_6) δ 21.8, 24.0, 50.0, 70.9, 84.5, 110.7, 123.3, 123.8, 129.8, 139.2, 158.0, 169.3. FTIR (thin film) 3389, 1685, 1426, 1124, 961 cm^{-1}.

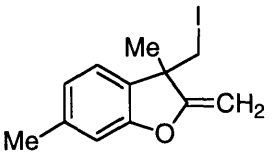

3-Iodomethyl-3,6-dimethyl-2-methylene-2,3-dihydro-benzofuran (Scheme 1.1, compound 1.8). To a round-bottomed flask with stirbar was added PPh_3 (828 mg, 3.16 mmol) and I_2 (438 mg, 2.84 mmol). Next, 10 mL of dry toluene was added and the mixture stirred at 80 °C for 5 minutes. Then a 10 mL toluene solution of alcohol **1.7** (300 mg, 1.58 mmol) was added to the reaction mixture. The solution was stirred at 80 °C for an additional 2 hours. The reaction was then cooled to room temperature and added to a separatory funnel. The contents were extracted into Et_2O, and the organic portion was washed with water, and dried with $MgSO_4$. Solvent was removed by rotary evaporation and the product was isolated by column chromatography (90% hexanes : 10% CH_2Cl_2) as a colorless oil (107 mg; 23% yield).

^1H NMR (500 MHz, C_6D_6) δ 1.22 (s, 3H), 2.02 (s, 3H), 2.93 (m, 2H), 4.05 (d, 1H, J = 2.5 Hz), 4.79 (d, 1H, J = 2 Hz), 6.62 (d, 1H, J = 7.5 Hz), 6.68 (s, 1H), 6.86 (d, 1H, J = 7.5 Hz).

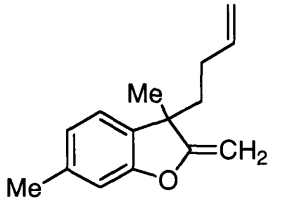

3-But-3-enyl-3,6-dimethyl-2-methylene-2,3-dihydro-benzofuran (Scheme 1.1, compound 1.9). To a vial with stirbar was added iodide **1.8** (26.6 mg, 0.0886 mmole). The vial was purged with argon and the substrate was dissolved in 0.45

mL of dry Et_2O. The mixture was cooled to –78 °C and *t*-BuLi (109 μL, 1.7M in pentanes, 0.186 mmol) was added. The reaction was stirred for 30 minutes at –78 °C then allyl bromide (53.6 mg, 38.3 μL, 0.443 mmol) was added. The reaction was warmed to room temperature and diluted with ~2 mL of hexanes and filtered through a plug of silica gel with hexanes/Et_2O (9:1) washings. The solvent was removed by rotary evaporation and the product was isolated by column chromatography (99.5% hexanes : 0.5% Et_2O) as a colorless oil (11.5 mg; 61% yield).

^{1}H NMR (500 MHz, C_6D_6) δ 1.24 (s, 3H), 1.58 (m, 1H), 1.71 (m, 2H), 2.06 (m, 4H), 4.05 (d, 1H, J = 3 Hz), 4.84 (d, 1H, J = 3 Hz), 4.89 (m, 2H), 5.64 (m, 1H), 6.65 (m, 1H), 6.71 (s, 1H) 6.72 (s, 1H).

V. X-ray Crystallographic Data

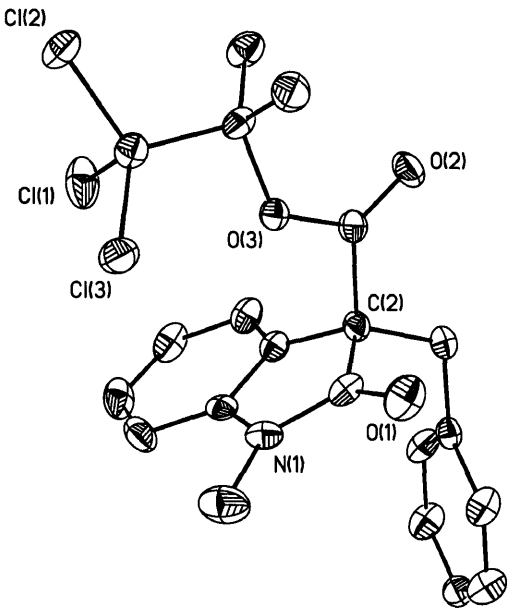

(*R*)-(–)-3-Benzyl-1-methyl-2-oxo-2,3-dihydro-1*H*-indole-3-carboxylic acid 2,2,2-trichloro-1,1-dimethyl-ethyl ester (Table 2, entry 3) [02133IHS]

A colorless pentane solution of (*R*)-(–)-3-benzyl-1-methyl-2-oxo-2,3-dihydro-1*H*-indole-3-carboxylic acid 2,2,2-trichloro-1,1-dimethyl-ethyl ester was prepared. Crystals suitable for X-ray structural analysis were obtained by solvent evaporation.

A colorless block of dimensions 0.45 x 0.25 x 0.15 mm^3 was mounted under STP and transferred to a Bruker AXS/CCD three-circle diffractometer (γ fixed at 54.78°) equipped with a cold stream of N_2 gas. An initial unit cell was determined by harvesting reflections $I > 20\ \sigma(I)$ from 45 x 10-s frames of 0.30° ω scan data with monochromated Mo K_α radiation ($\lambda = 0.71073$ Å). The cell thus determined was monoclinic.

A hemisphere of data was then collected using w scans of 0.30° and 30-s frames. The raw data frames were integrated using the Bruker program SAINT+

for NT version 6.01. An initial background was determined from the first 12° of data. Actual integration was performed with constant spot sizes of 1.6° in the detector plane and 0.6° in w. Backgrounds were then calculated as a continuing average over 8 frames of data. The data that were collected (8364 total reflections, 5076 unique, R_{int} = 0.0305) had the following Miller index ranges: –10 to 10 in h, –24 to 27 in k, and –9 to 10 in l. The data were corrected for Lorentz and polarization effects. SADABS absorption correction was performed.

All aspects of the solution and refinement were handled by SHELXTL NT version 5.10. The structure was solved by direct methods in the monoclinic space group P2(1), a = 9.0721(5) Å; b = 24.4432(14) Å; c = 9.6326(6) Å; α = 90°; β = 101.8800(10)°; γ = 90°, and refined using standard difference Fourier techniques. Final, full-matrix least-squares refinement (5076 data for 512 parameters) on F^2 yielded residuals of R_1 and wR_2 of 0.0454 and 0.1132 for data $I > 2\sigma(I)$, and 0.0465 and 0.1140, respectively, for all data. During the final refinement, all non-hydrogen atoms were treated anisotropically. Hydrogen atoms were included in calculated positions and refined isotropically on a riding model. Residual electron density amounted to a maximum of 0.387 e/Å^3 and a minimum of –0.205 e/Å^3.

The absolute structure (Flack) parameter for the correct enantiomer is 0.0000(4). The structure was also inverted and refined in order to confirm the initial assignment of absolute stereochemistry.

See Appendix A for tables containing full crystallographic data for the X-ray structure.

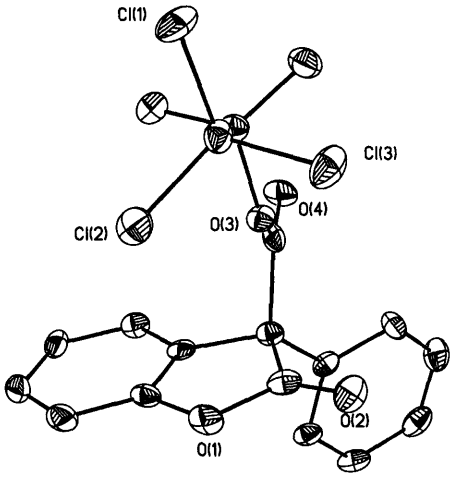

(*R*)-(–)-2-Oxo-3-phenyl-2,3-dihydro-benzofuran-3-carboxylic acid 2,2,2-trichloro-1,1-dimethyl-ethyl ester (Table 1.3, entry 1) [02163IHS]

A colorless Et_2O solution of (*R*)-(–)-2-oxo-3-phenyl-2,3-dihydro-benzofuran-3-carboxylic acid 2,2,2-trichloro-1,1-dimethyl-ethyl ester was prepared. Crystals suitable for X-ray structural analysis were obtained by solvent evaporation.

A colorless block of dimensions 0.32 x 0.21 x 0.17 mm^3 was mounted under STP and transferred to a Bruker AXS/CCD three-circle diffractometer (γ fixed at 54.78°) equipped with a cold stream of N_2 gas. An initial unit cell was determined by harvesting reflections $I > 20\ \sigma(I)$ from 45 x 10-s frames of 0.30° ω scan data with monochromated Mo K_α radiation (λ = 0.71073 Å). The cell thus determined was monoclinic.

A hemisphere of data was then collected using ω scans of 0.30° and 30-s frames. The raw data frames were integrated using the Bruker program SAINT+ for NT version 6.01. An initial background was determined from the first 12° of data. Actual integration was performed with constant spot sizes of 1.6° in the detector plane and 0.6° in ω. Backgrounds were then calculated as a continuing

average over 8 frames of data. The data that were collected (3726 total reflections, 2152 unique, R_{int} = 0.0407) had the following Miller index ranges: –8 to 9 in h, –8 to 10 in k, and –10 to 13 in l. The data were corrected for Lorentz and polarization effects. SADABS absorption correction was performed.

All aspects of the solution and refinement were handled by SHELXTL NT version 5.10. The structure was solved by direct methods in the monoclinic space group P2(1), a = 8.8316(7) Å; b = 9.4908(8) Å; c = 11.8129(10) Å; α = 90°; β = 110.5570(10)°; γ = 90°, and refined using standard difference Fourier techniques. Final, full-matrix least-squares refinement (2152 data for 237 parameters) on F^2 yielded residuals of R_1 and wR_2 of 0.0488 and 0.1251 for data $I > 2\sigma(I)$, and 0.0495 and 0.1256, respectively, for all data. During the final refinement, all non-hydrogen atoms were treated anisotropically. Hydrogen atoms were included in calculated positions and refined isotropically on a riding model. Residual electron density amounted to a maximum of 0.414 e/Å^3 and a minimum of –0.302 e/Å^3.

The absolute structure (Flack) parameter for the correct enantiomer is 0.05(10). The structure was also inverted and refined in order to confirm the initial assignment of absolute stereochemistry.

See Appendix A for tables containing full crystallographic data for the X-ray structure.

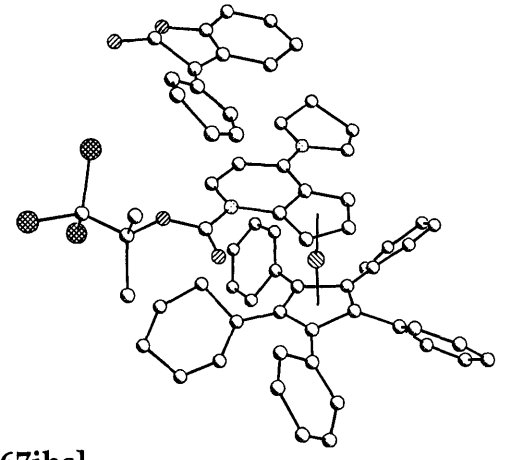

Ion Pair, Figure 2 [02167ihs]

To a vial was added catalyst (–)-**1** (10 mg) and carbonic acid 3-phenyl-benzofuran-2-yl ester 2,2,2-trichloro-1,1-dimethyl-ethyl ester (10 mg). Next, CH_2Cl_2 (0.2 mL) was added, affording a purple solution. The vial was kept at room temperature for 20 min, after which the color was between dark-purple and blue. The vial was then cooled to –35 °C for 24 h, at which time crystals suitable for X-ray structural analysis were harvested.

A blue-green needle of dimensions 0.5 x 0.04 x 0.04 mm^3 was mounted under STP and transferred to a Bruker AXS/CCD three-circle diffractometer (γ fixed at 54.78°) equipped with a cold stream of N_2 gas. An initial unit cell was determined by harvesting reflections $I > 20\ \sigma(I)$ from 45 x 10-s frames of 0.30° ω scan data with monochromated Mo K_α radiation (λ = 0.71073 Å). The cell thus determined was orthorhombic.

A hemisphere of data was then collected using w scans of 0.30° and 40-s frames. The raw data frames were integrated using the Bruker program SAINT+ for NT version 6.01. An initial background was determined from the first 12° of data. Actual integration was performed with constant spot sizes of 1.6° in the detector plane and 0.6° in ω. Backgrounds were then calculated as a continuing

average over 8 frames of data. The data that were collected (20328 total reflections, 8923 unique, $R_{int} = 0.4093$) had the following Miller index ranges: –11 to 9 in h, –18 to 17 in k, and –38 to 40 in l. The data were corrected for Lorentz and polarization effects. SADABS absorption correction was performed.

All aspects of the solution and refinement were handled by SHELXTL NT version 5.10. The structure was solved by direct methods in the orthorhombic space group P2(1)2(1)2(1), a = 9.9(8) Å; b = 16.8(17) Å; c = 37(4) Å; $\alpha = 90°$; $\beta = 90°$; $\gamma = 90°$, and refined using standard difference Fourier techniques. Final, full-matrix least-squares refinement (8923 data for 307 parameters) on F^2 yielded residuals of R_1 and wR_2 of 0.2498 and 0.4775 for data $I > 2\sigma(I)$, and 0.4056 and 0.5523, respectively, for all data. During the final refinement, all non-hydrogen atoms were treated *isotropically*. Hydrogen atoms were included in calculated positions and refined isotropically on a riding model. Residual electron density amounted to a maximum of 2.743 e/Å^3 and a minimum of –1.792 e/Å^3.

The absolute structure (Flack) parameter for the correct enantiomer is 0.10(13). The structure was also inverted and refined in order to confirm the initial assignment of absolute stereochemistry.

See Appendix A for tables containing full crystallographic data for the X-ray structure.

Part II

Reactions of Palladium Bisphosphine Complexes Relevant to Catalytic C-C Bond Formation

Chapter 2

Oxidative Addition of Alkyl Electrophiles to Palladium Bisphosphine Complexes

A. Introduction

Palladium-catalyzed cross-couplings are valuable tools for the synthetic organic chemist (eq 2.1);[41] however, until just a few years ago these cross-couplings were mostly restricted to aryl and vinyl halides and sulfonates. Recently, several groups have made advances in the palladium-catalyzed cross-coupling of alkyl halides and sulfonates.[42,43,44,45,46,47]

---

[41] For reviews of metal-catalyzed cross-coupling reactions, see: (a) *Cross-Coupling Reactions: A Practical Guide*; Miyaura, N., Ed.; Topics in Current Chemistry Series 219; Springer-Verlag: New York, 2002. (b) *Metal-Catalyzed Cross-Coupling Reactions*; Diederich, F.; Stang, P. J., Eds.; Wiley-VCH: New York, 1998.

[42] For an overview of the difficulty of achieving coupling reactions of C_{sp3}-electrophiles, see: (a) Cárdenas, D. J. *Angew. Chem. Int. Ed.* **2003**, *42*, 384-387. (b) Luh, T.-Y.; Leung, M.-K.; Wong, K.-T. *Chem. Rev.* **2000**, *100*, 3187-3204. (c) Cárdenas, D. J. *Angew. Chem. Int. Ed.* **1999**, *38*, 3018-3020.

[43] Suzuki reaction: (a) Kirchhoff, J. H.; Netherton, M. R.; Hills, I. D.; Fu, G. C. *J. Am. Chem. Soc.* **2002**, *124*, 13662-13663. (b) Netherton, M. R.; Fu, G. C. *Angew. Chem. Int. Ed.* **2002**, *41*, 3910-3912. (c) Kirchhoff, J. H.; Dai, C.; Fu, G. C. *Angew. Chem. Int. Ed.* **2002**, *41*, 1945-1947. (d) Netherton, M. R.; Dai, C.; Neuschütz, K.; Fu, G. C. *J. Am. Chem. Soc.* **2001**, *123*, 10099-10100. (e) Ishiyama, T.; Abe, S.; Miyaura, N.; Suzuki, A. *Chem. Lett.* **1992**, 691-694.

[44] Kumada reaction: (a) Terao, J.; Ikumi, A.; Kuniyasu, H.; Kambe, N. *J. Am. Chem. Soc.* **2003**, *125*, 5646-5647. (b) Frisch, A. C.; Shaikh, N.; Zapf, A.; Beller, M. *Angew. Chem. Int. Ed.* **2002**, *41*, 4056-4059. (c) Terao, J.; Watanabe, H.; Ikumi, A.; Kuniyasu, H.; Kambe, N. *J. Am. Chem. Soc.* **2002**, *124*, 4222-4223.

[45] Hiyama reaction: Lee, J.-Y., Fu, G. C. *J. Am. Chem. Soc.* **2003**, *125*, 5616-5617.

[46] Stille reaction: (a) Tang, H.; Menzel, K.; Fu, G. C. *Angew. Chem. Int. Ed.* **2003**, *42*, 5079-5082. (b) Menzel, K.; Fu, G. C. *J. Am. Chem. Soc.* **2003**, *125*, 3718-3719.

[47] Negishi reaction: (a) Wiskur, S. L.; Korte, A.; Fu, G. C. *J. Am. Chem. Soc.* **2004**, *126*, 82-83. (b) Zhou, J.; Fu, G. C. *J. Am. Chem. Soc.* **2003**, *125*, 12527-12530. (c) Jensen, A. E.; Knochel, P. *J. Org. Chem.* **2002**, *67*, 79-85. (d) Piber, M.; Jensen, A. E.; Rottländer, M.; Knochel, P. *Org. Lett.* **1999**, *1*, 1323-1326. (e) Giovannini, R.; Stüdemann, T.; Devasagayaraj, A.; Dussin, G.; Knochel, P. *J. Org. Chem.* **1999**, *64*, 3544-3553. (f) Giovannini, R.; Knochel, P. *J. Am. Chem. Soc.* **1998**, *120*, 11186-11187. (g) Giovannini, R.; Stüdemann, T.; Dussin, G.; Knochel, P. *Angew. Chem. Int. Ed.* **1998**, *37*, 2387-2390. (h) Devasagayaraj, A.; Stüdemann, T.; Knochel, P. *Angew. Chem. Int. Ed. Engl.* **1995**, *107*, 2952-2954.

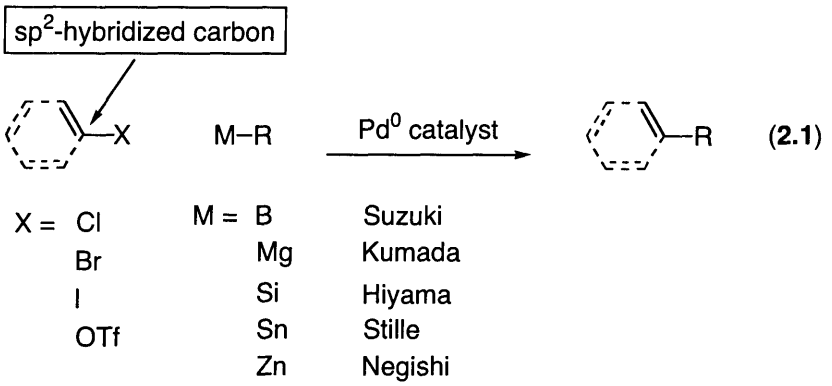

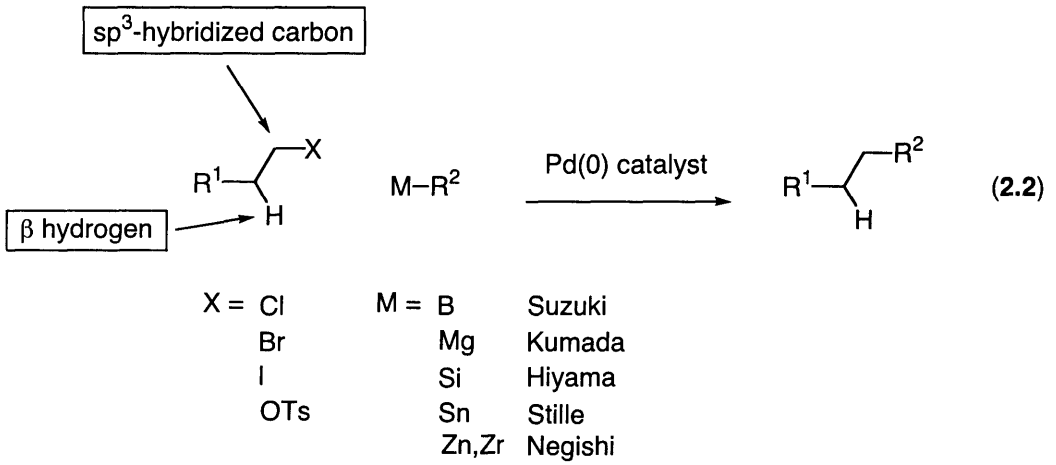

The catalytic cycle for most palladium-catalyzed cross-coupling reactions presumably includes a sequence of oxidative addition, transmetalation, and reductive elimination (Figure 2.1). The difficulty in developing methods capable of cross-coupling C_{sp3}-electrophiles has been attributed to relatively slow oxidative addition and an undesired side-reaction of β-hydride elimination. Our group has successfully overcome these obstacles by employing palladium catalysts bearing sterically-demanding trialkylphosphines, such as PCy_3 and $P(t\text{-}Bu)_2Me$. We were intrigued as to why these two ligands succeed in the cross-coupling of alkyl electrophile, while many other trialkylphosphines fail.

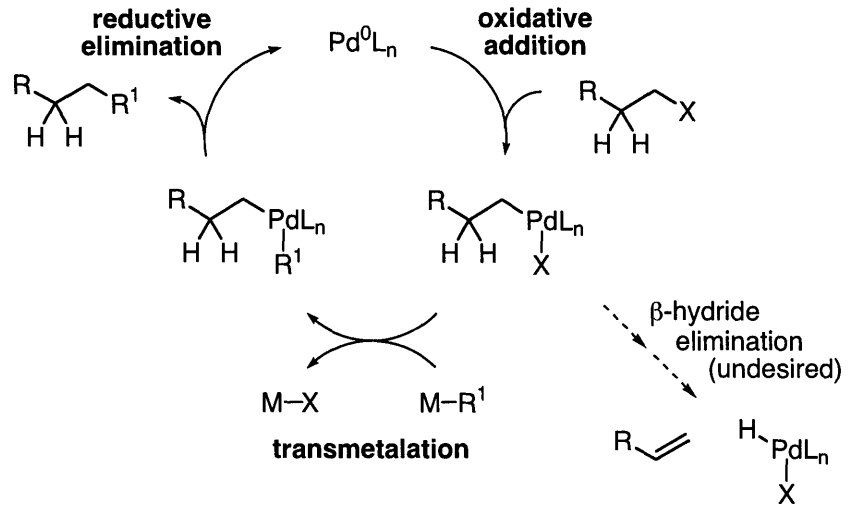

Figure 2.1. Generalized mechanism for a palladium-catalyzed cross-coupling reaction of alkyl electrophiles.

During attempts to further develop and explore the palladium-catalyzed couplings of C_{sp^3}-electrophiles, we discovered that oxidative addition adducts of bisphosphine-palladium complexes and alkyl bromides could be isolated and characterized crystallographically (Figure 2.2).[48] This result was a pleasant surprise, since oxidative addition appeared to be far more facile than previously thought and the resulting alkyl-palladium complexes seemed at least moderately stable to β-hydride elimination.

[48] The crystals were synthesized and grown by Dr. Matthew R. Netherton. The X-ray crystal structures were solved by I.D.H.

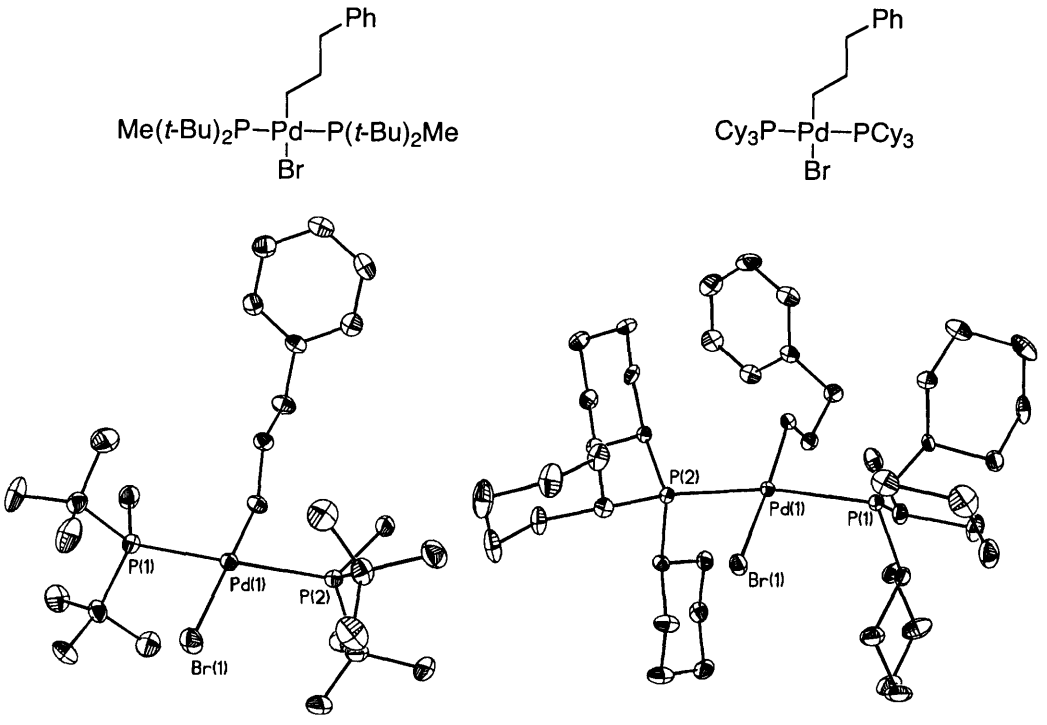

Figure 2.2. X-ray crystal structures of oxidative addition adducts of palladium bisphosphine complexes.

Furthermore, the choice of phosphine ligand has a profound effect on these cross-coupling reactions. For example, even a seemingly small change in the ligand structure from P(*t*-Bu)$_2$Me to P(*t*-Bu)$_2$Et has a deleterious effect on the outcome of Suzuki cross-coupling reactions (eq 2.3).[43b] This observation compelled us to conduct further studies on the mechanism of the palladium-catalyzed cross-couplings of alkyl electrophiles.

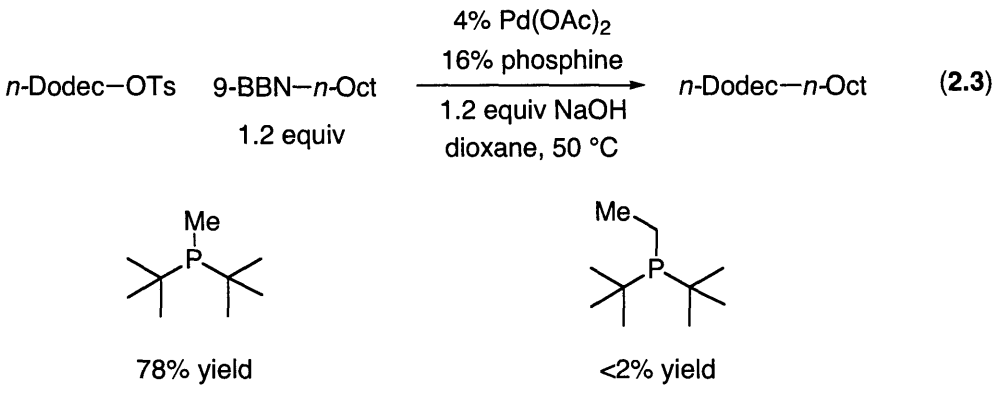

Intrigued by these results, we began an in-depth study of the oxidative addition of bisphosphine-palladium complexes to alkyl electrophiles.[49,50,51] There have been a plethora of mechanisms proposed for the oxidative addition of many different electrophiles to a diverse array of transition-metal complexes in various oxidation states. Despite the overwhelming number of mechanistic proposals, it is generally accepted that most mechanisms can be categorized as either a nucleophilic addition,[52] a concerted insertion,[53] or a radical process[54] (Figure 2.3).[55] We believed that a better understanding of this important step of the

[49] For examples of early studies performed on the oxidative addition of benzyl halides to Pd(0) complexes, see: (a) Milstein, D.; Stille, J. K. *J. Am. Chem. Soc.* **1979**, *101*, 4981. (b) Stille, J. K.; Lau, K. S. Y. *Acc. Chem. Res.* **1977**, *10*, 434-442. (c) Lau, K. S. Y.; Wong, P. K.; Stille, J. K. *J. Am. Chem. Soc.* **1976**, *98*, 5832-5840. (d) Stille, J. K.; Lau, K. S. Y. *J. Am. Chem. Soc.* **1976**, *98*, 5841-5849.

[50] For a recent discussion of the oxidative addition of Pd(0) to allylic acetates, see: Amatore, C.; Gamez, S.; Jutand, A.; Meyer, G.; Mottier, L. *Electrochim. Acta* **2001**, *46*, 3237-3244.

[51] The term 'oxidative addition' is used to merely name a transformation that takes place at a metal center and does not connote any specific mechanistic information. For basic discussions concerning reactions at metal centers and specifically oxidative addition, see: (a) Spessard, G. O.; Miessler, G. L. *Organometallic Chemistry*; Prentice Hall: Upper Saddle River, New Jersey, 1997; 161-178. (b) Collman, J. P.; Hegedus, L. S.; Norton, J. R.; Finke, R. G. *Principles and Applications of Organotransition Metal Chemistry*; University Science Books: Mill Valley, California, 1987; 279-353.

[52] For a review concerning oxidative addition through nucleophilic pathways, see: Cross, R. J. *Chem. Soc. Rev.* **1985**, *14*, 197-223.

[53] A concerted insertion mechanism is believed to be operative for the oxidative addition of dihydrogen to a diverse array of metal complexes, for examples see: (a) Zhou, P.; Vitale, A. A.; San Filippo, Jr., J.; Saunders, Jr., W. H. *J. Am. Chem. Soc.* **1985**, *107*, 8049-8054. (b) Low, J. J.; Goddard, III, W. A. *J. Am. Chem. Soc.* **1984**, *106*, 6928-6937. (c) Vaska, L.; Diluzio, J. W. *J. Am. Chem. Soc.* **1962**, *84*, 679-680.

[54] For an example of oxidative addition via a radical process, see: (a) Labinger, J. A.; Osborn, J. A. *Inorg. Chem.* **1980**, *19*, 3230-3236. (b) Labinger, J. A.; Osborn, J. A. *Inorg. Chem.* **1980**, *19*, 3236-3243.

[55] These three categories represent an oversimplification of the oxidative addition topic; however, they represent a starting point that helps the reader understand the issues one may encounter during the course of these mechanistic investigations.

catalytic cycle could lead to improved catalyst systems, thereby increasing the synthetic utility of this cross-coupling reaction. Thus, we proceeded to explore the mechanism of the oxidative addition of alkyl electrophiles to bisphosphine-palladium complexes, aware that any of the three mechanisms outlined in Figure 2.3, as well as others, may be operative.

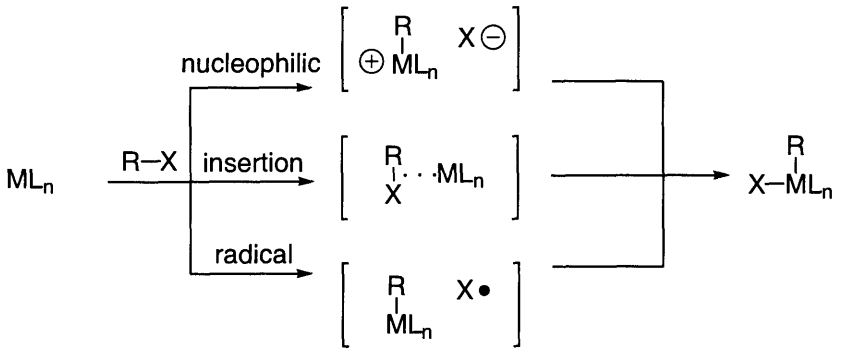

Figure 2.3. Possible mechanisms for the oxidative addition of a substrate to a metal center.[56]

[56] This figure is meant to a be an introduction to the general classes of oxidative addition mechanisms and does not adequately display the complexities involved in this area of chemistry. For example, the intermediate for the radical pathway is shown to have a discrete M–R bond and a free X•, but certain reaction conditions may give a different intermediate, such as M–X and R•, or M–R$^+$ and X$^-$•.

B. Results and Discussion

To-date, all of our results are consistent with the oxidative addition of an alkyl halide to a bisphosphine-palladium complex occurring through an S_N2-type mechanism. Through kinetics studies, we have determined that for the oxidative addition of *n*-nonyl bromide to $Pd(P(t\text{-}Bu)_2Me)_2$ (eq 2.4), the activation parameters are: $\Delta G^{\ddagger}$ = 20.8 kcal/mol at 20 °C; $\Delta H^{\ddagger}$ = 2.4 kcal/mol; $\Delta S^{\ddagger}$ = -63 eu. The large negative $\Delta S^{\ddagger}$ and preliminary stereochemical studies (eq 2.5) are consistent with an associative S_N2-type pathway.[57,58,59,60] We have also discovered that addition of $P(t\text{-}Bu)_2Me$ (e.g., 2 or 4 equiv) to the reaction illustrated in equation 2.4 does not affect the rate, suggesting that the alkyl bromide oxidatively adds to PdL_2 not PdL_1 or PdL_3.[61,62] In contrast, for cross-couplings of aryl bromides that are catalyzed by $Pd/P(t\text{-}Bu)_3$, the available data indicate that a palladium-monophosphine adduct undergoes oxidative addition.[63]

---

[57] These reaction conditions have been optimized for the Suzuki cross-coupling of alkyl bromides. For details, see: Kirchhoff, J. H.; Netherton, M. R.; Hills, I. D.; Fu, G. C. *J. Am. Chem. Soc.* **2002**, *124*, 13662-13663.

[58] Similar stereo-labeled substrates have been previously employed. For examples, see: (a) Bock, P. L.; Whitesides, G. M. *J. Am. Chem. Soc.* **1974**, *96*, 2826-2829. (b) Bock, P. L.; Boschetto, D. J. Rasmussen, J. R.; Demers, J. P.; Whitesides, G. M. *J. Am. Chem. Soc.* **1974**, *96*, 2814-2825.

[59] For other relevant stereochemical studies, see: Netherton, M. R.; Fu, G. C. *Angew. Chem. Int. Ed.* **2002**, *41*, 3910-3912.

[60] It has been proposed that the lack of complete stereoinversion for the oxidative addition may be attributed to nucleophilic exchange between an alkylpalladium intermediate and Pd(0). For details, see: Wong, P. K.; Lau, K. S. Y.; Stille, J. K. *J. Am. Chem. Soc.* **1974**, *96*, 5956-5957.

[61] When $Pd(P(t\text{-}Bu)_2Me)_2$ is dissolved in THF, the only phosphorus-containing species that is present according to ^{31}P NMR spectroscopy is the PdL_2 adduct (e.g., no PdL_1), and there is no change in the spectrum in the presence of excess $P(t\text{-}Bu)_2Me$ (e.g., no PdL_3).

[62] Attempts to crystallographically characterize a PdL_2 adduct bearing $P(t\text{-}Bu)_2Me$ have failed. Instead, crystals grown from a solution of $Pd(P(t\text{-}Bu)_2Me)_2$ were determined to be a PdL_3 adduct. See experimental for details.

[63] (a) Prashad, M.; Mak, X. Y.; Liu, Y.; Repic, O. *J. Org. Chem.* **2003**, *68*, 1163-1164. (b) Hii, K. K.; Jutand, A. *Angew. Chem. Int. Ed.* **2002**, *41*, 1760-1763. (c) Stambuli, J. P.; Kuwano, R.; Hartwig, J. F. *Angew. Chem. Int. Ed.* **2002**, *41*, 4746-4748. (d) Littke, A. F.; Dai, C.; Fu, G. C. *J. Am. Chem. Soc.* **2000**, *122*, 4020-4028. (e) Littke, A. F.; Fu, G. C. *Angew. Chem. Int. Ed.* **1998**, *37*, 3387-3388.

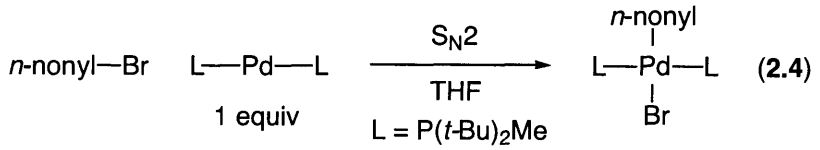

(2.4)

- $\Delta G^{\ddagger}$ = 20.8 kcal/mol (20 °C); $\Delta H^{\ddagger}$ = 2.4 kcal/mol; $\Delta S^{\ddagger}$ = –63 eu
- added phosphine does not affect the rate

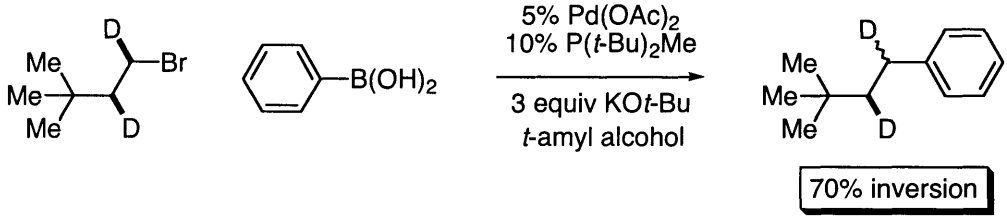

(2.5)

The effect of solvent polarity on the rate of oxidative addition was examined (Table 2.1).[64] A relatively high activation barrier for oxidative addition was observed when the reaction was performed in hexanes (entry 1). However, as the polarity of the solvent increases, the activation energy for oxidative addition decreases (entries 1→6). This trend is consistent with an S_N2-type nucleophilic attack of PdL_2 on an alkyl electrophile.[65]

[64] The values for solvent polarity are according to the S' scale. For an overview, see: Zou, J.; Yu, Q.; Shang, Z. *J. Chem. Soc., Perkin Trans. 2* **2001**, 1439-1443.
[65] In our methods-development studies, we have consistently found nonpolar solvents such as hexanes and toluene to be unsuitable for cross-coupling reactions of alkyl electrophiles.

Table 2.1. Correlation between solvent polarity and the activation barrier for oxidative addition.

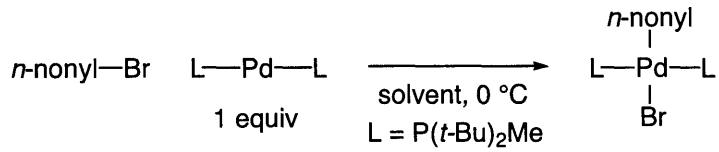

entry	solvent	polarity	$\Delta G^{\ddagger}$ (kcal/mol)
1	hexanes	0.68	>23.0[a]
2	toluene	1.66	20.0
3	THF	2.08	19.5
4	*t*-amyl alcohol	2.46[b]	18.1
5	NMP	2.62	18.0
6	DMF	2.80	17.8

All data are the average of two runs. [a] No reaction at 0-60 °C. $\Delta G^{\ddagger}$ was calculated for 60 °C. [b] Value for *t*-butanol.

We investigated the effect of the leaving group on the rate of oxidative addition of $Pd(P(t\text{-}Bu)_2Me)_2$ to a variety of alkyl electrophiles (Table 2.2). We found that an alkyl iodide undergoes oxidative addition very rapidly, and even at –60 °C the half-life is only 2.2 hours (entry 1). An alkyl bromide is significantly less reactive and has a comparable half-life of 2.3 hours at a much higher temperature (i.e., 0 °C, entry 2). A slower reaction is observed for *n*-nonyl tosylate, and heating at 40 °C is required to achieve a half-life of 10.4 hours (entry 3). Alkyl chlorides undergo considerably slower oxidative addition and have afford a half-life of 2 days at 60 °C (entry 4). Finally, alkyl fluorides were relatively inert under the conditions studied, which may explain why they are unable to undergo efficient cross-coupling (entry 5). The relative reactivity of these substrates further supports the hypothesis that oxidative addition occurs through an S_N2-type pathway.

Table 2.2. Effect of the leaving group on the rate of oxidative addition.

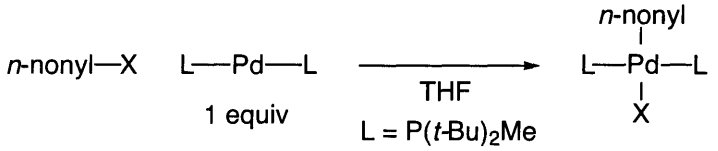

entry	X	half-life
1	I	2.2 h at –60 °C
2	Br	2.3 h at 0 °C
3	OTs	10.4 h at 40 °C
4	Cl	2.0 days at 60 °C
5	F	<2% reaction after 43 h at 60 °C

All data are the average of two runs.

We chose to explore the rate of oxidative addition of $Pd(P(t\text{-}Bu)_2Me)_2$ with substrates of varying steric demand (Table 2.3). As expected for an S_N2-process, the least bulky substrates have the most rapid rate of oxidative addition, with *n*-nonyl bromide having the lowest measured activation energy (19.5 kcal/mol, entry 1). Substitution in the γ-position leads to a ~5-fold decrease in reaction rate (entry 2), and β–substitution reduces the rate even further (entry 3). Finally, a secondary alkyl bromide did not undergo oxidative addition under these conditions (entry 4), which is consistent with both the expected trend for an S_N2-reaction and the inability for this catalyst system to cross-couple secondary electrophiles.

Table 2.3. Correlation between the steric demand of the electrophile and the activation barrier for oxidative addition.

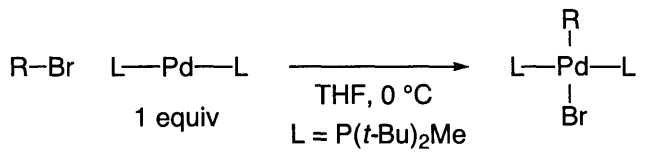

entry	R–Br	k_{rel}	$\Delta G^{\ddagger}$ (kcal/mol)
1	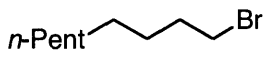	1.0	19.5
2	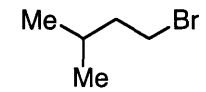	0.19	20.3
3	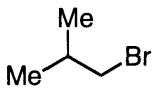	0.054	21.0
4	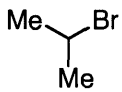	<0.0001	>24.0[a]

All data are the average of two runs. [a] Extrapolated from a reaction run at 60 °C.

Finally, in order to better understand the role of the phosphine ligand, we studied the oxidative addition of *n*-nonyl bromide to four bisphosphine complexes (Table 2.4). The phosphines capable of promoting the cross-couplings of alkyl electrophiles, PCy_3 and $P(t\text{-}Bu)_2Me$, furnish palladium complexes that undergo oxidative addition with a relatively low activation energy (entries 1 and 2). However, phosphines that are known to be poor ligands in the coupling of alkyl electrophiles provide palladium complexes that have significantly higher activation energies for oxidative addition. Despite its apparent similarity to $P(t\text{-}Bu)_2Me$, when $P(t\text{-}Bu)_2Et$ is used as a ligand the resulting palladium complex has an activation energy ~6 kcal/mol higher (measured at 60 °C), and $Pd(P(t\text{-}Bu)_3)_2$ was not observed to undergo oxidative addition (entry 3 and 4). It is reasonable to expect the very sterically demanding $P(t\text{-}Bu)_3$ to have an adverse effect on the

rate of this S_N2-process; however, we believe a more subtle explanation is responsible for the large difference in reactivity between $Pd(P(t\text{-}Bu)_2Me)_2$ and $Pd(P(t\text{-}Bu)_2Et)_2$. Thus, we conducted computational studies to better understand the conformation of these two palladium complexes.

Table 2.4. Effect of the phosphine on the activation barrier for oxidative addition.

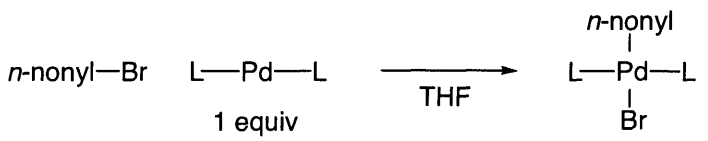

entry	L	$\Delta G^{\ddagger}$ (kcal/mol)[a]
1	$P(t\text{-}Bu)_2Me$	19.5 (0 °C)
2	PCy_3	20.0 (0 °C)
3	$P(t\text{-}Bu)_2Et$	25.4 (60 °C)
4	$P(t\text{-}Bu)_3$	>28.4 (60 °C)

All data are the average of two runs. [a] The temperature at which $\Delta G^{\ddagger}$ was measured is noted in parentheses.

We employed DFT calculations to determine the favored conformations of relevant species. First we computed the relative energies for three conformations of $P(t\text{-}Bu)_2Et$ (Figure 2.3).[66] The results indicate that the conformation with the lowest energy (**A**) has the ethyl group essentially aligned (eclipsed) with the lone-pair electrons of the phosphorus atom. This finding is sensible based on steric considerations, since conformations **B** and **C** have one and two *syn*-pentane interactions, respectively. If conformation **A** is indeed the lowest-energy conformation, then the ethyl group blocks a palladium atom bound to the

[66] Computations were performed with B3LYP/6-31G*; see experimental for details. All conformers are minima on the energy landscape and conformer **A** is believed to represent the global minimum. This has been verified by manually testing many conformations in a 'dihedral driver' type fashion.

phosphorus, which has negative consequences for an oxidative addition that occurs through an S_N2-type pathway.

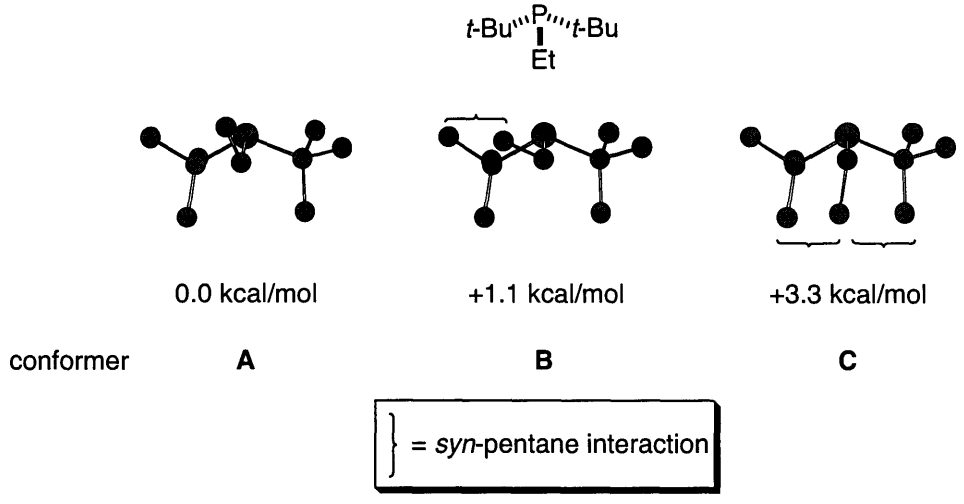

Figure 2.3. Conformations and relative energies for P(*t*-Bu)$_2$Et.

To verify that these computations were indeed relevant to the palladium complexes in question, we performed similar calculations for a palladium-ligated phosphine. Incorporation of the steric bulk associated with the palladium atom could raise the energy of a conformation in which the ethyl group is eclipsed with the non-bonding electrons of the phosphorus (Figure 2.4).[67] Indeed, this appears to be the case, since addition of the palladium atom seems to destabilize conformation **D** relative to conformation **E**; however, both of these conformations are still significantly lower in energy than conformation **F**, which exhibits two *syn*-pentane interactions. This result is still consistent with Pd(P(*t*-Bu)$_2$Et)$_2$ undergoing more sluggish oxidative addition than Pd(P(*t*-Bu)$_2$Me)$_2$ since

[67] Computations were performed with B3LYP/ LanL2DZ; see experimental for details. All conformers are minima on the energy landscape and conformer **D** is believed to represent the global minimum. This has been verified by manually testing many conformations in a 'dihedral driver' type fashion.

in the more highly populated conformations, **D** and **E**, the ethyl group blocks the nucleophilic metal.

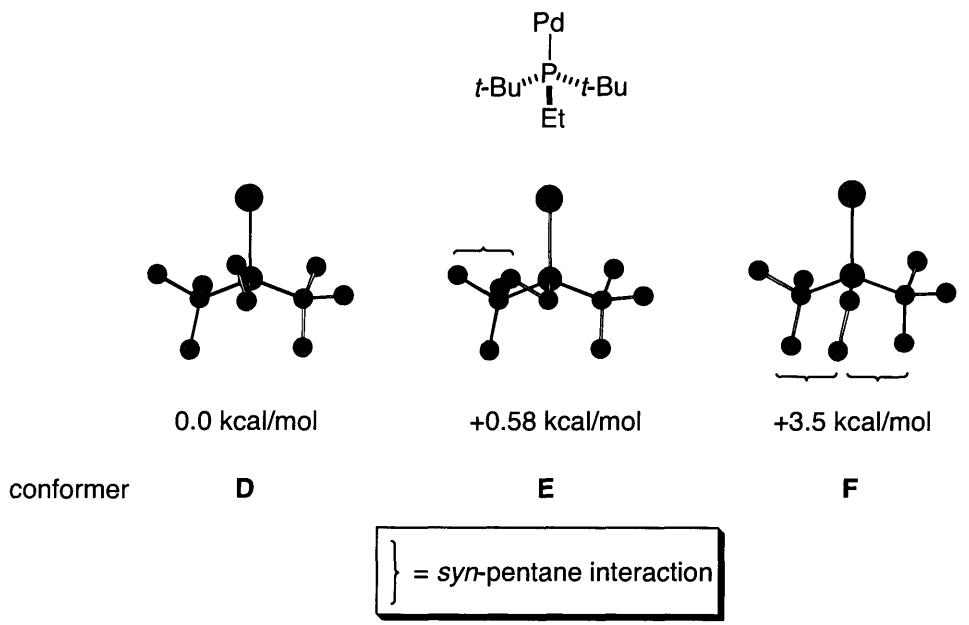

Figure 2.4. Conformations and relative energies for PdP(*t*-Bu)$_2$Et.

This is more clearly seen in a simple drawing of the two bisphosphine complexes (Figure 2.5). When P(*t*-Bu)$_2$Et adopts its lowest energy conformation, the palladium complex resembles **2.1**, and it can not readily engage in oxidative addition. In order for **2.1** to become more reactive, the complex must rearrange to a conformation more resembling **2.3**, such as conformation **2.2**.[68] This comes at a steep energetic cost, due to the introduction of many *syn*-pentane interactions. We believe that this simple conformational analysis adequately explains the profound difference in reactivity towards oxidative addition of alkyl

[68] It is likely that the reactivity of **2.1** toward oxidative addition will increase even if only one of the phosphine ligands undergoes conformational reorganization. Thus, structure **2.2** simply represents an endpoint on a continuum of reactive conformations. Also, we are unable to comment on the likelihood that the P-Pd-P angle deviates from the idealized 180°, which would lead to a more open and thus reactive palladium center.

electrophiles to Pd(P(*t*-Bu)$_2$Me)$_2$ and Pd(P(*t*-Bu)$_2$Et)$_2$, which in turn explains why P(*t*-Bu)$_2$Et performs poorly in cross-coupling reactions for this class of substrates.

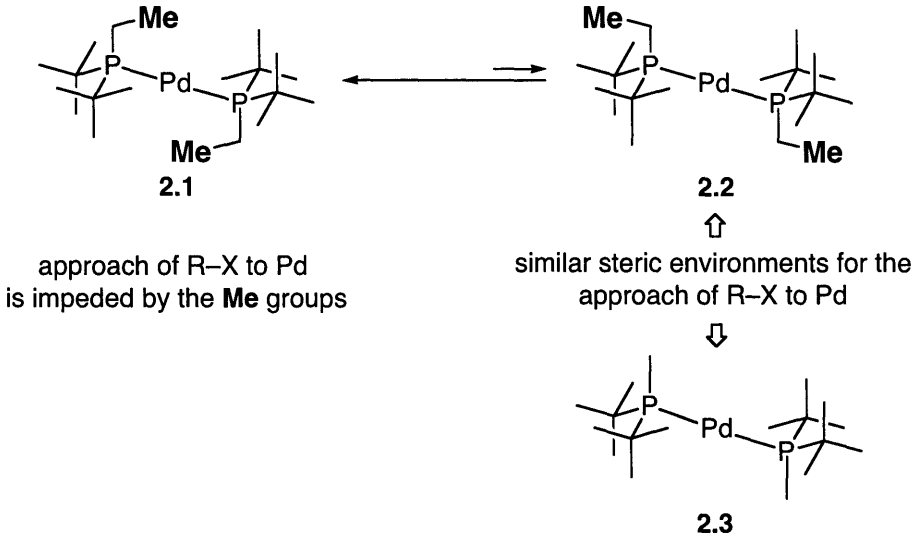

Figure 2.5. A rationale for the divergent reactivity of Pd(P(*t*-Bu)$_2$Me)$_2$ and Pd(P(*t*-Bu)$_2$Et)$_2$.

C. Conclusions

We have described the first systematic investigation of the oxidative addition of alkyl electrophiles to bisphosphine-palladium(0) complexes. The species that undergoes oxidative addition is PdL_2 (not PdL_1 or PdL_3), and the activation parameters for the oxidative addition of *n*-nonyl bromide to Pd(P(*t*-Bu)$_2$Me)$_2$ are: $\Delta G^{\ddagger}$ = 20.8 kcal/mol at 20 °C; $\Delta H^{\ddagger}$ = 2.4 kcal/mol; $\Delta S^{\ddagger}$ = -63 eu. We have quantified the effect of various parameters on the rate of oxidative addition, including solvent, leaving group (I, Br, Cl, F, OTs), steric demand of the substrate, and steric demand of the phosphine ligand. Additionally, based on DFT calculations, we have provided a rationale for the difference in reactivity between Pd(P(*t*-Bu)$_2$Me)$_2$ and Pd(P(*t*-Bu)$_2$Et)$_2$. We hope that these studies will aid in the design of a new generation of cross-coupling catalysts.

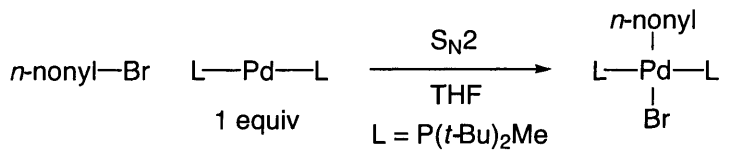

- $\Delta G^{\ddagger}$ = 20.8 kcal/mol (20 °C); $\Delta H^{\ddagger}$ = 2.4 kcal/mol; $\Delta S^{\ddagger}$ = –63 eu
- added phosphine does not affect the rate

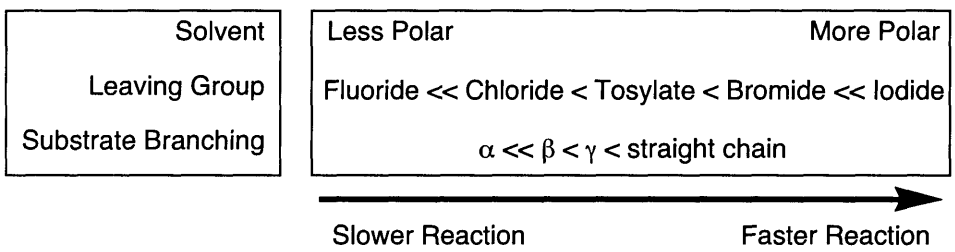

D. Experimental

I. General

All reactions were carried out under an atmosphere of nitrogen or argon in oven-dried glassware with magnetic stirring, unless otherwise indicated. Toluene and THF were purified by passage through a neutral alumina column, and *t*-amyl alcohol was purified by distillation from CaH_2. All other solvents were used as received: hexane (Aldrich; Sure/Seal); NMP (Aldrich; Sure/Seal); DMF (Aldrich; Sure/Seal).

All alkyl halides were purified by either distillation or vacuum transfer: *n*-nonyl iodide (Aldrich); *n*-nonyl bromide (Aldrich); *n*-nonyl chloride (Aldrich); *n*-nonyl fluoride (Aldrich); 1-bromo-3-methylbutane (Aldrich); isobutylbromide (Aldrich); isopropylbromide (Aldrich). *n*-Nonyl tosylate was prepared by tosylation of *n*-nonyl alcohol.

P(*t*-Bu)$_2$Me (Strem) and Pd(P(*t*-Bu)$_3$)$_2$ (Strem) were used without further purification. Pd(PCy$_3$)$_2$ (Strem) was purified by recrystallization from toluene/methanol. P(*t*-Bu)$_2$Et was prepared as previously described.[69] ^{1}H and ^{13}C NMR resonances are referenced to the solvent. ^{31}P NMR resonances are referenced to external 85% H_3PO_4.

[69] Netherton, M. R.; Fu, G. C. *Angew. Chem. Int. Ed.* **2002**, *41*, 3910-3912.

II. Preparation of PdL_2 Complexes

General procedure: Pd(π-allyl)(η^5-Cp) (1.0 equiv), the trialkylphosphine (2.2 equiv), and toluene (amount required for a 0.10 M solution in Pd) were added to a Schlenk tube equipped with a stirbar. The tube was sealed and then heated at 75 °C for 3 hours. The reaction mixture was then cooled to r.t., and the solvent was removed under vacuum. The resulting red solid was dissolved in pentane, and the solution was filtered and concentrated, furnishing a semi-crystalline solid.

$Pd(P(t\text{-}Bu)_2Me)_2$ [479210-19-0]. The general procedure was followed using 840 mg (3.9 mmol) of Pd(π-allyl)(η^5-Cp), 1.4 g (8.7 mmol) of $P(t\text{-}Bu)_2Me$, and 39 mL of toluene. The product (1.69 g, 101%) was isolated as an orange-brown solid. ^1H NMR (300 MHz, THF-d_8) δ 1.12 (s, 36H), 1.26 (s, 6H). ^{13}C NMR (300 MHz, THF-d_8) δ 7.4, 30.5, 33.6. ^{31}P NMR (300 MHz, THF-d_8) δ 42.3.

$Pd(P(t\text{-}Bu)_2Et)_2$. The general procedure was followed using 250 mg (1.2 mmol) of Pd(p-allyl)(h^5-Cp), 450 mg (2.6 mmol), $P(t\text{-}Bu)_2Et$, and 12 mL of toluene. The product (500 mg, 93% yield) was isolated as a brown-black solid.
^1H NMR (300 MHz, THF-d_8) δ 1.28 (m, 46H). ^{13}C NMR (300 MHz, THF-d_8) δ 16.1, 16.6, 31.0, 34.8. ^{31}P NMR (300 MHz, THF-d_8) δ 63.3. FTIR (thin film) 3402, 2894, 2864, 1469, 901 cm^{-1}. HRMS (ESI) calcd for $C_{20}H_{46}P_2PdNa$ ($M+Na^+$) 477.20, found 477.21.

III. Rates of Oxidative Addition[70]

Kinetic Analysis. Our kinetic analysis is based on an overall second-order rate law:

$$\text{Rate} = k[PdL_2][RX]$$

$$\text{When } [PdL_2] = [RX], \text{ Rate} = k[PdL_2]^2$$

$$\frac{d[PdL_2]}{dt} = -k[PdL_2]^2 \xrightarrow{\text{integration}} \int_{t_0}^{t} \frac{1}{[PdL_2]^2} d[PdL_2] = -k\int_{t_0}^{t} dt$$

$$\frac{1}{[PdL_2]_{t_0}} - \frac{1}{[PdL_2]_t} = -k(t - t_0) \xrightarrow{\text{simplification}} \frac{1}{[PdL_2]_t} - \frac{1}{[PdL_2]_{t_0}} = kt$$

Thus, a plot of $\frac{1}{[PdL_2]_t} - \frac{1}{[PdL_2]_{t_0}}$ versus time furnishes a linear plot, with a slope equal to the rate constant k.

The half-life is found by setting $[PdL_2] = \frac{1}{2}[PdL_2]_0$ and $t = t_{1/2}$, giving:

$$t_{1/2} = \frac{1}{[PdL_2]_0 k}$$

Using the Eyring equation:

$$k = \frac{\kappa T}{h} e^{\frac{-\Delta G^{\ddagger}}{RT}}$$

The free energy of activation ($\Delta G^{\ddagger}$) can be solved for by rearrangement:

---

[70] For additional details, see: a) Levine, I. N. *Physical Chemistry*, 4th ed.; McGraw-Hill: New York, 1995; pp 498-501. b) Lowry, T. H.; Richardson, K. S. *Mechanism and Theory in Organic Chemistry*, 3rd ed.; HarperCollins: New York, 1987; pp 208-209.

$$\Delta G^{\ddagger} = -RT\ln(\frac{kh}{\kappa T})$$

$$R = 1.9872\, cal \bullet mol^{-1} \bullet K^{-1}$$

$$T = temperature\ in\ Kelvin$$

$$k = rate\ constant$$

$$h = 6.62608 \times 10^{-34} J \bullet s$$

$$\kappa = 1.3806 \times 10^{-23}\ J \bullet K^{-1}$$

General procedure: In a vial in a glovebox, PdL_2 (0.040 mmol) was dissolved in the appropriate solvent (0.20 mL), and the resulting solution was transferred to a screw-cap NMR tube. The vial was then washed with additional solvent (2 x 0.10 mL), and the washings were added to the NMR tube. The NMR tube was closed with a Teflon-lined cap and removed from the glovebox. A solution of the alkyl electrophile (0.16 mmol) in the solvent (0.40 mL) was prepared in a glovebox. Outside of a glovebox, 0.10 mL of this solution was added through the septum of the cap of the NMR tube.

The reaction was monitored by ^{31}P NMR, and the percent conversion of PdL_2 was determined by integrating the resonances for PdL_2, PdL_2RX, and, in some cases, PdL_2HX. All experiments were performed twice. The data for a single run are provided below.

The ^{31}P NMR shifts (δ) for species of interest are listed below.

L	PdL_2	PdL_2RX	PdL_2HX
$P(t\text{-Bu})_2Me$	42.3	27.6	53.1
$P(t\text{-Bu})_2Et$	63.3	–[a]	63.9
PCy_3	39.7	22.0	42.0
$P(t\text{-Bu})_3$	85.9	–[a]	–[a]

[a] Not observed.

Note: PdL_2HX is sometimes formed as a secondary reaction product.

Activation Parameters (eq 2.4). All experiments were conducted according to the general procedure, with 17.1 mg of $Pd(P(t\text{-Bu})_2Me)_2$ and 8.3 mg of *n*-nonyl bromide. Prior to the addition of *n*-nonyl bromide, the NMR tubes were equilibrated to the appropriate temperature.

Rate constants were determined for reactions conducted from 263-303 K. Free energies of activation ($\Delta G^{\ddagger}$) were determined from the rate constants and plotted versus reaction temperature.

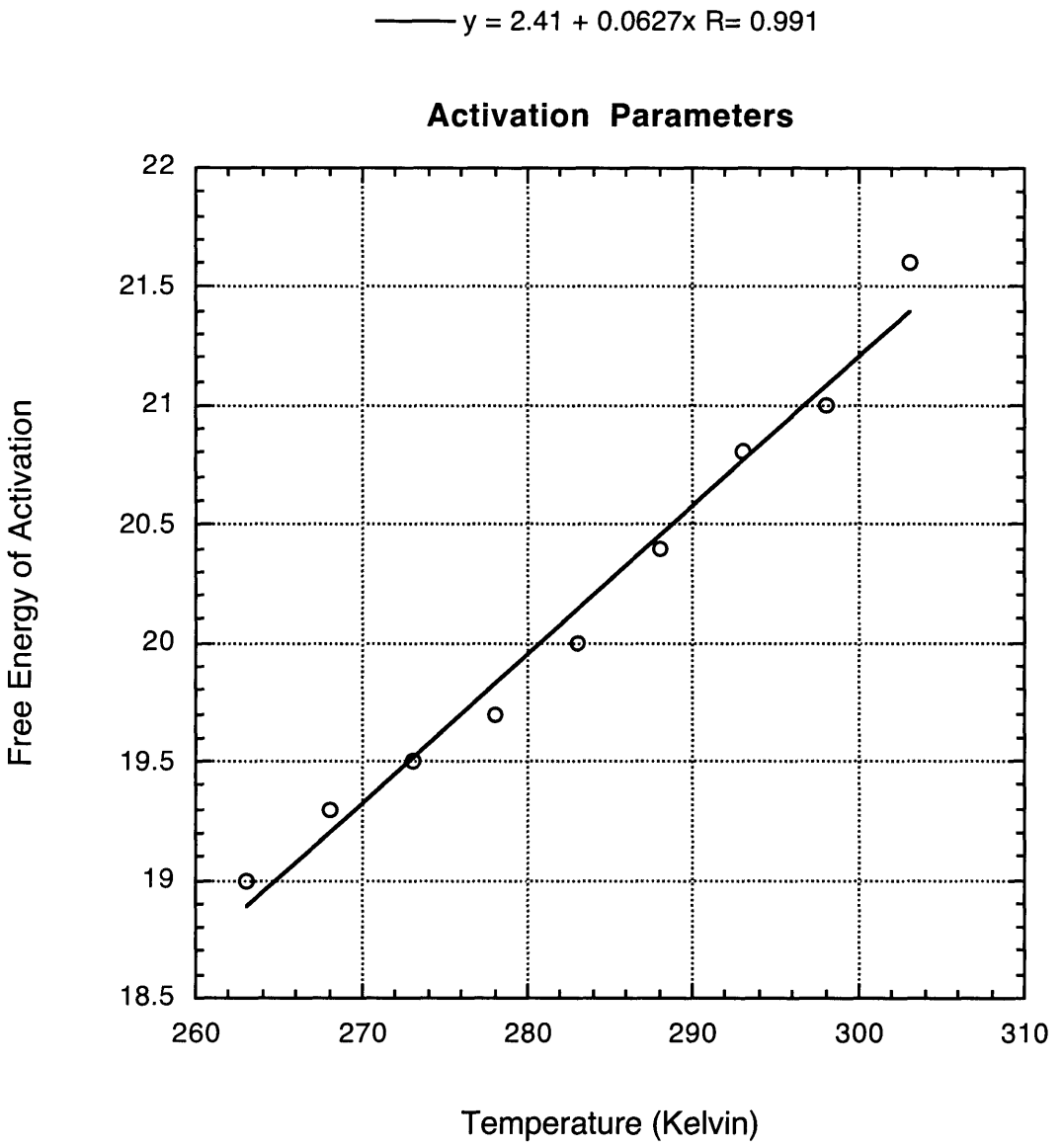

These data indicate: $\Delta H^{\ddagger} = 2.4$ kcal/mol and $\Delta S^{\ddagger} = -63$ eu.

Solvent Effect (Table 2.1). All experiments were conducted according to the general procedure, with 17.1 mg of $Pd(P(t\text{-}Bu)_2Me)_2$ and 8.3 mg of *n*-nonyl bromide. Prior to the addition of *n*-nonyl bromide, the NMR tubes were equilibrated to 0 °C. The reactions were monitored by ^{31}P NMR spectroscopy at 0 °C.

Hexane (Table 2.1, entry 1). An initial experiment showed no reaction (<2%) after 3 hours at 0 °C. This indicates: $k < 2.36 \times 10^{-5}\ M^{-1}s^{-1}$ and $\Delta G^{\ddagger} > 21.7$ kcal/mol.

An additional experiment was performed at 60 °C. The reaction proceeded to 13.9% conversion after 15 min ($k = 0.00224\ M^{-1}s^{-1}$ and $\Delta G^{\ddagger} = 23.6$ kcal/mol) and 27.5% conversion after 30 minutes ($k = 0.00263\ M^{-1}s^{-1}$ and $\Delta G^{\ddagger} = 23.5$ kcal/mol).

Toluene (Table 2.1, entry 2).

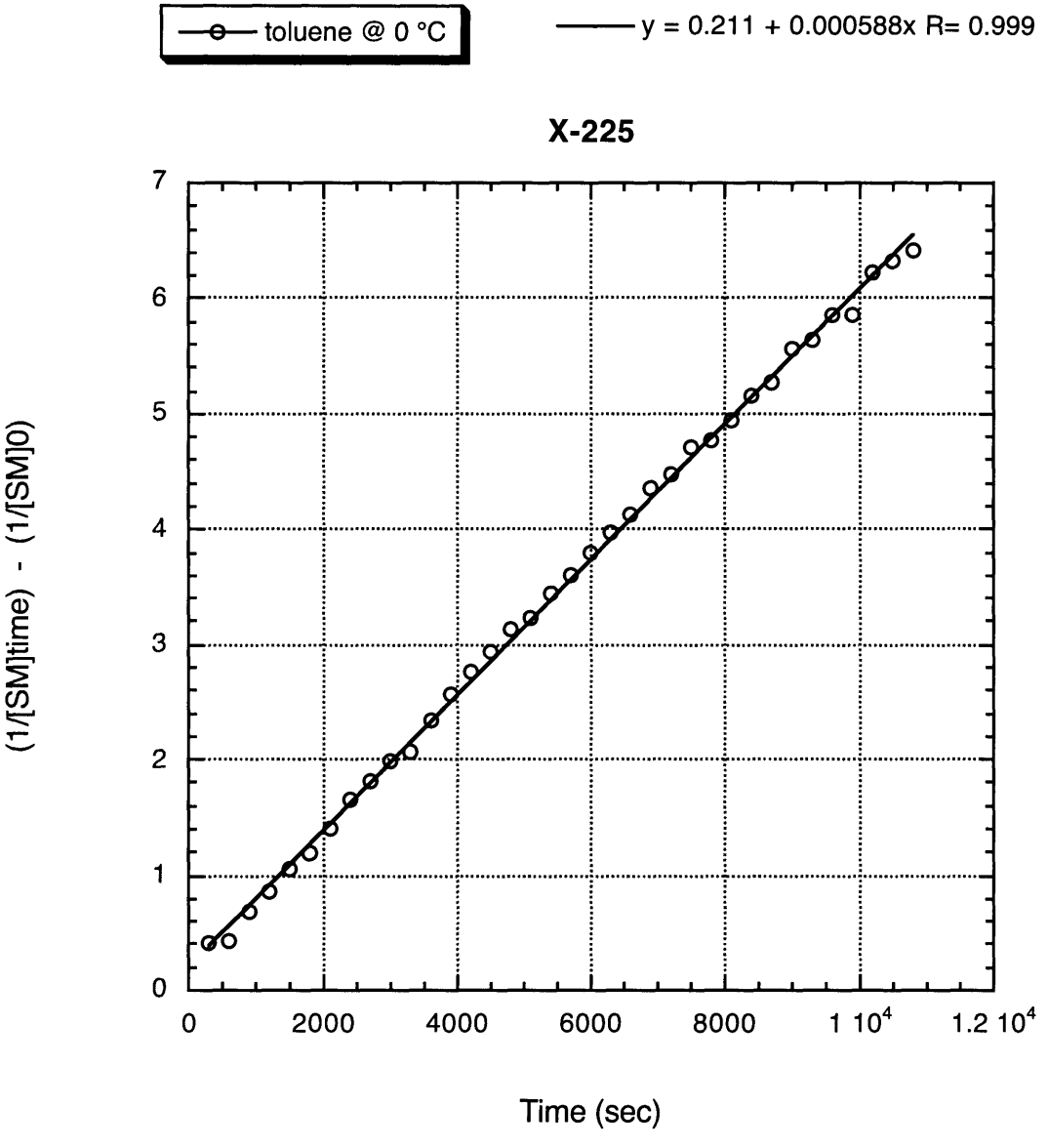

These data indicate: $k = 0.000588\ M^{-1}s^{-1}$ and $\Delta G^{\ddagger} = 20.0$ kcal/mol.

THF (Table 2.1, entry 3).

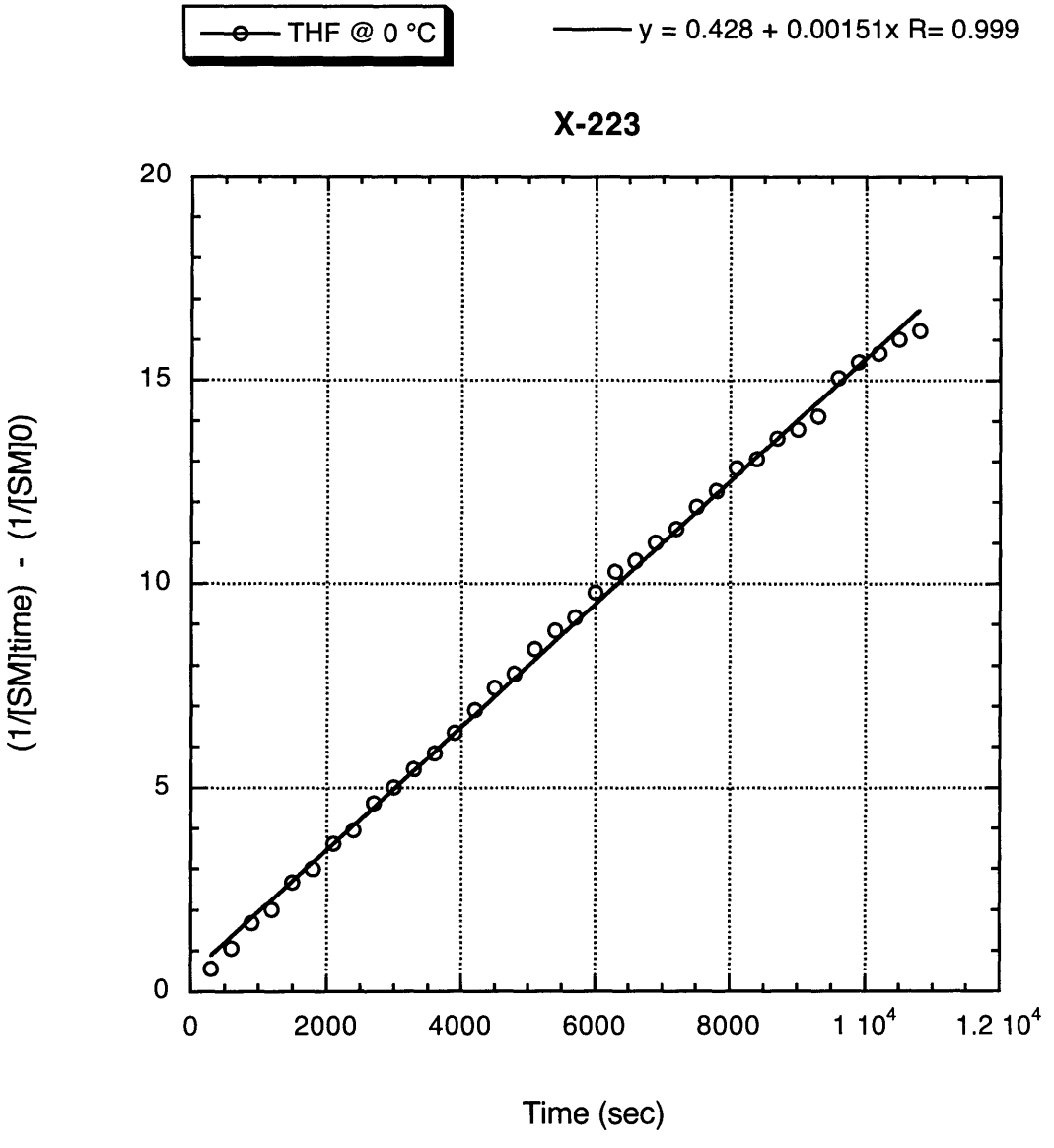

These data indicate: $k = 0.00151\ M^{-1}s^{-1}$ and $\Delta G^{\ddagger} = 19.5$ kcal/mol.

t-Amyl Alcohol (Table 2.1, entry 4).

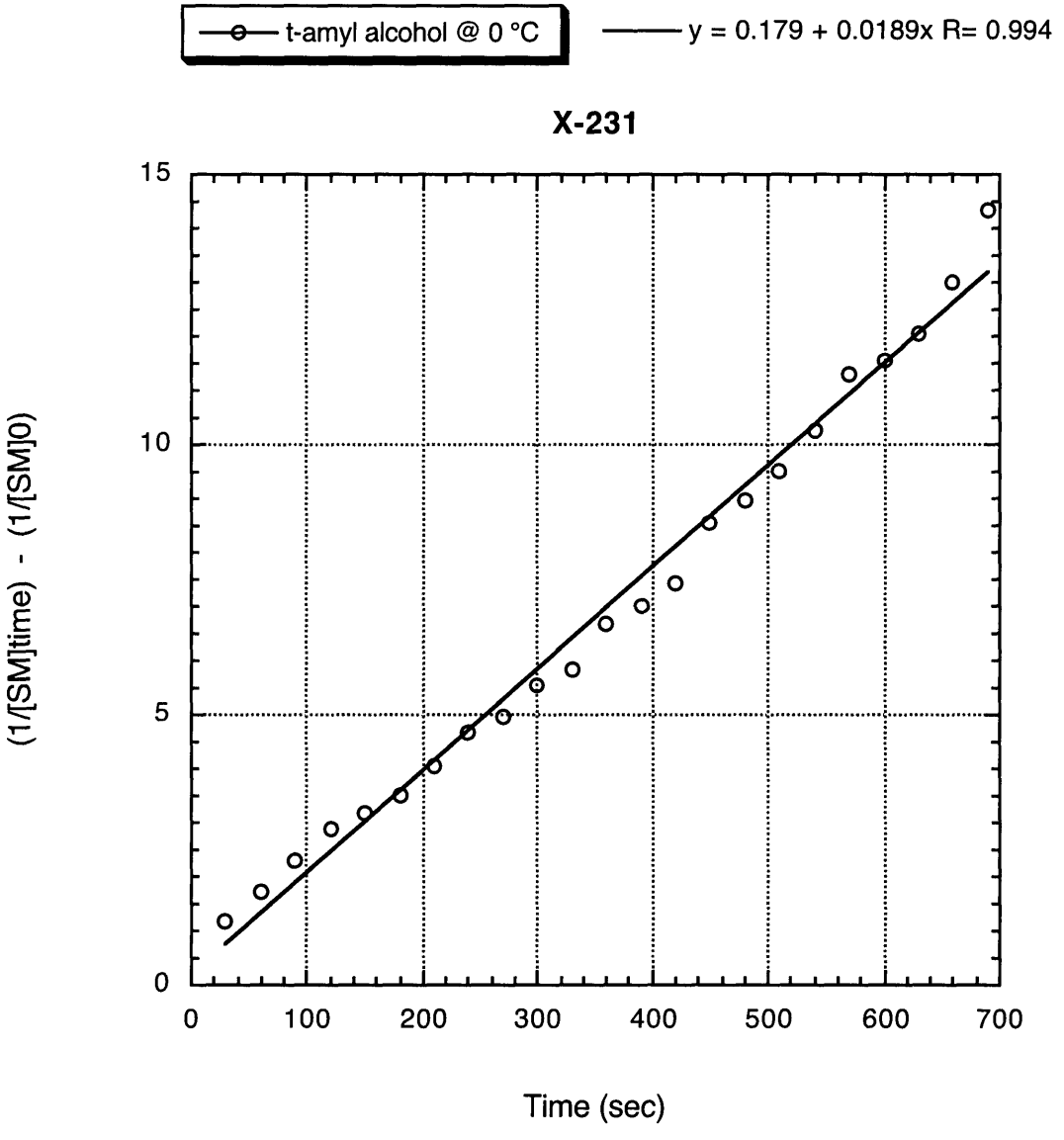

These data indicate: k = 0.0189 $M^{-1}s^{-1}$ and $\Delta G^{\ddagger}$ = 18.1 kcal/mol.

NMP (Table 2.1, entry 5).

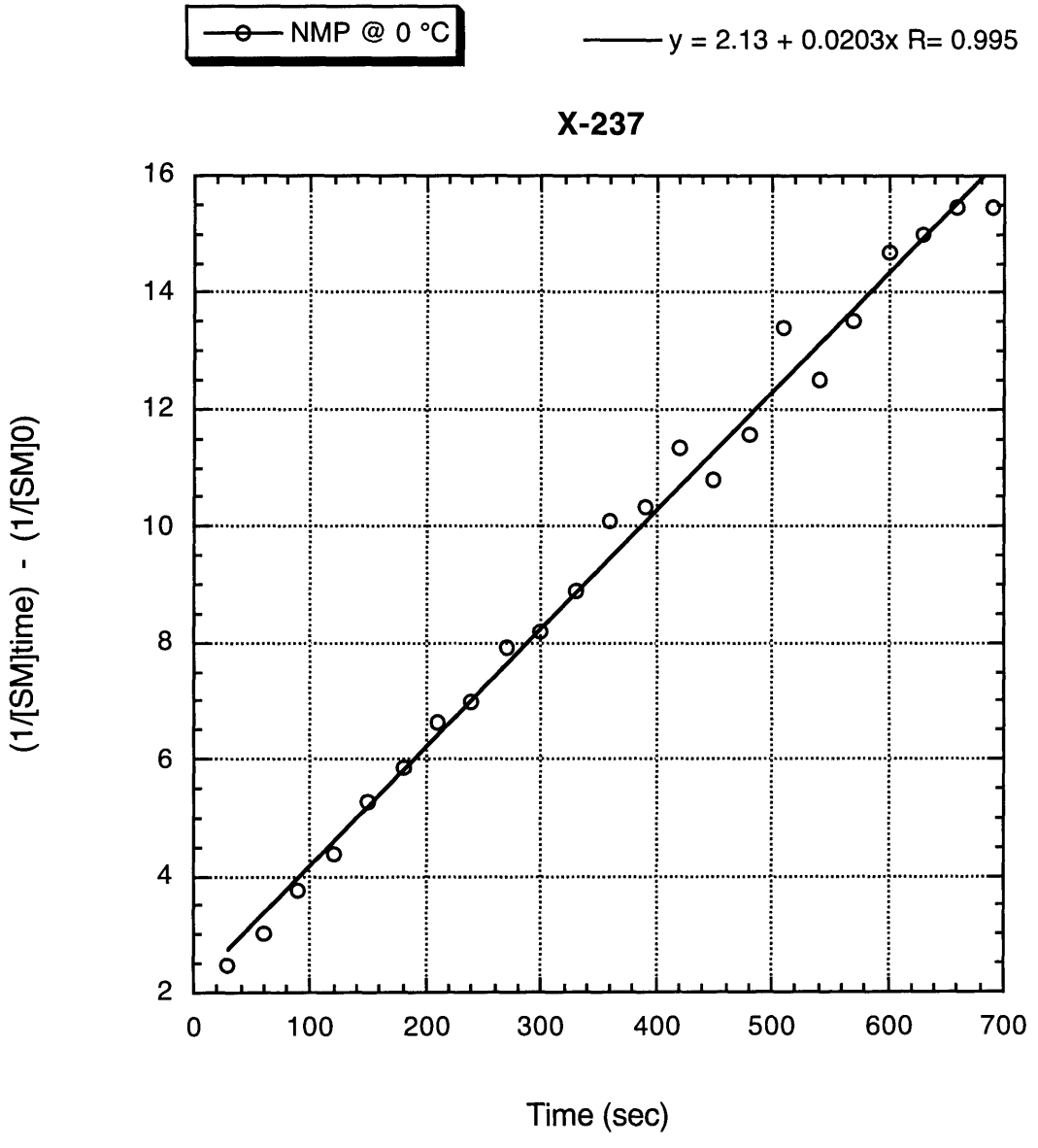

These data indicate: $k = 0.0203\ M^{-1}s^{-1}$ and $\Delta G^{\ddagger} = 18.0$ kcal/mol.

DMF (Table 2.1, entry 6).

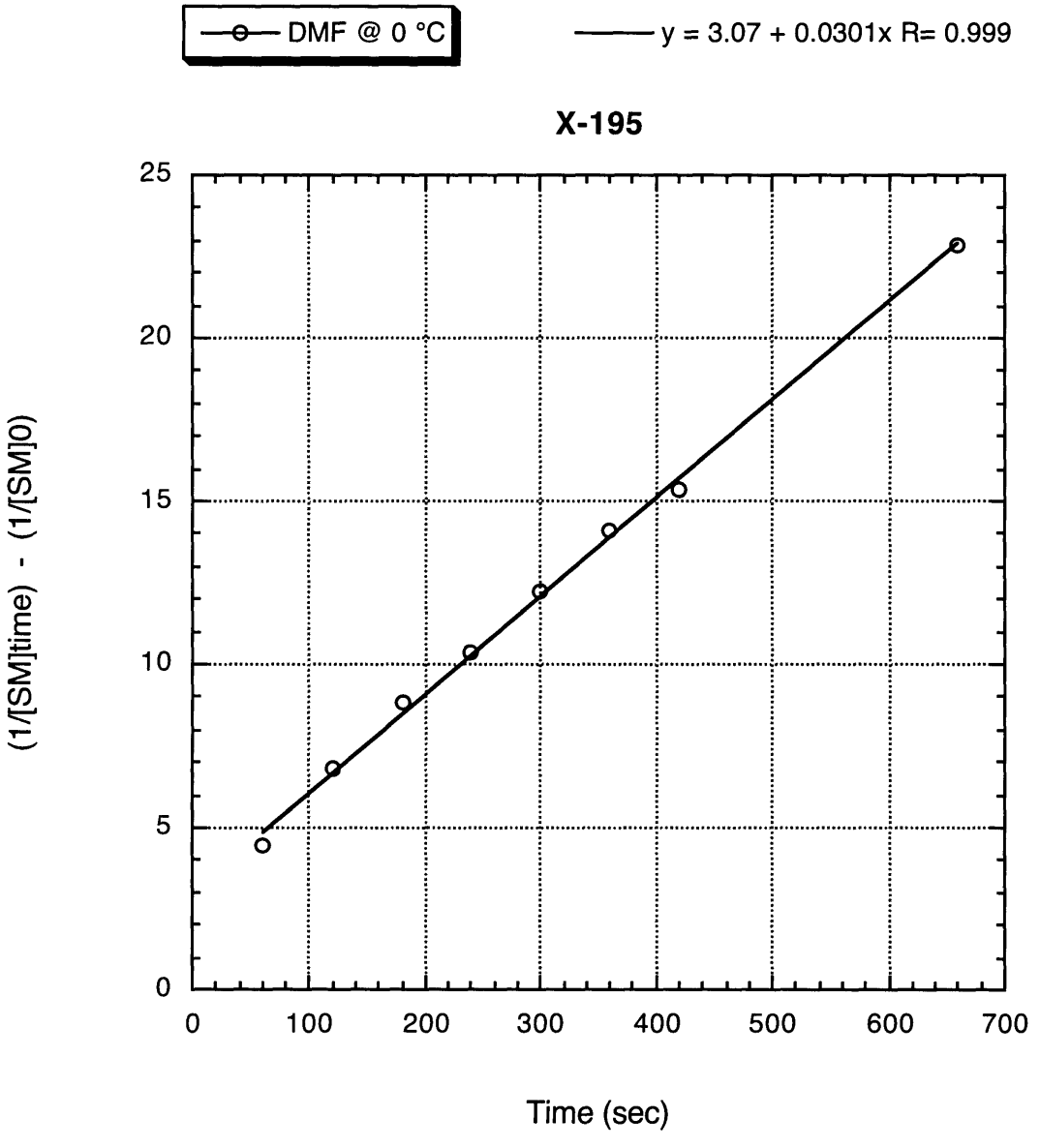

These data indicate: k = 0.0301 $M^{-1}s^{-1}$ and $\Delta G^{\ddagger}$ = 17.8 kcal/mol.

Leaving-Group Effect (Table 2.2). All experiments were conducted according to the general procedure, with 17.1 mg of $Pd(P(t\text{-}Bu)_2Me)_2$ and 0.040 mmol of *n*-nonyl–X. Prior to the addition of the electrophile, the NMR tubes were

equilibrated to the appropriate temperature. The reactions were monitored by ^{31}P NMR spectroscopy.

Iodide (Table 2.2, entry 1).

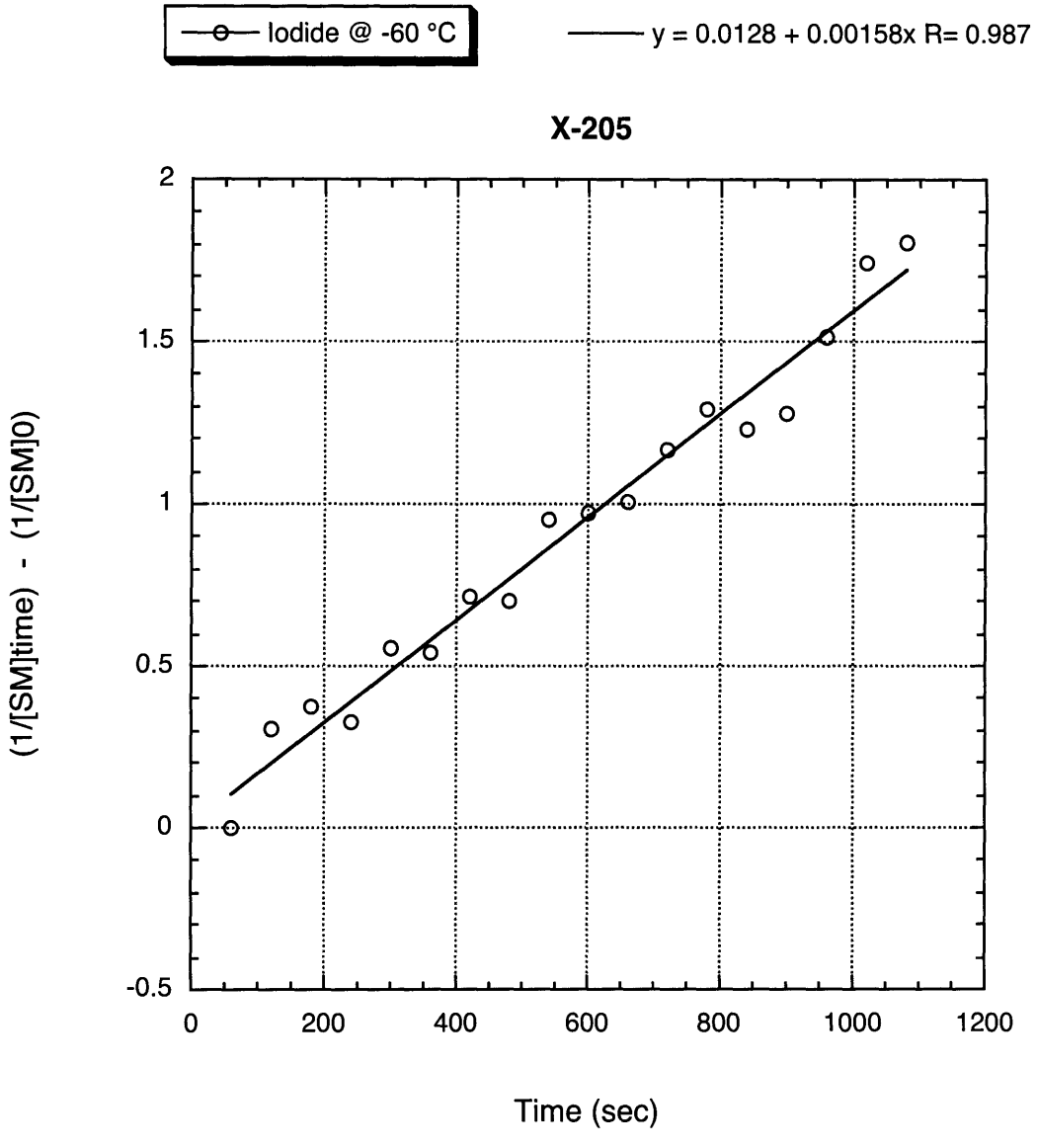

These data indicate: $k = 0.00158\ M^{-1}s^{-1}$ and $\Delta G^{\ddagger} = 15.1$ kcal/mol. This corresponds to a half-life of 2.20 hours at –60 °C.

Bromide (Table 2.2, entry 2).

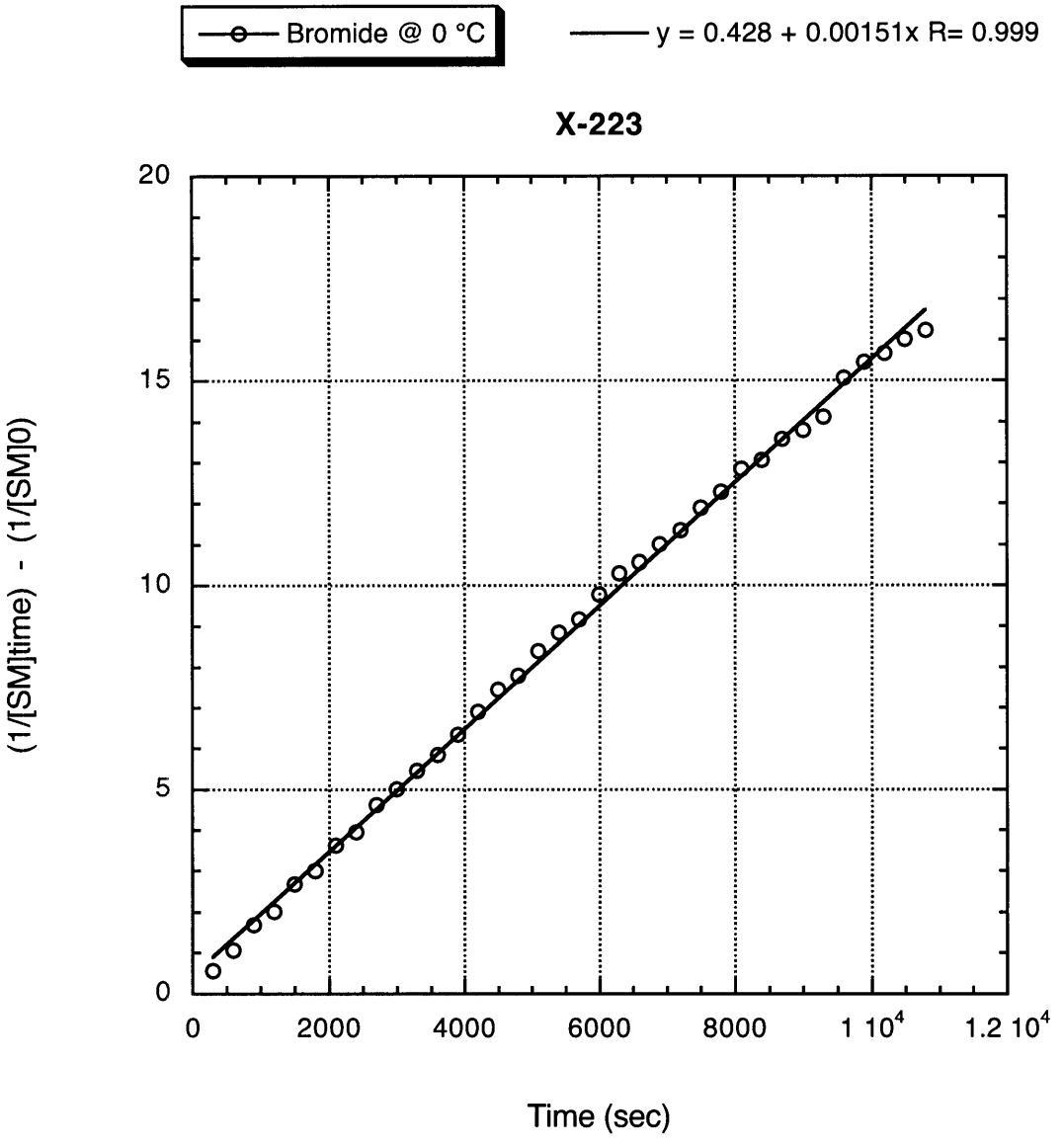

These data indicate: $k = 0.00151\ M^{-1}s^{-1}$ and $\Delta G^{\ddagger} = 19.5$ kcal/mol. This corresponds to a half-life of 2.30 hours at 0 °C.

Chloride (Table 2.2, entry 3).

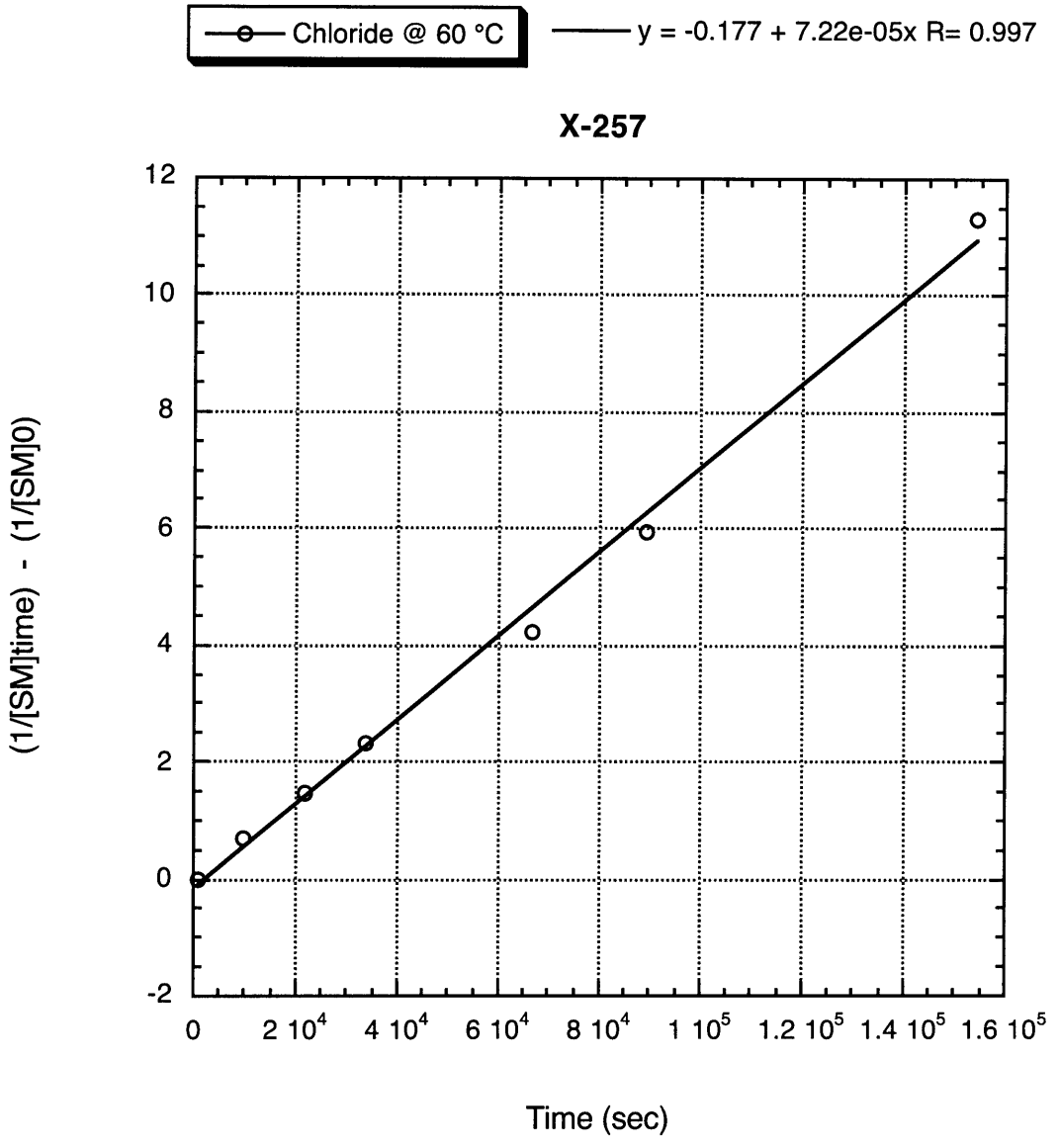

These data indicate: k = 0.0000722 $M^{-1}s^{-1}$ and $\Delta G^{\ddagger}$ = 25.9 kcal/mol. This corresponds to a half-life of 2.00 days at 60 °C.

Fluoride (Table 2.2, entry 4).

Addition of *n*-nonyl fluoride gave no (< 2%) PdL_2RF or PdL_2HF after 43 hours at 60 °C. This corresponds to k < 1.64 x 10^{-6} $M^{-1}s^{-1}$ and $\Delta G^{\ddagger}$ > 28.4 kcal/mol.

Tosylate (Table 2.2, entry 5).

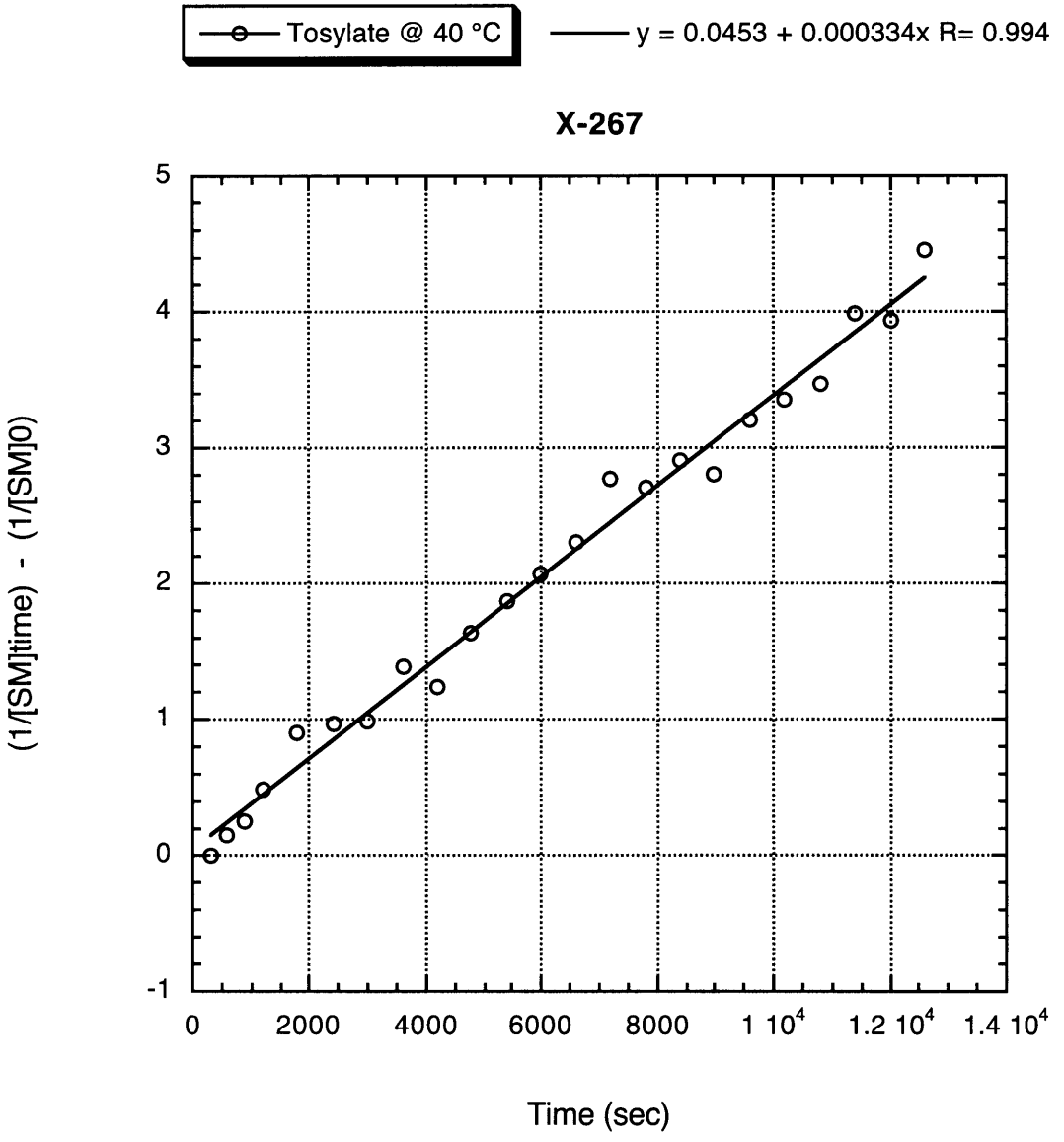

These data indicate: k = 0.000334 $M^{-1}s^{-1}$ and $\Delta G^{\ddagger}$ = 23.3 kcal/mol. This corresponds to a half-life of 10.4 hours at 40 °C.

Steric Effect of R (Table 2.3). All experiments were conducted according to the general procedure, with 17.1 mg of Pd(P(*t*-Bu)$_2$Me)$_2$ and 0.040 mmol of the alkyl

bromide. Prior to the addition of the electrophile, the NMR tubes were equilibrated to 0 °C. The reactions were monitored by ^{31}P NMR spectroscopy.

***n*-Nonyl bromide (Table 2.3, entry 1).**

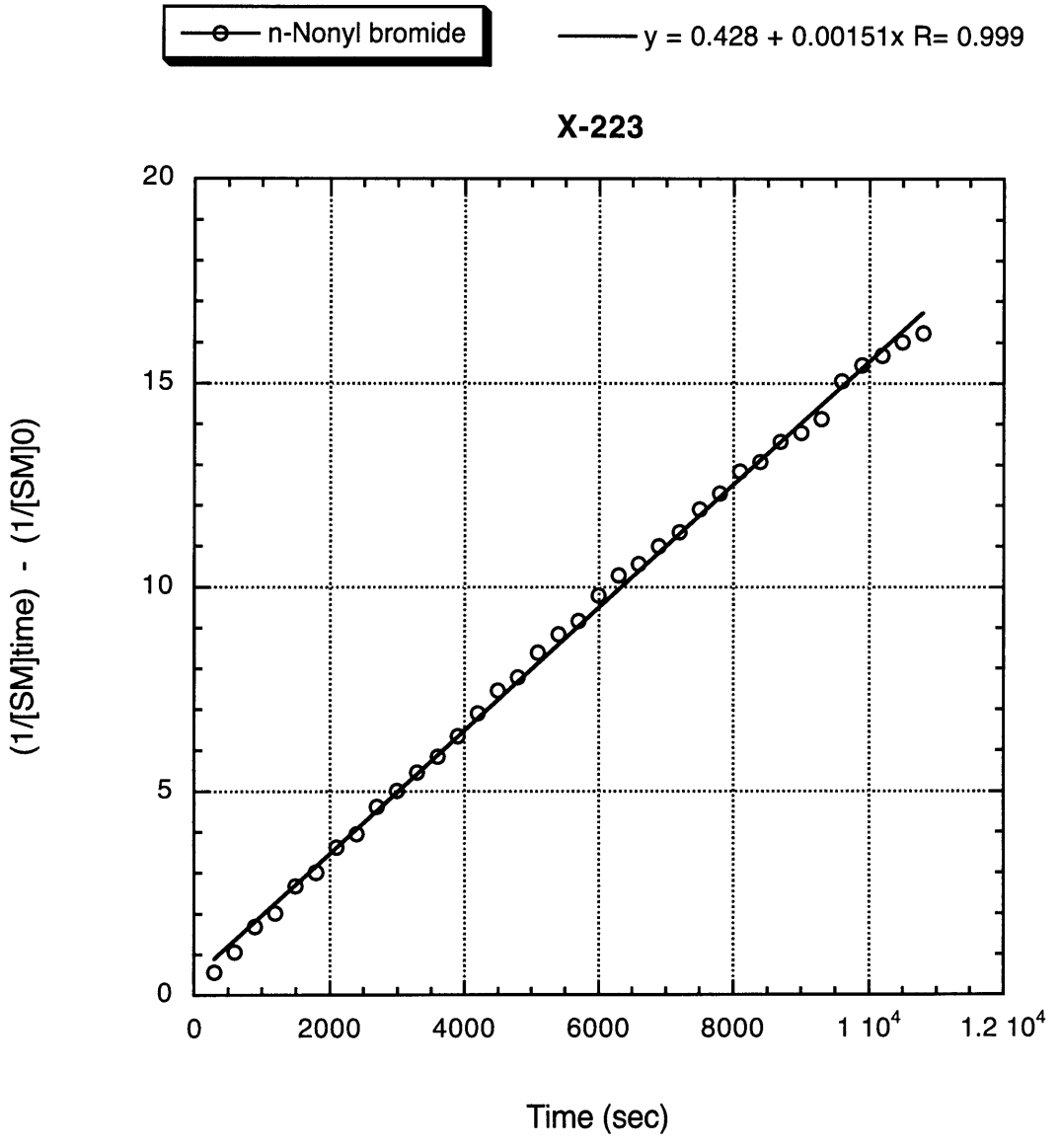

These data indicate: $k = 0.00151\ M^{-1}s^{-1}$, $\Delta G^{\ddagger} = 19.5$ kcal/mol, and $k_{rel} = 1.0$.

1-Bromo-3-methylbutane (Table 2.3, entry 2).

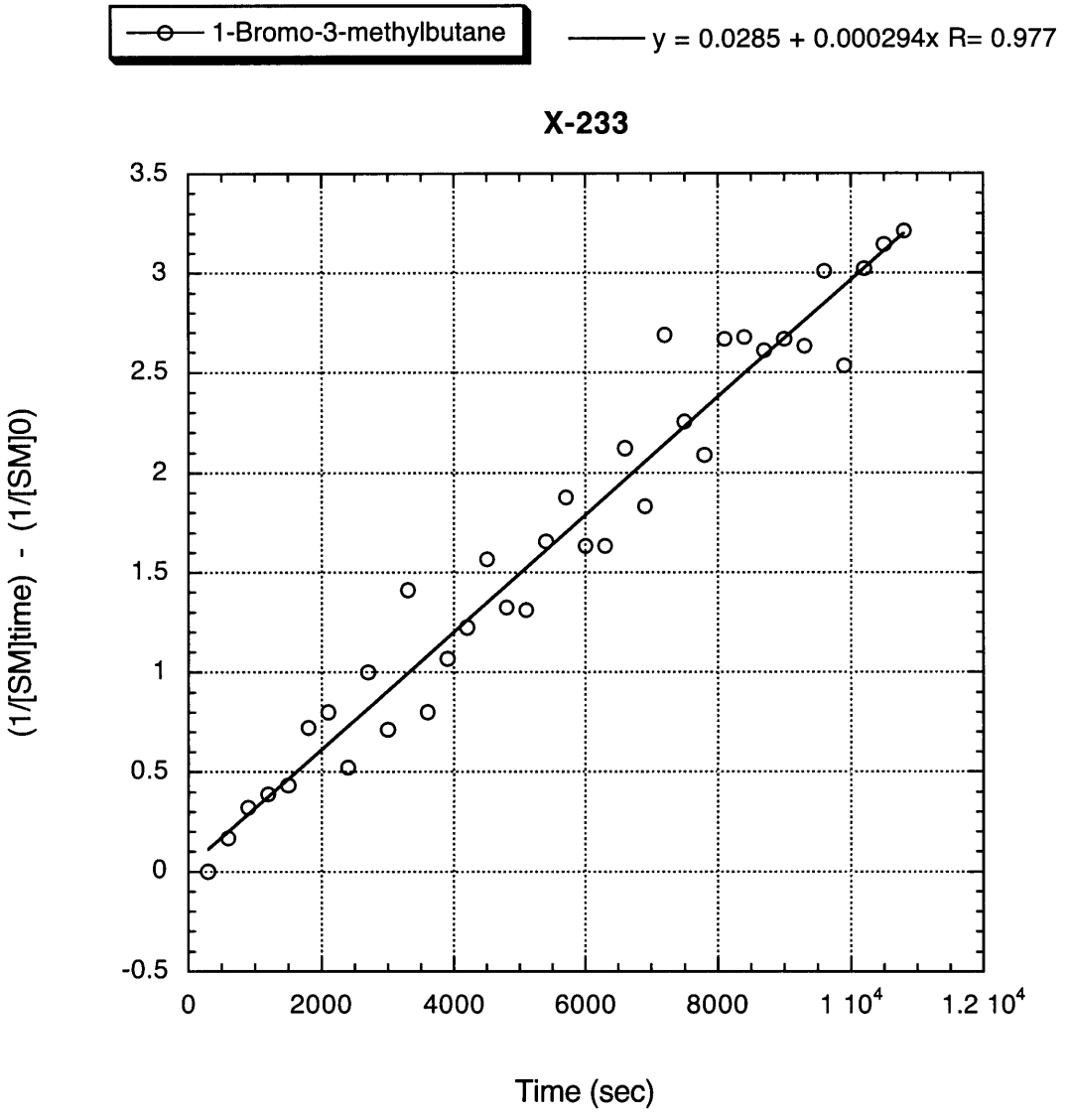

These data indicate: $k = 0.000294\ M^{-1}s^{-1}$, $\Delta G^{\ddagger} = 20.3$ kcal/mol, and $k_{rel} = 0.19$.

Isobutyl bromide (Table 2.3, entry 3).

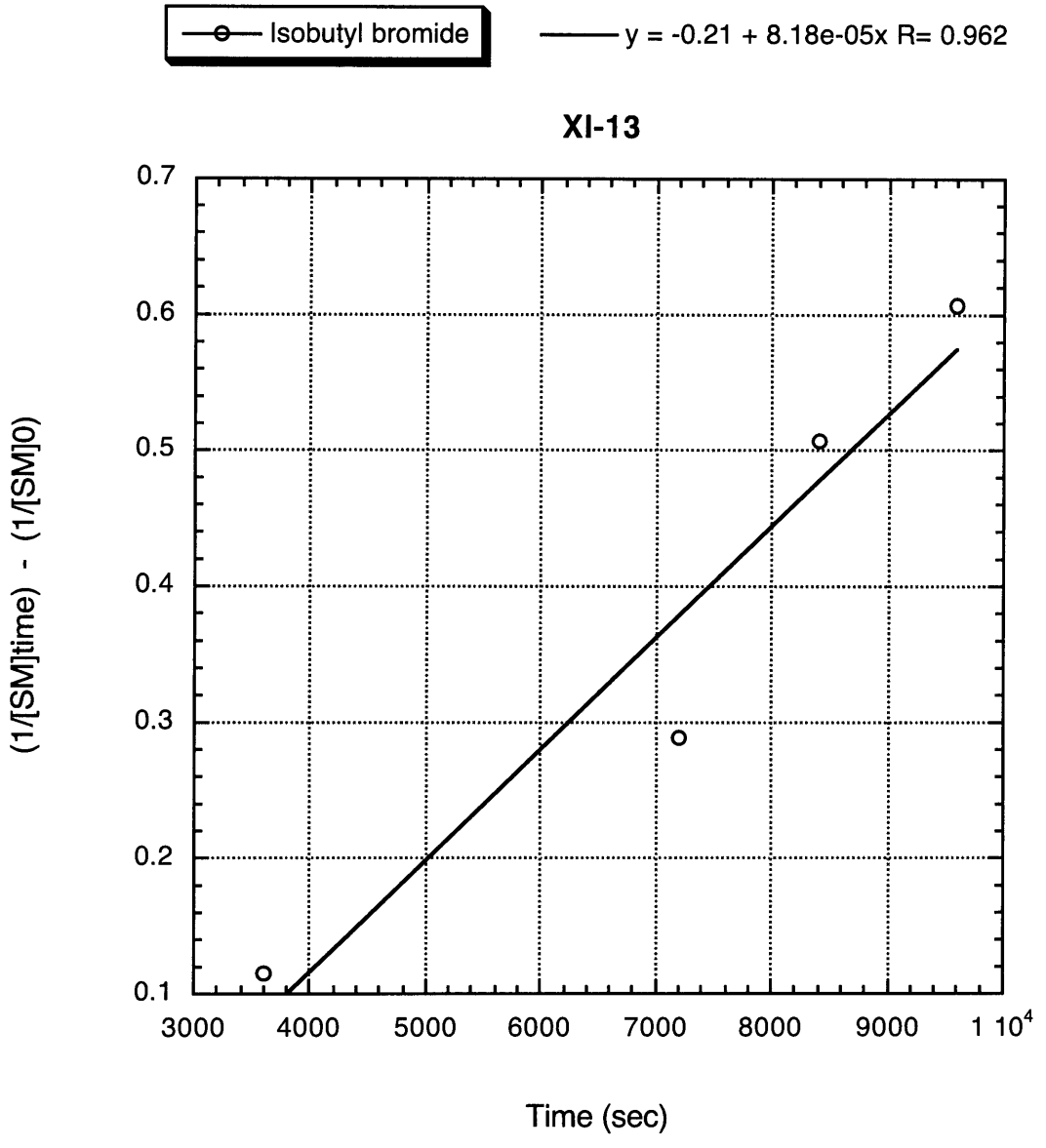

These data indicate: k = 0.0000818 $M^{-1}s^{-1}$, $\Delta G^{\ddagger}$ = 21.0 kcal/mol, and k_{rel} = 0.0542.

Isopropyl bromide (Table 2.3, entry 4). An initial experiment showed no reaction (<2%) after 3 hours at 0 °C. This indicates: k < 2.36 x 10-5 $M^{-1}s^{-1}$ and $\Delta G^{\ddagger}$ > 21.7 kcal/mol.

An additional experiment was performed at 60 °C. The reaction proceeded to 3.0% conversion after 15 min ($k = 0.000430\ M^{-1}s^{-1}$ and $\Delta G^{\ddagger} = 24.7$ kcal/mol) and 6.0% after 30 min ($k = 0.000443\ M^{-1}s^{-1}$ and $\Delta G^{\ddagger} = 24.7$ kcal/mol). Assuming a $\Delta G^{\ddagger}$ of 24.7 kcal/mol at 0 °C, these data correspond to $k = 9.0 \times 10^{-8}\ M^{-1}s^{-1}$ and $k_{rel} = 6.0 \times 10^{-6}$.

Ligand Effect (Table 2.4). All experiments were conducted according to the general procedure, with 0.040 mmol of PdL_2 and 8.3 mg of *n*-nonyl bromide. Prior to the addition of the electrophile, the NMR tubes were equilibrated to the appropriate temperature. The reactions were monitored by ^{31}P NMR spectroscopy.

P(*t*-Bu)$_2$Me (Table 2.4, entry 1).

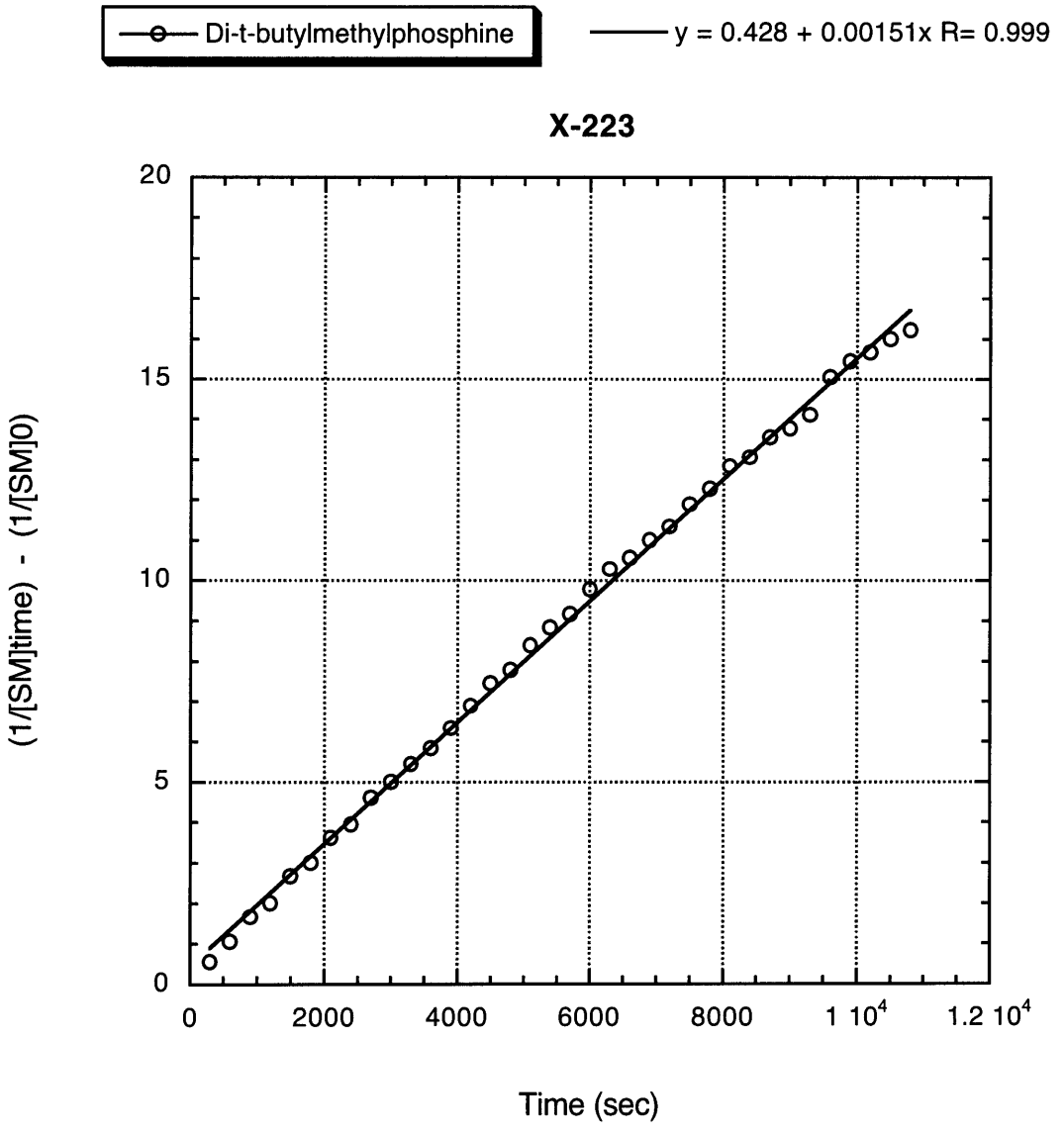

These data indicate: k = 0.00151 $M^{-1}s^{-1}$ and $\Delta G^{\ddagger}$ = 19.5 kcal/mol.

PCy_3 (Table 2.4, entry 2).

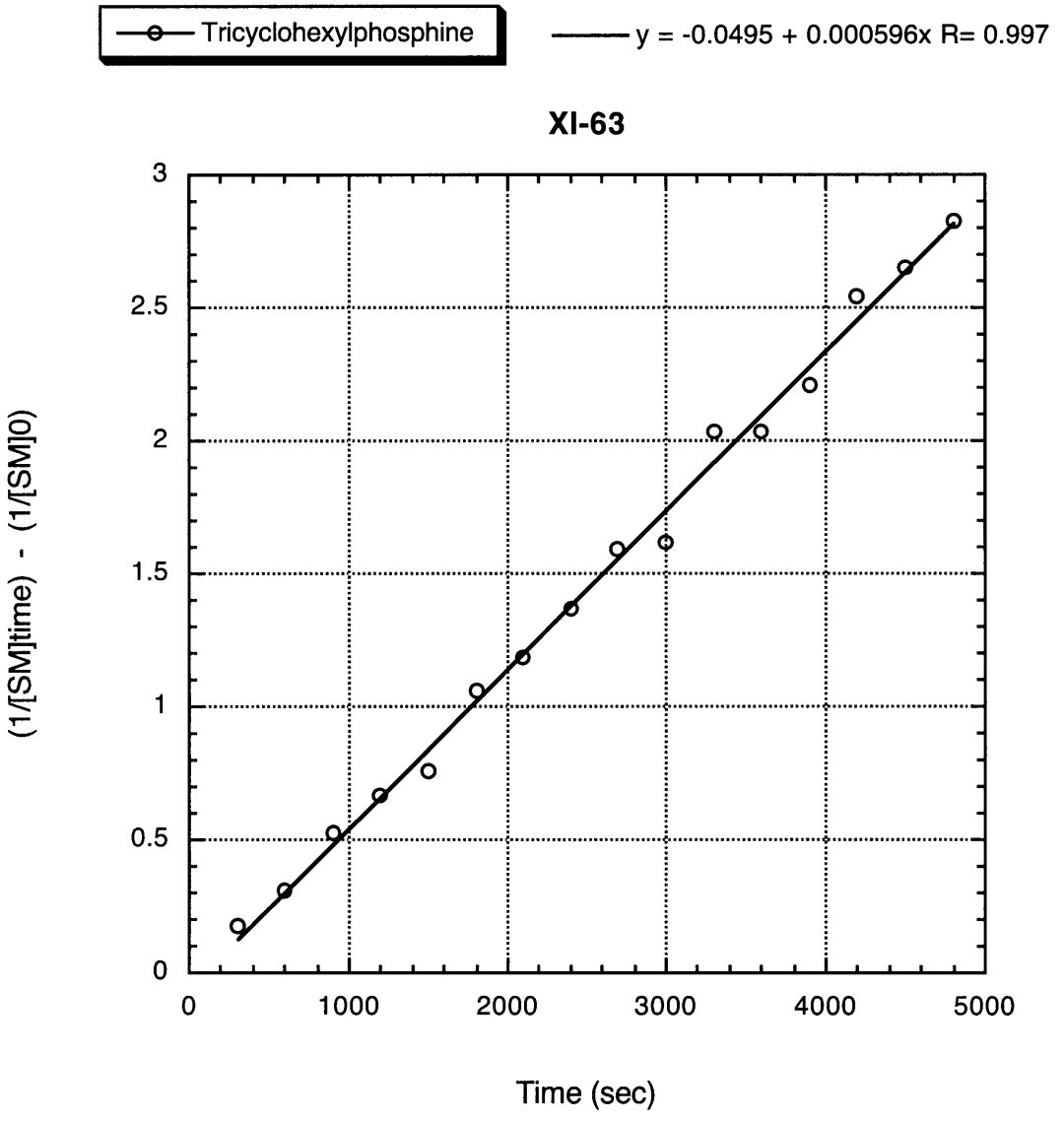

These data indicate: k = 0.000596 $M^{-1}s^{-1}$ and $\Delta G^{\ddagger}$ = 20.0 kcal/mol.

P(*t*-Bu)$_2$Et (Table 2.4, entry 3).

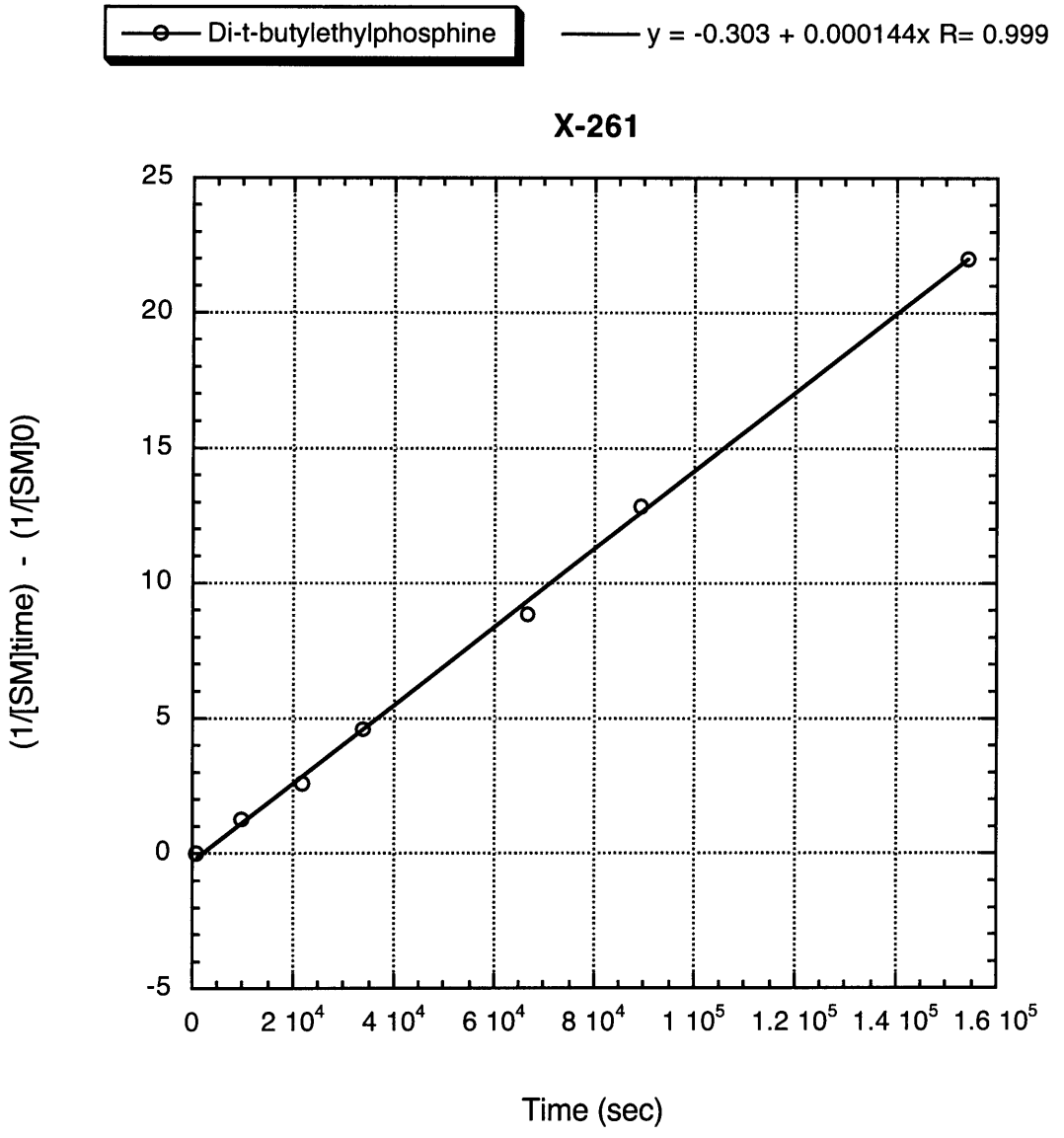

These data indicate: k = 0.000144 $M^{-1}s^{-1}$ and $\Delta G^{\ddagger}$ = 25.4 kcal/mol.

P(*t*-Bu)$_3$ (Table 2.4, entry 4). The reaction showed no product (<2%) after 43 hours at 60 °C. This gives an estimate of: k < 1.63 x 10^{-6} $M^{-1}s^{-1}$ and $\Delta G^{\ddagger}$ > 28.4 kcal/mol.

IV. Computations[71]

All calculations were performed using Gaussian 98 Rev. A.11.4.[72] Optimization of free-phosphine structures was performed using the B3LYP method and 6-31G* basis-set. Optimization of structures containing palladium was performed using the B3LYP method and LanL2DZ basis-set. Frequency calculations were performed on all solutions, and each stationary point was determined to be a local minimum (i.e., no imaginary frequencies were determined). All solutions were also checked for stability and were found to be stable under the perturbations considered.

The absolute electronic energies in hartrees are given below, along with corrected energies taking into account thermal energy (i.e., calculated zero-point vibrational energy and thermal energy at 298.15 K).

Picture	Description	Electronic Energy (hartrees)	Thermally Corrected Energy (hartrees)	Relative Energy[a]
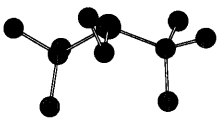	P(*t*-Bu)$_2$Et/eclipsed	–736.269658	–735.940378	0.0 kcal/mol[b]

[71] For an excellent introduction into computational methods, see: Foresman, J. B.; Frisch, Æ. *Exploring Chemistry with Electronic Structure Methods*; Gaussian, Inc.: Pittsburgh, 1996.

[72] Gaussian 98, Revision A.11.4, Frisch, M. J.; Trucks, G. W.; Schlegel, H. B.; Scuseria, G. E.; Robb, M. A.; Cheeseman, J. R.; Zakrzewski, V. G.; Montgomery, J. A., Jr.; Stratmann, R. E.; Burant, J. C.; Dapprich, S.; Millam, J. M.; Daniels, A. D.; Kudin, K. N.; Strain, M. C.; Farkas, O.; Tomasi, J.; Barone, V.; Cossi, M.; Cammi, R.; Mennucci, B.; Pomelli, C.; Adamo, C.; Clifford, S.; Ochterski, J.; Petersson, G. A.; Ayala, P. Y.; Cui, Q.; Morokuma, K.; Rega, N.; Salvador, P.; Dannenberg, J. J.; Malick, D. K.; Rabuck, A. D.; Raghavachari, K.; Foresman, J. B.; Cioslowski, J.; Ortiz, J. V.; Baboul, A. G.; Stefanov, B. B.; Liu, G.; Liashenko, A.; Piskorz, P.; Komaromi, I.; Gomperts, R.; Martin, R. L.; Fox, D. J.; Keith, T.; Al-Laham, M. A.; Peng, C. Y.; Nanayakkara, A.; Challacombe, M.; Gill, P. M. W.; Johnson, B.; Chen, W.; Wong, M. W.; Andres, J. L.; Gonzalez, C.; Head-Gordon, M.; Replogle, E. S.; Pople, J. A. Gaussian, Inc., Pittsburgh, PA, 2002.

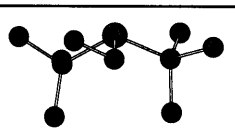	P(*t*-Bu)$_2$Et/gauche	–736.268374	–735.938657	+1.1 kcal/mol[b]
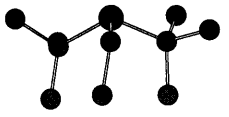	P(*t*-Bu)$_2$Et/anti	–736.264555	–735.935191	+3.3 kcal/mol[b]
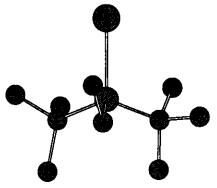	(P(*t*-Bu)$_2$Et)Pd/ eclipsed	–528.109929	–527.777394	0.0 kcal/mol[c]
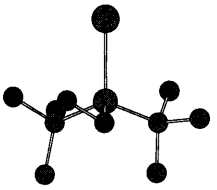	(P(*t*-Bu)$_2$Et)Pd/ gauche	–528.109059	–527.776475	+0.58 kcal/mol[c]
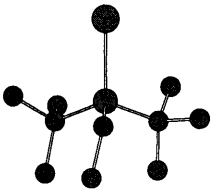	(P(*t*-Bu)$_2$Et)Pd/ anti	–528.104501	–527.771825	+3.5 kcal/mol[c]
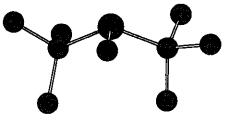	P(*t*-Bu)$_2$Me	–696.960417	–696.661463	
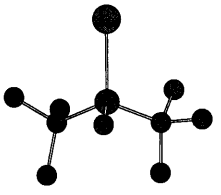	(P(*t*-Bu)$_2$Me)Pd	–488.806647	–488.504342	

[a] Relative energies are based on thermally corrected energies. [b] Relative energies are with respect to the various conformations of P(*t*-Bu)$_2$Et. [c] Relative energies are with respect to various conformations of (P(*t*-Bu)$_2$Et)Pd.

V. X-ray Crystallographic Data

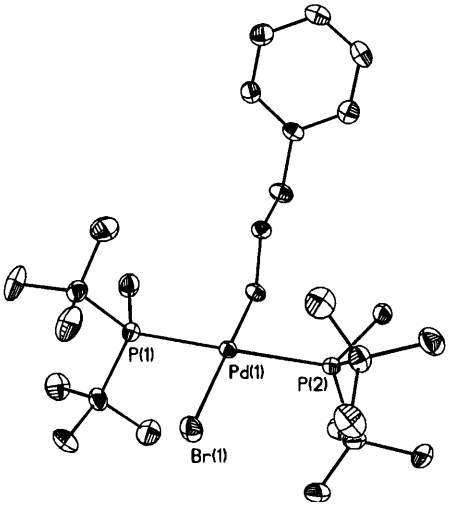

[02152MNS] (Figure 2.2). A light-yellow block of dimensions 0.39 x 0.33 x 0.16 mm^3 was mounted under STP and transferred to a Bruker AXS/CCD three-circle diffractometer (γ fixed at 54.78°) equipped with a cold stream of N2 gas. An initial unit cell was determined by harvesting reflections $I > 20\ \sigma(I)$ from 45 x 10-s frames of 0.30° ω scan data with monochromated Mo k_α radiation (λ = 0.71073 Å). The cell thus determined was orthorhombic.

A hemisphere of data was then collected using ω scans of 0.30° and 10-s frames. The raw data frames were integrated using the Bruker program SAINT+ for NT version 6.01. The data that were collected (22703 total reflections, 4332 unique, Rint = 0.0660) had the following Miller index ranges: –10 to 12 in h, –18 to 20 in k, and –32 to 32 in l. The data were corrected for Lorentz and polarization effects. An SADABS absorption correction was applied with μ = 2.06 mm^{-1}.

All aspects of the solution and refinement were handled by SHELXTL

Windows NT version 5.10. The structure was solved by direct methods in the orthorhombic space group *Pbca*, a = 11.1382(7) Å; b = 18.3329(11) Å; c = 29.5216(18) Å; $\alpha = 90°$; $\beta = 90°$; $\gamma = 90°$, and refined using standard difference Fourier techniques. Final, full-matrix least squares refinement (4332 data for 294 parameters) on F2 yielded residuals of R1 and wR2 of 0.0613 and 0.1410 for data I > 2σ(I), and 0.0631 and 0.1420, respectively, for all data. During the final refinement, all non-hydrogen atoms were treated anisotropically. Hydrogen atoms were included in calculated positions and refined isotropically on a riding model. No secondary extinction coefficient was used in the refinement. Residual electron density amounted to a maximum of 0.994 e/Å^3 and a minimum of –0.982 e/Å^3.

See Appendix A for tables containing full crystallographic data for the X-ray structure.

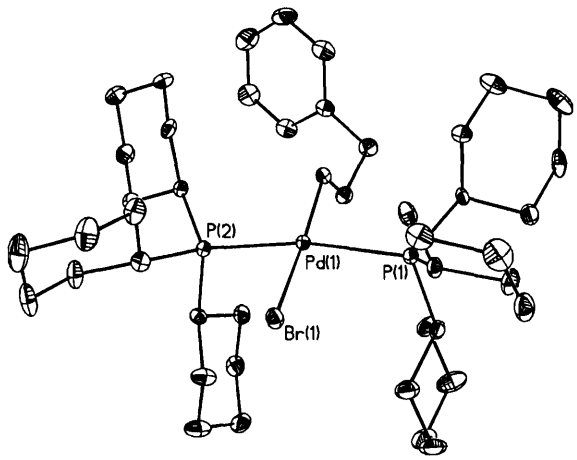

[02110MNS] (Figure 2.2). A gray plate of dimensions 0.27 x 0.18 x 0.10 mm^3 was mounted under STP and transferred to a Bruker AXS/CCD three-circle diffractometer (γ fixed at 54.78°) equipped with a cold stream of N2 gas. An initial unit cell was determined by harvesting reflections $I > 20\ \sigma(I)$ from 45 x 10-s frames of 0.30° ω scan data with monochromated Mo k_α radiation (λ = 0.71073 Å). The cell thus determined was monoclinic.

A hemisphere of data was then collected using ω scans of 0.30° and 10-s frames. The raw data frames were integrated using the Bruker program SAINT+ for NT version 6.01. The data that were collected (19303 total reflections, 7017 unique, Rint = 0.0328) had the following Miller index ranges: –15 to 10 in h, –18 to 18 in k, and –23 to 23 in l. The data were corrected for Lorentz and polarization effects.

All aspects of the solution and refinement were handled by SHELXTL Windows NT version 5.10. The structure was solved by direct methods in the monoclinic space group *P2(1)/n*, a = 13.7755(9) Å; b = 17.0727(11) Å; c = 21.0506(14) Å; α = 90°; β = 98.5560(10)°; γ = 90°, and refined using standard

difference Fourier techniques. Final, full-matrix least squares refinement (7017 data for 489 parameters) on F2 yielded residuals of R1 and wR2 of 0.0686 and 0.1139 for data $I > 2\sigma(I)$, and 0.0722 and 0.1149, respectively, for all data. During the final refinement, all non-hydrogen atoms were treated anisotropically. Hydrogen atoms were included in calculated positions and refined isotropically on a riding model. No secondary extinction coefficient was used in the refinement. Residual electron density amounted to a maximum of 0.626 $e/Å^3$ and a minimum of –1.096 $e/Å^3$.

See Appendix A for tables containing full crystallographic data for the X-ray structure.

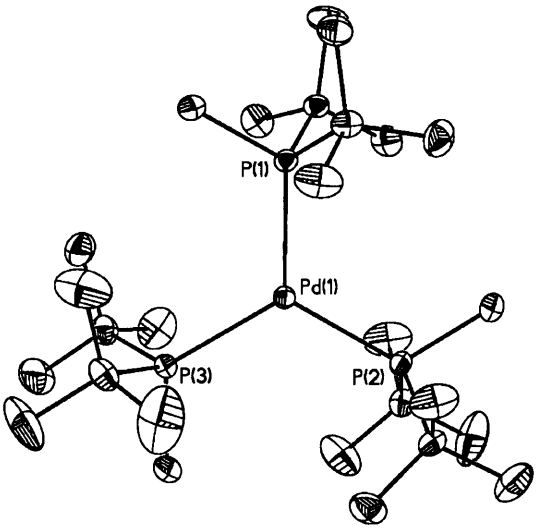

[03068IHS] (Footnote 62). A brown needle of dimensions 0.43 x 0.19 x 0.19 mm^3 was mounted under STP and transferred to a Bruker AXS/CCD three-circle diffractometer (γ fixed at 54.78°) equipped with a cold stream of N2 gas. An initial unit cell was determined by harvesting reflections $I > 20\ \sigma(I)$ from 45 x 10-s frames of 0.30° ω scan data with monochromated Mo k_α radiation (λ = 0.71073 Å). The cell thus determined was monoclinic.

A hemisphere of data was then collected using ω scans of 0.30° and 10-s frames. The raw data frames were integrated using the Bruker program SAINT+ for NT version 6.01. The data that were collected (12788 total reflections, 4678 unique, Rint = 0.0276) had the following Miller index ranges: –9 to 9 in h, –29 to 34 in k, and –13 to 10 in l. The data were corrected for Lorentz and polarization effects.

All aspects of the solution and refinement were handled by SHELXTL Windows NT version 5.10. The structure was solved by direct methods in the monoclinic space group *P2(1)/n*, a = 8.9087(11) Å; b = 31.047(4) Å; c = 11.8390(14) Å; α = 90°; β = 94.481(2)°; γ = 90°, and refined using standard difference Fourier techniques. Final, full-matrix least squares refinement (4678 data for 301

parameters) on F2 yielded residuals of R1 and wR2 of 0.0428 and 0.0900 for data I $> 2\sigma(I)$, and 0.0490 and 0.0921, respectively, for all data. During the final refinement, all non-hydrogen atoms were treated anisotropically. Hydrogen atoms were included in calculated positions and refined isotropically on a riding model. No secondary extinction coefficient was used in the refinement. Residual electron density amounted to a maximum of 0.762 e/Å^3 and a minimum of –0.969 e/Å^3.

See Appendix A for tables containing full crystallographic data for the X-ray structure.

Chapter 3

Reductive Elimination of H-X from Palladium Hydrides

A. Introduction

In recent years, much progress has been made in the palladium-catalyzed *cross-coupling* of aryl chlorides.[73] It has been shown that sterically demanding trialkylphosphines, including $P(t\text{-Bu})_3$ and PCy_3, are generally good ligands[74,75] for performing these transformations under relatively mild conditions. Despite these successes, only modest advances in the palladium-catalyzed *Heck coupling* of aryl chlorides have been achieved.[76,77] This disparity must be connected to the reaction mechanism, which in the case of the Heck coupling is presumably a series of oxidative addition, olefin insertion, β-hydride elimination, and finally a reductive elimination to regenerate the active catalyst (Figure 3.1).

---

[73] For reviews, see: (a) *Cross-Coupling Reactions: A Practical Guide*; Miyaura, N., Ed.; Topics in Current Chemistry Series 219; Springer-Verlag: New York, 2002. (b) *Handbook of Organopalladium Chemistry for Organic Synthesis*; Negishi, E.-i., Ed.; Wiley Interscience: New York, 2002. (c) Littke, A. F.; Fu, G. C. *Angew. Chem. Int. Ed.* **2002**, *41*, 4176-4211.

[74] Some sterically demanding dialkylmonoarylphosphines perform exceptionally well in the cross-coupling of aryl electrophiles. For examples, see: (a) Walker, S. D.; Barder, T. E.; Martinelli, J. R.; Buchwald, S. L. *Angew. Chem. Int. Ed.* **2004**, *43*, 1871-1876. (b) Gelman, D.; Buchwald, S. L. *Angew. Chem. Int. Ed.* **2003**, *42*, 5993-5996. (c) Wolfe, J. P.; Singer, R. A.; Yang, B. H.; Buchwald, S. L. *J. Am. Chem. Soc.* **1999**, *121*, 9550-9561. (d) Old, D. W.; Wolfe, J. P.; Buchwald, S. L. *J. Am. Chem. Soc.* **1998**, *120*, 9722-9723.

[75] Some carbene ligands can also promote the cross-coupling of aryl chlorides under mild conditions. For examples, see: (a) Navarro, O.; Kelly, R. A., III; Nolan, S. P. *J. Am. Chem. Soc.* **2003**, *125*, 16194-16195. (b) Gstöttmayr, C. W. K.; Bohm, V. P. W.; Herdtweck, E.; Grosche, M.; Herrmann, W. A. *Angew. Chem. Int. Ed.* **2002**, *41*, 1363-1365

[76] For an overview of the Heck reaction, see: Beletskaya, I. P.; Cheprakov, A. V. *Chem. Rev.* **2000**, *100*, 3009-3066.

[77] For specific examples of the Heck coupling of aryl chlorides, see: (a) Schnyder, A.; Indolese, A. F.; Studer, M.; Blaser, H.-U. *Angew. Chem. Int. Ed.* **2002**, *41*, 3668-3671. (b) Selvakumar, K.; Zapf, A.; Beller, M. *Org. Lett.* **2002**, *4*, 3031-3033. (c) Mukhopadhyay, S.; Rothenberg, G.; Joshi, A. Baidossi, M. Sasson, Y. *Adv. Syn. Cat.* **2002**, *344*, 348-354. (d) Littke, A. F.; Fu, G. C. *J. Am. Chem. Soc.* **2001**, *123*, 6989-7000.

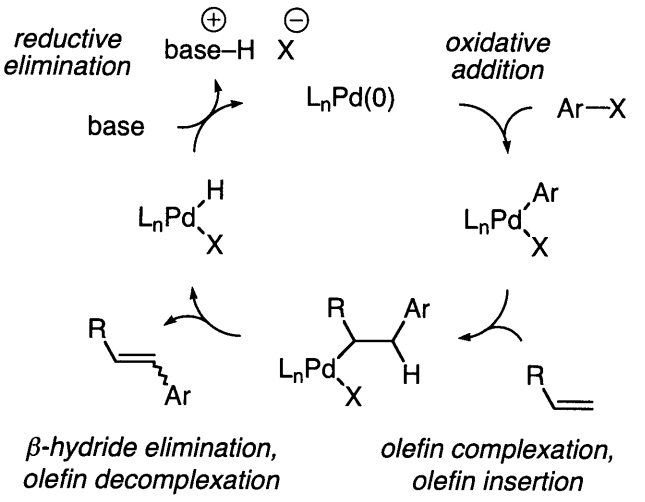

Figure 3.1. Generalized catalytic cycle for Heck arylations.

One might attribute the slow development of Heck couplings of aryl chlorides to the relatively low reactivity of aryl chlorides toward oxidative addition.[78] However, if this were the only barrier to efficient Heck couplings, then palladium/ligand combinations that have proved effective for cross-couplings of aryl chlorides should also be effective for Heck reactions of these compounds. Our group has discovered that some conditions that work well for cross-coupling reactions can not be extended to the Heck reaction. Both a Pd/PCy_3 and a $Pd/P(t\text{-}Bu)_3$ system succeed in the Suzuki-coupling of aryl chlorides (eq 3.1);[79] however, in the Heck coupling of aryl chlorides Pd/PCy_3 fails to furnish any product (eq 3.2).[80,81] This observation intrigued us, but we did not immediately perform mechanistic investigations to understand the basis for this divergence in reactivity.

---

[78] For discussions, see: (a) Grushin, V. V.; Alper, H. In *Activation of Unreactive Bonds and Organic Synthesis*; Murai, S., Ed.; Springer-Verlag: Berlin, 1999; pp. 193-226. (b) Grushin, V. V.; Alper, H. *Chem. Rev.* **1994**, *94*, 1047-1062.

[79] Littke, A. F.; Fu, G. C. *Angew. Chem. Int. Ed.* **1998**, *37*, 3387-3388.

[80] Littke, A. F.; Fu, G. C. *J. Org. Chem.* **1999**, *64*, 10-11.

[81] This difference in reactivity has been confirmed by others; for example, see: Galardon, E.; Ramdeehul, S.; Brown, J. M.; Cowley, A.; Hii, K. K.; Jutand, A. *Angew. Chem. Int. Ed.* **2002**, *41*, 1760-1763.

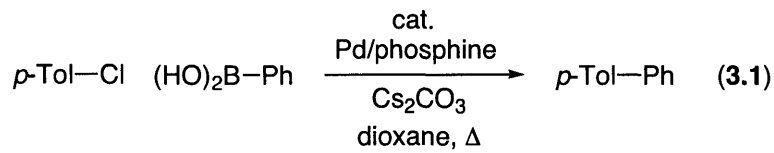

phosphine	yield
PCy_3	75%
$P(t\text{-Bu})_3$	86%

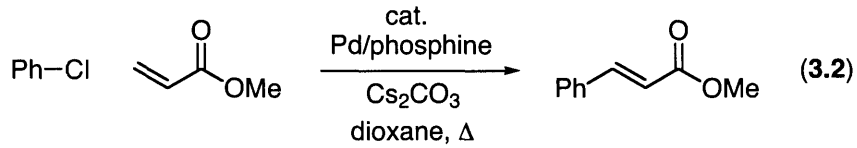

phosphine	yield
PCy_3	<2%
$P(t\text{-Bu})_3$	56%

We continued to optimize the Heck coupling of aryl chlorides and developed a second-generation system (eq 3.3),[82] which was closely related to our initial system except for the choice of base. We found that by using Cy_2NMe instead of Cs_2CO_3 the Heck coupling with $Pd/P(t\text{-Bu})_3$ was more effective for a greater diversity of aryl chlorides and could even be performed at room temperature for some cases. We reasoned that the change of base most directly affects the last step of the catalytic cycle (Figure 3.1), and perhaps Cy_2NMe more efficiently regenerates the active catalyst through reductive elimination. We were intrigued by this possibility, since seldom had anyone suggested that regeneration of the active catalyst through reductive elimination was the

[82] Littke, A. F.; Fu, G. C. *J. Am. Chem. Soc.* **2001**, *123*, 6989-7000.

'difficult step' in the Heck coupling cycle for aryl chlorides.[83] Thus, we initiated a mechanistic investigation into the factors that affect the reductive elimination of H–X from palladium hydrides.[84]

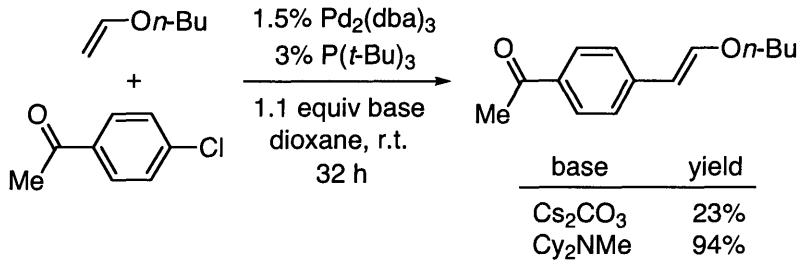

(3.3)

[83] Jeffery has postulated that the success of the "Jeffery conditions" for Heck reactions of aryl and vinyl iodides ($Pd(OAc)_2$, HCO_3^-, R_4NX) may be attributable in part to efficient regeneration of Pd(0): Jeffery, T. In *Advances in Metal-Organic Chemistry*; Liebeskind, L. S., Ed.; JAI: London, 1996; Vol. 5, pp. 153-260.

[84] For reviews of palladium-hydride chemistry, see: (a) Hii, K. K. In *Handbook of Organopalladium Chemistry for Organic Synthesis*; Negishi, E.-i., Ed.; Wiley Interscience: New York, 2002, ; Chapter II.2.5. (b) Grushin, V. V. *Chem. Rev.* **1996**, *96*, 2011-2033.

B. Results and Discussion

We first decided to follow the Heck reactions by ^{31}P NMR and discovered that the resting state for the two catalytic systems is different (eq 3.4). With Cs_2CO_3 only L_2PdHCl is observed, whereas for Cy_2NMe the resting state is PdL_2. To the best of our knowledge, the arylation mediated by Cs_2CO_3 represents the first time that a palladium hydride has been identified during the course of a catalyzed Heck reaction.[85]

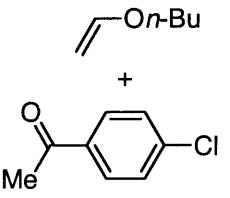

1.5% $Pd_2(dba)_3$
3% P(*t*-Bu)$_3$
1.1 equiv base
dioxane, r.t.
4 h

^{31}P NMR (**3.4**)

base	L_2PdHCl : PdL_2
Cs_2CO_3 (~8% conversion)	>98 : <2
Cy_2NMe (~30% conversion)	<2 : >98

L = P(*t*-Bu)$_3$

These NMR data show that Cs_2CO_3 is not especially effective at regenerating Pd(0) from L_2PdHCl, correlating with the lower coupling activity of Pd/P(*t*-Bu)$_3$ in the presence of this particular base. It is possible that the inefficiency of reductive elimination in the presence of Cs_2CO_3 is attributable to the heterogeneity of the reaction. In order to further probe the reductive elimination of palladium hydrides, we synthesized an array of bisphosphine

[85] In a recent review of "Hydridopalladium Complexes" [Hii, K. K. In *Handbook of Organopalladium Chemistry for Organic Synthesis*; Negishi, E.-i., Ed.; Wiley Interscience: New York, 2002; Chapter II.2.5], Hii has noted that hydridopalladium complexes "have never been detected under true catalytic conditions...The involvement of these species in the β-hydrogen elimination step is...only implied based on mechanistic considerations."

palladium-hydride complexes and explored their behavior in the presence of a homogeneous base, such as Cy_2NMe (Table 3.1).[86] We were surprised to discover that only the palladium hydride bearing the sterically-demanding P(*t*-Bu)$_3$ undergoes reductive elimination,[87] while the equilibrium for all other trialkylphosphines, including PCy_3, favors L_2PdHCl.[88] The equilibrium ratios provided in Table 3.1 were confirmed by treating PdL_2 with $[Cy_2NHMe]Cl$ (1 equiv) in the presence of Cy_2NMe (34 equiv). These results indicate that in addition to any *kinetic* barrier that one might encounter in the reductive elimination of H-X from a palladium hydride (e.g., due to the heterogeneity of Cs_2CO_3), there exists the possibility that reductive elimination is disfavored based on *thermodynamic* considerations!

[86] In order to mimic the stoichiometry of a palladium-catalyzed Heck reaction, we employed a large excess (35 equiv) of Cy_2NMe.
[87] The activation energy for this process is: $\Delta G^{\ddagger}$ = 22 kcal/mol at 20 °C. See experimental for details.
[88] $(PCy_3)_2PdHCl$ will undergo reductive elimination in the presence of K(O(*t*-Bu)).

Table 3.1. Examination of the role of phosphine ligand on the equilibrium between L_2PdHCl and PdL_2.

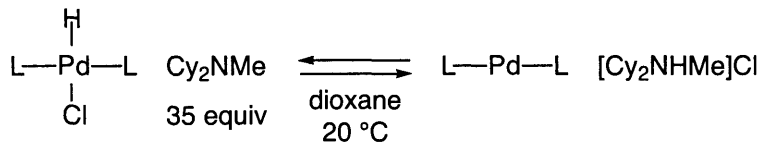

entry	ligand	cone angle	L_2PdHCl : PdL_2
1	$P(t\text{-Bu})_3$	182°	<2 : >98
2	$P(t\text{-Bu})_2Cy$	178°	>98 : <2
3	$P(t\text{-Bu})Cy_2$	174°	>98 : <2
4	PCy_3	170°	>98 : <2
5	$P(t\text{-Bu})_2Et$	165°	>98 : <2
6	$P(t\text{-Bu})_2Me$	161°	>98 : <2

We next performed a preliminary examination on the effect of the halide ligand on the equilibrium between L_2PdHX and PdL_2 (Table 3.2). We found that even for a bromide and iodide ligand the palladium hydrides bearing PCy_3 do not undergo reductive elimination in the presence of Cy_2NMe (entry 4 and 5). These observations suggest that the nature of the phosphine ligand controls whether or not PdL_2 will be the favored complex.

Table 3.2. Examination of the role of the halide ligand on the equilibrium between L_2PdHX and PdL_2.

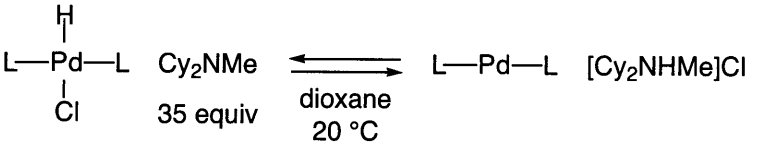

entry	ligand	X	PdL_2HX : PdL_2
1	P(*t*-Bu)$_3$	Cl	<2 : >98
2		Br	<2 : >98
3	PCy_3	Cl	>98 : <2
4		Br	>98 : <2
5		I	>98 : <2
6	P(*t*-Bu$_2$)Me	Cl	>98 : <2
7		Br	>98 : <2
8		I	>98 : <2

We postulated that the difference between the propensity of complexes bearing either P(*t*-Bu)$_3$ or PCy_3 to undergo reductive elimination is related to the disparity in the steric demand of the two ligands.[89] To verify this hypothesis, we obtained X-ray crystal structures of (P(*t*-Bu)$_3$)$_2$PdHCl and (PCy_3)$_2$PdHCl (Figure 3.2). In the case of the PCy_3 adduct, the P–Pd–P geometry is linear (180°). In contrast, for the P(*t*-Bu)$_3$ complex, the P–Pd–P angle is 161°; specifically, the P(*t*-Bu)$_3$ ligands are bent away from Cl, at the cost of increased interaction between

[89] Electronic considerations do not appear to furnish a suitable explanation, since P(*t*-Bu)$_3$ is generally regarded as more electron-donating than PCy_3, which should lead to a more stable Pd(II) complex.

the two phosphines and with the hydride.[90] These unfavorable steric effects are relieved upon reductive elimination to generate $Pd(P(t\text{-}Bu)_3)_2$, thereby providing a driving force for this process.

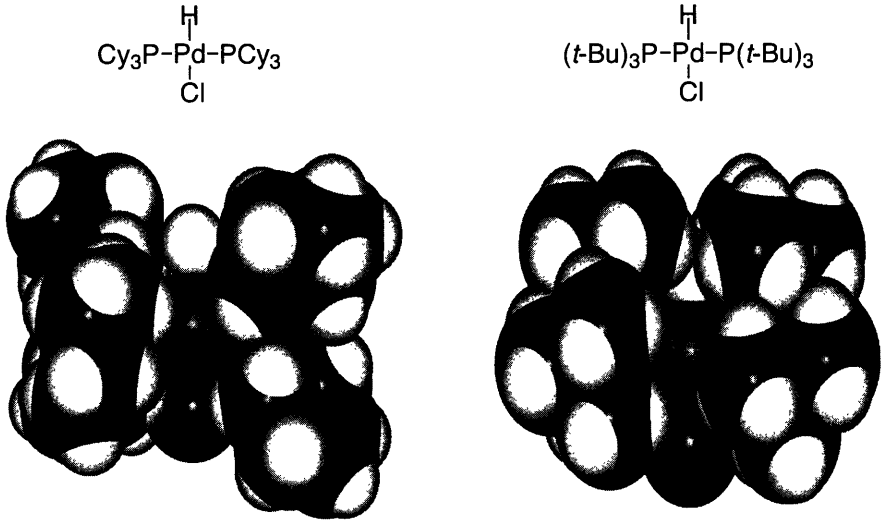

3.1 **3.2**

Figure 3.2. Space-filling (van der Waals radii) based on the X-ray crystal structures of L_2PdHCl (left: L = PCy_3; right: L = $P(t\text{-}Bu)_3$).

Based on these data, we postulate that the comparatively low activity of Pd/PCy_3 as a catalyst for Heck reactions of aryl chlorides (e.g., 3.2) may be attributable in part to the relative reluctance of $(PCy_3)_2PdHCl$ to undergo reductive elimination in the presence of Cy_2NMe, the critical Pd(0)-regenerating step of the catalytic cycle (Figure 3.1). For $(P(t\text{-}Bu)_3)_2PdHCl$, on the other hand, loss of HCl is favored and facile.

[90] Notes: The hydrides in the crystal structures have not been explicitly located, but are modeled for illustrative purposes, see experimental for details; Pd–P bond lengths for L_2PdHCl: 2.306(3) Å for L = PCy_3; 2.361(11) Å for L = $P(t\text{-}Bu)_3$

We have examined the kinetics of the Cy_2NMe-mediated reductive elimination of HCl from L_2PdHCl (L = P(*t*-Bu)$_3$; eq 3.5). The rate of the reaction is first-order in L_2PdHCl and zero-order in Cy_2NMe, inhibited by the addition of P(*t*-Bu)$_3$, and comparable for L_2PdHCl and L_2PdDCl.[91] These data are consistent with a mechanism for reductive elimination that involves an initial slow and reversible dissociation of L from L_2PdHCl (eq 3.5). We are currently uncertain of the role of the base in the later stages of this reaction, and a better understanding will require additional study.

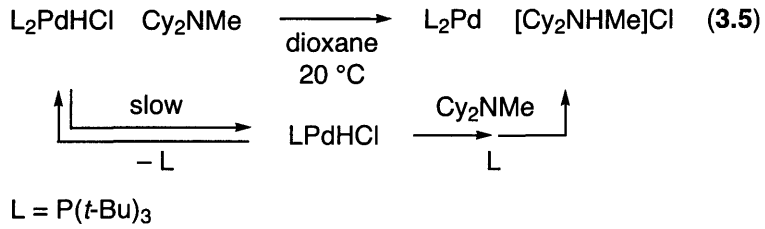

[91] (a) During the course of the reductive elimination, no intermediate is evident by ^{31}P NMR spectroscopy. (b) A preliminary kinetics study indicates that $k_H/k_D \sim 1.0\text{-}1.5$ for reactions of L_2PdHCl/L_2PdDCl.

C. Conclusions

In summary, we have described a series of studies that provide insight into the Heck arylation process. Specifically, we have detected, for the first time, the postulated palladium-hydride intermediate (L_2PdHX) in the catalytic cycle. We have determined that the base-mediated Pd(0)-regeneration step ($L_2PdHX \rightarrow PdL_2$) of the cycle can be kinetically slow and thermodynamically unfavorable. This reductive elimination process is remarkably sensitive to the structure of L (PCy_3 vs. $P(t\text{-}Bu)_3$), which we believe, on the basis of crystallographic studies, may be a consequence of steric effects. Finally, we have correlated slow rates of Heck arylation with reluctant reductive elimination of L_2PdHX, furnishing a possible rationalization for our observed Brønsted-base (Cs_2CO_3 vs. Cy_2NMe) and ligand (PCy_3 vs. $P(t\text{-}Bu)_3$) effects.

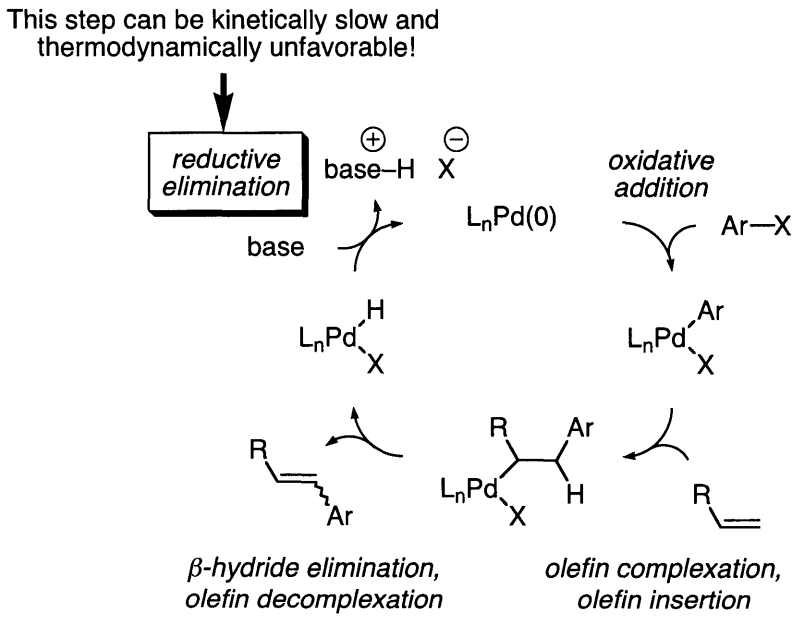

D. Experimental

I. General

All reactions were carried out under an atmosphere of nitrogen or argon in oven-dried glassware with magnetic stirring, unless otherwise indicated.

$Pd(P(t\text{-}Bu)_3)_2$ (Strem and Johnson Matthey), $Pd_2(dba)_3$ (Aldrich), PCy_3 (Strem), and $P(t\text{-}Bu)_3$ (FMC) were used as received. $Pd(PCy_3)_2$ (Strem) was purified by recrystallization from toluene/methanol.

THF was purified under argon by passage through a neutral alumina column. Dioxane (Aldrich; Sure Seal), Cs_2CO_3 (Strem), phenyl boronic acid (Frontier Scientific), and 1.0 M HCl in Et_2O (Aldrich) were used as received. Cy_2NMe (Aldrich), *n*-butyl vinyl ether (Aldrich), and 4'-chloroacetophenone (Aldrich) were de-gassed by bubbling dry argon through the liquids.

^1H and ^{13}C NMR resonances are referenced to the solvent. ^{31}P NMR resonances are referenced to external 85% H_3PO_4.

II. Preparation of L_2PdHCl Complexes

General procedure. In a glovebox, HCl (1.0 M in Et_2O; 1.1 equiv) was added dropwise over 2 minutes to a stirring 0.1 M solution of the PdL_2 complex (1.0 equiv) in THF. Upon the initial addition of HCl, the reaction mixture darkened; however, after approximately 15 minutes of stirring at room temperature, the solution turned light-yellow. The reaction mixture was stirred for a total of 1 h, and then it was filtered. The solvent and the excess HCl were removed under vacuum, and the resulting solid was washed with pentanes and then dried under vacuum.

$(P(t\text{-}Bu)_3)_2PdHCl$ [63166-71-2]. The general procedure was followed, using 250 mg (0.49 mmol) of $Pd(P(t\text{-}Bu)_3)_2$ and 0.54 mL of 1.0 M HCl in Et_2O. The product (260 mg, 97% yield) was isolated as an off-white powder.

^1H NMR (300 MHz, THF-d_8) δ –16.41 (t, 1H, $^2J_{H\text{-}P}$ = 6.0 Hz), 1.57 (m, 54H). ^{13}C NMR (300 MHz, THF) δ 32.7 (t, $^2J_{C\text{-}P}$ = 11.7 Hz), 39.6 (t, $^1J_{C\text{-}P}$ = 14.4 Hz). ^{31}P NMR (300 MHz, THF) δ 83.1. FTIR (thin film) 2901, 2021, 1477, 1393, 1361, 1170, 808 cm^{-1}.

$(PCy_3)_2PdHCl$ [28016-71-9]. The general procedure was followed, using 300 mg (0.45 mmol) of $Pd(PCy_3)_2$ and 0.50 mL of 1.0 M HCl in Et_2O. The product (310 mg, 98% yield) was isolated as a gray powder.

^1H NMR (300 MHz, THF-d_8) δ –14.61 (t, 1H, $^2J_{H\text{-}P}$ = 4.2 Hz), 1.29 (m, 18H), 1.55 (m, 12H), 1.73 (m, 18H), 2.15 (m, 12H), 2.14 (m, 6H). ^{13}C NMR (300 MHz, THF) δ 26.8, 27.7 (t, $^2J_{C\text{-}P}$ = 23.4 Hz), 30.7, 34.4 (t, $^1J_{C\text{-}P}$ = 40.2 Hz). ^{31}P NMR (300

MHz, THF) δ 42.6. FTIR (thin film) 2926, 2850, 1446, 1266, 1174, 1070, 1004, 888, 849 cm^{-1}.

III. Reactivity Studies

Procedure for eq 3.3 and eq 3.4. In a nitrogen-filled glovebox, $Pd_2(dba)_3$ (3.6 mg, 0.018 mmol) and 4'-chloroacetophenone (66 mg, 0.66 mmol) were added to a Teflon-capped vial equipped with a stir bar. The Brønsted base (0.66 mmol of either Cs_2CO_3 (220 mg) or Cy_2NMe (130 mg)), P(*t*-Bu)$_3$ (59 mg, 0.30 mmol), *n*-butyl vinyl ether (8.2 mg, 0.0090 mmol), tetradecane (59 mg, 0.30 mmol; internal standard for GC analysis), and dioxane (0.60 mL) were added via syringe. The reaction mixture was stirred at room temperature. To measure the yields of the Heck arylation product, aliquots were removed after 4 hours and after 32 hours of reaction, filtered through a plug of silica with copious washings with Et_2O, and analyzed by GC.

^{31}P NMR analysis (eq 3.4). Aliquots were removed after 4 hours and transferred directly to an NMR tube for ^{31}P NMR analysis. For the reaction in the presence of Cy_2NMe, a resonance (>98%) at 86 ppm was observed; this coincides with the resonance for Pd(P(*t*-Bu)$_3$)$_2$. For the reaction in the presence of Cs_2CO_3, a resonance (>98%) at 83 ppm was observed; this coincides with the resonance for (P(*t*-Bu)$_3$)$_2$PdHCl (see spectra below).

Reference ^{31}P NMR shifts (δ).

	L_2PdHCl	PdL_2	L
P(*t*-Bu)$_3$	83.1	85.9	63.4
PCy_3	42.6	39.7	10.9

^{31}P NMR spectra for Heck reactions (eq 3.4).

Reaction with Cs_2CO_3 as the Brønsted base

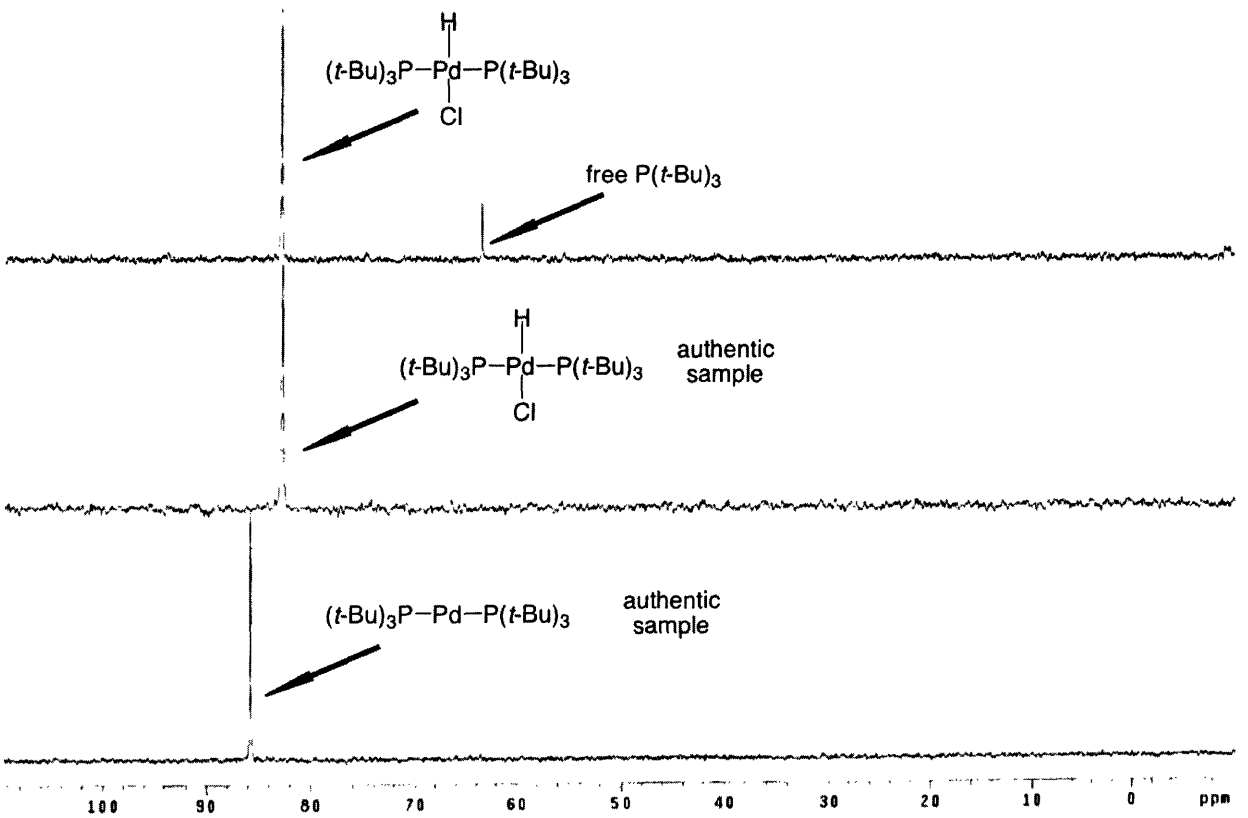

Reaction with Cy_2NMe as the Brønsted base

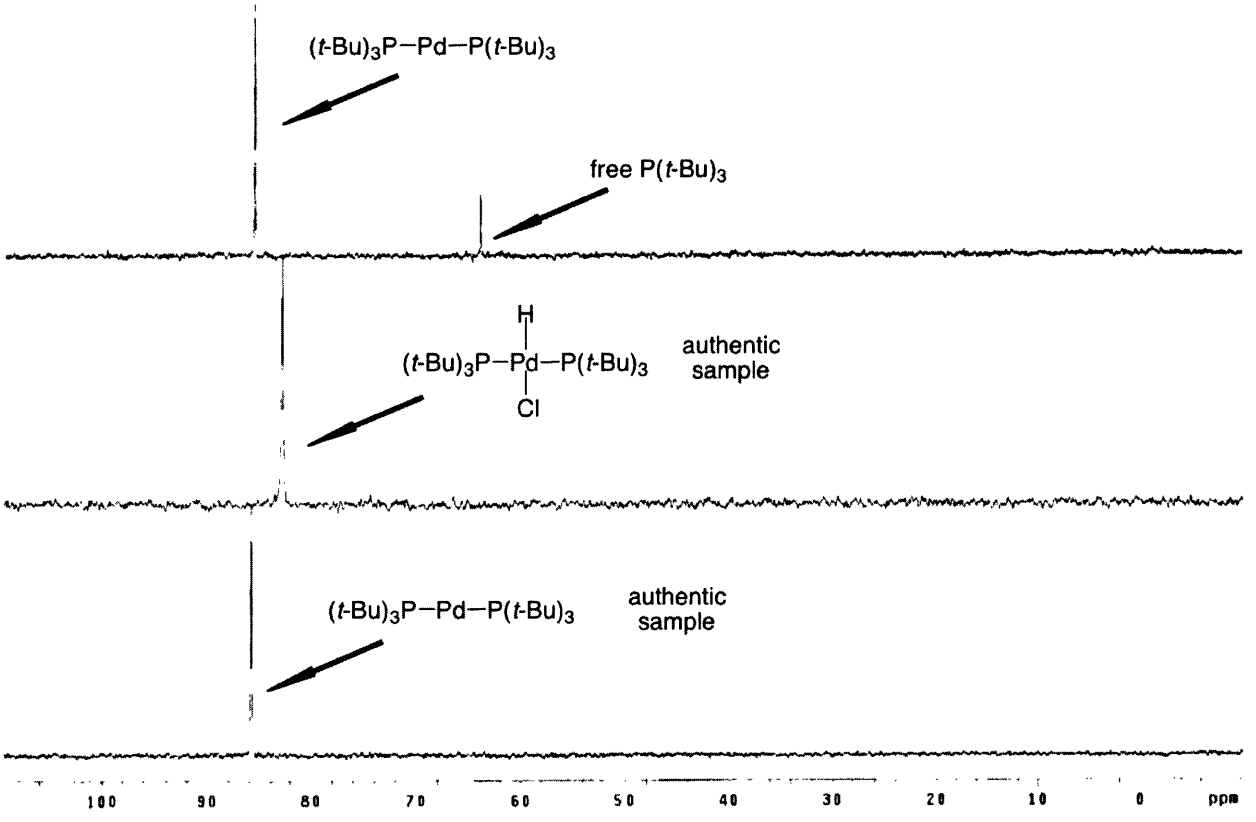

Procedure for Table 3.1 and Table 3.2, starting with L_2PdHCl. In a glovebox, L_2PdHCl (1.0 equiv) was added to a vial and dissolved in dioxane. Then, Cy_2NMe (35 equiv) was added to the reaction mixture, and the entire contents of the vial were transferred to an NMR tube for ^{31}P NMR analysis.

Table 3.1, L = P(*t*-Bu)$_3$. The general procedure was followed, using $(P(t\text{-}Bu)_3)_2PdHCl$ (9.9 mg, 0.018 mmol), Cy_2NMe (120 mg, 0.63 mmol), and dioxane (0.60 mL). ^{31}P NMR analysis was performed 30 minutes and 5.5 hours after the start of the reaction. After 30 minutes, the ratio of $(P(t\text{-}Bu)_3)_2PdHCl$ and $Pd(P(t\text{-}Bu)_3)_2$ was 36 : 64, with a trace (<5%) of free $P(t\text{-}Bu)_3$. After 5.5 hours, the ratio of

$(P(t\text{-}Bu)_3)_2PdHCl$ and $Pd(P(t\text{-}Bu)_3)_2$ was <2 : >98, with a trace (<5%) of free $P(t\text{-}Bu)_3$ (see spectra below).

Table 3.1, L = PCy_3. The general procedure was followed, using $(PCy_3)_2PdHCl$ (13.0 mg, 0.018 mmol), Cy_2NMe (120 mg, 0.63 mmol), and dioxane (0.60 mL). ^{31}P NMR analysis was performed 30 minutes and 5.5 hours after the start of the reaction. After 30 minutes, the ratio of $(PCy_3)_2PdHCl$ and $Pd(PCy_3)_2$ was >98 : <2, and no free PCy_3 was observed. After 5.5 hours, the ratio of $(P(t\text{-}Bu)_3)_2PdHCl$ and $Pd(P(t\text{-}Bu)_3)_2$ remained at >98 : <2, and no free PCy_3 was observed (see spectra below).

The data for the other ligands in table 3.1 and table 3.2 were collected in a fashion similar to that described above for $(P(t\text{-}Bu)_3)_2PdHCl$ and $(PCy_3)_2PdHCl$.

^{31}P NMR spectra for reactions of L_2PdHCl with Cy_2NMe (Table 3.1).

Reaction with $P(t\text{-}Bu)_3$ as the ligand

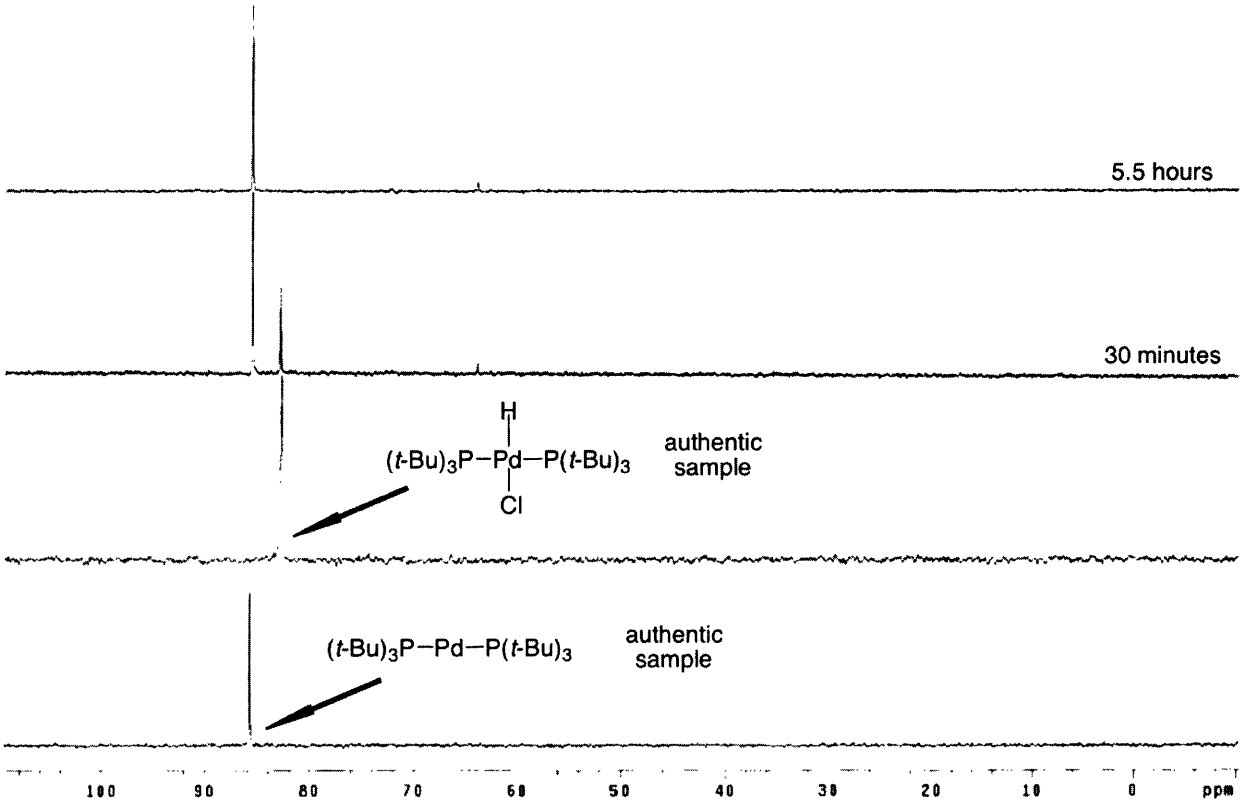
5.5 hours
30 minutes
H
(t-Bu)3P–Pd–P(t-Bu)3
Cl
authentic sample
(t-Bu)3P–Pd–P(t-Bu)3
authentic sample
100
90
80
70
60
50
40
30
20
10
0
ppm

Reaction with PCy_3 as the ligand

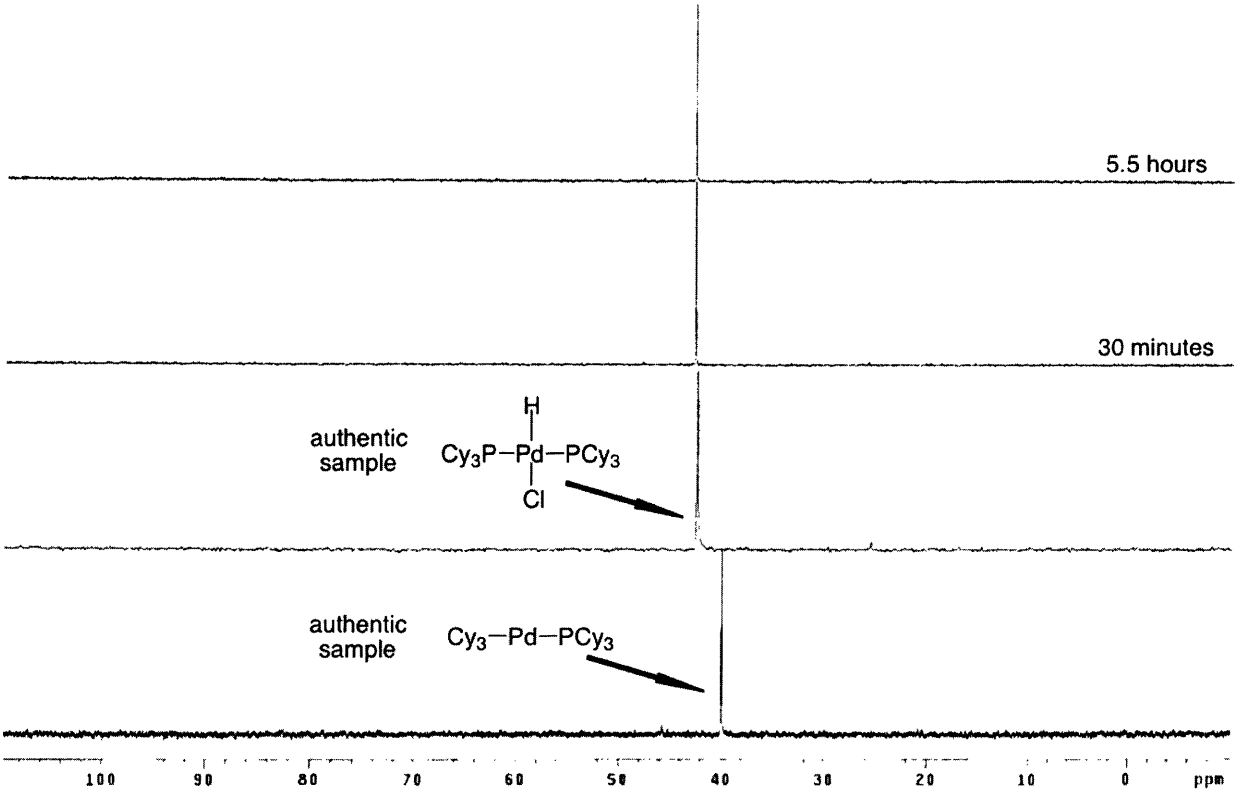

Procedure for Table 3.1, starting with PdL_2. In order to verify that the ratios of L_2PdHCl : PdL_2 in eq 5 are equilibrium ratios, the equilibrium was approached from the opposite direction (starting from the right-hand side of eq 5).

In a glovebox, PdL_2 (1.0 equiv) was added to a vial and dissolved in dioxane. Then, $[Cy_2NHMe]Cl$ (1.0 equiv) was added, followed by Cy_2NMe (34 equiv). The entire contents of the vial were transferred to an NMR tube for ^{31}P NMR analysis.

Table 3.1, L = P(*t*-Bu)$_3$. The general procedure was followed, using $Pd(P(t\text{-}Bu)_3)_2$ (9.2 mg, 0.018 mmol), $[Cy_2NHMe]Cl$ (4.2 mg, 0.018 mmol), Cy_2NMe (120

mg, 0.61 mmol), and dioxane (0.60 mL). The entire contents of the vial were transferred after 30 minutes to an NMR tube and analyzed by ^{31}P NMR. The ratio of $(P(t\text{-}Bu)_3)_2PdHCl$: $Pd(P(t\text{-}Bu)_3)_2$ was <2 : >98.

Table 3.1, L = PCy_3. The general procedure was followed, using $Pd(PCy_3)_2$ (12 mg, 0.018 mmol), $[Cy_2HNMe]Cl$ (4.2 mg, 0.018 mmol), Cy_2NMe (120 mg, 0.61 mmol), and dioxane (0.60 mL). The entire contents of the vial were transferred after 30 minutes to an NMR tube and analyzed by ^{31}P NMR. The ratio of $(PCy_3)_2PdHCl$: $Pd(PCy_3)_2$ was >98 : <2.

The data for the other phosphines in table 3.1 were collected in fashion similar to that described above for $P(t\text{-}Bu)_3$ and PCy_3.

Equation 3.5.

$$\text{Rate} = k[HClPdL_2]$$

$$\frac{d[HClPdL_2]}{dt} = -k[HClPdL_2] \xrightarrow{\text{integration}} \int_{t_0}^{t} \frac{1}{[HClPdL_2]}\, d[HClPdL_2] = -\int_{t_0}^{t} k\, dt$$

$$\ln\left(\frac{[HClPdL_2]_t}{[HClPdL_2]_{t_0}}\right) = -k(t - t_0) \xrightarrow{\text{simplification}} \ln\left(\frac{[HClPdL_2]}{[HClPdL_2]_0}\right) = -kt$$

Thus, if the reductive elimination obeys the above rate law, a plot of the conversion as a function of time (see above) will furnish a line, the slope of which is the first-order rate constant, k.

Using the Eyring equation:

$$k = \frac{\kappa T}{h} e^{\frac{-\Delta G^{\ddagger}}{RT}}$$

The free energy of activation ($\Delta G^{\ddagger}$) can be solved for by rearrangement:

$$\Delta G^{\ddagger} = -RT \ln\left(\frac{kh}{\kappa T}\right)$$

$$R = 1.9872\, cal \bullet mol^{-1} \bullet K^{-1}$$

$$T = temperature\ in\ Kelvin$$

$$k = rate\ constant$$

$$h = 6.62608 \times 10^{-34} J \bullet s$$

$$\kappa = 1.3806 \times 10^{-23}\ J \bullet K^{-1}$$

General procedure for kinetics studies. In a glovebox, $(P(t\text{-}Bu)_3)_2PdHCl$ (9.9 mg, 0.018 mmol, 1.0 equiv) was added to a vial, dissolved in dioxane (0.20 mL), and transferred to an NMR tube. The vial was washed with dioxane (2 x 0.20 mL), and the washings were transferred to the NMR tube, giving an overall concentration of 0.03 M in the palladium complex. The tube was sealed with a Teflon screw-cap and cooled to 15 °C in the spectrometer. After the temperature had reached equilibrium, Cy_2NMe (3.4 μL, 3.5 mg, 0.018 mmol, 1.0 equiv) was added to the NMR tube through the Teflon septum.

The reaction was monitored by ^{31}P NMR at 15 °C, and the percent conversion of $(P(t\text{-}Bu)_3)_2PdHCl$ to $Pd(P(t\text{-}Bu)_3)_2$ was determined by integrating the two resonances (attempts to use an internal standard led to anomalous results).

Support for a first-order reaction (eq 3.5). A reaction was set up and monitored according to the general procedure. The data were plotted using the kinetic analysis for a first-order reaction outlined above, which furnished a linear plot (see graph below). These data indicate that k = 0.000155 s^{-1}.

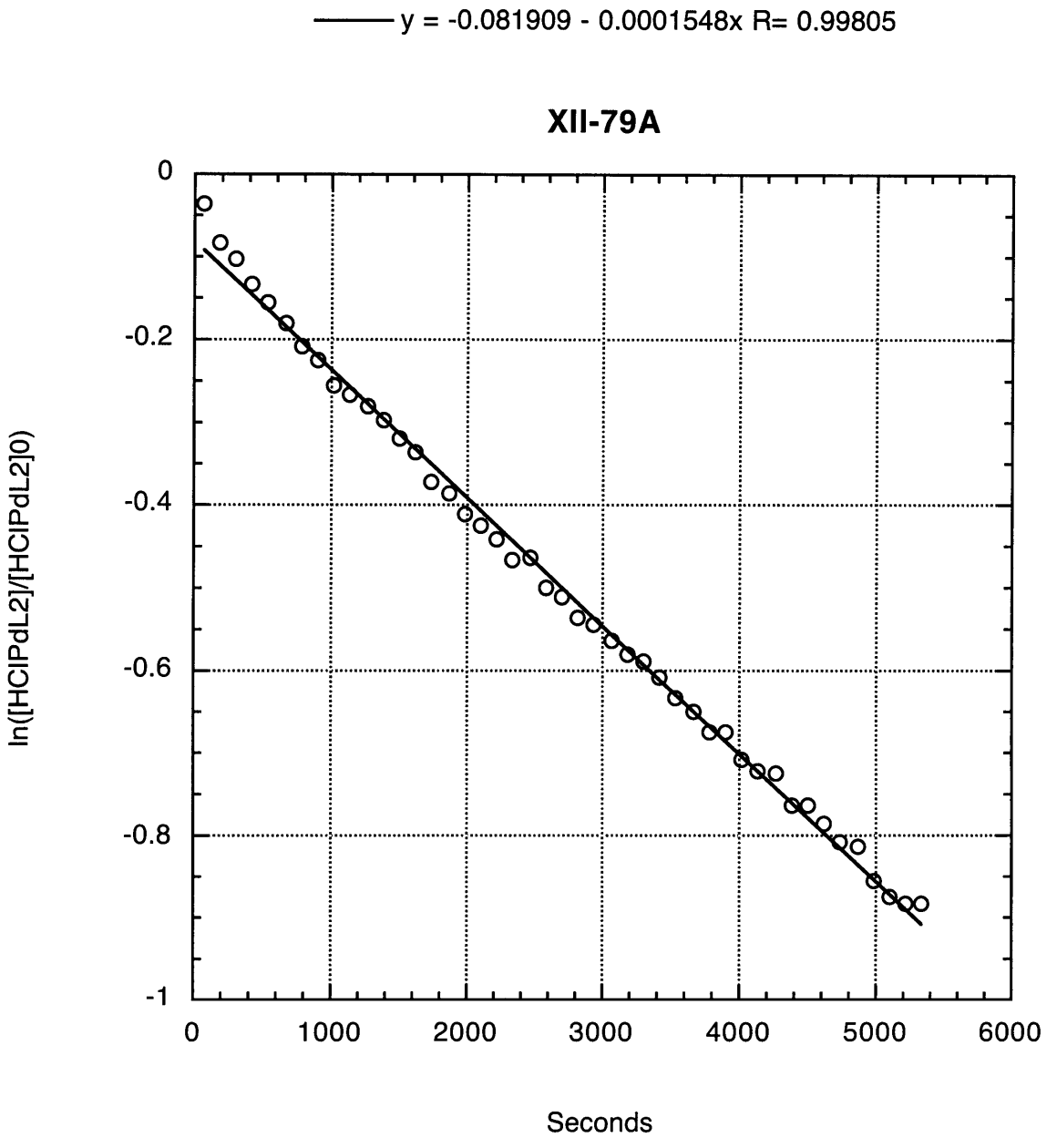

Order of the reaction in Cy_2NMe (eq 3.5). Three reactions were set up and monitored according to the general procedure. The three reactions had 1.0, 2.0, or 4.0 equiv of Cy_2NMe. The data (see graph below) indicate that k = 0.000155 s^{-1}, 0.000162 s^{-1}, and 0.000167 s^{-1} for 1.0, 2.0, and 4.0 equiv of Cy_2NMe, respectively. These values are consistent with a zero-order dependence on Cy_2NMe.

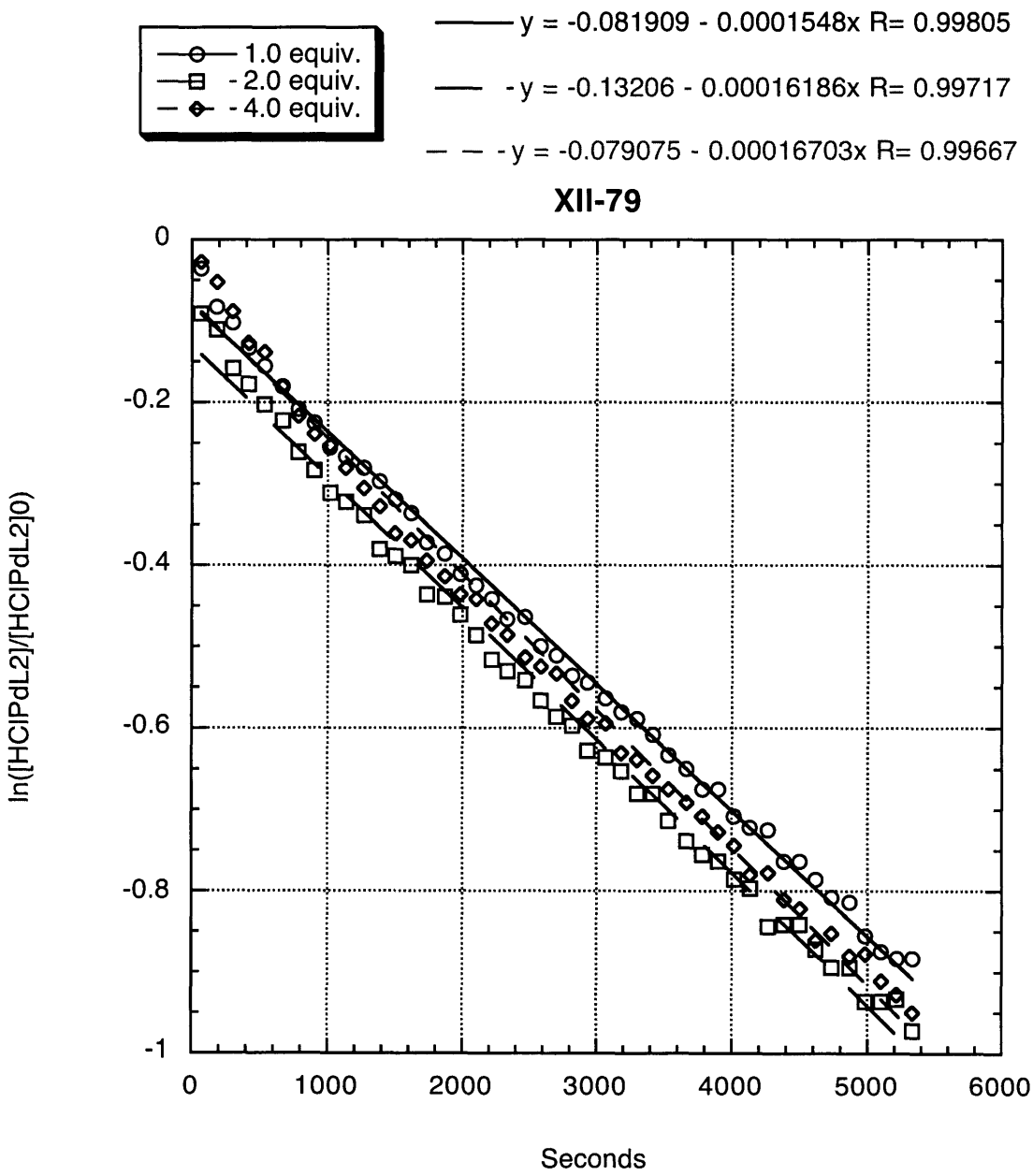

Effect of added P(*t*-Bu)$_3$ (eq 3.5). Three reactions were set up and monitored according to the general procedure. The three reactions had 0.0, 2.0, or 4.0 equiv of added P(*t*-Bu)$_3$. These data indicate that k = 0.000155 s^{-1}, 0.000111 s^{-1}, and 0.000107 s^{-1} for 0.0, 2.0, and 4.0 equiv of added P(*t*-Bu)$_3$, respectively. These values are consistent with an inhibitory effect of added P(*t*-Bu)$_3$ (see graph below).

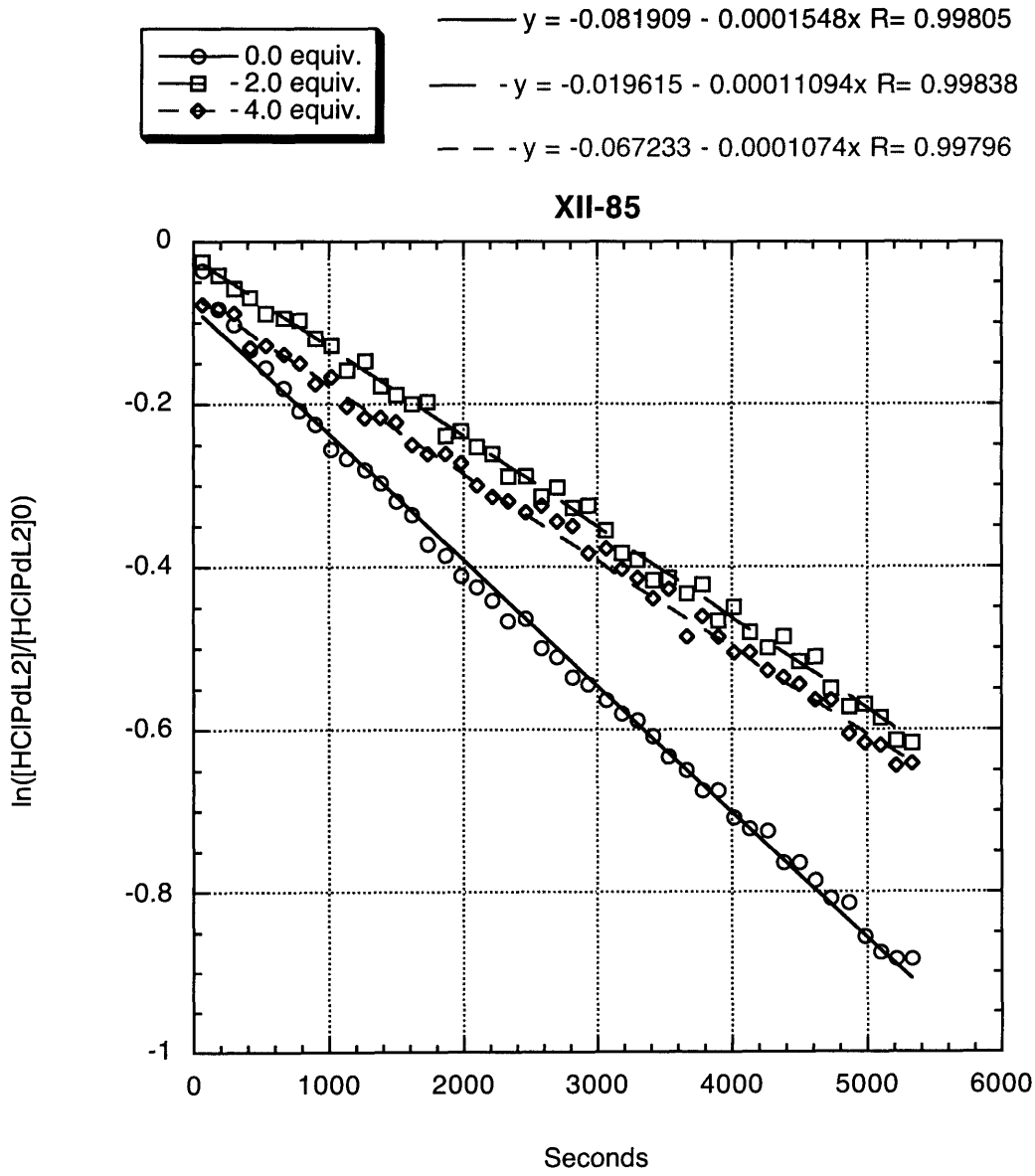

Activation energy for reductive elimination (Table 3.1, entry 1). Two reactions were set up at 20 °C using 35 equiv of Cy_2NMe (mimicking the conditions found in a Pd/P(*t*-Bu)$_3$-catalyzed Heck reaction) and monitored according to the general procedure. These data indicate that k = 0.000143 s^{-1} and 0.000129 s^{-1} for run 1 and run 2, respectively. These rate constants correspond to $\Delta G^{\ddagger}$ = 22.3 kcal/mol and 22.4 kcal/mol, respectively.

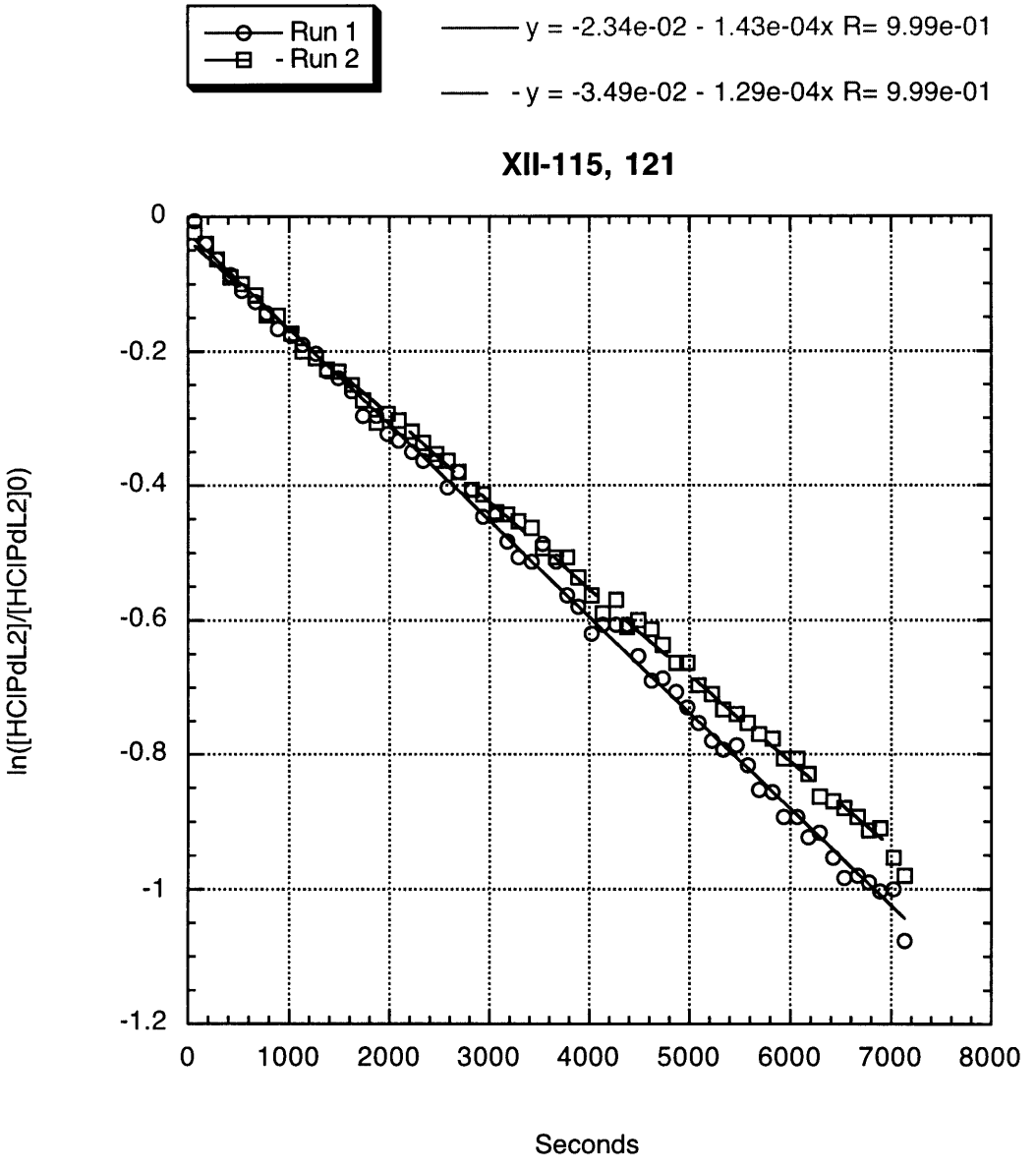

IV. X-ray Crystallographic Data

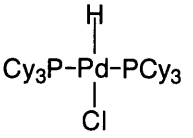

3.1

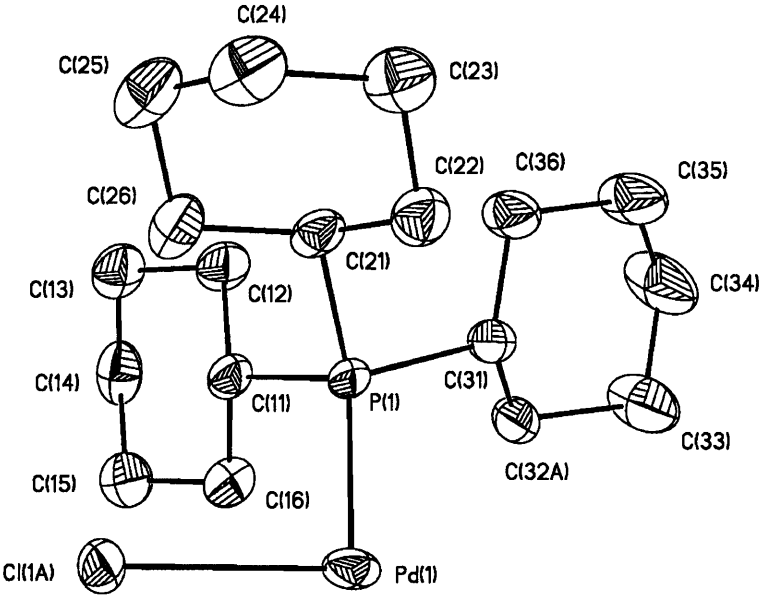

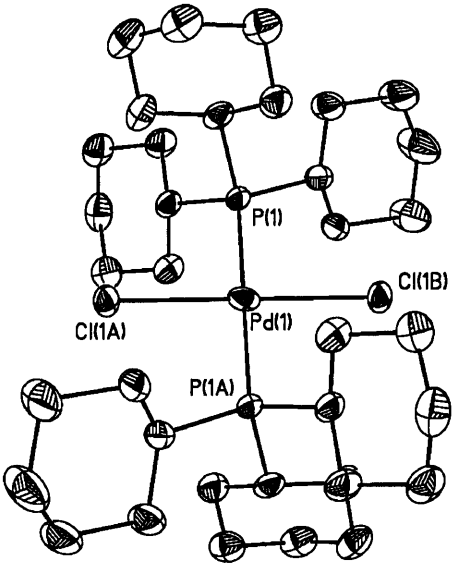

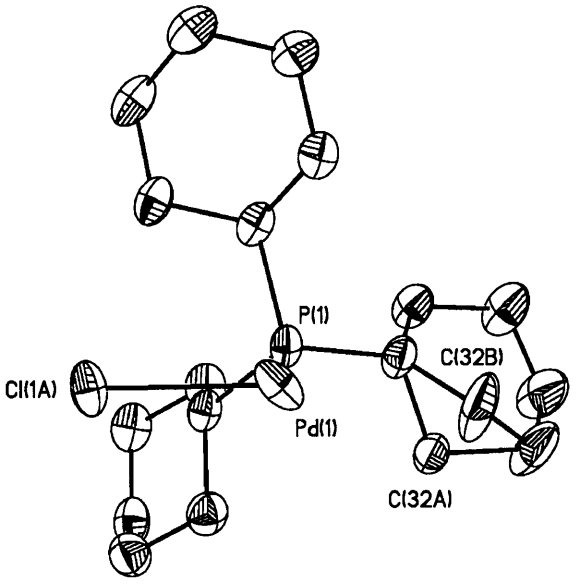

A light-gray ether solution of **3.1** was prepared. Crystals suitable for X-ray structural analysis were obtained by solvent evaporation.

A colorless block of dimensions 0.28 x 0.19 x 0.16 mm^3 was mounted under STP and transferred to a Bruker AXS/CCD three-circle diffractometer (c fixed at 54.78°) equipped with a cold stream of N_2 gas. An initial unit cell was determined by harvesting reflections I > 20 s(I) from 45 x 10-s frames of 0.30° w scan data with monochromated Mo K_a radiation (l = 0.71073 Å). The cell thus determined was triclinic.

A hemisphere of data was then collected using w scans of 0.30° and 30-s frames. The raw data frames were integrated using the Bruker program SAINT+ for NT version 6.01. The data that were collected (4013 total reflections, 3242 unique, R_{int} = 0.0229) had the following Miller index ranges: –10 to 10 in h, –10 to 11 in k, and –11 to 11 in l. No absorption correction was performed.

All aspects of the solution and refinement were handled by SHELXTL NT version 5.10. The structure was solved by direct methods in the triclinic space

group P-1, a = 9.8843(5) Å; b =10.2473(5) Å; c = 10.6255(6) Å; a = 66.6700(10)°; b = 70.1810(1)°; g = 89.9180(10)°, and refined using standard difference Fourier techniques. Final, full-matrix least-squares refinement (2596 data for 197 parameters) on F^2 yielded residuals of R_1 and wR_2 of 0.0371 and 0.0884 for data I > 2s(I), and 0.0397 and 0.0905, respectively, for all data. During the final refinement, all non-hydrogen atoms were treated anisotropically. Hydrogen atoms were included in calculated positions and refined isotropically on a riding model. Residual electron density amounted to a maximum of 0.557 e/Å^3 and a minimum of –1.033 e/Å^3.

The chlorine, **Cl(1A)**, has been refined with a partial occupancy and through symmetry generates **Cl(1A)#** (~50% in each position). There is disorder in **C(32)**, represented by **C(32A)** and **C(32B)**. The cyclohexyl ring incorporating **C(32)** is partially in a chair (~80%) and boat (~20%) conformation. The metal-hydride has not been definitively located and is merely represented graphically in Figure 2 for illustrative purposes.

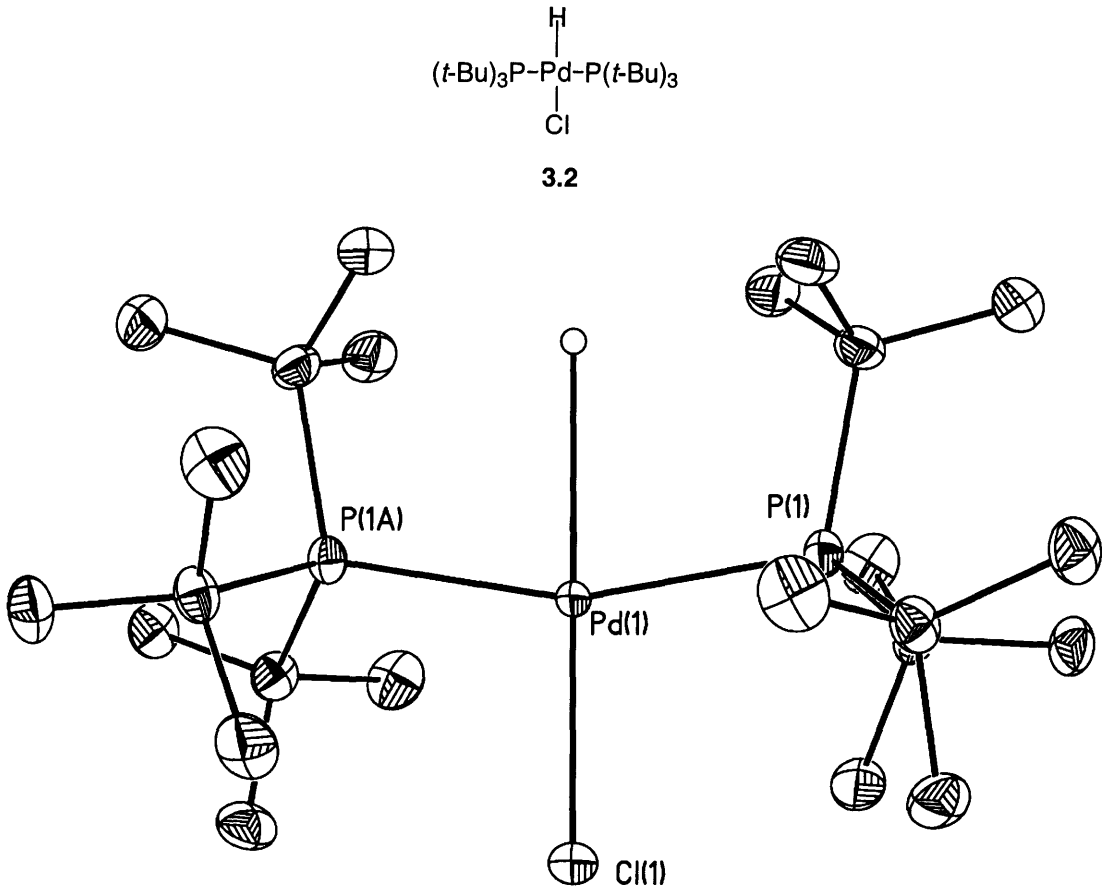

3.2

A light-gray solution of **3.2** in Et_2O was prepared. Crystals suitable for X-ray structural analysis were obtained by the diffusion of pentanes into the Et_2O solution.

A colorless plate of dimensions 0.27 x 0.26 x 0.07 mm^3 was mounted under STP and transferred to a Bruker AXS/CCD three-circle diffractometer (γ fixed at 54.78°) equipped with a cold stream of N_2 gas. An initial unit cell was determined by harvesting reflections $I > 20\ \sigma(I)$ from 45 x 10-s frames of 0.30° ω scan data with monochromated Mo K_α radiation (λ = 0.71073 Å). The cell thus determined was monoclinic.

A hemisphere of data was then collected using ω scans of 0.30° and 30-s frames. The raw data frames were integrated using the Bruker program SAINT+

for NT version 6.01. The data that were collected (5946 total reflections, 2015 unique, R_{int} = 0.0366) had the following Miller index ranges: –12 to 14 in h, –9 to 7 in k, and –15 to 15 in l. No absorption correction was performed.

All aspects of the solution and refinement were handled by SHELXTL NT version 5.10. The structure was solved by direct methods in the monoclinic space group P2/n, a = 12.7692(12) Å; b = 8.7306(9) Å; c = 13.8817(14) Å; α = 90°; β = 114.718(2)°; γ = 90°, and refined using standard difference Fourier techniques. Final, full-matrix least-squares refinement (2015 data for 139 parameters) on F^2 yielded residuals of R_1 and wR_2 of 0.0475 and 0.1198 for data $I > 2\sigma(I)$, and 0.0511 and 0.1237, respectively, for all data. During the final refinement, all non-hydrogen atoms were treated anisotropically. Hydrogen atoms were included in calculated positions and refined isotropically on a riding model. Residual electron density amounted to a maximum of 3.011 e/Å^3 and a minimum of –0.357 e/Å^3.

See Appendix A for tables containing full crystallographic data for the X-ray structure.

Part III

Miscellaneous

Chapter 4

Palladium-Hydride Catalyzed Isomerizations of Allylic Alcohols

A. Introduction

The isomerization of allylic alcohols is a simple atom-economical method for furnishing either aldehydes or ketones in a single step (Scheme 4.1).[92,93] Another attractive aspect of a simple isomerization protocol is the avoidance of reactions (i.e., oxidation and reduction) that may not be compatible with a complex substrate bearing sensitive functional groups.

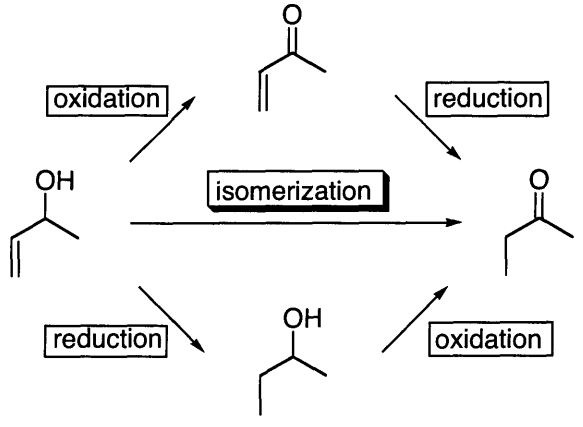

Scheme 4.1. Illustration of the potential efficiency of an allylic alcohol isomerization compared with a 2-step process.

A number of transition-metal catalysts capable of isomerizing allylic alcohols to their corresponding carbonyl compounds have been developed. These catalysts are structurally diverse and are based on both early- and late-transition metals. A subclass of these catalysts are metal hydrides, which can

[92] For reviews concerning catalysts, substrates, and mechanisms commonly encountered in allylic alcohol isomerizations, see: (a) Uma, R.; Crévisy, C.; Grée, R. *Chem. Rev.* **2003**, *103*, 27-51. (b) Van der Drift, R. C.; Bouwman, E.; Drent, E. *J. Organomet. Chem.* **2002**, *650*, 1-24.
[93] For a discussion on the concept of atom economy, see: Trost, B. M. *Pure Appl. Chem.* **1992**, *64*, 315-322.

presumably mediate the isomerization of an allylic alcohol through a sequence of olefin insertion and β-hydride elimination. The resulting enol that is formed at the end of this cycle undergoes tautomerization to provide the desired aldehyde or ketone (Figure 4.1).

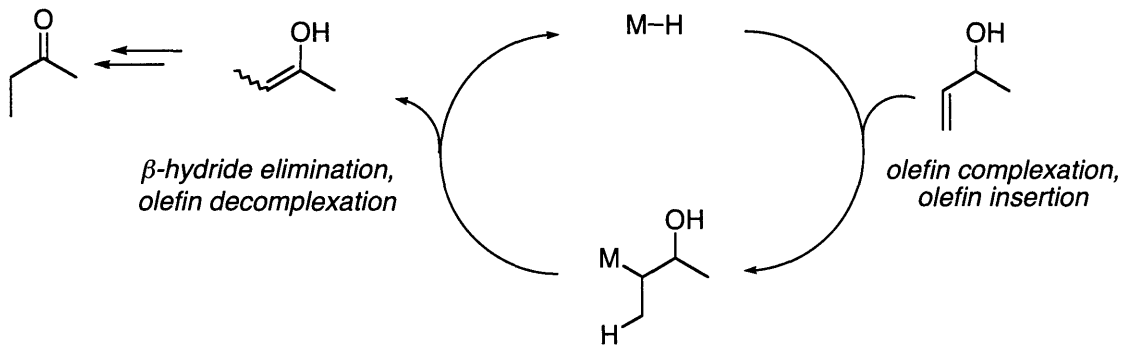

Figure 4.1. Generally accepted catalytic cycle for the isomerization of allylic alcohols by metal hydrides.

During our investigation on the reductive elimination of H-X from palladium hydrides (Chapter 3), we performed preliminary experiments directed toward determining if an isolated bisphosphine palladium-hydride complex could serve as an effective allylic alcohol isomerization catalyst. Our first experiment was simply the addition of 5 mol% $(P(t\text{-}Bu)_3)_2PdHCl$ to a solution of allyl alcohol in $CDCl_3$. Using ^1H NMR, we were excited to observe that after 2.5 hours the majority of the starting material was consumed and a new resonance appeared in the aldehyde region (eq 4.1).[94] Although the literature on catalysts for the isomerization of allylic alcohols is extensive, there are very few examples

[94] No internal standard was employed in this preliminary experiment. The new ^1H NMR resonance is presumed to be indicative of propionaldehyde.

of palladium catalysts for isomerizations of this type.[95,96] Furthermore, to the best of our knowledge there are no examples of an isolated palladium hydride catalyst performing this transformation. Despite this initial success, allyl alcohol is widely believed to be the least-challenging substrate possible. We therefore proceeded to further optimize and explore the scope of this isomerization employing isolated palladium hydrides.

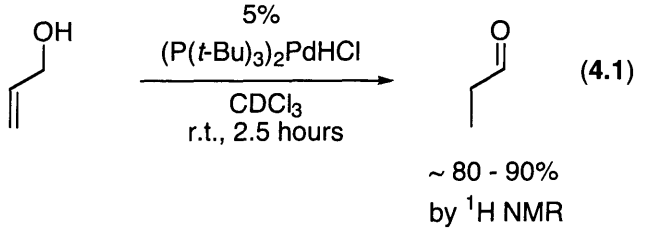

(**4.1**)

[95] For examples of palladium-catalyzed isomerizations of unsaturated alcohols (e.g., homoallylic or propargylic alcohols), see: (a) Ganchegui, B.; Bouquillon, S.; Hénin, F.; Muzart, J. *J. Mol. Catal. A: Chem.* **2004**, 65-69. (b) Lu, X.; Ji, J.; Ma, D.; Shen, W. *J. Org. Chem.* **1991**, *56*, 5774-5778.

[96] For examples of palladium-catalyzed isomerizations of allylic ethers, see: Boss, R.; Scheffold, R. *Angew. Chem.* **1976**, *88*, 578-579.

B. Results and Discussion

In order to rapidly determine if $(P(t\text{-}Bu)_3)_2PdHCl$ (**4.1**) is capable of isomerizing substrates more challenging than allyl alcohol, we performed a series of NMR experiments in which we simply attempted to observe a new resonance indicative of either an aldehyde or a ketone (Table 4.1). We were pleased to see that more challenging substrates do indeed undergo isomerization in the presence of **4.1**. 1,1- and 1,2-disubstituted (1,1 and 1,2) allylic alcohols furnish product in this initial examination (entries 2 – 5). A cyclic tri-substituted alcohol yields 5 – 10% product under these unoptimized conditions (entry 6). An allylic ether isomerizes very cleanly to a vinyl ether, which presumably can undergo acid-catalyzed hydrolysis, thereby effecting the deprotection of an alcohol (entry 7). Reaction of 3-butene-1-ol (homoallyl alcohol) occurs cleanly, but very slowly, to furnish the aldehyde (entry 8). Alkynes did not undergo the desired reaction, and instead palladium black was formed (entries 9 and 10). The attempted isomerization of an allylic amine furnished no desired product (entry 11), presumably due to the base-induced reductive elimination of HCl from the palladium hydride (see Chapter 3). Finally, the reaction of geraniol with **4.1** yields only a trace of an aldehyde peak by ^1H NMR (entry 12). This rough survey of reactivity gave us the confidence to move forward with additional optimization studies.

Table 4.1. Preliminary survey of scope and reactivity in the $(P(t\text{-}Bu)_3)_2PdHCl$ catalyzed isomerization of allylic alcohols.

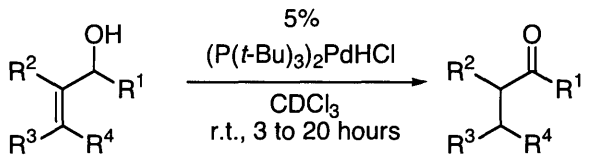

entry	substrate	estimated yield[a]	entry	substrate	estimated yield[a]
1	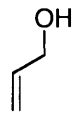	80 - 90%	7	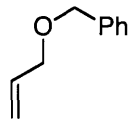	90 - 100%[c]
2	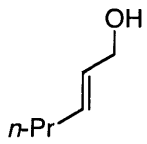	50 - 60%	8	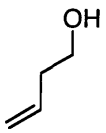	5 - 10%[d]
3	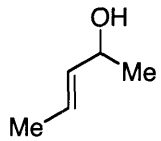	50 - 60%	9	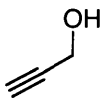	no reaction[e]
4	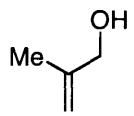	90 - 100%	10	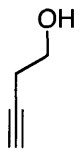	no reaction[e]
5	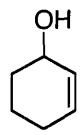	80 - 90%	11	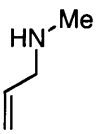	no reaction[f]
6	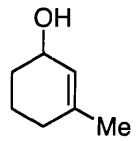	5 - 10%[b]	12	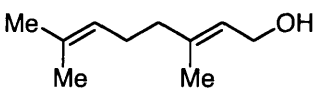	trace[g]

[a] Estimated yields based on uncalibrated ^1H NMR spectra. [b] The reaction only proceeds to ~50% conversion, and the major product seems to be 3-methyl-cyclohex-3-enol. [c] The product obtained is a ~1:1 mixture of Z and E enol ethers. [d] The remainder of the material is mostly unreacted substrate. [e] No product was formed, and palladium black was observed. [f] The amine likely induces reductive elimination/deprotonation of the palladium hydride. [g] There is ~50% conversion to form other olefin-containing products.

We next examined the effect of the phosphine ligand on the reactivity of the palladium-hydride catalysts (Table 4.2). To our initial surprise, only the palladium hydride bearing the very sterically demanding P(*t*-Bu)$_3$ catalyzed the formation of the ketone product (entries 1-4). P(*t*-Bu)$_3$ may be uniquely effective for this reaction, because a tri-coordinate palladium-hydride (LPdHCl) may be the active catalyst in this isomerization process.[97]

Table 4.2. Examination of the effect of the phosphine on L_2PdHCl-catalyzed isomerization of an allylic alcohol.

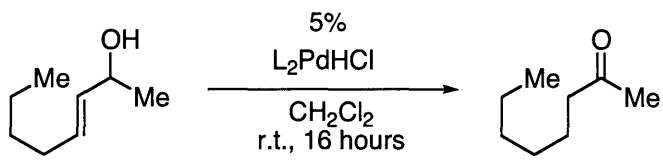

entry	phosphine	GC yield[a]
1	P(*t*-Bu)$_3$	12%
2	PCy$_3$	<2%
3	P(*t*-Bu)$_2$Et	<2%
4	P(*t*-Bu)$_2$Me	<2%

[a] GC yield determined using a calibrated internal standard.

Next, we attempted to determine if the halide ligand could be tuned to increase catalyst reactivity (eq 4.2). We were delighted to see that substituting the chloride ligand with a bromide ligand leads to a higher yield. We also discovered that heating has a beneficial effect on the reaction. Thus, the

[97] Based on a steric argument, it is expected that the equilibrium between L_2PdHCl and LPdHCl plus free L will be shifted toward the LPdHCl species when L is the sterically demanding P(*t*-Bu)$_3$. However, only L_2PdHCl can be observed in solution by ^{1}H NMR.

combination of $(P(t\text{-}Bu)_3)_2PdHBr$ and heat (80 °C) isomerizes the model substrate in 67% yield after a 20-hour reaction (eq 4.2).[98] Unfortunately we were unable to examine the reactivity of $(P(t\text{-}Bu)_3)_2PdHI$, since attempts to cleanly isolate this compound failed. However, we were able to examine the reactivity of a $Pd(P(t\text{-}Bu)_3)_2$ / HI (aq) combination.

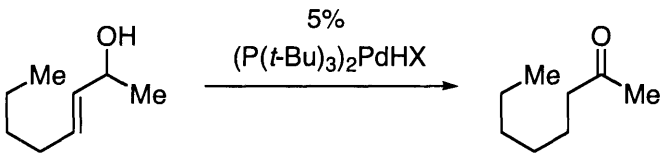

(4.2)

		GC yield
X = Cl	@ r.t.	12 %
Br		36 %
X = Cl	@ 80 °C	56 %
Br		67 %

We were pleased to see that the combination of 5% $Pd(P(t\text{-}Bu)_3)_2$ and 5% HI (aq) furnish a catalyst capable of isomerizing moderately challenging substrates at room temperature (Table 4.3). Incorporation of iodide[99] into the system provides a more a active catalyst; however, a brief solvent survey shows that THF is now preferred over CH_2Cl_2 (entries 1 – 3). This system is also suitable for the rearrangement of a tri-substituted olefin (entry 4). These optimized conditions are more convenient than those utilizing a discrete palladium hydride, since both the palladium(0) complex and the aqueous acid are commercially available. However, the in situ generated catalyst does not lend itself to thorough mechanistic investigation. In light of the many in situ

[98] The reactions were performed in a sealed vial. See experimental for details.
[99] Aqueous HI is employed, and we currently do not fully understand the possible effects of added water. When a combination of $Pd(P(t\text{-}Bu)_3)_2$ and HCl(aq) is employed, the reactivity appears to be similar to that observed for $(P(t\text{-}Bu)_3)_2PdHCl$.

generated catalysts capable of performing the isomerization of allylic alcohols, we chose to postpone further development of this catalytic system.

Table 4.3. Isomerizations performed by a catalyst generated in situ from Pd(P(*t*-Bu)$_3$)$_2$ and HI (aq).

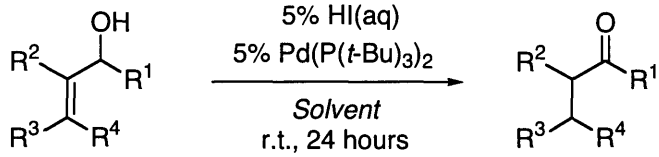

entry	substrate	solvent	GC yield
1	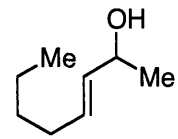	CH_2Cl_2	34%
2		NMP	66%
3		THF	89%
4	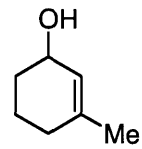	THF	77%

C. Conclusion

We have shown in this preliminary investigation that the isomerization of allylic alcohols can be catalyzed by a bisphosphine palladium-hydride. Initial screens suggest that a sterically demanding phosphine, such as P(*t*-Bu)$_3$, is required to achieve good reactivity. A more active catalyst is furnished when the halide at the metal is changed from Cl to Br, and we have found a catalyst generated from HI (aq) is the best. Under these optimized conditions, moderately challenging substrates, such as 3-methyl-cyclohex-2-enol, can be rearranged to the corresponding ketone (eq 4.3).

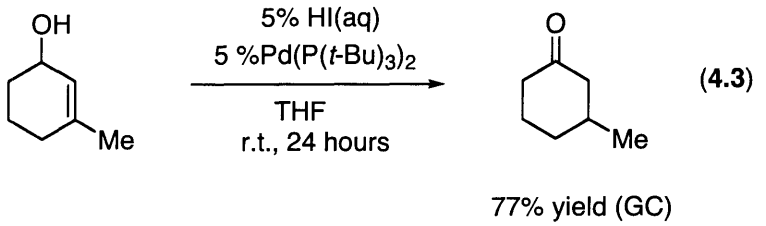

(4.3)

D. Experimental

I. General

All reactions were carried out under an atmosphere of nitrogen or argon in oven-dried glassware with magnetic stirring, unless otherwise indicated.

$Pd(P(t\text{-}Bu)_3)_2$ (Strem and Johnson Matthey), and 55% HI (aq) (Fluka) were used as received. Allyl alcohol, *trans*-3-penten-2-ol, *trans*-2-hexen-1-ol, *trans*-3-octene-2-ol, methallyl alcohol, cyclohex-2-enol, 3-methyl-cyclohex-2-enol, allylbenzyl ether, homoallyl alcohol, propargyl alcohol, homopropargyl alcohol, allyl methyl amine, and geraniol were degassed by bubbling with argon for 20 minutes. L_2PdHX (L = $P(t\text{-}Bu)_3$, $P(t\text{-}Bu)_2Et$, $P(t\text{-}Bu)_2Me$, and PCy_3; X = Cl and Br) was prepared following the general procedure outlined in the experimental of Chapter 3.

THF and CH_2Cl_2 were purified under argon by passage through a neutral alumina column. $CDCl_3$ was purified by distillation from CaH_2. NMP (Aldrich; Sure Seal) was used as received.

GC yields were determined using a calibrated internal standard (dodecane).

II. Isomerization Reactions

General procedure for Table 4.1. Reactions were setup in a nitrogen-filled glovebox. To a vial was added $(P(t\text{-}Bu)_3)_2PdHCl$ (5.0 mg, 0.0091 mmol), and 0.7 mL of $CDCl_3$. Next the substrate (0.18 mmol) was added and the resulting reaction mixture transferred to an NMR tube. The tube was sealed and kept at room temperature for between 3 and 20 hours and then analyzed by ^1H NMR. The yields were estimated by comparing the newly formed aldehyde or ketone peaks versus the remaining starting material and the residual protonated $CHCl_3$ of the solvent. No additional calibrated standard was employed.

Table 4.1, entry 1. The general procedure was followed and the reaction was performed for 3 hours before analysis. The reaction proceeded cleanly with 80 – 90% yield of the desired product.

Table 4.1, entry 2. The general procedure was followed and the reaction was performed for 15 hours before analysis. The reaction proceeded cleanly with 50 – 60% yield of the desired product.

Table 4.1, entry 3. The general procedure was followed and the reaction was performed for 15 hours before analysis. The reaction proceeded cleanly with 50 – 60% yield of the desired product.

Table 4.1, entry 4. The general procedure was followed and the reaction was performed for 3 hours before analysis. The reaction proceeded cleanly with 90 – 100% yield of the desired product.

Table 4.1, entry 5. The general procedure was followed and the reaction was performed for 15 hours before analysis. The reaction proceeded cleanly with 80 – 90% yield of the desired product.

Table 4.1, entry 6. The general procedure was followed and the reaction was performed for 15 hours before analysis. Approximately 50% of the starting material was consumed, and partitioned as 5 – 10% yield of the desired product and 30 – 40% yield of a product assigned as 3-methyl-cyclohex-3-enol.

Table 4.1, entry 7. The general procedure was followed and the reaction was performed for 3 hours before analysis. The reaction proceeded cleanly to produce 90 – 100% yield of a ~ 1:1 mixture of Z and E vinyl ethers.

Table 4.1, entry 8. The general procedure was followed and the reaction was performed for 3 hours before analysis. Between 5 and 10% product was observed, while roughly 80 – 90% of the starting material remained.

Table 4.1, entry 9. The general procedure was followed; however, upon combination of the catalyst and substrate palladium black formed coating the NMR tube (over a period of ~3 hours)

Table 4.1, entry 10. The general procedure was followed; however, upon combination of the catalyst and substrate palladium black formed coating the NMR tube (over a period of ~3 hours).

Table 4.1, entry 11. The general procedure was followed and the reaction was performed for 3 hours before analysis. No desired product was observed.

Table 4.1, entry 12. The general procedure was followed and the reaction was performed for 20 hours before analysis. Only a trace of a new aldehyde peak was observed.

General procedure for Table 4.2, and eq 4.2. Reactions were setup in a nitrogen-filled glovebox. To a vial with a stirbar was added L_2PdHCl (0.015 mmol), and 0.30 mL of CH_2Cl_2. Next the substrate (0.30 mmol) and dodecane (10.0 mg, 0.060 mmol; internal standard) were added. The vial was sealed and stirred at room temperature outside of the glovebox for 16 hours. Then an aliquot was taken from each reaction and filtered through a plug of silica gel with Et_2O. The resulting filtrate was subjected to GC analysis to determine the product yield.

Table 4.2, entry 1. The reaction was setup following the general procedure using $(P(t\text{-}Bu)_3)_2PdHCl$ (8.2 mg, 0.015 mmol) and *trans*-3-octene-2-ol (39 mg, 0.30 mmol). GC analysis showed 12% yield of the desired product.

Table 4.2, entry 2. The reaction was setup following the general procedure using $(PCy_3)_2PdHCl$ (11 mg, 0.015 mmol) and *trans*-3-octene-2-ol (39 mg, 0.30 mmol). GC analysis showed no desired product.

Table 4.2, entry 3. The reaction was setup following the general procedure using $(P(t\text{-}Bu)_2Et)_2PdHCl$ (7.4 mg, 0.015 mmol) and *trans*-3-octene-2-ol (39 mg, 0.30 mmol). GC analysis showed no desired product.

Table 4.2, entry 4. The reaction was setup following the general procedure using $(P(t\text{-}Bu)_2Me)_2PdHCl$ (7.6 mg, 0.015 mmol) and *trans*-3-octene-2-ol (39 mg, 0.30 mmol). GC analysis showed no desired product.

Equation 4.2. The reaction was setup following the general procedure using $(P(t\text{-}Bu)_3)_2PdHCl$ (8.2 mg, 0.015 mmol) or $(P(t\text{-}Bu)_3)_2PdHBr$ (8.9 mg, 0.015 mmol) and *trans*-3-octene-2-ol (39 mg, 0.30 mmol) then performed at either room temperature or 80 °C.

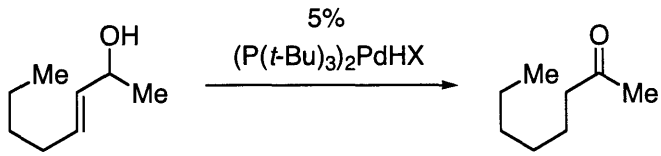

		GC yield
X = Cl	@ r.t.	12 %
Br		36 %
X = Cl	@ 80 °C	56 %
Br		67 %

General procedure for Table 4.3. Reactions were setup in a nitrogen-filled glovebox. To a vial with a stirbar was added $Pd(P(t\text{-}Bu)_3)_2$ (7.7 mg, 0.015 mmol), and 0.30 mL of solvent. Next the substrate (0.30 mmol) and dodecane (10.0 mg, 0.060 mmol; internal standard) were added. The vial was sealed with a septum-cap and removed from the glovebox. Then HI (aq) (0.015 mmol) was added through the septum. The reaction was stirred at room temperature outside of the glovebox for 24 hours. Then an aliquot was taken from each reaction and filtered through a plug of silica gel with Et_2O. The resulting filtrate was subjected to GC analysis to determine the product yield.

Table 4.3, entry 1. The reaction was setup following the general procedure using *trans*-3-octene-2-ol (39 mg, 0.30 mmol) and CH_2Cl_2 as solvent. GC analysis showed 34% yield of the desired product.

Table 4.3, entry 2. The reaction was setup following the general procedure using *trans*-3-octene-2-ol (39 mg, 0.30 mmol) and NMP as solvent. GC analysis showed 66% yield of the desired product.

Table 4.3, entry 3. The reaction was setup following the general procedure using *trans*-3-octene-2-ol (39 mg, 0.30 mmol) and THF as solvent. GC analysis showed 89% yield of the desired product.

Table 4.3, entry 4. The reaction was setup following the general procedure using 3-methyl-cyclohex-2-enol (34 mg, 0.30 mmol) and THF as solvent. GC analysis showed 77% yield of the desired product.

Chapter 5

Mechanistic Investigations of Nickel-Catalyzed Cross-Couplings of Secondary Alkyl Electrophiles

A. Introduction

In recent years, the palladium-catalyzed cross-coupling of unactivated alkyl electrophiles has seen much development.[100] However, these systems are generally limited to primary alkyl-electrophiles. Multiple groups have attempted to address the more challenging problem of cross-coupling unactivated secondary alkyl electrophiles(eq 5.1).[101,102,103,104,105] Clearly further development of this transformation would provide a powerful tool for the synthetic chemist.

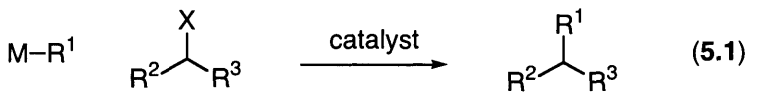

(5.1)

Our group has found success for these cross-coupling reactions by employing nickel-based catalysts.[102] In an attempt to further develop these useful catalytic systems, we have initiated mechanistic studies of these reactions.[106,107] We currently believe that two mechanistic pathways may be operative in our cross-coupling reactions (Scheme 5.1).

---

[100] See the introduction of Chapter 2.
[101] For the cross-coupling of activated secondary alkyl-electrophiles, see: Chen, G. J.; Chen, L. S.; Eapen, K. C. *J. Fluorine Chem.* **1993**, *65*, 59-65.
[102] For nickel-catalyzed couplings, see: (a) Powell, D. A.; Fu, G. C. *J. Am. Chem. Soc.* **2004**, *126*, 7788-7789. (b) Zhou, J.; Fu, G. C. *J. Am. Chem. Soc.* **2004**, *126*, 1340-1341. (c) Zhou, J.; Fu, G. C. *J. Am. Chem. Soc.* **2003**, *125*, 14726-14727.
[103] For iron-catalyzed couplings, see: (a) Nagano, T.; Hayashi, T. *Org. Lett*, **2004**, *6*, 1297-1299. (b) Nakamura, M.; Matsuo, K.; Ito, S.; Nakamura, E. *J. Am. Chem. Soc.* **2004**, *126*, 3686-3687.
[104] For cobalt-catalyzed couplings, see: Tsuji, T.; Yorimitsu, H.; Oshima, K. *Angew. Chem. Int. Ed.* **2002**, *41*, 4137-4139.
[105] For copper-catalyzed couplings, see: (a) Berkowitz, W. F.; Wu, Y. *Tetrahedron Lett.* **1997**, *38*, 3171-3174. (b) Nunomoto, S.; Kawakami, Y.; Yamashita, Y. *J. Org. Chem.* **1983**, *48*, 1912-1914.
[106] Preliminary studies of the reaction mechanism have been performed using substrate-based probes. For details see, footnote 102.

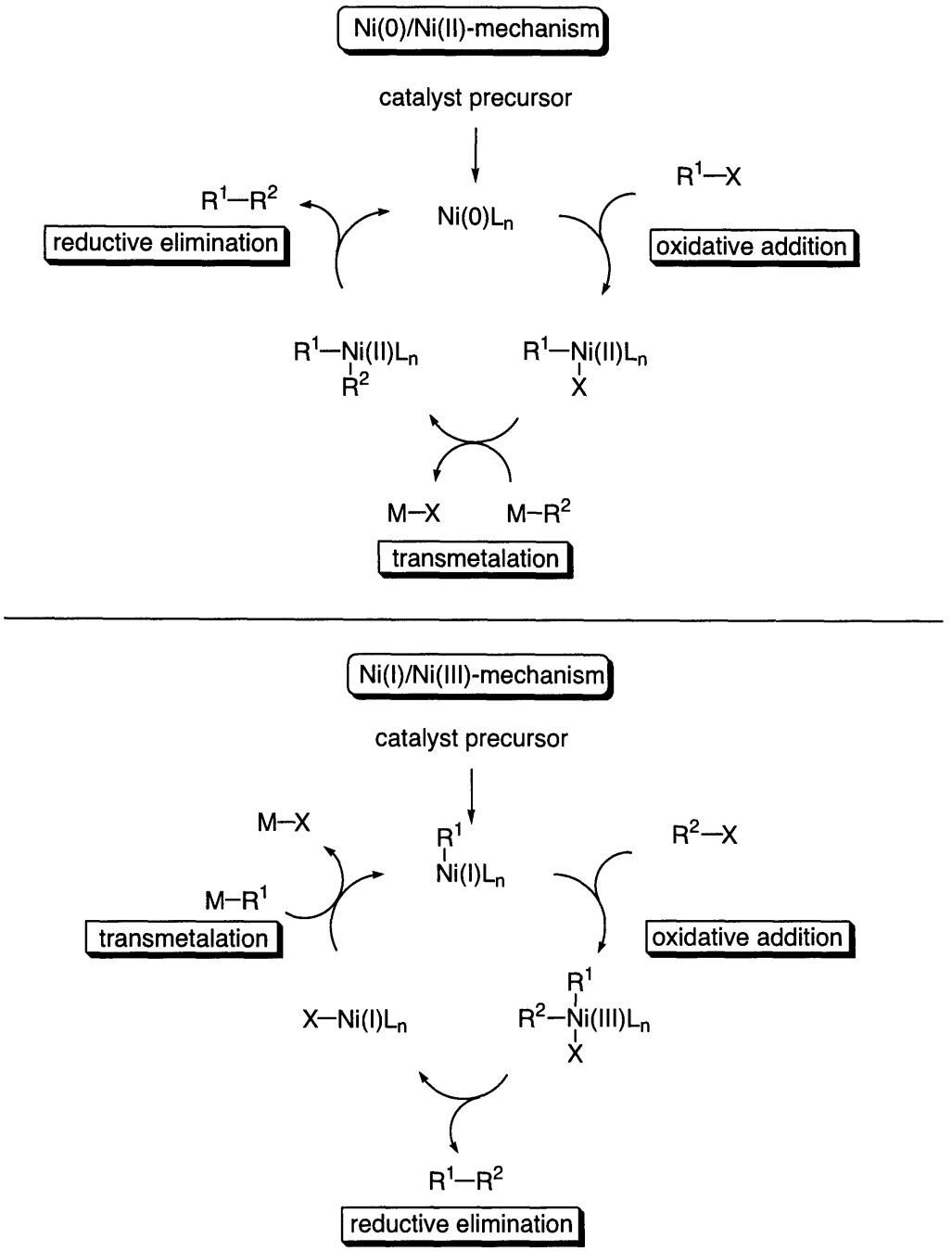

Scheme 5.1. Two possible catalytic cycles for the nickel-catalyzed coupling of unactivated alkyl electrophiles.

[107] Mechanistic studies relevant to nickel-catalyzed cross-coupling of unactivated alkyl-electrophiles have been performed by Vicic and co-workers. For details, see: (a) Anderson, T. J.; Jones, G. D.; Vicic, D. A. *J. Am. Chem. Soc.* **2004**, *126*, 8100-8101. (b) Anderson, T. J.; Vicic, D. A. *Organometallics* **2004**, *23*, 623-625.

In the first mechanism (Ni(0)/Ni(II)-mechanism; Scheme 5.1, top), the catalytic cycle resembles the commonly accepted pathway for palladium-catalyzed cross-couplings. While each of the steps could proceed either through polar or radical type mechanisms, we would expect the resting state of the catalyst to be one of the intermediates illustrated. In the second mechanism (Ni(I)/Ni(III)-mechanism; Scheme 5.1, bottom), the resting state of the catalyst is expected to have an odd electron count, and thus be paramagnetic. The intermediates encountered in both of these mechanistic proposals have support in the literature.[108,109]

To date our group has been able to perform the nickel-catalyzed cross-coupling of unactivated secondary electrophiles using both bidentate and tridentate amine ligands (Figure 5.1).[102] Interestingly, use of the tridentate ligand *s*-Bu-Pybox furnishes a system that couples secondary alkyl electrophiles and *alkyl* nucleophiles (Procedure A); whereas, a catalyst bearing a bidentate ligand such as bathophenanthroline (BP) is effective for coupling secondary alkyl electrophiles and *aryl* nucleophiles (Procedure B and C). Another observation is that for certain procedures the reaction is very sensitive to the choice of catalyst precursor (Figure 5.2). For example, Procedure B fails when $Ni(cod)_2$ is replaced with $NiBr_2$, whereas in procedure C, $Ni(cod)_2$ and $NiBr_2$ give comparable yields of product. This may suggest that these two procedures operate with different mechanisms.

---

[108] For early studies of nickel-catalyzed cross-couplings of aryl electrophiles, see: (a) Smith, G.; Kochi, J. K. *J. Organomet. Chem.* **1980**, *198*, 199-214. (b) Tsou, T. T.; Kochi, J. K. *J. Am. Chem. Soc.* **1979**, *101*, 6319-6332. (c) Tsou, T. T.; Kochi, J. K. *J. Am. Chem. Soc.* **1979**, *101*, 7547-7560. (c) Morrell, D. G.; Kochi, J. K. *J. Am. Chem. Soc.* **1975**, *97*, 7262-7270. (d) Elson, I. H.; Morrell, D. G.; Kochi, J. K. *J. Organomet. Chem.* **1975**, *84*, C7-C10.

[109] For electrochemical studies in which Ni(0), Ni(I), Ni(II), and Ni(III) intermediates have been detected in nickel-catalyzed methods, see: (a) Amatore, C.; Jutand, A. *J. Am. Chem. Soc.* **1991**, *113*, 2819-2825. (b) Amatore, C.; Jutand, A. *Organometallics* **1988**, *7*, 2203-2214.

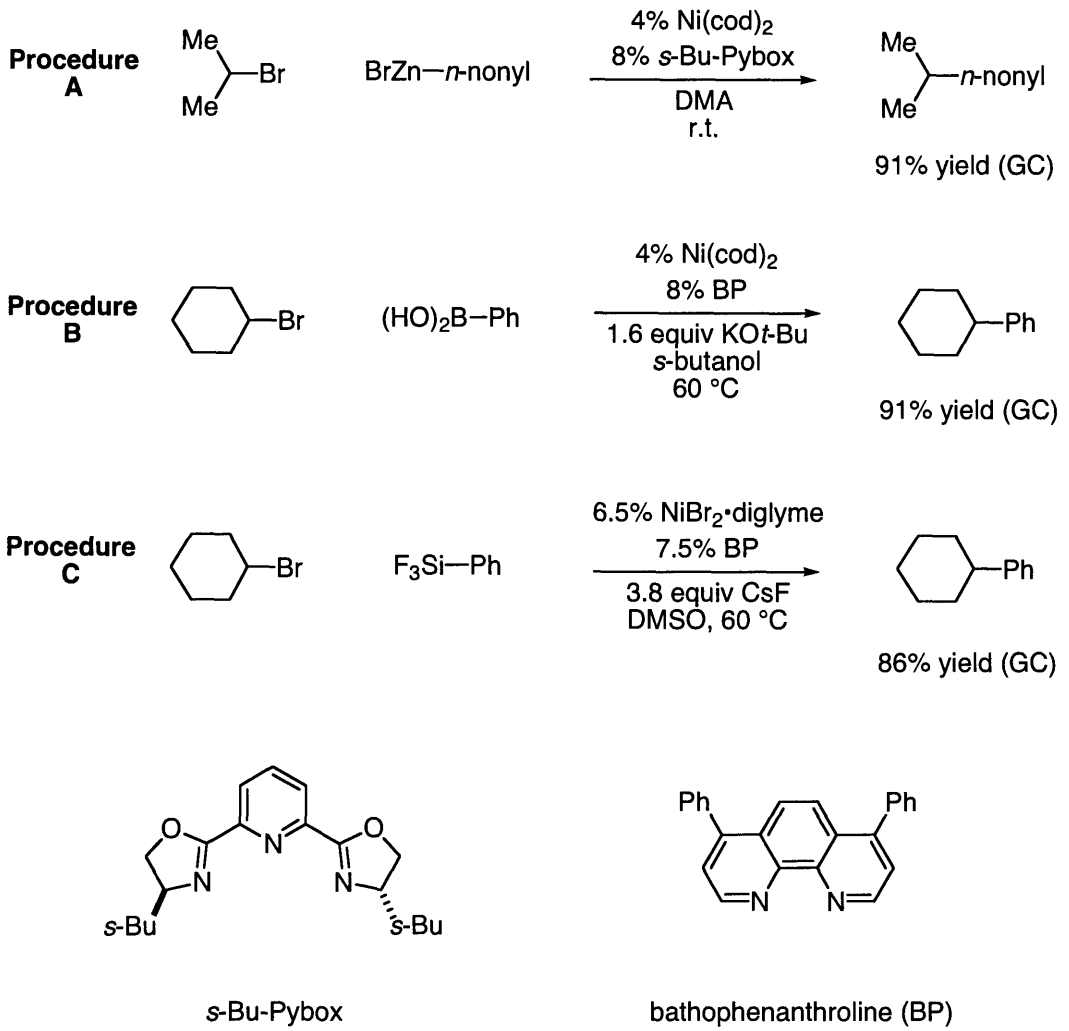

Figure 5.1. Summary of nickel-catalyzed cross-couplings of secondary alkyl electrophiles developed in the Fu group.

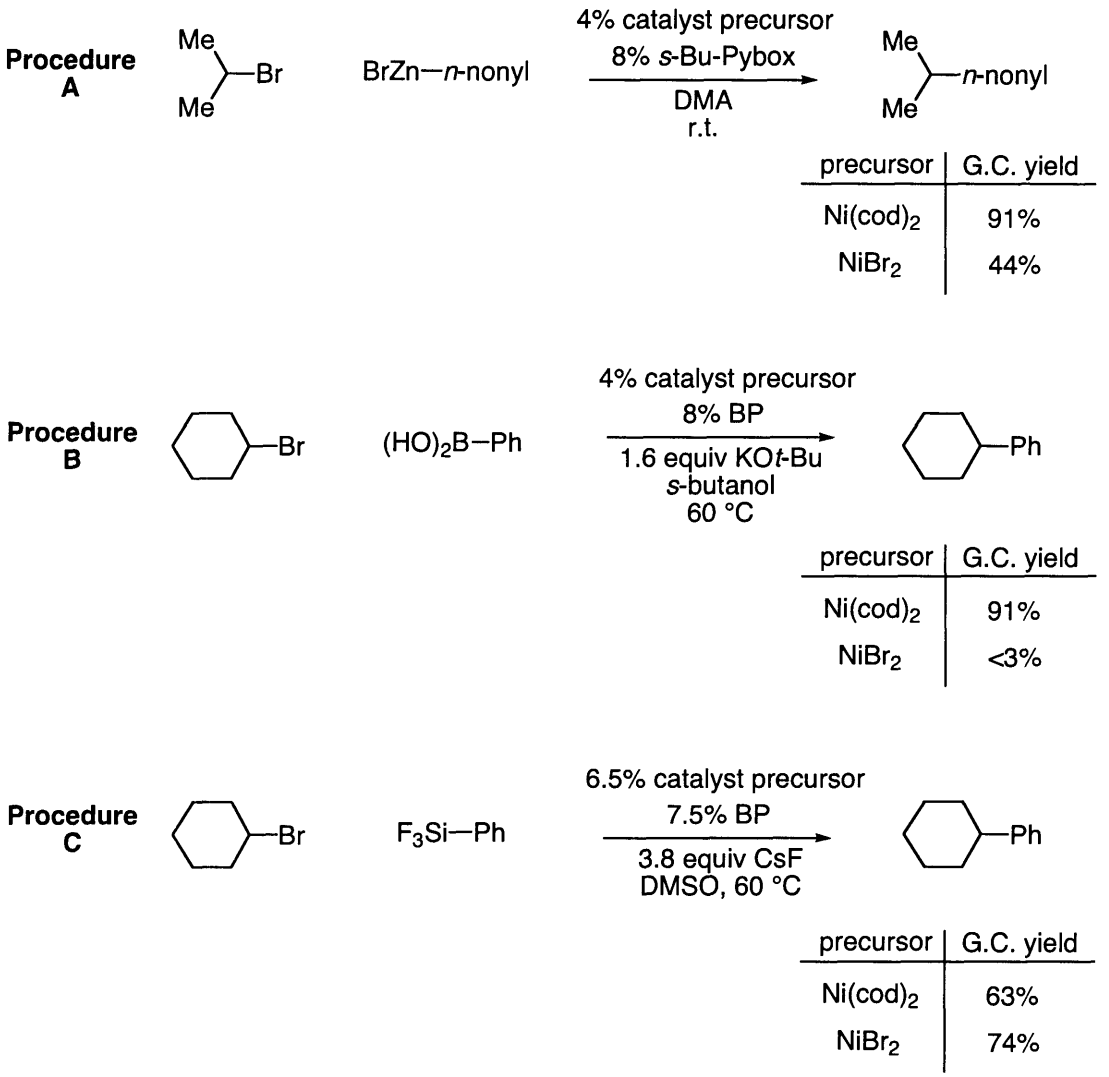

Figure 5.2. Effect of catalyst precursors on cross-coupling efficiency.

Our initial goal was to synthesize discrete nickel-ligand complexes that are competent catalysts for the reactions described above. More specifically, we sought to prepare compounds that might be intermediates (for our working hypotheses, see Scheme 5.1) and test their kinetic and chemical competence.[110]

[110] This has been performed by Vicic and coworkers in the context of a nickel-catalyzed cross-coupling of secondary alkyl iodides. See ref. 107a.

Thus we attempted the syntheses of relevant nickel complexes, which are illustrated in Figure 5.3.

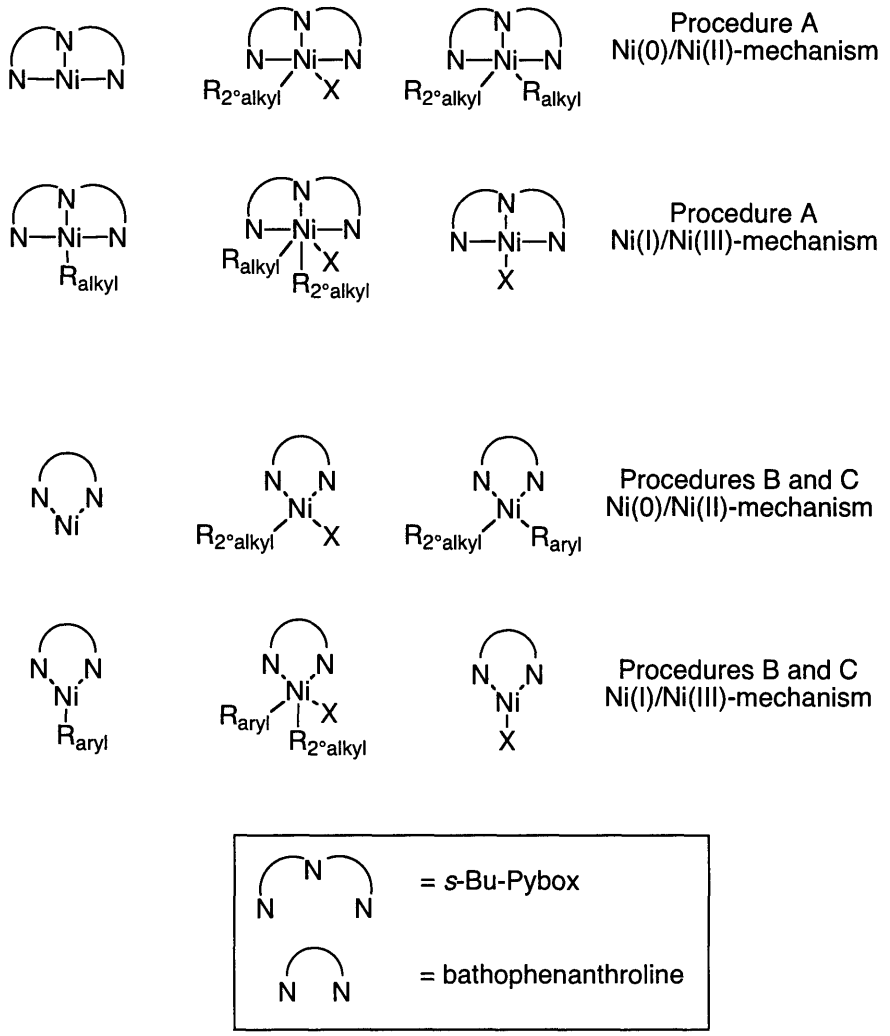

Figure 5.3. Possible intermediates in the nickel-catalyzed cross-coupling of secondary alkyl-electrophiles.

B. Results and Discussion

We have attempted to prepare relevant nickel complexes bearing either *s*-Bu-Pybox or bathophenanthroline (BP). Due to the relatively high cost of BP, we have also attempted to make nickel complexes using 2,2'-Bipyridine (bpy) as a BP surrogate. Many of the attempts to synthesize the compounds illustrated in Figure 5.3 have failed, either due to the inherent instability of the target compounds or to unsuitable reaction conditions. Below are described noteworthy attempts to synthesize relevant compounds, as well as successful syntheses of less pertinent compounds.[111]

Complexes bearing *s*-Bu-Pybox (Procedure A)

We first attempted to synthesize a Ni(0) complex bearing *s*-Bu-Pybox, hoping ultimately to test the catalytic competence of such a complex. We were aware that a simple (*s*-Bu-Pybox)Ni complex was unlikely, since it is coordinatively unsaturated; however, we thought it possible that the vacant coordination site could be occupied by cyclooctadiene (cod), since $Ni(cod)_2$ is a competent catalyst precursor (Figure 5.4). Although combination of $Ni(cod)_2$ and *s*-Bu-Pybox in various solvents (e.g., Et_2O, THF, DMF, and DMA) led to a rapid

[111] Notes: Use of ^1H NMR as a spectroscopic tool in these studies was hampered by the fact that some of the synthetic targets are paramagnetic, thus furnishing broad and unintelligible spectra. Even the diamagnetic targets exhibited broadened ^1H NMR spectra, which is presumably due to traces of paramagnetic impurities. Thus, we focused on isolating compounds and characterizing them crystallographically.

color change,[112] suggesting the formation of a new nickel complex, no well-defined single-component solid could be isolated.

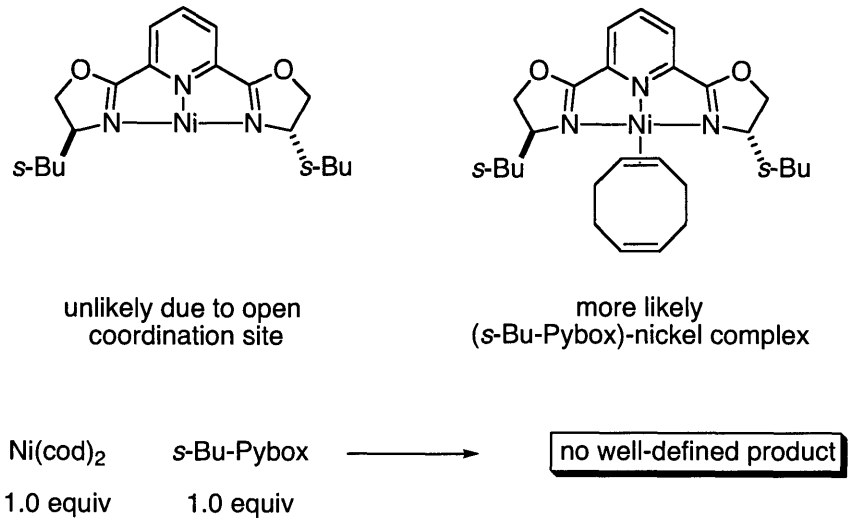

Figure 5.4. Possible Ni(0) complexes bearing *s*-Bu-Pybox.

Next we attempted to prepare a Ni(II) compound bearing *s*-Bu-Pybox. Thus, we combined 1 equivalent each of $NiBr_2$ and *s*-Bu-Pybox in various solvents at elevated temperature and found that a new compound could be isolated (Figure 5.5). We were able to acquire a low resolution X-ray crystal structure, and to our surprise the metal complex bore two *s*-Bu-Pybox ligands! We believed, due to the lack of coordinative unsaturation, this compound could not serve as an active catalyst, but could possibly represent a reservoir for the catalyst.[113] Hoping to synthesize more pertinent compounds, we next attempted to prepare an oxidative addition adduct between "(*s*-Bu-Pybox)Ni(0)" and an organic electrophile.

[112] $Ni(cod)_2$ is a yellow crystalline-solid. When $Ni(cod)_2$ is added to a colorless solution of *s*-Bu-Pybox, a deep blue-purple color results.
[113] We have not tested the catalytic activity of this compound.

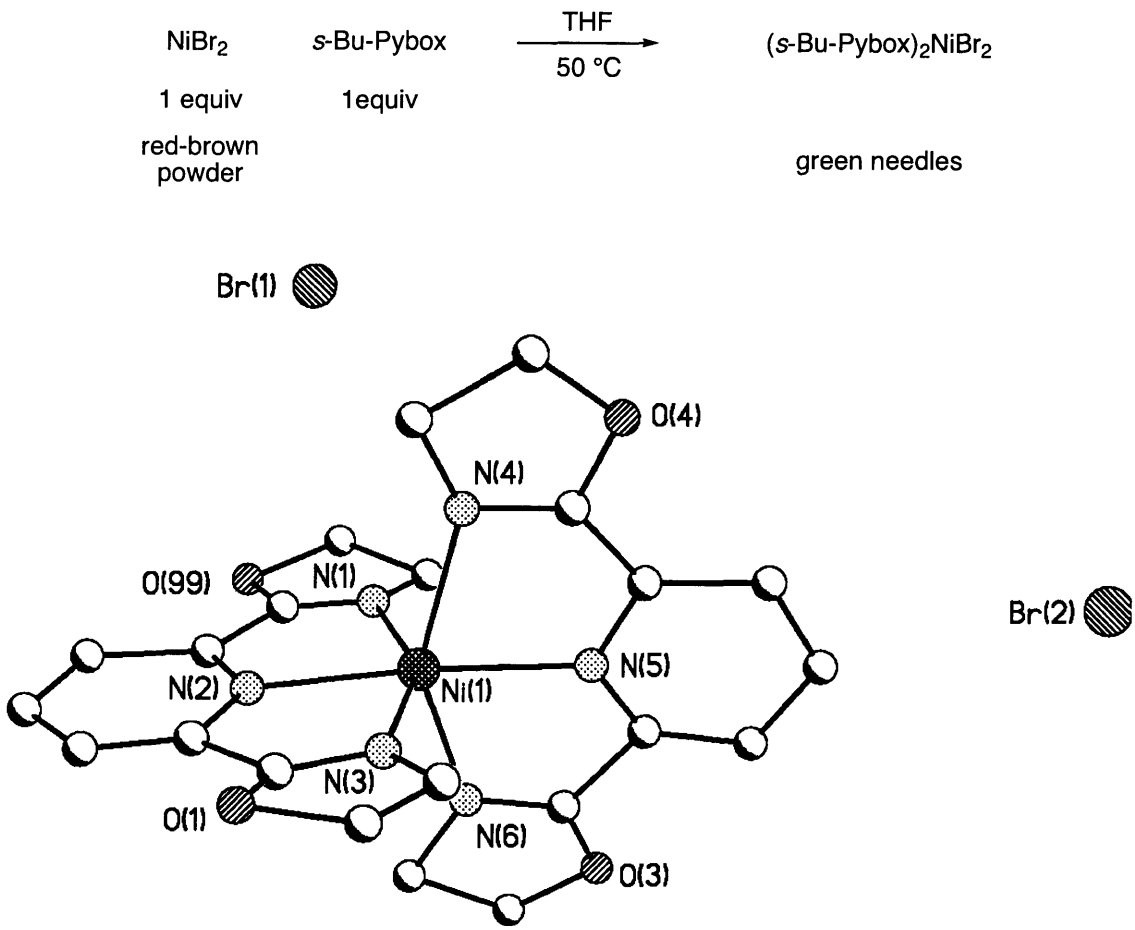

Figure 5.5. Low resolution X-ray structure of (*s*-Bu-Pybox)$_2$NiBr$_2$ (*s*-Bu groups are omitted for clarity).

Thus, we combined equimolar amounts of Ni(cod)$_2$ and *s*-Bu-Pybox to generate "(*s*-Bu-Pybox)Ni(0)" in situ. Next we added an array of electrophiles, hoping to isolate an oxidative-addition adduct (Figure 5.6). Upon addition of many of the electrophiles, the reaction instantly changed color from blue-purple[114] to orange-red. The reactions were then cooled to –35 °C and layered with pentanes in an attempt to induce crystallization of the products. After an extended time, the reaction mixtures became dark green, which is possibly due

[114] Indicative of the putative "(*s*-Bu-Pybox)Ni(0)".

to formation of (*s*-Bu-Pybox)$_2$NiX$_2$ via disproportionation reactions. No further attempt was made to isolate the reaction products.

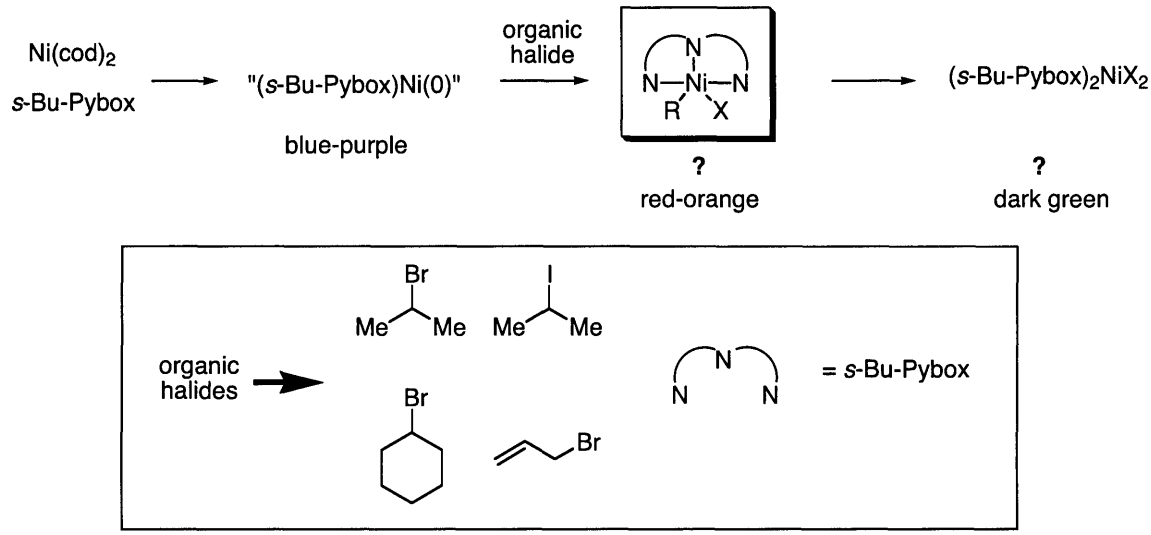

Figure 5.6. Attempts to isolate an oxidative-addition adduct bearing *s*-Bu-Pybox.

However, upon addition of 1-bromo-2-cyclohexene to the reaction mixture, the blue-purple color persisted, and a purple crystal could be isolated for X-ray analysis (Figure 5.7). To our surprise, the low resolution X-ray structure was not of a Ni(II) oxidative addition adduct, but rather a Ni(I) halide![115] Since the electrophile used to generate this novel nickel species was activated (allylic) rather than one of our targeted class of simple unactivated secondary electrophiles, we chose to postpone further investigations of this compound, and to shift our attention to compounds relevant to procedures B and C.

[115] Vicic has acquired evidence that suggests a Ni(I) species may play an important role in some nickel-catalyzed cross-couplings. See ref. 107a.

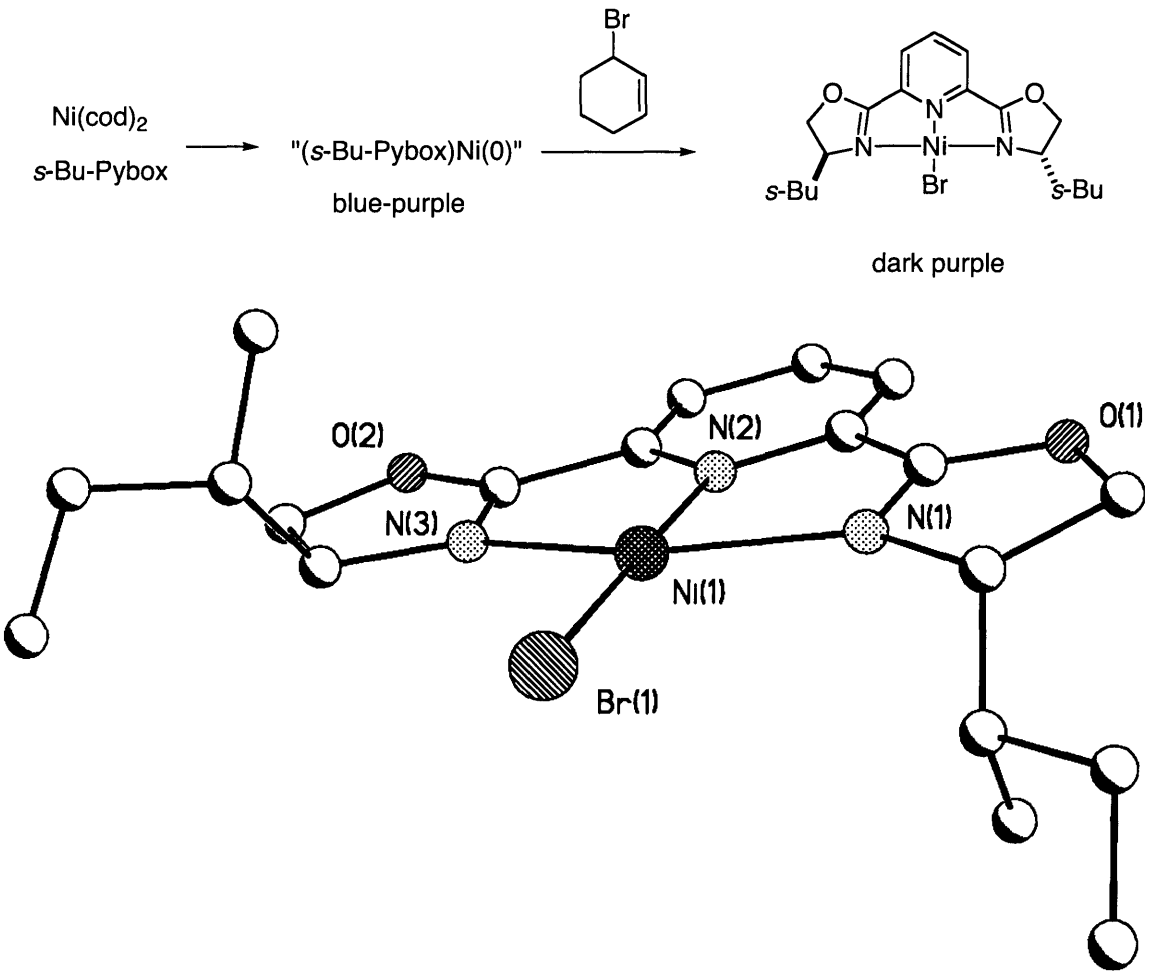

Figure 5.7. Unexpected isolation of a Ni(I) species instead of an oxidative addition adduct.

Complexes Bearing 2,2′-Bipyridine (Procedures B and C)

As mentioned above, we employed 2,2′-biypyridine (bpy) as a model ligand for bathophenanthroline, due to its relatively low cost. Again, we attempted to isolate oxidative-addition adducts by adding a diverse array of organic electrophiles to a blue-purple solution of in situ generated "(bpy)Ni(0)" (Figure 5.8). Upon addition of the organic electrophiles, the reaction again

instantly turned red-orange and then dark green in color. The only exception was when an acid chloride was employed, which led to the isolation of a dark-red powder that is presumably the nickel-acyl compound (eq 5.2). Thus, relevant organonickel compounds could not be isolated for further study.

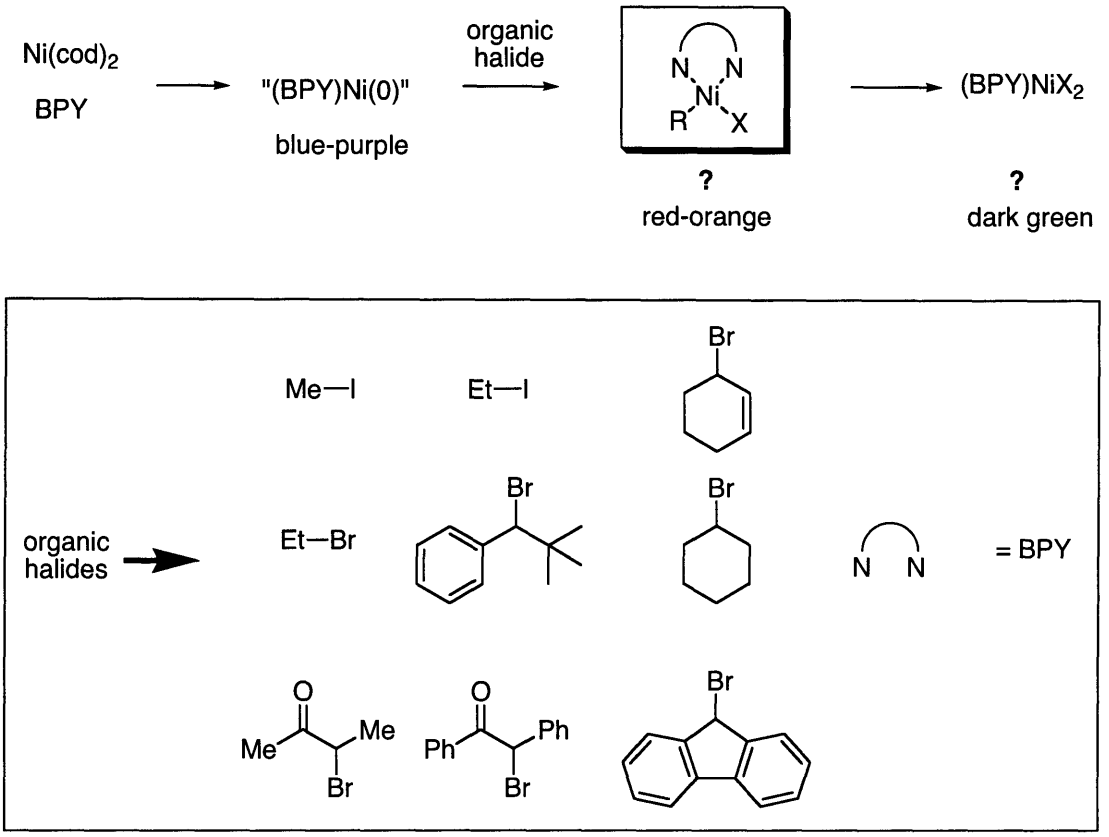

Figure 5.6. Attempts to isolate an oxidative-addition adduct bearing bpy.

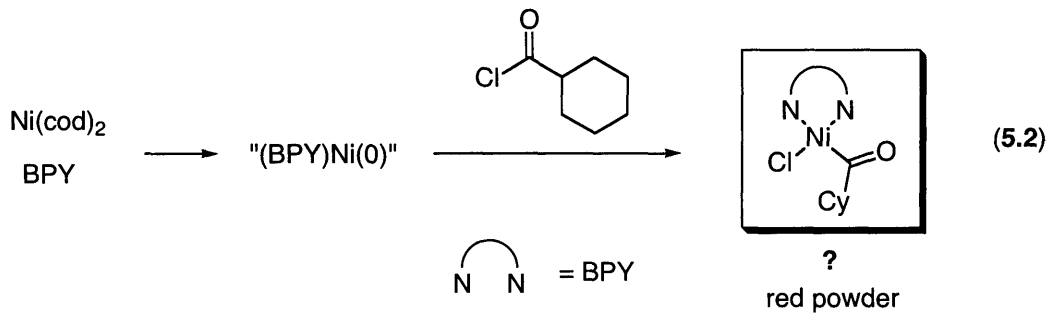

(5.2)

C. Conclusion

Gaining a better understanding of the mechanism(s) of nickel-catalyzed cross-coupling reactions of unactivated secondary alkyl electrophiles continues to represent a worthy goal. However, initial attempts to synthesize relevant intermediates in the catalytic cycle have been unsuccessful. Further study in this area is underway.

D. Experimental

I. General

All reactions were carried out under an atmosphere of nitrogen or argon in oven-dried glassware with magnetic stirring, unless otherwise indicated.

$Ni(cod)_2$ (Strem), $NiBr_2$ (Strem), 2,2'-bipyridine (Aldrich), DMA (Aldrich), DMF (Aldrich), and pentanes (Aldrich) were used as received. *s*-Bu-Pybox was prepared according to published methods.[116]

THF and Et_2O were purified under argon by passage through a neutral alumina column.

[116] Zhou, J.; Fu, G. C. *J. Am. Chem. Soc.* **2003**, *125*, 14726-14727.

II. Synthesis of Nickel Complexes

Synthesis of "(*s*-Bu-Pybox)Ni(0)". The reaction was conducted in a nitrogen-filled glove box. To a vial with a stir-bar was added $Ni(cod)_2$ (50 mg, 0.18 mmol) and *s*-Bu-Pybox (60 mg, 0.18 mmol). Next these two components were dissolved by adding 2.0 mL of Et_2O. The reaction was stirred at room temperature and after 15 minutes the color was dark blue-purple. The reaction was stirred for an additional 45 minutes and then the solvent was removed by vacuum to furnish a blue-purple solid mixed with streaks of a white solid (*s*-Bu-Pybox?). The isolated solid was dissolved in pentanes to give a suspension of a white powder in a blue-purple solution. The mixture was filtered and the solvent was removed from the filtrate to once again provide a blue-purple solid mixed with streaks of a white solid. The mixture was once again dissolved in pentanes to afford a suspension that was filtered. The solvent was once again removed from the filtrate by vacuum to give an orange-red solid. The reaction was abandoned at this point.

Synthesis of (*s*-Bu-Pybox)$_2$NiBr$_2$ (Figure 5.5). The reaction was conducted in a nitrogen-filled glovebox. To a vial with a stir-bar was added $NiBr_2$ (22 mg, 0.10 mmol) and *s*-Bu-Pybox (33 mg, 0.10 mmol). Next 1 mL of THF was added to furnish an orange-brown suspension. The vial was sealed and stirred outside of the glovebox at 50 °C. After 3 hours of heating the reaction was cooled to room temperature and taken back into the glovebox. The mixture was filtered and the filtrate layered with pentanes and cooled to –35 °C to afford green needles that were analyzed by X-ray crystallography (see section III).

Attempted Synthesis of an Oxidative-Addition Adduct. Numerous approaches were tried to prepare an oxidative-addition adduct of nickel bearing *s*-Bu-Pybox or bpy; below is a representative procedure.

In a nitrogen-filled glove box, $Ni(cod)_2$ (42 mg, 0.15 mmol) and *s*-Bu-Pybox (50 mg, 0.15 mmol) were added to a stir-bar containing vial. Next 2mL of THF was added and the mixture was stirred for 15 minutes at room temperature to afford a blue-purple solution. Then cyclohexyl bromide (25 mg, 0.15 mmol) was added and the reaction stirred at room temperature. After 1 hour the reaction the was a deep red color. The reaction was layered with pentanes and cooled to –35 °C. After approximately 12-16 hours the mixture was a dark green color and a small amount of green powder was isolated.

Synthesis of (*s*-Bu-Pybox)NiBr. In a nitrogen-filled glove box, $Ni(cod)_2$ (20 mg, 0.073 mmol) and *s*-Bu-Pybox (24 mg, 0.073 mmol) were added to a stir-bar containing vial. Next 2mL of THF was added and the mixture was stirred for 15 minutes at room temperature to afford a blue-purple solution. Then 1-bromo-2-cyclohexen (12 mg, 0.073 mmol) was added and the reaction stirred at room temperature. After 1 hour the reaction the was still a blue-purple color, but no longer homogeneous. Next 1 mL of THF was added to dissolve most of the mixture and then the reaction was filtered. The filtrate was cooled to –35 °C. Purple plate-like crystals were isolated and analyzed by X-ray crystallography (see section III).

III. X-ray Crystallographic Data

The X-ray crystal structures of both (*s*-Bu-Pybox)$_2$NiBr$_2$ and (*s*-Bu-Pybox)NiBr are severely disordered and have not been refined anisotropically, nor have the hydrogen atoms added to the model. Relevant data tables are presented in Appendix A.

Education

Ph. D., Organic Chemistry, Massachusetts Institute of Technology, August 2004
Thesis title: "Catalytic Enantioselective Synthesis of Oxindoles and Benzofuranones bearing a Quaternary Stereocenter and Reactions of Palladium Bisphosphine Complexes Relevant to Catalytic C-C Bond Formation"
Adviser: Professor Gregory C. Fu

B.S., Chemistry, University of North Carolina–Chapel Hill
Adviser: Professor Joseph L. Templeton

Awards and Scholarships

2003	MIT-Wyeth Scholar
2002	Recipient of ACS Division of Organic Chemistry Graduate Fellowship, s ponsored by Abbott Laboratories
1995 – 1999	William Davie Scholarship, University of North Carolina – Chapel Hill

Publications

(5) **Elucidating Reactivity Differences in Palladium-Catalyzed Coupling Processes: The Chemistry of Palladium Hydrides**
Accepted.
Hills, I. D.; Fu, G. C.

(4) **Toward an Improved Understanding of the Unusual Reactivity of Pd^0/Trialkylphosphine Catalysts in Cross-Couplings of Alkyl Electrophiles: Quantifying the Factors That Determine the Rate of Oxidative Addition**
Angew. Chem. Int. Ed. **2003**, *42*, 5749-5752.
Hills, I. D.; Netherton, M. R.; Fu, G. C.

(3) **Catalytic Enantioselective Synthesis of Oxindoles and Benzofuranones that Bear a Quaternary Stereocenter**
Angew. Chem. Int. Ed. **2003**, *42*, 3921-3924.
Hills, I. D.; Fu, G. C.

(2) **Boronic Acids: New Coupling Partners in Room-Temperature Suzuki Reactions of Alkyl Bromides. Crystallographic Characterization of an Oxidative-Addition Adduct Generated Under Remarkably Mild Conditions**
J. Am. Chem. Soc. **2002**, *124*, 13662-13663.
Kirchhoff, J. H.; Netherton, M. R.; Hills, I. D.; Fu, G. C.

(1) **The First General Method for the Synthesis of Transition-Metal π Complexes of an Electronically Diverse Family of 1,2-Azaborolyls**
Organometallics **2002**, *21*, 4323-4325.
Liu, S.-Y.; Hills, I. D.; Fu, G. C.

Appendix A

X-ray Crystal Structure Data

02133ihs (Table 1.2, entry 3)

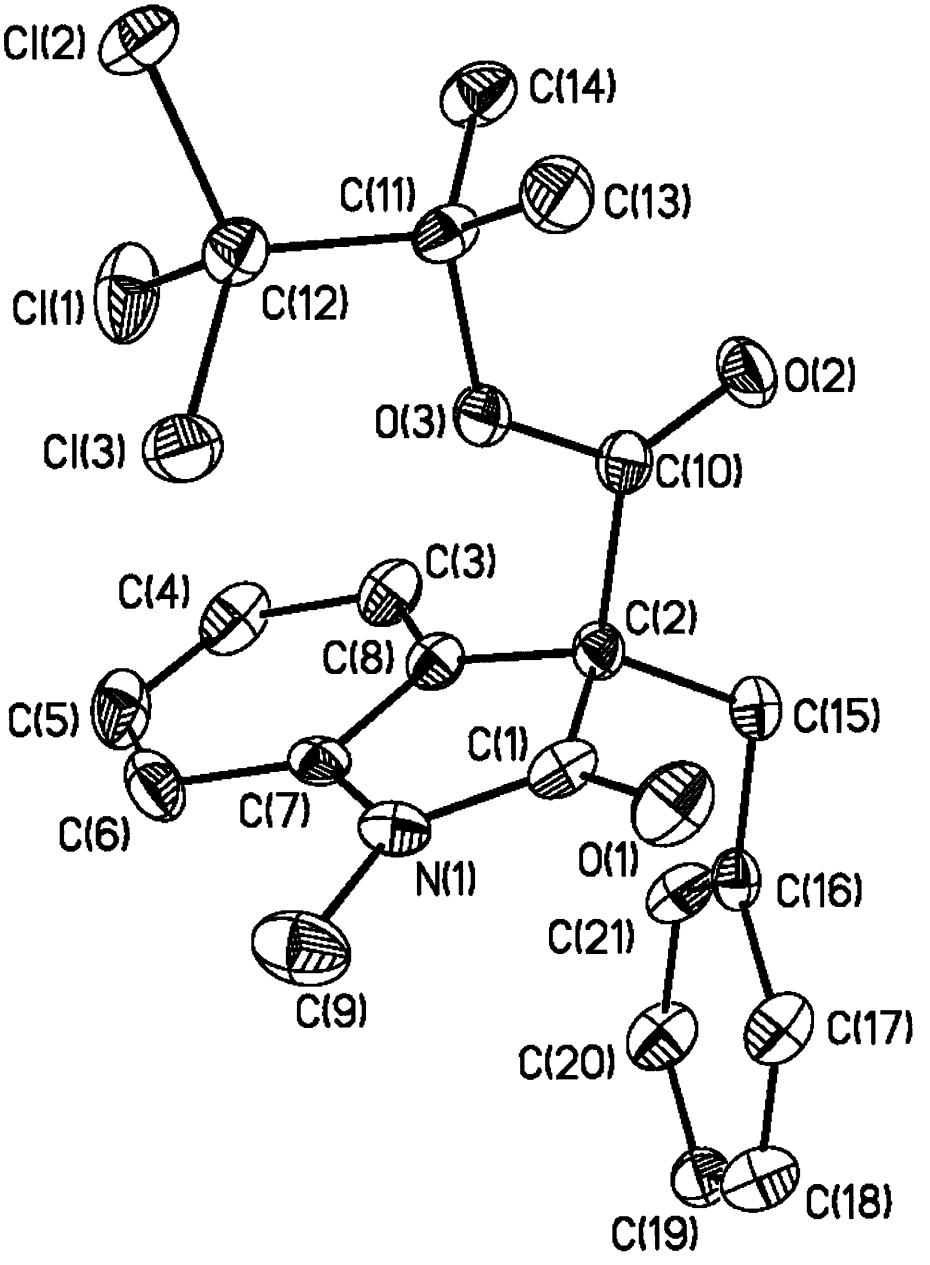

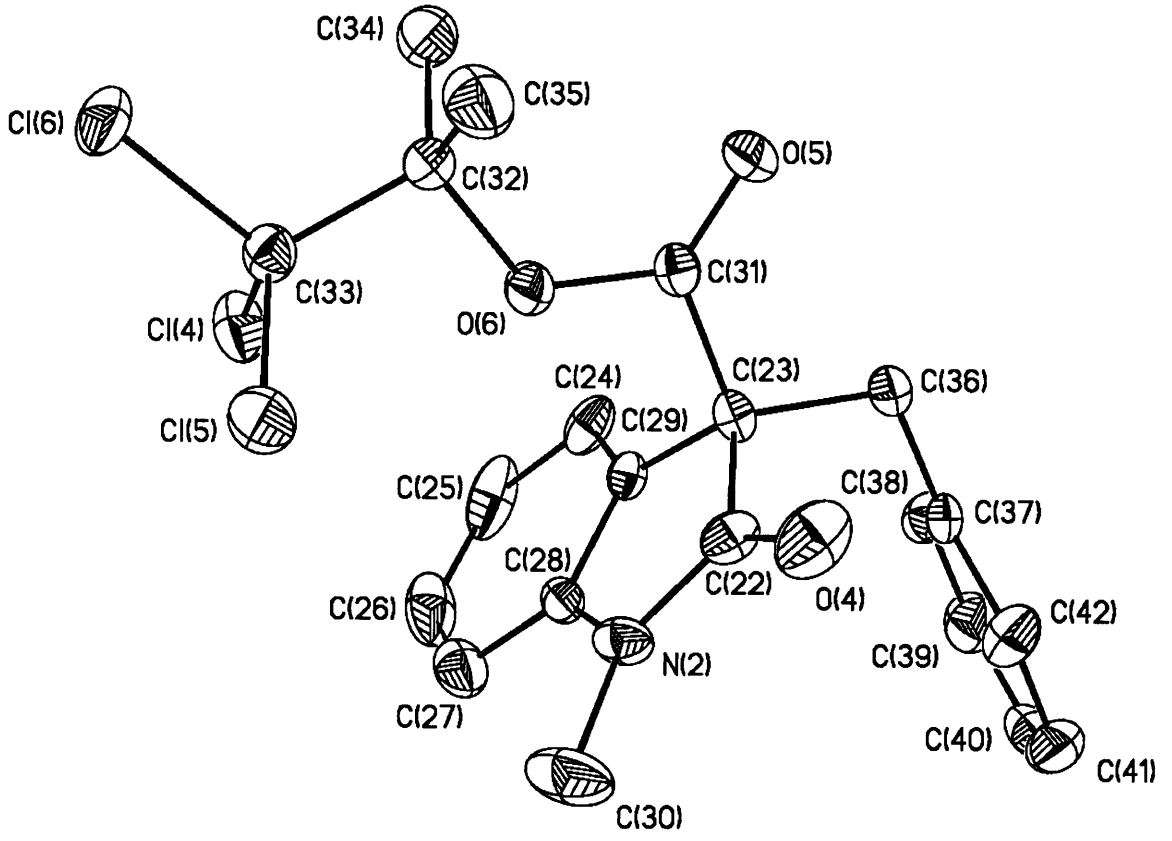
C(34)
C(35)
Cl(6)
C(32)
O(5)
C(33)
C(31)
Cl(4)
O(6)
C(24)
C(23)
C(36)
Cl(5)
C(29)
C(25)
C(38)
C(37)
C(28)
C(22)
O(4)
C(26)
C(42)
N(2)
C(39)
C(27)
C(40)
C(41)
C(30)

Table 1. Crystal data and structure refinement for 02133IHs.

Identification code	02133ihs
Empirical formula	C21 H20 Cl3 N1 O2
Formula weight	220.37
Temperature	183(2) K
Wavelength	0.71073 Å
Crystal system	Monoclinic
Space group	P2(1)
Unit cell dimensions	a = 9.0721(5) Å α = 90°. b = 24.4432(14) Å β = 101.8800(10)°. c = 9.6326(6) Å γ = 90°.
Volume	2090.3(2) $Å^3$
Z	4
Density (calculated)	0.700 Mg/m^3
Absorption coefficient	0.230 mm^{-1}
F(000)	456
Crystal size	0.45 x 0.25 x 0.15 mm^3
Theta range for data collection	2.29 to 23.27°.
Index ranges	-10<=h<=10, -24<=k<=27, -9<=l<=10
Reflections collected	8364
Independent reflections	5076 [R(int) = 0.0305]
Completeness to theta = 23.27°	99.6 %
Refinement method	Full-matrix least-squares on F^2
Data / restraints / parameters	5076 / 1 / 512
Goodness-of-fit on F^2	1.107
Final R indices [I>2sigma(I)]	R1 = 0.0454, wR2 = 0.1132
R indices (all data)	R1 = 0.0465, wR2 = 0.1140
Absolute structure parameter	0.06(7)
Extinction coefficient	0.0000(4)
Largest diff. peak and hole	0.387 and -0.205 $e.Å^{-3}$

Table 2. Atomic coordinates (x 10^4) and equivalent isotropic displacement parameters ($Å^2$x 10^3) for 02133IHs. U(eq) is defined as one third of the trace of the orthogonalized U^{ij} tensor.

	x	y	z	U(eq)
Cl(1)	7670(2)	7772(1)	2433(2)	58(1)
Cl(2)	8349(1)	7302(1)	-99(1)	40(1)
Cl(3)	7659(1)	6609(1)	2084(1)	50(1)
Cl(4)	-2795(1)	5035(1)	2431(1)	48(1)
Cl(5)	-2667(2)	3865(1)	2560(1)	51(1)
Cl(6)	-3245(1)	4476(1)	4934(1)	51(1)
O(1)	3287(4)	6091(1)	2940(4)	48(1)
O(2)	2431(3)	7371(2)	779(3)	47(1)
O(3)	4841(3)	7150(1)	1666(3)	36(1)
O(4)	1830(5)	3601(2)	1095(4)	55(1)
O(5)	2570(4)	4581(2)	3900(3)	51(1)
O(6)	88(3)	4520(1)	2914(3)	34(1)
N(1)	5109(4)	6529(2)	4558(4)	33(1)
N(2)	-94(4)	4096(2)	-242(4)	35(1)
C(1)	3851(5)	6502(2)	3540(5)	33(1)
C(2)	3227(5)	7092(2)	3243(4)	29(1)
C(3)	4450(5)	7973(2)	4539(5)	39(1)
C(4)	5680(6)	8169(2)	5537(5)	44(1)
C(5)	6767(6)	7819(3)	6231(5)	48(1)
C(6)	6686(5)	7257(3)	5974(4)	44(1)
C(7)	5443(5)	7073(2)	5004(4)	28(1)
C(8)	4344(5)	7421(2)	4273(4)	29(1)
C(9)	6038(7)	6054(2)	5074(6)	56(2)
C(10)	3400(5)	7227(2)	1726(4)	29(1)
C(11)	5500(5)	7260(2)	448(4)	32(1)
C(12)	7208(5)	7238(2)	1167(4)	34(1)

C(13)	5090(6)	6806(2)	-630(5)	44(1)
C(14)	5077(6)	7822(2)	-175(6)	41(1)
C(15)	1569(4)	7135(2)	3352(4)	31(1)
C(16)	1315(5)	7025(2)	4828(4)	29(1)
C(17)	1098(5)	6497(2)	5287(5)	40(1)
C(18)	875(6)	6400(2)	6633(6)	46(1)
C(19)	848(5)	6828(2)	7559(5)	43(1)
C(20)	1054(6)	7355(2)	7129(5)	44(1)
C(21)	1270(5)	7446(2)	5768(5)	40(1)
C(22)	1195(5)	4029(2)	733(5)	32(1)
C(23)	1721(5)	4596(2)	1342(4)	27(1)
C(24)	391(6)	5527(2)	516(5)	39(1)
C(25)	-885(7)	5749(3)	-390(7)	58(2)
C(26)	-1921(6)	5427(3)	-1217(6)	59(2)
C(27)	-1766(6)	4869(3)	-1246(5)	46(1)
C(28)	-520(5)	4648(2)	-398(4)	31(1)
C(29)	550(5)	4970(2)	480(4)	26(1)
C(30)	-1005(7)	3638(3)	-933(6)	64(2)
C(31)	1563(5)	4577(2)	2882(5)	28(1)
C(32)	-480(5)	4500(2)	4215(4)	32(1)
C(33)	-2191(5)	4474(2)	3560(5)	34(1)
C(34)	-90(6)	5024(2)	5070(6)	47(1)
C(35)	87(6)	3998(3)	5061(6)	55(2)
C(36)	3382(5)	4722(2)	1284(5)	37(1)
C(37)	3623(5)	4791(2)	-214(5)	32(1)
C(38)	3679(6)	5306(2)	-760(5)	41(1)
C(39)	3891(6)	5383(3)	-2134(6)	53(2)
C(40)	4054(6)	4945(3)	-2945(5)	54(2)
C(41)	4001(6)	4430(3)	-2422(6)	61(2)
C(42)	3790(6)	4349(2)	-1038(5)	45(1)

Table 3. Bond lengths [Å] and angles [°] for 02133IHs.

Cl(1)-C(12)	1.777(5)
Cl(2)-C(12)	1.762(4)
Cl(3)-C(12)	1.778(5)
Cl(4)-C(33)	1.765(5)
Cl(5)-C(33)	1.778(5)
Cl(6)-C(33)	1.786(4)
O(1)-C(1)	1.219(6)
O(2)-C(10)	1.183(5)
O(3)-C(10)	1.333(5)
O(3)-C(11)	1.448(5)
O(4)-C(22)	1.210(6)
O(5)-C(31)	1.195(5)
O(6)-C(31)	1.352(5)
O(6)-C(32)	1.451(5)
N(1)-C(1)	1.344(6)
N(1)-C(7)	1.412(6)
N(1)-C(9)	1.460(6)
N(2)-C(22)	1.351(6)
N(2)-C(28)	1.403(6)
N(2)-C(30)	1.467(6)
C(1)-C(2)	1.555(7)
C(2)-C(8)	1.497(6)
C(2)-C(15)	1.533(6)
C(2)-C(10)	1.536(6)
C(3)-C(8)	1.374(7)
C(3)-C(4)	1.398(7)
C(4)-C(5)	1.370(8)
C(5)-C(6)	1.397(8)
C(6)-C(7)	1.383(6)
C(7)-C(8)	1.386(6)
C(11)-C(13)	1.515(7)

C(11)-C(14)	1.515(7)
C(11)-C(12)	1.562(6)
C(15)-C(16)	1.511(6)
C(16)-C(21)	1.377(7)
C(16)-C(17)	1.390(7)
C(17)-C(18)	1.374(7)
C(18)-C(19)	1.380(7)
C(19)-C(20)	1.377(8)
C(20)-C(21)	1.383(7)
C(22)-C(23)	1.542(6)
C(23)-C(29)	1.512(6)
C(23)-C(31)	1.521(6)
C(23)-C(36)	1.549(6)
C(24)-C(29)	1.371(7)
C(24)-C(25)	1.407(8)
C(25)-C(26)	1.354(9)
C(26)-C(27)	1.371(9)
C(27)-C(28)	1.363(7)
C(28)-C(29)	1.391(6)
C(32)-C(35)	1.504(7)
C(32)-C(34)	1.524(7)
C(32)-C(33)	1.551(6)
C(36)-C(37)	1.513(6)
C(37)-C(42)	1.368(7)
C(37)-C(38)	1.369(7)
C(38)-C(39)	1.388(7)
C(39)-C(40)	1.351(9)
C(40)-C(41)	1.361(10)
C(41)-C(42)	1.399(8)
C(10)-O(3)-C(11)	125.5(3)
C(31)-O(6)-C(32)	123.6(3)
C(1)-N(1)-C(7)	111.4(4)
C(1)-N(1)-C(9)	123.6(4)

C(7)-N(1)-C(9)	124.9(4)
C(22)-N(2)-C(28)	111.8(4)
C(22)-N(2)-C(30)	123.3(5)
C(28)-N(2)-C(30)	124.6(4)
O(1)-C(1)-N(1)	126.7(4)
O(1)-C(1)-C(2)	125.2(4)
N(1)-C(1)-C(2)	108.1(4)
C(8)-C(2)-C(15)	117.2(4)
C(8)-C(2)-C(10)	109.1(4)
C(15)-C(2)-C(10)	110.1(3)
C(8)-C(2)-C(1)	101.8(3)
C(15)-C(2)-C(1)	112.1(4)
C(10)-C(2)-C(1)	105.6(4)
C(8)-C(3)-C(4)	118.7(5)
C(5)-C(4)-C(3)	121.0(5)
C(4)-C(5)-C(6)	121.4(5)
C(7)-C(6)-C(5)	116.4(5)
C(6)-C(7)-C(8)	123.1(5)
C(6)-C(7)-N(1)	127.2(4)
C(8)-C(7)-N(1)	109.6(4)
C(3)-C(8)-C(7)	119.5(4)
C(3)-C(8)-C(2)	131.5(4)
C(7)-C(8)-C(2)	109.0(4)
O(2)-C(10)-O(3)	126.0(4)
O(2)-C(10)-C(2)	126.3(4)
O(3)-C(10)-C(2)	107.7(3)
O(3)-C(11)-C(13)	109.6(4)
O(3)-C(11)-C(14)	112.1(4)
C(13)-C(11)-C(14)	112.7(4)
O(3)-C(11)-C(12)	99.9(3)
C(13)-C(11)-C(12)	111.0(4)
C(14)-C(11)-C(12)	110.8(4)
C(11)-C(12)-Cl(2)	111.1(3)

C(11)-C(12)-Cl(3)	110.9(3)
Cl(2)-C(12)-Cl(3)	108.2(3)
C(11)-C(12)-Cl(1)	110.5(3)
Cl(2)-C(12)-Cl(1)	108.7(3)
Cl(3)-C(12)-Cl(1)	107.3(2)
C(16)-C(15)-C(2)	113.2(3)
C(21)-C(16)-C(17)	117.3(4)
C(21)-C(16)-C(15)	121.1(4)
C(17)-C(16)-C(15)	121.6(4)
C(18)-C(17)-C(16)	121.3(5)
C(17)-C(18)-C(19)	120.3(5)
C(20)-C(19)-C(18)	119.6(5)
C(19)-C(20)-C(21)	119.3(5)
C(16)-C(21)-C(20)	122.3(5)
O(4)-C(22)-N(2)	126.7(4)
O(4)-C(22)-C(23)	125.2(4)
N(2)-C(22)-C(23)	108.1(4)
C(29)-C(23)-C(31)	110.9(4)
C(29)-C(23)-C(22)	101.9(3)
C(31)-C(23)-C(22)	105.0(4)
C(29)-C(23)-C(36)	116.1(4)
C(31)-C(23)-C(36)	109.2(3)
C(22)-C(23)-C(36)	113.0(4)
C(29)-C(24)-C(25)	116.5(5)
C(26)-C(25)-C(24)	121.5(6)
C(25)-C(26)-C(27)	122.0(5)
C(28)-C(27)-C(26)	117.2(5)
C(27)-C(28)-C(29)	122.0(5)
C(27)-C(28)-N(2)	128.4(4)
C(29)-C(28)-N(2)	109.6(4)
C(24)-C(29)-C(28)	120.8(4)
C(24)-C(29)-C(23)	130.6(4)
C(28)-C(29)-C(23)	108.5(4)

O(5)-C(31)-O(6)	125.1(4)
O(5)-C(31)-C(23)	126.2(4)
O(6)-C(31)-C(23)	108.6(3)
O(6)-C(32)-C(35)	110.6(4)
O(6)-C(32)-C(34)	110.7(4)
C(35)-C(32)-C(34)	112.2(4)
O(6)-C(32)-C(33)	98.8(3)
C(35)-C(32)-C(33)	112.9(4)
C(34)-C(32)-C(33)	110.8(4)
C(32)-C(33)-Cl(4)	112.1(3)
C(32)-C(33)-Cl(5)	111.4(3)
Cl(4)-C(33)-Cl(5)	107.9(2)
C(32)-C(33)-Cl(6)	110.0(3)
Cl(4)-C(33)-Cl(6)	108.0(3)
Cl(5)-C(33)-Cl(6)	107.2(3)
C(37)-C(36)-C(23)	112.9(4)
C(42)-C(37)-C(38)	119.1(4)
C(42)-C(37)-C(36)	121.4(5)
C(38)-C(37)-C(36)	119.6(5)
C(37)-C(38)-C(39)	121.0(5)
C(40)-C(39)-C(38)	119.8(6)
C(39)-C(40)-C(41)	120.2(5)
C(40)-C(41)-C(42)	120.4(6)
C(37)-C(42)-C(41)	119.6(6)

Table 4. Anisotropic displacement parameters ($Å^2 x\ 10^3$) for 02133IHs. The anisotropic displacement factor exponent takes the form: $-2p^2[\ h^2\ a^{*2}U^{11} + ... + 2\ h\ k\ a^*\ b^*\ U^{12}\ ]$

	U^{11}	U^{22}	U^{33}	U^{23}	U^{13}	U^{12}
Cl(1)	37(1)	78(1)	58(1)	-30(1)	7(1)	-9(1)
Cl(2)	38(1)	40(1)	50(1)	6(1)	23(1)	-1(1)
Cl(3)	36(1)	61(1)	56(1)	26(1)	17(1)	13(1)
Cl(4)	33(1)	53(1)	56(1)	13(1)	8(1)	4(1)
Cl(5)	45(1)	49(1)	59(1)	-18(1)	13(1)	-16(1)
Cl(6)	44(1)	66(1)	49(1)	-7(1)	27(1)	-13(1)
O(1)	56(2)	25(2)	63(2)	-8(2)	15(2)	-9(2)
O(2)	26(2)	80(3)	33(2)	8(2)	0(2)	6(2)
O(3)	23(2)	54(2)	33(2)	8(2)	7(1)	3(2)
O(4)	75(3)	34(2)	59(2)	6(2)	22(2)	18(2)
O(5)	31(2)	92(3)	28(2)	-1(2)	-1(2)	4(2)
O(6)	27(2)	47(2)	30(2)	3(2)	7(1)	-3(2)
N(1)	43(2)	27(2)	30(2)	5(2)	11(2)	5(2)
N(2)	40(2)	30(2)	34(2)	-8(2)	5(2)	-11(2)
C(1)	37(3)	27(3)	38(2)	0(2)	18(2)	-5(2)
C(2)	21(2)	39(3)	26(2)	-1(2)	6(2)	1(2)
C(3)	34(3)	41(3)	46(3)	-7(2)	21(2)	1(2)
C(4)	49(3)	39(3)	49(3)	-20(2)	23(3)	-14(3)
C(5)	39(3)	67(4)	37(3)	-20(3)	3(2)	-13(3)
C(6)	34(3)	69(4)	26(2)	1(3)	0(2)	8(3)
C(7)	32(3)	37(3)	19(2)	3(2)	13(2)	5(2)
C(8)	29(2)	31(3)	30(2)	-4(2)	13(2)	1(2)
C(9)	68(4)	46(4)	55(3)	14(3)	19(3)	22(3)
C(10)	28(2)	28(3)	31(2)	-4(2)	5(2)	-2(2)
C(11)	34(2)	33(3)	32(2)	0(2)	15(2)	-5(2)
C(12)	32(2)	32(3)	38(2)	1(2)	9(2)	0(2)

C(13)	43(3)	52(4)	36(3)	-7(2)	9(2)	-7(3)
C(14)	41(3)	32(3)	54(3)	11(2)	19(2)	6(2)
C(15)	24(2)	34(3)	32(2)	-4(2)	2(2)	1(2)
C(16)	22(2)	28(3)	34(2)	-3(2)	2(2)	3(2)
C(17)	41(3)	34(3)	49(3)	-10(2)	18(2)	-4(2)
C(18)	53(3)	38(3)	52(3)	3(3)	22(3)	-1(3)
C(19)	34(3)	63(4)	33(2)	6(2)	11(2)	-7(3)
C(20)	50(3)	43(3)	46(3)	-12(3)	25(2)	-4(3)
C(21)	38(3)	28(3)	58(3)	4(2)	22(2)	1(2)
C(22)	44(3)	24(3)	30(2)	1(2)	12(2)	4(2)
C(23)	20(2)	26(3)	33(2)	2(2)	3(2)	0(2)
C(24)	48(3)	29(3)	49(3)	0(2)	30(2)	-3(2)
C(25)	63(4)	40(4)	85(4)	32(3)	45(3)	28(3)
C(26)	37(3)	87(5)	52(3)	29(3)	9(3)	18(3)
C(27)	36(3)	69(4)	33(3)	10(3)	4(2)	-5(3)
C(28)	23(2)	50(4)	21(2)	3(2)	6(2)	-5(2)
C(29)	23(2)	28(3)	29(2)	2(2)	11(2)	0(2)
C(30)	72(4)	68(5)	48(3)	-14(3)	6(3)	-43(4)
C(31)	25(2)	26(3)	33(2)	2(2)	5(2)	2(2)
C(32)	29(2)	36(3)	29(2)	0(2)	7(2)	-1(2)
C(33)	32(2)	31(3)	40(2)	-3(2)	11(2)	-7(2)
C(34)	42(3)	51(4)	50(3)	-15(3)	13(2)	-16(3)
C(35)	45(3)	72(4)	45(3)	15(3)	6(2)	-5(3)
C(36)	23(2)	55(3)	32(2)	-3(2)	5(2)	2(2)
C(37)	18(2)	45(3)	35(2)	-4(2)	8(2)	1(2)
C(38)	37(3)	48(3)	42(3)	-8(2)	17(2)	-8(2)
C(39)	42(3)	70(5)	51(3)	3(3)	16(3)	-1(3)
C(40)	31(3)	98(5)	33(3)	3(3)	4(2)	-12(3)
C(41)	45(3)	88(5)	55(3)	-33(4)	20(3)	-11(3)
C(42)	50(3)	38(3)	52(3)	-5(2)	22(2)	1(2)

Table 5. Hydrogen coordinates (x 10^4) and isotropic displacement parameters ($Å^2$x 10^3) for 02133IHs.

	x	y	z	U(eq)
H(3)	3703	8217	4055	47
H(4)	5762	8549	5737	53
H(5)	7593	7963	6901	58
H(6)	7444	7013	6441	53
H(9A)	5623	5729	4539	83
H(9B)	6047	5999	6083	83
H(9C)	7069	6116	4946	83
H(13A)	5433	6454	-188	65
H(13B)	5577	6872	-1433	65
H(13C)	3995	6796	-967	65
H(14A)	4065	7808	-776	62
H(14B)	5802	7935	-746	62
H(14C)	5091	8086	594	62
H(15A)	1198	7507	3059	37
H(15B)	972	6871	2685	37
H(17)	1105	6198	4657	48
H(18)	738	6035	6927	55
H(19)	689	6761	8488	51
H(20)	1048	7653	7761	53
H(21)	1391	7811	5472	47
H(24)	1104	5751	1121	47
H(25)	-1022	6135	-422	70
H(26)	-2782	5591	-1794	71
H(27)	-2498	4646	-1832	56
H(30A)	-501	3292	-614	96
H(30B)	-1124	3670	-1964	96
H(30C)	-1998	3646	-682	96

H(34A)	1001	5040	5435	71
H(34B)	-612	5027	5864	71
H(34C)	-406	5341	4458	71
H(35A)	-52	3678	4436	82
H(35B)	-476	3947	5817	82
H(35C)	1160	4043	5480	82
H(36A)	3698	5061	1825	44
H(36B)	4027	4420	1748	44
H(38)	3572	5615	-191	49
H(39)	3921	5743	-2502	64
H(40)	4207	4997	-3883	65
H(41)	4107	4124	-3000	73
H(42)	3764	3989	-673	54

Table 6. Torsion angles [°] for 02133IHs.

C(7)-N(1)-C(1)-O(1)	179.4(4)
C(9)-N(1)-C(1)-O(1)	2.2(7)
C(7)-N(1)-C(1)-C(2)	-0.3(5)
C(9)-N(1)-C(1)-C(2)	-177.5(4)
O(1)-C(1)-C(2)-C(8)	179.6(4)
N(1)-C(1)-C(2)-C(8)	-0.7(4)
O(1)-C(1)-C(2)-C(15)	53.5(6)
N(1)-C(1)-C(2)-C(15)	-126.8(4)
O(1)-C(1)-C(2)-C(10)	-66.4(5)
N(1)-C(1)-C(2)-C(10)	113.3(4)
C(8)-C(3)-C(4)-C(5)	0.5(7)
C(3)-C(4)-C(5)-C(6)	-0.3(8)
C(4)-C(5)-C(6)-C(7)	-1.0(7)
C(5)-C(6)-C(7)-C(8)	2.2(7)
C(5)-C(6)-C(7)-N(1)	179.5(4)
C(1)-N(1)-C(7)-C(6)	-176.4(4)
C(9)-N(1)-C(7)-C(6)	0.8(7)
C(1)-N(1)-C(7)-C(8)	1.3(5)
C(9)-N(1)-C(7)-C(8)	178.4(4)
C(4)-C(3)-C(8)-C(7)	0.6(7)
C(4)-C(3)-C(8)-C(2)	-177.0(4)
C(6)-C(7)-C(8)-C(3)	-2.0(6)
N(1)-C(7)-C(8)-C(3)	-179.8(4)
C(6)-C(7)-C(8)-C(2)	176.1(4)
N(1)-C(7)-C(8)-C(2)	-1.7(5)
C(15)-C(2)-C(8)-C(3)	-58.2(6)
C(10)-C(2)-C(8)-C(3)	67.9(6)
C(1)-C(2)-C(8)-C(3)	179.2(5)
C(15)-C(2)-C(8)-C(7)	124.1(4)
C(10)-C(2)-C(8)-C(7)	-109.9(4)
C(1)-C(2)-C(8)-C(7)	1.4(4)

C(11)-O(3)-C(10)-O(2)	3.9(8)
C(11)-O(3)-C(10)-C(2)	-176.4(4)
C(8)-C(2)-C(10)-O(2)	-126.5(5)
C(15)-C(2)-C(10)-O(2)	3.6(7)
C(1)-C(2)-C(10)-O(2)	124.8(5)
C(8)-C(2)-C(10)-O(3)	53.8(5)
C(15)-C(2)-C(10)-O(3)	-176.1(4)
C(1)-C(2)-C(10)-O(3)	-54.9(4)
C(10)-O(3)-C(11)-C(13)	-77.5(6)
C(10)-O(3)-C(11)-C(14)	48.5(6)
C(10)-O(3)-C(11)-C(12)	165.8(4)
O(3)-C(11)-C(12)-Cl(2)	175.0(3)
C(13)-C(11)-C(12)-Cl(2)	59.5(5)
C(14)-C(11)-C(12)-Cl(2)	-66.6(4)
O(3)-C(11)-C(12)-Cl(3)	54.6(4)
C(13)-C(11)-C(12)-Cl(3)	-61.0(4)
C(14)-C(11)-C(12)-Cl(3)	172.9(3)
O(3)-C(11)-C(12)-Cl(1)	-64.3(4)
C(13)-C(11)-C(12)-Cl(1)	-179.8(3)
C(14)-C(11)-C(12)-Cl(1)	54.1(4)
C(8)-C(2)-C(15)-C(16)	-52.8(5)
C(10)-C(2)-C(15)-C(16)	-178.3(4)
C(1)-C(2)-C(15)-C(16)	64.4(5)
C(2)-C(15)-C(16)-C(21)	94.1(5)
C(2)-C(15)-C(16)-C(17)	-86.8(5)
C(21)-C(16)-C(17)-C(18)	-1.2(7)
C(15)-C(16)-C(17)-C(18)	179.7(4)
C(16)-C(17)-C(18)-C(19)	0.6(8)
C(17)-C(18)-C(19)-C(20)	-0.3(8)
C(18)-C(19)-C(20)-C(21)	0.6(8)
C(17)-C(16)-C(21)-C(20)	1.5(7)
C(15)-C(16)-C(21)-C(20)	-179.4(4)
C(19)-C(20)-C(21)-C(16)	-1.3(8)

C(28)-N(2)-C(22)-O(4)	179.7(5)
C(30)-N(2)-C(22)-O(4)	5.7(8)
C(28)-N(2)-C(22)-C(23)	0.8(5)
C(30)-N(2)-C(22)-C(23)	-173.3(4)
O(4)-C(22)-C(23)-C(29)	178.3(5)
N(2)-C(22)-C(23)-C(29)	-2.7(4)
O(4)-C(22)-C(23)-C(31)	-65.9(6)
N(2)-C(22)-C(23)-C(31)	113.0(4)
O(4)-C(22)-C(23)-C(36)	53.0(6)
N(2)-C(22)-C(23)-C(36)	-128.0(4)
C(29)-C(24)-C(25)-C(26)	2.1(8)
C(24)-C(25)-C(26)-C(27)	-1.8(9)
C(25)-C(26)-C(27)-C(28)	0.3(8)
C(26)-C(27)-C(28)-C(29)	0.8(7)
C(26)-C(27)-C(28)-N(2)	-179.5(5)
C(22)-N(2)-C(28)-C(27)	-178.0(5)
C(30)-N(2)-C(28)-C(27)	-4.0(8)
C(22)-N(2)-C(28)-C(29)	1.8(5)
C(30)-N(2)-C(28)-C(29)	175.7(4)
C(25)-C(24)-C(29)-C(28)	-1.0(6)
C(25)-C(24)-C(29)-C(23)	-176.8(4)
C(27)-C(28)-C(29)-C(24)	-0.5(7)
N(2)-C(28)-C(29)-C(24)	179.8(4)
C(27)-C(28)-C(29)-C(23)	176.2(4)
N(2)-C(28)-C(29)-C(23)	-3.5(5)
C(31)-C(23)-C(29)-C(24)	68.6(6)
C(22)-C(23)-C(29)-C(24)	180.0(5)
C(36)-C(23)-C(29)-C(24)	-56.8(6)
C(31)-C(23)-C(29)-C(28)	-107.7(4)
C(22)-C(23)-C(29)-C(28)	3.7(4)
C(36)-C(23)-C(29)-C(28)	127.0(4)
C(32)-O(6)-C(31)-O(5)	5.3(7)
C(32)-O(6)-C(31)-C(23)	-178.6(4)

C(29)-C(23)-C(31)-O(5)	-138.8(5)
C(22)-C(23)-C(31)-O(5)	111.8(5)
C(36)-C(23)-C(31)-O(5)	-9.7(7)
C(29)-C(23)-C(31)-O(6)	45.1(5)
C(22)-C(23)-C(31)-O(6)	-64.3(4)
C(36)-C(23)-C(31)-O(6)	174.2(4)
C(31)-O(6)-C(32)-C(35)	-65.1(6)
C(31)-O(6)-C(32)-C(34)	59.9(6)
C(31)-O(6)-C(32)-C(33)	176.2(4)
O(6)-C(32)-C(33)-Cl(4)	-57.2(4)
C(35)-C(32)-C(33)-Cl(4)	-174.1(4)
C(34)-C(32)-C(33)-Cl(4)	59.0(4)
O(6)-C(32)-C(33)-Cl(5)	63.8(4)
C(35)-C(32)-C(33)-Cl(5)	-53.1(5)
C(34)-C(32)-C(33)-Cl(5)	-179.9(3)
O(6)-C(32)-C(33)-Cl(6)	-177.4(3)
C(35)-C(32)-C(33)-Cl(6)	65.7(5)
C(34)-C(32)-C(33)-Cl(6)	-61.2(5)
C(29)-C(23)-C(36)-C(37)	-49.4(6)
C(31)-C(23)-C(36)-C(37)	-175.6(4)
C(22)-C(23)-C(36)-C(37)	67.8(5)
C(23)-C(36)-C(37)-C(42)	-81.7(6)
C(23)-C(36)-C(37)-C(38)	98.4(5)
C(42)-C(37)-C(38)-C(39)	0.5(8)
C(36)-C(37)-C(38)-C(39)	-179.6(4)
C(37)-C(38)-C(39)-C(40)	-0.5(8)
C(38)-C(39)-C(40)-C(41)	0.5(8)
C(39)-C(40)-C(41)-C(42)	-0.6(8)
C(38)-C(37)-C(42)-C(41)	-0.6(7)
C(36)-C(37)-C(42)-C(41)	179.6(4)
C(40)-C(41)-C(42)-C(37)	0.7(8)

002163s (Table 1.3, entry 1)

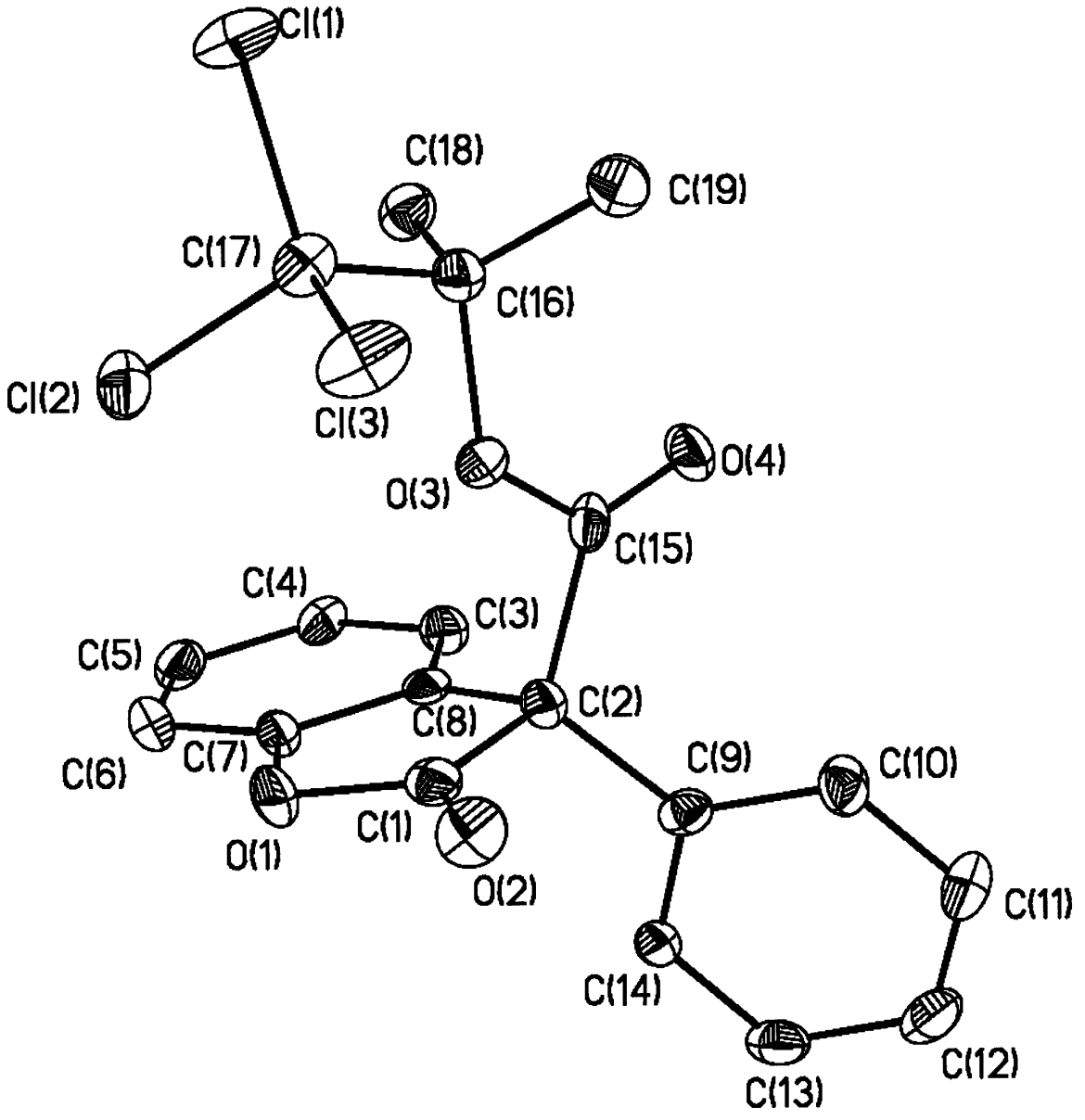

Table 1. Crystal data and structure refinement for 002163s.

Identification code	002163s
Empirical formula	C19 H15 Cl3 O4
Formula weight	413.66
Temperature	193(2) K
Wavelength	0.71073 Å
Crystal system	Monoclinic
Space group	P2(1)
Unit cell dimensions	a = 8.8316(7) Å α = 90°.
	b = 9.4908(8) Å β = 110.5570(10)°.
	c = 11.8129(10) Å γ = 90°.
Volume	927.10(13) $Å^3$
Z	2
Density (calculated)	1.482 Mg/m^3
Absorption coefficient	0.516 mm^{-1}
F(000)	424
Crystal size	0.32 x 0.21 x 0.17 mm^3
Theta range for data collection	2.83 to 23.25°.
Index ranges	-8<=h<=9, -8<=k<=10, -10<=l<=13
Reflections collected	3726
Independent reflections	2152 [R(int) = 0.0407]
Completeness to theta = 23.25°	99.2 %
Absorption correction	Semi-empirical from equivalents
Max. and min. transmission	0.935988 and 0.540818
Refinement method	Full-matrix least-squares on F^2
Data / restraints / parameters	2152 / 1 / 237
Goodness-of-fit on F^2	1.090
Final R indices [I>2sigma(I)]	R1 = 0.0488, wR2 = 0.1251
R indices (all data)	R1 = 0.0495, wR2 = 0.1256
Absolute structure parameter	0.05(10)
Largest diff. peak and hole	0.414 and -0.302 $e.Å^{-3}$

Table 2. Atomic coordinates (x 10^4) and equivalent isotropic displacement parameters ($Å^2$x 10^3) for 002163s. U(eq) is defined as one third of the trace of the orthogonalized U^{ij} tensor.

	x	y	z	U(eq)
Cl(1)	11455(2)	8559(2)	450(1)	45(1)
Cl(2)	8321(2)	7349(2)	17(1)	40(1)
Cl(3)	9070(2)	10078(2)	1118(2)	45(1)
O(1)	5391(4)	6603(5)	1421(3)	34(1)
O(2)	5761(5)	8677(5)	2398(3)	39(1)
O(3)	9056(4)	7580(4)	2599(3)	26(1)
O(4)	10174(4)	6649(5)	4471(3)	35(1)
C(1)	6095(5)	7481(7)	2400(4)	28(1)
C(2)	7275(6)	6582(6)	3446(4)	26(1)
C(3)	7772(6)	3857(6)	3311(5)	30(1)
C(4)	7414(6)	2710(6)	2543(4)	31(1)
C(5)	6343(6)	2851(7)	1355(5)	37(2)
C(6)	5609(6)	4131(7)	922(5)	37(2)
C(7)	6005(5)	5238(7)	1708(4)	27(1)
C(8)	7055(5)	5138(6)	2876(4)	24(1)
C(9)	6863(6)	6709(6)	4587(4)	26(1)
C(10)	7675(6)	7597(6)	5539(4)	32(1)
C(11)	7258(7)	7670(7)	6548(5)	39(1)
C(12)	5964(7)	6907(7)	6620(5)	41(2)
C(13)	5116(6)	6032(7)	5673(5)	36(1)
C(14)	5564(6)	5934(7)	4667(4)	30(1)
C(15)	9058(6)	6958(6)	3616(4)	27(1)
C(16)	10557(6)	7674(6)	2320(4)	28(1)
C(17)	9888(6)	8363(6)	1051(5)	31(1)
C(18)	11188(6)	6225(7)	2251(5)	33(1)
C(19)	11796(7)	8607(8)	3220(5)	40(1)

Table 3. Bond lengths [Å] and angles [°] for 002163s.

Cl(1)-C(17)	1.773(5)
Cl(2)-C(17)	1.774(6)
Cl(3)-C(17)	1.794(6)
O(1)-C(1)	1.384(7)
O(1)-C(7)	1.400(7)
O(2)-C(1)	1.172(8)
O(3)-C(15)	1.338(6)
O(3)-C(16)	1.476(6)
O(4)-C(15)	1.174(6)
C(1)-C(2)	1.561(7)
C(2)-C(8)	1.509(8)
C(2)-C(9)	1.519(7)
C(2)-C(15)	1.558(7)
C(3)-C(4)	1.380(8)
C(3)-C(8)	1.384(8)
C(4)-C(5)	1.397(8)
C(5)-C(6)	1.387(9)
C(6)-C(7)	1.364(9)
C(7)-C(8)	1.369(7)
C(9)-C(10)	1.387(8)
C(9)-C(14)	1.394(8)
C(10)-C(11)	1.367(8)
C(11)-C(12)	1.380(9)
C(12)-C(13)	1.383(9)
C(13)-C(14)	1.381(7)
C(16)-C(18)	1.497(8)
C(16)-C(19)	1.515(8)
C(16)-C(17)	1.550(7)
C(1)-O(1)-C(7)	109.4(4)
C(15)-O(3)-C(16)	120.6(4)
O(2)-C(1)-O(1)	122.8(5)

O(2)-C(1)-C(2)	129.0(5)
O(1)-C(1)-C(2)	108.1(5)
C(8)-C(2)-C(9)	115.8(4)
C(8)-C(2)-C(15)	103.4(4)
C(9)-C(2)-C(15)	114.4(4)
C(8)-C(2)-C(1)	101.4(4)
C(9)-C(2)-C(1)	110.9(4)
C(15)-C(2)-C(1)	109.9(4)
C(4)-C(3)-C(8)	118.7(5)
C(3)-C(4)-C(5)	120.1(5)
C(6)-C(5)-C(4)	121.3(5)
C(7)-C(6)-C(5)	116.6(5)
C(6)-C(7)-C(8)	123.6(6)
C(6)-C(7)-O(1)	124.3(4)
C(8)-C(7)-O(1)	112.1(5)
C(7)-C(8)-C(3)	119.6(5)
C(7)-C(8)-C(2)	108.8(5)
C(3)-C(8)-C(2)	131.4(4)
C(10)-C(9)-C(14)	118.0(5)
C(10)-C(9)-C(2)	123.5(5)
C(14)-C(9)-C(2)	118.5(5)
C(11)-C(10)-C(9)	121.1(5)
C(10)-C(11)-C(12)	120.6(5)
C(11)-C(12)-C(13)	119.4(5)
C(14)-C(13)-C(12)	119.9(5)
C(13)-C(14)-C(9)	120.9(5)
O(4)-C(15)-O(3)	128.2(5)
O(4)-C(15)-C(2)	124.0(5)
O(3)-C(15)-C(2)	107.6(4)
O(3)-C(16)-C(18)	109.7(4)
O(3)-C(16)-C(19)	111.2(4)
C(18)-C(16)-C(19)	112.6(5)
O(3)-C(16)-C(17)	100.1(3)

C(18)-C(16)-C(17)	111.0(4)
C(19)-C(16)-C(17)	111.6(5)
C(16)-C(17)-Cl(2)	112.2(4)
C(16)-C(17)-Cl(1)	110.2(3)
Cl(2)-C(17)-Cl(1)	108.1(3)
C(16)-C(17)-Cl(3)	111.2(4)
Cl(2)-C(17)-Cl(3)	107.1(3)
Cl(1)-C(17)-Cl(3)	107.8(3)

Table 4. Anisotropic displacement parameters ($Å^2 x\ 10^3$) for 002163s. The anisotropic displacement factor exponent takes the form: $-2p^2[\ h^2\ a^{*2}U^{11} + ... + 2\ h\ k\ a^*\ b^*\ U^{12}\ ]$

	U^{11}	U^{22}	U^{33}	U^{23}	U^{13}	U^{12}
Cl(1)	45(1)	49(1)	55(1)	10(1)	36(1)	8(1)
Cl(2)	38(1)	53(1)	25(1)	-2(1)	7(1)	5(1)
Cl(3)	58(1)	29(1)	62(1)	12(1)	37(1)	13(1)
O(1)	28(2)	48(3)	20(2)	4(2)	-1(1)	2(2)
O(2)	45(2)	32(3)	40(2)	9(2)	16(2)	9(2)
O(3)	27(2)	30(2)	24(2)	2(2)	12(1)	-2(2)
O(4)	25(2)	52(3)	21(2)	3(2)	0(2)	-4(2)
C(1)	23(2)	39(4)	25(3)	10(3)	11(2)	2(3)
C(2)	22(2)	32(3)	20(2)	2(2)	5(2)	1(2)
C(3)	26(3)	36(4)	25(2)	5(3)	7(2)	2(2)
C(4)	35(3)	31(3)	31(3)	-4(3)	17(2)	2(2)
C(5)	35(3)	46(4)	36(3)	-17(3)	19(2)	-11(3)
C(6)	26(3)	54(4)	25(3)	-6(3)	3(2)	-2(3)
C(7)	20(2)	41(3)	18(2)	1(3)	5(2)	-4(2)
C(8)	18(2)	35(3)	22(2)	4(2)	12(2)	-2(2)
C(9)	25(2)	28(3)	26(3)	6(2)	11(2)	7(2)
C(10)	35(3)	29(3)	30(3)	-7(3)	11(2)	-10(3)
C(11)	52(3)	40(4)	28(3)	-7(3)	18(2)	-1(3)
C(12)	43(3)	54(4)	33(3)	4(3)	21(3)	17(3)
C(13)	24(3)	50(4)	38(3)	8(3)	15(2)	3(3)
C(14)	21(2)	46(4)	20(2)	0(2)	5(2)	5(2)
C(15)	33(3)	28(3)	19(2)	-7(2)	8(2)	-5(2)
C(16)	25(2)	32(3)	26(2)	1(3)	9(2)	-2(2)
C(17)	38(3)	23(3)	34(3)	0(2)	17(2)	-1(2)
C(18)	33(3)	38(4)	28(3)	5(3)	12(2)	7(2)
C(19)	38(3)	45(4)	38(3)	-7(3)	16(3)	-13(3)

Table 5. Hydrogen coordinates (x 10^4) and isotropic displacement parameters ($Å^2$x 10^3) for 002163s.

	x	y	z	U(eq)
H(3)	8497	3768	4121	35
H(4)	7896	1822	2824	37
H(5)	6113	2056	834	45
H(6)	4869	4232	118	44
H(10)	8536	8165	5490	38
H(11)	7863	8251	7206	47
H(12)	5659	6981	7313	49
H(13)	4227	5499	5714	43
H(14)	4978	5330	4020	36
H(18A)	11554	5793	3056	49
H(18B)	12097	6284	1959	49
H(18C)	10327	5648	1693	49
H(19A)	11283	9491	3318	60
H(19B)	12680	8809	2924	60
H(19C)	12228	8123	4001	60

Table 6. Torsion angles [°] for 002163s.

C(7)-O(1)-C(1)-O(2)	-178.5(4)
C(7)-O(1)-C(1)-C(2)	-1.0(5)
O(2)-C(1)-C(2)-C(8)	176.4(5)
O(1)-C(1)-C(2)-C(8)	-0.9(5)
O(2)-C(1)-C(2)-C(9)	52.9(7)
O(1)-C(1)-C(2)-C(9)	-124.4(4)
O(2)-C(1)-C(2)-C(15)	-74.7(6)
O(1)-C(1)-C(2)-C(15)	108.0(4)
C(8)-C(3)-C(4)-C(5)	-0.2(7)
C(3)-C(4)-C(5)-C(6)	-0.5(8)
C(4)-C(5)-C(6)-C(7)	0.9(8)
C(5)-C(6)-C(7)-C(8)	-0.5(8)
C(5)-C(6)-C(7)-O(1)	179.4(5)
C(1)-O(1)-C(7)-C(6)	-177.2(5)
C(1)-O(1)-C(7)-C(8)	2.8(5)
C(6)-C(7)-C(8)-C(3)	-0.1(7)
O(1)-C(7)-C(8)-C(3)	179.9(4)
C(6)-C(7)-C(8)-C(2)	176.6(5)
O(1)-C(7)-C(8)-C(2)	-3.4(5)
C(4)-C(3)-C(8)-C(7)	0.5(7)
C(4)-C(3)-C(8)-C(2)	-175.4(5)
C(9)-C(2)-C(8)-C(7)	122.7(4)
C(15)-C(2)-C(8)-C(7)	-111.4(4)
C(1)-C(2)-C(8)-C(7)	2.5(5)
C(9)-C(2)-C(8)-C(3)	-61.1(7)
C(15)-C(2)-C(8)-C(3)	64.8(6)
C(1)-C(2)-C(8)-C(3)	178.7(5)
C(8)-C(2)-C(9)-C(10)	146.0(5)
C(15)-C(2)-C(9)-C(10)	25.9(7)
C(1)-C(2)-C(9)-C(10)	-99.2(6)
C(8)-C(2)-C(9)-C(14)	-36.4(6)

C(15)-C(2)-C(9)-C(14)	-156.6(5)
C(1)-C(2)-C(9)-C(14)	78.4(6)
C(14)-C(9)-C(10)-C(11)	2.6(8)
C(2)-C(9)-C(10)-C(11)	-179.9(5)
C(9)-C(10)-C(11)-C(12)	-3.0(9)
C(10)-C(11)-C(12)-C(13)	1.8(9)
C(11)-C(12)-C(13)-C(14)	-0.3(9)
C(12)-C(13)-C(14)-C(9)	-0.1(9)
C(10)-C(9)-C(14)-C(13)	-1.0(8)
C(2)-C(9)-C(14)-C(13)	-178.7(5)
C(16)-O(3)-C(15)-O(4)	14.2(8)
C(16)-O(3)-C(15)-C(2)	-161.3(4)
C(8)-C(2)-C(15)-O(4)	-87.6(6)
C(9)-C(2)-C(15)-O(4)	39.3(8)
C(1)-C(2)-C(15)-O(4)	164.8(5)
C(8)-C(2)-C(15)-O(3)	88.2(5)
C(9)-C(2)-C(15)-O(3)	-145.0(5)
C(1)-C(2)-C(15)-O(3)	-19.4(6)
C(15)-O(3)-C(16)-C(18)	59.5(6)
C(15)-O(3)-C(16)-C(19)	-65.7(6)
C(15)-O(3)-C(16)-C(17)	176.2(4)
O(3)-C(16)-C(17)-Cl(2)	-57.5(5)
C(18)-C(16)-C(17)-Cl(2)	58.2(5)
C(19)-C(16)-C(17)-Cl(2)	-175.3(4)
O(3)-C(16)-C(17)-Cl(1)	-178.1(3)
C(18)-C(16)-C(17)-Cl(1)	-62.3(5)
C(19)-C(16)-C(17)-Cl(1)	64.1(5)
O(3)-C(16)-C(17)-Cl(3)	62.4(4)
C(18)-C(16)-C(17)-Cl(3)	178.1(4)
C(19)-C(16)-C(17)-Cl(3)	-55.4(5)

02167ihs (Figure 1.3)

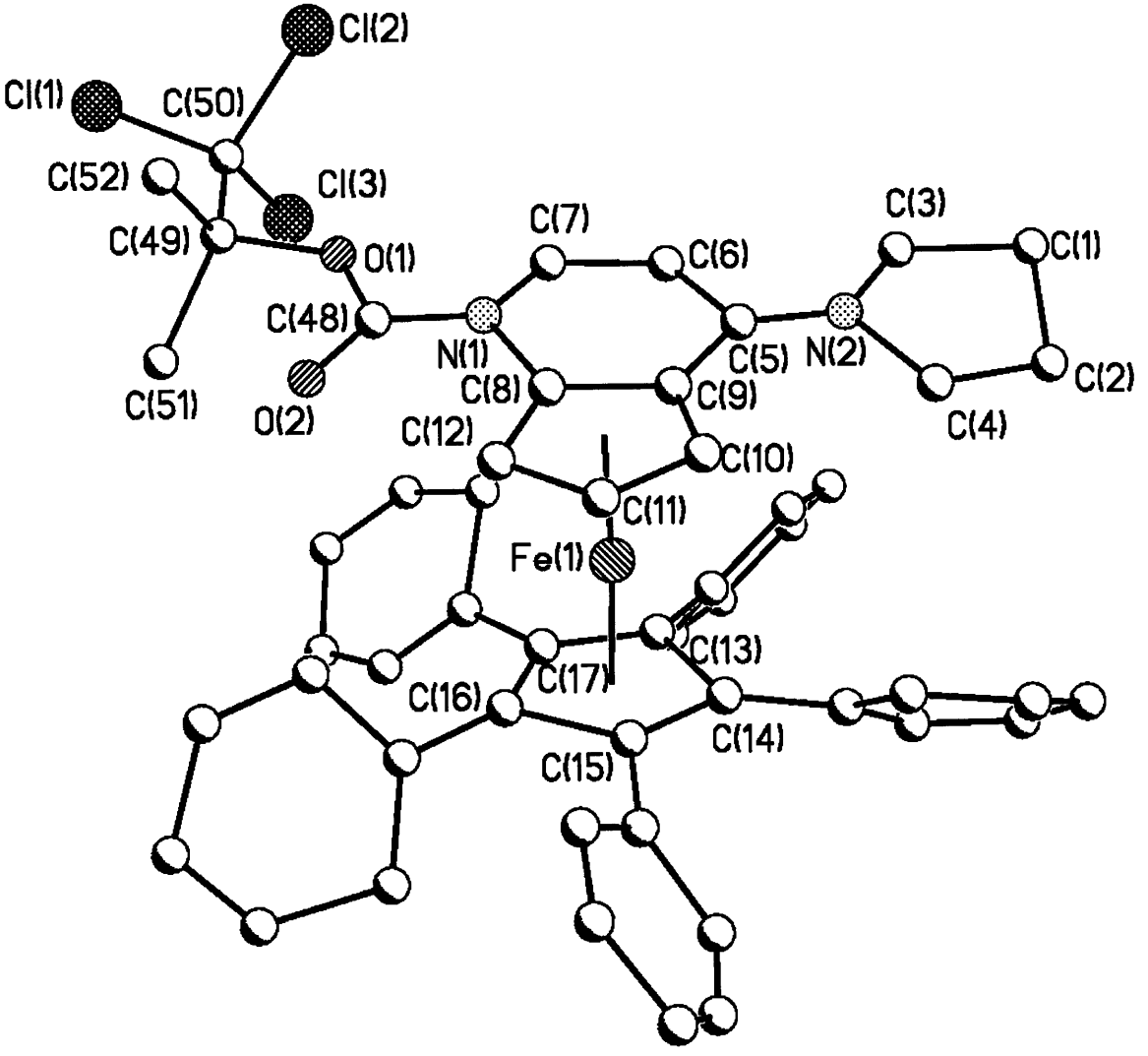

Table 1. Crystal data and structure refinement for 02167ihs.

Identification code	02167ihs	
Empirical formula	C66 H53 Cl3 Fe N2 O4	
Formula weight	1100.30	
Temperature	293(2) K	
Wavelength	0.71073 Å	
Crystal system	Orthorhombic	
Space group	P2(1)2(1)2(1)	
Unit cell dimensions	a = 9.9(8) Å	α = 90°.
	b = 16.8(17) Å	β = 90°.
	c = 37(4) Å	γ = 90°.
Volume	6066(1002) $Å^3$	
Z	4	
Density (calculated)	1.205 Mg/m^3	
Absorption coefficient	0.428 mm^{-1}	
F(000)	2288	
Crystal size	0.5 x 0.04 x 0.04 mm^3	
Theta range for data collection	2.06 to 23.56°.	
Index ranges	-11<=h<=9, -18<=k<=17, -38<=l<=40	
Reflections collected	20328	
Independent reflections	8923 [R(int) = 0.4093]	
Completeness to theta = 23.56°	99.0 %	
Refinement method	Full-matrix least-squares on F^2	
Data / restraints / parameters	8923 / 0 / 307	
Goodness-of-fit on F^2	1.227	
Final R indices [I>2sigma(I)]	R1 = 0.2498, wR2 = 0.4775	
R indices (all data)	R1 = 0.4056, wR2 = 0.5523	
Absolute structure parameter	0.10(13)	
Largest diff. peak and hole	2.743 and -1.792 e.$Å^{-3}$	

Table 2. Atomic coordinates (x 10^4) and equivalent isotropic displacement parameters ($Å^2$x 10^3) for 02167IHs. U(eq) is defined as one third of the trace of the orthogonalized U^{ij} tensor.

	x	y	z	U(eq)
Fe(1)	3082(4)	1502(2)	1550(1)	17(1)
Cl(1)	6931(12)	-2085(6)	82(3)	68(3)
Cl(2)	5973(10)	-545(6)	-142(3)	52(3)
Cl(3)	7887(11)	-709(6)	442(3)	62(3)
O(1)	5050(20)	-336(11)	596(6)	26(5)
O(2)	3470(20)	-547(13)	993(6)	40(6)
O(3)	4780(20)	1810(13)	9321(6)	37(6)
O(4)	4910(30)	579(17)	9223(8)	75(9)
N(1)	3940(30)	656(15)	799(7)	30(7)
N(2)	3730(20)	3135(13)	791(6)	16(6)
C(1)	4290(40)	4490(20)	582(10)	52(11)
C(2)	3330(50)	4510(20)	954(12)	87(14)
C(3)	4660(40)	3580(20)	587(12)	71(13)
C(4)	2860(30)	3669(12)	1014(7)	7(6)
C(5)	3790(30)	2410(20)	822(9)	35(9)
C(6)	4770(30)	1966(17)	630(9)	20(8)
C(7)	4930(40)	1140(20)	625(10)	43(10)
C(8)	2940(30)	1056(16)	1023(8)	20(7)
C(9)	2810(30)	1902(18)	1020(9)	34(9)
C(10)	1660(30)	2027(16)	1218(7)	14(7)
C(11)	1240(30)	1345(15)	1344(8)	16(7)
C(12)	1990(30)	691(14)	1239(6)	5(6)
C(13)	4820(30)	1903(15)	1801(8)	10(7)
C(14)	3530(30)	2292(17)	1977(8)	20(8)
C(15)	2790(30)	1603(18)	2086(8)	29(8)
C(16)	3500(30)	783(16)	2007(8)	17(8)

C(17)	4750(40)	1080(20)	1844(10)	39(10)
C(18)	5760(30)	558(15)	1740(8)	11(7)
C(19)	6580(40)	710(20)	1362(11)	70(13)
C(20)	6260(40)	-10(20)	1936(11)	54(11)
C(21)	7320(30)	-470(19)	1903(9)	38(10)
C(22)	8160(40)	-440(20)	1566(12)	69(12)
C(23)	7730(30)	159(17)	1370(9)	26(8)
C(24)	3050(30)	78(17)	2144(9)	32(8)
C(25)	2800(50)	10(20)	2522(11)	66(13)
C(26)	2450(30)	-862(17)	2626(9)	29(9)
C(27)	2410(40)	-1440(20)	2406(11)	59(12)
C(28)	2740(40)	-1240(30)	2026(13)	84(15)
C(29)	3100(40)	-526(19)	1890(10)	42(9)
C(30)	1520(30)	1610(20)	2313(9)	39(9)
C(31)	1510(30)	2103(18)	2626(8)	27(9)
C(32)	380(40)	2039(19)	2812(10)	38(10)
C(33)	-730(30)	1721(14)	2783(8)	13(7)
C(34)	-670(40)	1210(20)	2496(11)	53(12)
C(35)	510(30)	1178(19)	2275(10)	39(10)
C(36)	3310(30)	3109(17)	2010(8)	27(8)
C(37)	2020(30)	3405(18)	1942(8)	33(8)
C(38)	1700(30)	4193(16)	1960(8)	26(8)
C(39)	2650(30)	4686(16)	1984(7)	13(7)
C(40)	4020(30)	4405(17)	2076(8)	20(7)
C(41)	4290(30)	3660(17)	2090(8)	28(9)
C(42)	5990(40)	2360(20)	1681(10)	46(10)
C(43)	6090(30)	2934(18)	1421(9)	33(9)
C(44)	7240(30)	3328(17)	1354(8)	28(8)
C(45)	8350(30)	3128(17)	1495(9)	29(9)
C(46)	8360(30)	2586(16)	1756(8)	22(8)
C(47)	7220(30)	2148(19)	1855(10)	42(10)
C(48)	4120(30)	-99(19)	811(9)	30(9)
C(49)	5290(30)	-1169(17)	532(9)	26(8)

C(50)	4030(40)	-1530(30)	367(11)	75(13)
C(51)	5690(50)	-1590(30)	933(12)	94(16)
C(52)	6520(30)	-1135(19)	258(9)	37(10)
C(86)	1990(40)	390(20)	10074(10)	44(10)
C(87)	1200(30)	-292(19)	10170(9)	36(9)
C(88)	1010(40)	-970(20)	10039(11)	56(12)
C(89)	1590(40)	-880(20)	9691(11)	59(12)
C(90)	2400(40)	-250(20)	9615(10)	48(11)
C(91)	2600(30)	378(18)	9780(9)	25(8)
C(92)	4000(30)	2313(17)	9514(8)	20(7)
C(93)	4020(40)	3140(20)	9483(12)	61(13)
C(94)	3210(30)	3591(19)	9724(8)	36(9)
C(95)	2270(40)	3199(18)	9966(10)	44(11)
C(96)	2370(30)	2300(16)	9974(8)	25(8)
C(97)	3200(30)	1837(16)	9719(8)	24(8)
C(98)	3370(40)	1080(20)	9693(10)	42(10)
C(99)	4360(40)	1190(30)	9354(12)	59(12)

Table 3. Bond lengths [Å] and angles [°] for 02167IHs.

Fe(1)-C(15)	2.0(2)
Fe(1)-C(11)	1.99(15)
Fe(1)-C(13)	2.06(13)
Fe(1)-C(10)	2.06(12)
Fe(1)-C(14)	2.10(15)
Fe(1)-C(9)	2.07(19)
Fe(1)-C(17)	2.09(13)
Fe(1)-C(8)	2.08(19)
Fe(1)-C(12)	2.07(12)
Fe(1)-C(16)	2.11(15)
Cl(1)-C(52)	1.77(15)
Cl(2)-C(52)	1.85(13)
Cl(3)-C(52)	1.67(11)
O(1)-C(48)	1.27(8)
O(1)-C(49)	1.44(14)
O(2)-C(48)	1.19(8)
O(3)-C(99)	1.13(10)
O(3)-C(92)	1.35(8)
O(4)-C(99)	1.25(10)
N(1)-C(48)	1.28(13)
N(1)-C(8)	1.45(9)
N(1)-C(7)	1.42(9)
N(2)-C(5)	1.22(13)
N(2)-C(3)	1.40(9)
N(2)-C(4)	1.49(9)
C(1)-C(3)	1.57(16)
C(1)-C(2)	1.67(13)
C(2)-C(4)	1.49(14)
C(5)-C(6)	1.41(9)
C(5)-C(9)	1.48(9)
C(6)-C(7)	1.40(14)

C(8)-C(12)	1.37(8)
C(8)-C(9)	1.43(15)
C(9)-C(10)	1.37(10)
C(10)-C(11)	1.30(11)
C(11)-C(12)	1.38(10)
C(13)-C(17)	1.39(14)
C(13)-C(42)	1.45(10)
C(13)-C(14)	1.57(10)
C(14)-C(36)	1.39(14)
C(14)-C(15)	1.43(11)
C(15)-C(30)	1.50(11)
C(15)-C(16)	1.57(13)
C(16)-C(24)	1.36(11)
C(16)-C(17)	1.47(10)
C(17)-C(18)	1.38(9)
C(18)-C(20)	1.29(9)
C(18)-C(19)	1.62(13)
C(19)-C(23)	1.46(10)
C(20)-C(21)	1.30(9)
C(21)-C(22)	1.49(12)
C(22)-C(23)	1.30(10)
C(24)-C(29)	1.38(11)
C(24)-C(25)	1.41(14)
C(25)-C(26)	1.54(14)
C(26)-C(27)	1.26(10)
C(27)-C(28)	1.47(14)
C(28)-C(29)	1.34(12)
C(30)-C(35)	1.24(9)
C(30)-C(31)	1.42(11)
C(31)-C(32)	1.31(10)
C(32)-C(33)	1.22(9)
C(33)-C(34)	1.36(11)
C(34)-C(35)	1.42(10)

C(36)-C(41)	1.37(9)
C(36)-C(37)	1.39(11)
C(37)-C(38)	1.36(13)
C(38)-C(39)	1.25(9)
C(39)-C(40)	1.47(11)
C(40)-C(41)	1.28(13)
C(42)-C(43)	1.36(10)
C(42)-C(47)	1.42(10)
C(43)-C(44)	1.34(10)
C(44)-C(45)	1.25(9)
C(45)-C(46)	1.32(10)
C(46)-C(47)	1.39(10)
C(49)-C(50)	1.51(10)
C(49)-C(52)	1.58(11)
C(49)-C(51)	1.68(14)
C(86)-C(91)	1.23(11)
C(86)-C(87)	1.43(11)
C(87)-C(88)	1.25(11)
C(87)-C(89)	2.05(17)
C(88)-C(89)	1.41(13)
C(89)-C(90)	1.34(10)
C(90)-C(91)	1.23(10)
C(91)-C(98)	1.44(11)
C(92)-C(97)	1.35(8)
C(92)-C(93)	1.39(14)
C(92)-C(99)	2.01(18)
C(93)-C(94)	1.41(9)
C(94)-C(95)	1.44(9)
C(95)-C(96)	1.51(15)
C(96)-C(97)	1.47(9)
C(97)-C(98)	1.28(13)
C(98)-C(99)	1.59(12)
C(15)-Fe(1)-C(11)	105(4)

C(15)-Fe(1)-C(13)	70(4)
C(11)-Fe(1)-C(13)	167.3(16)
C(15)-Fe(1)-C(10)	117(5)
C(11)-Fe(1)-C(10)	37(3)
C(13)-Fe(1)-C(10)	134(5)
C(15)-Fe(1)-C(14)	41(4)
C(11)-Fe(1)-C(14)	124.1(18)
C(13)-Fe(1)-C(14)	44(2)
C(10)-Fe(1)-C(14)	108(6)
C(15)-Fe(1)-C(9)	151(4)
C(11)-Fe(1)-C(9)	65(2)
C(13)-Fe(1)-C(9)	115(3)
C(10)-Fe(1)-C(9)	39(2)
C(14)-Fe(1)-C(9)	121(6)
C(15)-Fe(1)-C(17)	69(4)
C(11)-Fe(1)-C(17)	151(3)
C(13)-Fe(1)-C(17)	39(4)
C(10)-Fe(1)-C(17)	171.0(12)
C(14)-Fe(1)-C(17)	70(5)
C(9)-Fe(1)-C(17)	134(3)
C(15)-Fe(1)-C(8)	160(3)
C(11)-Fe(1)-C(8)	62(2)
C(13)-Fe(1)-C(8)	126(3)
C(10)-Fe(1)-C(8)	64(5)
C(14)-Fe(1)-C(8)	159.4(16)
C(9)-Fe(1)-C(8)	40(5)
C(17)-Fe(1)-C(8)	114(4)
C(15)-Fe(1)-C(12)	121(4)
C(11)-Fe(1)-C(12)	40(2)
C(13)-Fe(1)-C(12)	153.1(13)
C(10)-Fe(1)-C(12)	67(6)
C(14)-Fe(1)-C(12)	158.9(17)
C(9)-Fe(1)-C(12)	68(5)

C(17)-Fe(1)-C(12)	118(6)
C(8)-Fe(1)-C(12)	38.5(18)
C(15)-Fe(1)-C(16)	45(5)
C(11)-Fe(1)-C(16)	114(3)
C(13)-Fe(1)-C(16)	71(4)
C(10)-Fe(1)-C(16)	148(2)
C(14)-Fe(1)-C(16)	74(8)
C(9)-Fe(1)-C(16)	163.2(17)
C(17)-Fe(1)-C(16)	41(2)
C(8)-Fe(1)-C(16)	123(6)
C(12)-Fe(1)-C(16)	99(7)
C(48)-O(1)-C(49)	122(3)
C(99)-O(3)-C(92)	108(6)
C(48)-N(1)-C(8)	122(4)
C(48)-N(1)-C(7)	119(5)
C(8)-N(1)-C(7)	117(6)
C(5)-N(2)-C(3)	124(4)
C(5)-N(2)-C(4)	125(5)
C(3)-N(2)-C(4)	111(7)
C(3)-C(1)-C(2)	98(3)
C(4)-C(2)-C(1)	107(4)
N(2)-C(3)-C(1)	112(5)
N(2)-C(4)-C(2)	108(6)
N(2)-C(5)-C(6)	121(5)
N(2)-C(5)-C(9)	126(5)
C(6)-C(5)-C(9)	113(7)
C(5)-C(6)-C(7)	127(4)
N(1)-C(7)-C(6)	119(5)
C(12)-C(8)-N(1)	126(6)
C(12)-C(8)-C(9)	113(4)
N(1)-C(8)-C(9)	121(4)
C(12)-C(8)-Fe(1)	71(5)
N(1)-C(8)-Fe(1)	130(4)

C(9)-C(8)-Fe(1)	70(3)
C(10)-C(9)-C(8)	103(3)
C(10)-C(9)-C(5)	136(5)
C(8)-C(9)-C(5)	121(5)
C(10)-C(9)-Fe(1)	70(5)
C(8)-C(9)-Fe(1)	70(3)
C(5)-C(9)-Fe(1)	124(4)
C(11)-C(10)-C(9)	109(5)
C(11)-C(10)-Fe(1)	68(5)
C(9)-C(10)-Fe(1)	71(7)
C(10)-C(11)-C(12)	115(7)
C(10)-C(11)-Fe(1)	74(3)
C(12)-C(11)-Fe(1)	74(5)
C(8)-C(12)-C(11)	100(6)
C(8)-C(12)-Fe(1)	71(6)
C(11)-C(12)-Fe(1)	67(6)
C(17)-C(13)-C(42)	127(4)
C(17)-C(13)-C(14)	109(4)
C(42)-C(13)-C(14)	123(6)
C(17)-C(13)-Fe(1)	72(3)
C(42)-C(13)-Fe(1)	134(5)
C(14)-C(13)-Fe(1)	69(6)
C(36)-C(14)-C(15)	134(5)
C(36)-C(14)-C(13)	125(3)
C(15)-C(14)-C(13)	101(6)
C(36)-C(14)-Fe(1)	131(4)
C(15)-C(14)-Fe(1)	66(6)
C(13)-C(14)-Fe(1)	67(5)
C(14)-C(15)-C(30)	125(4)
C(14)-C(15)-C(16)	116(7)
C(30)-C(15)-C(16)	118(4)
C(14)-C(15)-Fe(1)	74(3)
C(30)-C(15)-Fe(1)	132(3)

C(16)-C(15)-Fe(1)	71.3(17)
C(24)-C(16)-C(17)	136(3)
C(24)-C(16)-C(15)	123(6)
C(17)-C(16)-C(15)	99(6)
C(24)-C(16)-Fe(1)	137(3)
C(17)-C(16)-Fe(1)	69(4)
C(15)-C(16)-Fe(1)	64(5)
C(18)-C(17)-C(13)	124(5)
C(18)-C(17)-C(16)	120(6)
C(13)-C(17)-C(16)	115(4)
C(18)-C(17)-Fe(1)	130(5)
C(13)-C(17)-Fe(1)	69(3)
C(16)-C(17)-Fe(1)	70(6)
C(20)-C(18)-C(17)	126(6)
C(20)-C(18)-C(19)	114(5)
C(17)-C(18)-C(19)	120(4)
C(23)-C(19)-C(18)	106(5)
C(21)-C(20)-C(18)	134(5)
C(20)-C(21)-C(22)	120(5)
C(23)-C(22)-C(21)	108(6)
C(22)-C(23)-C(19)	138(5)
C(16)-C(24)-C(29)	112(7)
C(16)-C(24)-C(25)	120(4)
C(29)-C(24)-C(25)	127(6)
C(24)-C(25)-C(26)	111(3)
C(27)-C(26)-C(25)	125(7)
C(26)-C(27)-C(28)	115(7)
C(29)-C(28)-C(27)	128(4)
C(28)-C(29)-C(24)	113(8)
C(35)-C(30)-C(31)	115(5)
C(35)-C(30)-C(15)	127(5)
C(31)-C(30)-C(15)	117(5)
C(32)-C(31)-C(30)	112(5)

C(33)-C(32)-C(31)	139(5)
C(32)-C(33)-C(34)	108(4)
C(33)-C(34)-C(35)	120(5)
C(30)-C(35)-C(34)	125(6)
C(41)-C(36)-C(14)	125(6)
C(41)-C(36)-C(37)	117(7)
C(14)-C(36)-C(37)	119(3)
C(38)-C(37)-C(36)	123(3)
C(39)-C(38)-C(37)	118(6)
C(38)-C(39)-C(40)	119(6)
C(41)-C(40)-C(39)	121(3)
C(40)-C(41)-C(36)	120(6)
C(43)-C(42)-C(47)	116(5)
C(43)-C(42)-C(13)	130(4)
C(47)-C(42)-C(13)	114(6)
C(44)-C(43)-C(42)	122(4)
C(45)-C(44)-C(43)	122(6)
C(44)-C(45)-C(46)	120(4)
C(45)-C(46)-C(47)	123(4)
C(42)-C(47)-C(46)	116(6)
O(2)-C(48)-O(1)	123(6)
O(2)-C(48)-N(1)	125(5)
O(1)-C(48)-N(1)	113(4)
O(1)-C(49)-C(50)	108(5)
O(1)-C(49)-C(52)	101(3)
C(50)-C(49)-C(52)	113(7)
O(1)-C(49)-C(51)	108(5)
C(50)-C(49)-C(51)	112(5)
C(52)-C(49)-C(51)	113(6)
C(49)-C(52)-Cl(3)	112(7)
C(49)-C(52)-Cl(1)	112(4)
Cl(3)-C(52)-Cl(1)	110(5)
C(49)-C(52)-Cl(2)	108(6)

Cl(3)-C(52)-Cl(2)	109(5)
Cl(1)-C(52)-Cl(2)	105(6)
C(91)-C(86)-C(87)	118(4)
C(88)-C(87)-C(86)	136(6)
C(88)-C(87)-C(89)	43(3)
C(86)-C(87)-C(89)	94(6)
C(87)-C(88)-C(89)	101(5)
C(88)-C(89)-C(90)	121(4)
C(88)-C(89)-C(87)	37(5)
C(90)-C(89)-C(87)	85(5)
C(91)-C(90)-C(89)	131(6)
C(90)-C(91)-C(86)	111(5)
C(90)-C(91)-C(98)	132(6)
C(86)-C(91)-C(98)	116(4)
C(97)-C(92)-O(3)	105(7)
C(97)-C(92)-C(93)	130(4)
O(3)-C(92)-C(93)	125(5)
C(97)-C(92)-C(99)	73(6)
O(3)-C(92)-C(99)	32(2)
C(93)-C(92)-C(99)	155(4)
C(94)-C(93)-C(92)	118(5)
C(93)-C(94)-C(95)	121(7)
C(94)-C(95)-C(96)	115(4)
C(97)-C(96)-C(95)	124(4)
C(98)-C(97)-C(92)	118(5)
C(98)-C(97)-C(96)	130(4)
C(92)-C(97)-C(96)	111(7)
C(97)-C(98)-C(91)	136(6)
C(97)-C(98)-C(99)	91(4)
C(91)-C(98)-C(99)	126(4)
O(3)-C(99)-O(4)	124(7)
O(3)-C(99)-C(98)	115(4)
O(4)-C(99)-C(98)	118(5)

O(3)-C(99)-C(92)	40(5)
O(4)-C(99)-C(92)	163(4)
C(98)-C(99)-C(92)	77(4)

Table 4. Hydrogen coordinates (x 10^4) and isotropic displacement parameters ($Å^2$x 10^3) for 02167IHs.

	x	y	z	U(eq)
H(1A)	3793	4643	364	62
H(1B)	5088	4832	606	62
H(2A)	3842	4692	1163	104
H(2B)	2554	4857	920	104
H(3A)	4687	3382	339	85
H(3B)	5563	3516	691	85
H(4A)	2935	3531	1270	8
H(4B)	1919	3614	941	8
H(6)	5380	2257	490	25
H(7)	5671	906	510	52
H(10)	1221	2545	1260	17
H(11)	431	1297	1499	19
H(12)	1825	122	1281	6
H(19A)	5997	597	1154	84
H(19B)	6885	1256	1346	84
H(20)	5750	-121	2143	65
H(21)	7558	-816	2091	46
H(22)	8868	-780	1506	83
H(23)	8326	267	1180	31
H(25A)	2059	353	2590	79
H(25B)	3602	174	2657	79
H(26)	2259	-968	2869	35
H(27)	2177	-1949	2479	71
H(28)	2694	-1655	1860	100
H(29)	3353	-449	1648	50
H(31)	2226	2436	2692	32

H(32)	444	2316	3032	45
H(33)	-1481	1813	2930	15
H(34)	-1404	884	2445	64
H(35)	517	805	2087	47
H(37)	1334	3046	1881	40
H(38)	804	4363	1954	32
H(39)	2493	5226	1945	16
H(40)	4697	4775	2125	24
H(41)	5159	3492	2153	34
H(43)	5321	3058	1283	40
H(44)	7226	3764	1197	33
H(45)	9153	3358	1417	35
H(46)	9165	2494	1880	27
H(47)	7267	1738	2025	51
H(50A)	4043	-2098	401	113
H(50B)	4000	-1410	111	113
H(50C)	3242	-1311	484	113
H(51A)	6302	-1246	1064	142
H(51B)	6124	-2095	891	142
H(51C)	4884	-1669	1074	142
H(86)	2043	826	10228	53
H(87)	324	-69	10093	43
H(88)	590	-1413	10142	67
H(89)	786	-724	9552	71
H(90)	2895	-305	9400	58
H(93)	4559	3391	9309	73
H(94)	3280	4144	9727	43
H(95A)	1352	3344	9894	53
H(95B)	2411	3399	10211	53
H(96A)	2674	2158	10217	30
H(96B)	1452	2098	9951	30
H(98)	4071	1022	9881	51

Table 5. Torsion angles [°] for 02167IHs.

C(3)-C(1)-C(2)-C(4)	-22(5)
C(5)-N(2)-C(3)-C(1)	177(3)
C(4)-N(2)-C(3)-C(1)	-14(4)
C(2)-C(1)-C(3)-N(2)	21(4)
C(5)-N(2)-C(4)-C(2)	167(3)
C(3)-N(2)-C(4)-C(2)	-2(4)
C(1)-C(2)-C(4)-N(2)	16(4)
C(3)-N(2)-C(5)-C(6)	-5(5)
C(4)-N(2)-C(5)-C(6)	-172(3)
C(3)-N(2)-C(5)-C(9)	-177(3)
C(4)-N(2)-C(5)-C(9)	15(5)
N(2)-C(5)-C(6)-C(7)	-177(3)
C(9)-C(5)-C(6)-C(7)	-3(5)
C(48)-N(1)-C(7)-C(6)	-176(3)
C(8)-N(1)-C(7)-C(6)	-10(5)
C(5)-C(6)-C(7)-N(1)	7(6)
C(48)-N(1)-C(8)-C(12)	-7(5)
C(7)-N(1)-C(8)-C(12)	-173(3)
C(48)-N(1)-C(8)-C(9)	176(3)
C(7)-N(1)-C(8)-C(9)	10(5)
C(48)-N(1)-C(8)-Fe(1)	87(5)
C(7)-N(1)-C(8)-Fe(1)	-79(5)
C(15)-Fe(1)-C(8)-C(12)	11(4)
C(11)-Fe(1)-C(8)-C(12)	-42(4)
C(13)-Fe(1)-C(8)-C(12)	149(3)
C(10)-Fe(1)-C(8)-C(12)	-85(7)
C(14)-Fe(1)-C(8)-C(12)	-156(3)
C(9)-Fe(1)-C(8)-C(12)	-125(5)
C(17)-Fe(1)-C(8)-C(12)	105(7)
C(16)-Fe(1)-C(8)-C(12)	59(5)
C(15)-Fe(1)-C(8)-N(1)	-110(7)

C(11)-Fe(1)-C(8)-N(1)	-164(3)
C(13)-Fe(1)-C(8)-N(1)	27(4)
C(10)-Fe(1)-C(8)-N(1)	154(3)
C(14)-Fe(1)-C(8)-N(1)	83(6)
C(9)-Fe(1)-C(8)-N(1)	114(4)
C(17)-Fe(1)-C(8)-N(1)	-16(3)
C(12)-Fe(1)-C(8)-N(1)	-121(6)
C(16)-Fe(1)-C(8)-N(1)	-62(3)
C(15)-Fe(1)-C(8)-C(9)	136(5)
C(11)-Fe(1)-C(8)-C(9)	82(2)
C(13)-Fe(1)-C(8)-C(9)	-87(3)
C(10)-Fe(1)-C(8)-C(9)	40(3)
C(14)-Fe(1)-C(8)-C(9)	-31(6)
C(17)-Fe(1)-C(8)-C(9)	-130(3)
C(12)-Fe(1)-C(8)-C(9)	125(5)
C(16)-Fe(1)-C(8)-C(9)	-176(2)
C(12)-C(8)-C(9)-C(10)	-6(4)
N(1)-C(8)-C(9)-C(10)	171(3)
Fe(1)-C(8)-C(9)-C(10)	-63(5)
C(12)-C(8)-C(9)-C(5)	176(3)
N(1)-C(8)-C(9)-C(5)	-7(5)
Fe(1)-C(8)-C(9)-C(5)	119(5)
C(12)-C(8)-C(9)-Fe(1)	57(5)
N(1)-C(8)-C(9)-Fe(1)	-126(5)
N(2)-C(5)-C(9)-C(10)	-1(7)
C(6)-C(5)-C(9)-C(10)	-174(4)
N(2)-C(5)-C(9)-C(8)	177(3)
C(6)-C(5)-C(9)-C(8)	3(5)
N(2)-C(5)-C(9)-Fe(1)	-97(6)
C(6)-C(5)-C(9)-Fe(1)	89(5)
C(15)-Fe(1)-C(9)-C(10)	-37(4)
C(11)-Fe(1)-C(9)-C(10)	36(4)
C(13)-Fe(1)-C(9)-C(10)	-130(6)

C(14)-Fe(1)-C(9)-C(10)	-80(4)
C(17)-Fe(1)-C(9)-C(10)	-172(2)
C(8)-Fe(1)-C(9)-C(10)	112(3)
C(12)-Fe(1)-C(9)-C(10)	79(5)
C(16)-Fe(1)-C(9)-C(10)	124(4)
C(15)-Fe(1)-C(9)-C(8)	-150(4)
C(11)-Fe(1)-C(9)-C(8)	-77(3)
C(13)-Fe(1)-C(9)-C(8)	118(4)
C(10)-Fe(1)-C(9)-C(8)	-112(3)
C(14)-Fe(1)-C(9)-C(8)	168(2)
C(17)-Fe(1)-C(9)-C(8)	75(3)
C(12)-Fe(1)-C(9)-C(8)	-33(4)
C(16)-Fe(1)-C(9)-C(8)	12(6)
C(15)-Fe(1)-C(9)-C(5)	95(7)
C(11)-Fe(1)-C(9)-C(5)	168(3)
C(13)-Fe(1)-C(9)-C(5)	2(3)
C(10)-Fe(1)-C(9)-C(5)	133(6)
C(14)-Fe(1)-C(9)-C(5)	53(4)
C(17)-Fe(1)-C(9)-C(5)	-40(5)
C(8)-Fe(1)-C(9)-C(5)	-115(5)
C(12)-Fe(1)-C(9)-C(5)	-148(3)
C(16)-Fe(1)-C(9)-C(5)	-103(7)
C(8)-C(9)-C(10)-C(11)	5(4)
C(5)-C(9)-C(10)-C(11)	-177(4)
Fe(1)-C(9)-C(10)-C(11)	-58(3)
C(8)-C(9)-C(10)-Fe(1)	63(3)
C(5)-C(9)-C(10)-Fe(1)	-119(5)
C(15)-Fe(1)-C(10)-C(11)	-79(5)
C(13)-Fe(1)-C(10)-C(11)	-166(2)
C(14)-Fe(1)-C(10)-C(11)	-123(5)
C(9)-Fe(1)-C(10)-C(11)	120(4)
C(17)-Fe(1)-C(10)-C(11)	158(8)
C(8)-Fe(1)-C(10)-C(11)	78(6)

C(12)-Fe(1)-C(10)-C(11)	36(4)
C(16)-Fe(1)-C(10)-C(11)	-33(3)
C(15)-Fe(1)-C(10)-C(9)	161(3)
C(11)-Fe(1)-C(10)-C(9)	-120(4)
C(13)-Fe(1)-C(10)-C(9)	74(4)
C(14)-Fe(1)-C(10)-C(9)	118(4)
C(17)-Fe(1)-C(10)-C(9)	38(9)
C(8)-Fe(1)-C(10)-C(9)	-42(4)
C(12)-Fe(1)-C(10)-C(9)	-84(4)
C(16)-Fe(1)-C(10)-C(9)	-153(3)
C(9)-C(10)-C(11)-C(12)	-3(4)
Fe(1)-C(10)-C(11)-C(12)	-63(6)
C(9)-C(10)-C(11)-Fe(1)	60(6)
C(15)-Fe(1)-C(11)-C(10)	115(4)
C(13)-Fe(1)-C(11)-C(10)	53(8)
C(14)-Fe(1)-C(11)-C(10)	75(7)
C(9)-Fe(1)-C(11)-C(10)	-36.9(18)
C(17)-Fe(1)-C(11)-C(10)	-173(3)
C(8)-Fe(1)-C(11)-C(10)	-82(6)
C(12)-Fe(1)-C(11)-C(10)	-123(7)
C(16)-Fe(1)-C(11)-C(10)	161.5(18)
C(15)-Fe(1)-C(11)-C(12)	-122(3)
C(13)-Fe(1)-C(11)-C(12)	177(5)
C(10)-Fe(1)-C(11)-C(12)	123(7)
C(14)-Fe(1)-C(11)-C(12)	-161.6(17)
C(9)-Fe(1)-C(11)-C(12)	86(6)
C(17)-Fe(1)-C(11)-C(12)	-50(7)
C(8)-Fe(1)-C(11)-C(12)	41.2(16)
C(16)-Fe(1)-C(11)-C(12)	-75(7)
N(1)-C(8)-C(12)-C(11)	-173(3)
C(9)-C(8)-C(12)-C(11)	4(3)
Fe(1)-C(8)-C(12)-C(11)	61(4)
N(1)-C(8)-C(12)-Fe(1)	126(4)

C(9)-C(8)-C(12)-Fe(1)	-57(4)
C(10)-C(11)-C(12)-C(8)	-1(3)
Fe(1)-C(11)-C(12)-C(8)	-64(6)
C(10)-C(11)-C(12)-Fe(1)	63(6)
C(15)-Fe(1)-C(12)-C(8)	-175.5(18)
C(11)-Fe(1)-C(12)-C(8)	110(5)
C(13)-Fe(1)-C(12)-C(8)	-68(5)
C(10)-Fe(1)-C(12)-C(8)	77(5)
C(14)-Fe(1)-C(12)-C(8)	157(3)
C(9)-Fe(1)-C(12)-C(8)	35(3)
C(17)-Fe(1)-C(12)-C(8)	-95(5)
C(16)-Fe(1)-C(12)-C(8)	-133(4)
C(15)-Fe(1)-C(12)-C(11)	74(4)
C(13)-Fe(1)-C(12)-C(11)	-178(2)
C(10)-Fe(1)-C(12)-C(11)	-34(3)
C(14)-Fe(1)-C(12)-C(11)	46(5)
C(9)-Fe(1)-C(12)-C(11)	-76(4)
C(17)-Fe(1)-C(12)-C(11)	155(3)
C(8)-Fe(1)-C(12)-C(11)	-110(5)
C(16)-Fe(1)-C(12)-C(11)	116(4)
C(15)-Fe(1)-C(13)-C(17)	81(3)
C(11)-Fe(1)-C(13)-C(17)	146(6)
C(10)-Fe(1)-C(13)-C(17)	-172(2)
C(14)-Fe(1)-C(13)-C(17)	120(5)
C(9)-Fe(1)-C(13)-C(17)	-130(3)
C(8)-Fe(1)-C(13)-C(17)	-85(4)
C(12)-Fe(1)-C(13)-C(17)	-39(5)
C(16)-Fe(1)-C(13)-C(17)	33(3)
C(15)-Fe(1)-C(13)-C(42)	-155(4)
C(11)-Fe(1)-C(13)-C(42)	-90(8)
C(10)-Fe(1)-C(13)-C(42)	-48(4)
C(14)-Fe(1)-C(13)-C(42)	-116(7)
C(9)-Fe(1)-C(13)-C(42)	-6(3)

C(17)-Fe(1)-C(13)-C(42)	124(4)
C(8)-Fe(1)-C(13)-C(42)	39(5)
C(12)-Fe(1)-C(13)-C(42)	85(6)
C(16)-Fe(1)-C(13)-C(42)	157(3)
C(15)-Fe(1)-C(13)-C(14)	-39(4)
C(11)-Fe(1)-C(13)-C(14)	26(6)
C(10)-Fe(1)-C(13)-C(14)	69(6)
C(9)-Fe(1)-C(13)-C(14)	110(6)
C(17)-Fe(1)-C(13)-C(14)	-120(5)
C(8)-Fe(1)-C(13)-C(14)	156(2)
C(12)-Fe(1)-C(13)-C(14)	-159(2)
C(16)-Fe(1)-C(13)-C(14)	-87(7)
C(17)-C(13)-C(14)-C(36)	175(3)
C(42)-C(13)-C(14)-C(36)	5(5)
Fe(1)-C(13)-C(14)-C(36)	-124(5)
C(17)-C(13)-C(14)-C(15)	-4(3)
C(42)-C(13)-C(14)-C(15)	-173(3)
Fe(1)-C(13)-C(14)-C(15)	57(5)
C(17)-C(13)-C(14)-Fe(1)	-61(5)
C(42)-C(13)-C(14)-Fe(1)	130(5)
C(15)-Fe(1)-C(14)-C(36)	-128(6)
C(11)-Fe(1)-C(14)-C(36)	-56(4)
C(13)-Fe(1)-C(14)-C(36)	117(4)
C(10)-Fe(1)-C(14)-C(36)	-18(3)
C(9)-Fe(1)-C(14)-C(36)	22(4)
C(17)-Fe(1)-C(14)-C(36)	152(4)
C(8)-Fe(1)-C(14)-C(36)	46(7)
C(12)-Fe(1)-C(14)-C(36)	-90(6)
C(16)-Fe(1)-C(14)-C(36)	-165(4)
C(11)-Fe(1)-C(14)-C(15)	71(4)
C(13)-Fe(1)-C(14)-C(15)	-115(4)
C(10)-Fe(1)-C(14)-C(15)	110(6)
C(9)-Fe(1)-C(14)-C(15)	150(3)

C(17)-Fe(1)-C(14)-C(15)	-80(6)
C(8)-Fe(1)-C(14)-C(15)	173(3)
C(12)-Fe(1)-C(14)-C(15)	37(4)
C(16)-Fe(1)-C(14)-C(15)	-37(4)
C(15)-Fe(1)-C(14)-C(13)	115(4)
C(11)-Fe(1)-C(14)-C(13)	-173.3(16)
C(10)-Fe(1)-C(14)-C(13)	-135(3)
C(9)-Fe(1)-C(14)-C(13)	-95(2)
C(17)-Fe(1)-C(14)-C(13)	36(3)
C(8)-Fe(1)-C(14)-C(13)	-71(5)
C(12)-Fe(1)-C(14)-C(13)	153(4)
C(16)-Fe(1)-C(14)-C(13)	78(2)
C(36)-C(14)-C(15)-C(30)	-6(6)
C(13)-C(14)-C(15)-C(30)	172(3)
Fe(1)-C(14)-C(15)-C(30)	-130(4)
C(36)-C(14)-C(15)-C(16)	-177(3)
C(13)-C(14)-C(15)-C(16)	2(3)
Fe(1)-C(14)-C(15)-C(16)	59(3)
C(36)-C(14)-C(15)-Fe(1)	124(4)
C(13)-C(14)-C(15)-Fe(1)	-58(3)
C(11)-Fe(1)-C(15)-C(14)	-126(3)
C(13)-Fe(1)-C(15)-C(14)	42.3(19)
C(10)-Fe(1)-C(15)-C(14)	-88(7)
C(9)-Fe(1)-C(15)-C(14)	-62(7)
C(17)-Fe(1)-C(15)-C(14)	84(6)
C(8)-Fe(1)-C(15)-C(14)	-173(3)
C(12)-Fe(1)-C(15)-C(14)	-165.1(17)
C(16)-Fe(1)-C(15)-C(14)	125(6)
C(11)-Fe(1)-C(15)-C(30)	-3(3)
C(13)-Fe(1)-C(15)-C(30)	165(4)
C(10)-Fe(1)-C(15)-C(30)	36(5)
C(14)-Fe(1)-C(15)-C(30)	123(5)
C(9)-Fe(1)-C(15)-C(30)	61(6)

C(17)-Fe(1)-C(15)-C(30)	-153(5)
C(8)-Fe(1)-C(15)-C(30)	-50(6)
C(12)-Fe(1)-C(15)-C(30)	-42(5)
C(16)-Fe(1)-C(15)-C(30)	-112(5)
C(11)-Fe(1)-C(15)-C(16)	109(4)
C(13)-Fe(1)-C(15)-C(16)	-83(5)
C(10)-Fe(1)-C(15)-C(16)	147.4(15)
C(14)-Fe(1)-C(15)-C(16)	-125(6)
C(9)-Fe(1)-C(15)-C(16)	173(2)
C(17)-Fe(1)-C(15)-C(16)	-40.7(15)
C(8)-Fe(1)-C(15)-C(16)	62(8)
C(12)-Fe(1)-C(15)-C(16)	70(7)
C(14)-C(15)-C(16)-C(24)	169(3)
C(30)-C(15)-C(16)-C(24)	-3(4)
Fe(1)-C(15)-C(16)-C(24)	-131(4)
C(14)-C(15)-C(16)-C(17)	1(3)
C(30)-C(15)-C(16)-C(17)	-171(3)
Fe(1)-C(15)-C(16)-C(17)	61(3)
C(14)-C(15)-C(16)-Fe(1)	-61(3)
C(30)-C(15)-C(16)-Fe(1)	128(4)
C(15)-Fe(1)-C(16)-C(24)	112(7)
C(11)-Fe(1)-C(16)-C(24)	25(4)
C(13)-Fe(1)-C(16)-C(24)	-168(4)
C(10)-Fe(1)-C(16)-C(24)	46(5)
C(14)-Fe(1)-C(16)-C(24)	146(4)
C(9)-Fe(1)-C(16)-C(24)	-56(8)
C(17)-Fe(1)-C(16)-C(24)	-136(5)
C(8)-Fe(1)-C(16)-C(24)	-47(5)
C(12)-Fe(1)-C(16)-C(24)	-14(4)
C(15)-Fe(1)-C(16)-C(17)	-112(4)
C(11)-Fe(1)-C(16)-C(17)	161(3)
C(13)-Fe(1)-C(16)-C(17)	-32(3)
C(10)-Fe(1)-C(16)-C(17)	-177(2)

C(14)-Fe(1)-C(16)-C(17)	-78(2)
C(9)-Fe(1)-C(16)-C(17)	81(5)
C(8)-Fe(1)-C(16)-C(17)	90(3)
C(12)-Fe(1)-C(16)-C(17)	123(3)
C(11)-Fe(1)-C(16)-C(15)	-87(5)
C(13)-Fe(1)-C(16)-C(15)	80(6)
C(10)-Fe(1)-C(16)-C(15)	-66(4)
C(14)-Fe(1)-C(16)-C(15)	34(4)
C(9)-Fe(1)-C(16)-C(15)	-168(4)
C(17)-Fe(1)-C(16)-C(15)	112(4)
C(8)-Fe(1)-C(16)-C(15)	-159(3)
C(12)-Fe(1)-C(16)-C(15)	-126(5)
C(42)-C(13)-C(17)-C(18)	-7(6)
C(14)-C(13)-C(17)-C(18)	-176(3)
Fe(1)-C(13)-C(17)-C(18)	125(7)
C(42)-C(13)-C(17)-C(16)	174(3)
C(14)-C(13)-C(17)-C(16)	5(4)
Fe(1)-C(13)-C(17)-C(16)	-55(7)
C(42)-C(13)-C(17)-Fe(1)	-132(6)
C(14)-C(13)-C(17)-Fe(1)	59(7)
C(24)-C(16)-C(17)-C(18)	12(6)
C(15)-C(16)-C(17)-C(18)	177(3)
Fe(1)-C(16)-C(17)-C(18)	-125(5)
C(24)-C(16)-C(17)-C(13)	-169(4)
C(15)-C(16)-C(17)-C(13)	-3(4)
Fe(1)-C(16)-C(17)-C(13)	54(4)
C(24)-C(16)-C(17)-Fe(1)	137(5)
C(15)-C(16)-C(17)-Fe(1)	-58(4)
C(15)-Fe(1)-C(17)-C(18)	158(4)
C(11)-Fe(1)-C(17)-C(18)	76(7)
C(13)-Fe(1)-C(17)-C(18)	-118(5)
C(10)-Fe(1)-C(17)-C(18)	-76(11)
C(14)-Fe(1)-C(17)-C(18)	-158(4)

C(9)-Fe(1)-C(17)-C(18)	-43(6)
C(8)-Fe(1)-C(17)-C(18)	0(4)
C(12)-Fe(1)-C(17)-C(18)	43(4)
C(16)-Fe(1)-C(17)-C(18)	113(7)
C(15)-Fe(1)-C(17)-C(13)	-84(3)
C(11)-Fe(1)-C(17)-C(13)	-165(3)
C(10)-Fe(1)-C(17)-C(13)	43(10)
C(14)-Fe(1)-C(17)-C(13)	-40(4)
C(9)-Fe(1)-C(17)-C(13)	75(3)
C(8)-Fe(1)-C(17)-C(13)	118(4)
C(12)-Fe(1)-C(17)-C(13)	161(3)
C(16)-Fe(1)-C(17)-C(13)	-128(4)
C(15)-Fe(1)-C(17)-C(16)	45(5)
C(11)-Fe(1)-C(17)-C(16)	-37(4)
C(13)-Fe(1)-C(17)-C(16)	128(4)
C(10)-Fe(1)-C(17)-C(16)	171(7)
C(14)-Fe(1)-C(17)-C(16)	88(6)
C(9)-Fe(1)-C(17)-C(16)	-157(3)
C(8)-Fe(1)-C(17)-C(16)	-113(6)
C(12)-Fe(1)-C(17)-C(16)	-70(5)
C(13)-C(17)-C(18)-C(20)	132(4)
C(16)-C(17)-C(18)-C(20)	-49(5)
Fe(1)-C(17)-C(18)-C(20)	-137(5)
C(13)-C(17)-C(18)-C(19)	-40(5)
C(16)-C(17)-C(18)-C(19)	140(4)
Fe(1)-C(17)-C(18)-C(19)	51(6)
C(20)-C(18)-C(19)-C(23)	-4(4)
C(17)-C(18)-C(19)-C(23)	169(3)
C(17)-C(18)-C(20)-C(21)	-168(4)
C(19)-C(18)-C(20)-C(21)	4(6)
C(18)-C(20)-C(21)-C(22)	-7(6)
C(20)-C(21)-C(22)-C(23)	8(5)
C(21)-C(22)-C(23)-C(19)	-11(6)

C(18)-C(19)-C(23)-C(22)	9(6)
C(17)-C(16)-C(24)-C(29)	-59(6)
C(15)-C(16)-C(24)-C(29)	138(4)
Fe(1)-C(16)-C(24)-C(29)	52(7)
C(17)-C(16)-C(24)-C(25)	112(5)
C(15)-C(16)-C(24)-C(25)	-51(5)
Fe(1)-C(16)-C(24)-C(25)	-137(5)
C(16)-C(24)-C(25)-C(26)	-174(3)
C(29)-C(24)-C(25)-C(26)	-5(6)
C(24)-C(25)-C(26)-C(27)	1(5)
C(25)-C(26)-C(27)-C(28)	1(5)
C(26)-C(27)-C(28)-C(29)	1(6)
C(27)-C(28)-C(29)-C(24)	-4(6)
C(16)-C(24)-C(29)-C(28)	176(3)
C(25)-C(24)-C(29)-C(28)	6(6)
C(14)-C(15)-C(30)-C(35)	141(5)
C(16)-C(15)-C(30)-C(35)	-49(6)
Fe(1)-C(15)-C(30)-C(35)	41(6)
C(14)-C(15)-C(30)-C(31)	-46(5)
C(16)-C(15)-C(30)-C(31)	125(5)
Fe(1)-C(15)-C(30)-C(31)	-145(4)
C(35)-C(30)-C(31)-C(32)	-3(4)
C(15)-C(30)-C(31)-C(32)	-177(3)
C(30)-C(31)-C(32)-C(33)	-7(6)
C(31)-C(32)-C(33)-C(34)	11(6)
C(32)-C(33)-C(34)-C(35)	-5(5)
C(31)-C(30)-C(35)-C(34)	7(5)
C(15)-C(30)-C(35)-C(34)	-180(3)
C(33)-C(34)-C(35)-C(30)	-2(6)
C(15)-C(14)-C(36)-C(41)	140(6)
C(13)-C(14)-C(36)-C(41)	-38(7)
Fe(1)-C(14)-C(36)-C(41)	-126(3)
C(15)-C(14)-C(36)-C(37)	-43(7)

C(13)-C(14)-C(36)-C(37)	139(6)
Fe(1)-C(14)-C(36)-C(37)	51(4)
C(41)-C(36)-C(37)-C(38)	-2(5)
C(14)-C(36)-C(37)-C(38)	-179(3)
C(36)-C(37)-C(38)-C(39)	11(5)
C(37)-C(38)-C(39)-C(40)	-14(5)
C(38)-C(39)-C(40)-C(41)	8(5)
C(39)-C(40)-C(41)-C(36)	1(5)
C(14)-C(36)-C(41)-C(40)	173(3)
C(37)-C(36)-C(41)-C(40)	-4(5)
C(17)-C(13)-C(42)-C(43)	131(6)
C(14)-C(13)-C(42)-C(43)	-62(7)
Fe(1)-C(13)-C(42)-C(43)	30(6)
C(17)-C(13)-C(42)-C(47)	-46(6)
C(14)-C(13)-C(42)-C(47)	121(6)
Fe(1)-C(13)-C(42)-C(47)	-147(3)
C(47)-C(42)-C(43)-C(44)	-6(5)
C(13)-C(42)-C(43)-C(44)	177(3)
C(42)-C(43)-C(44)-C(45)	9(5)
C(43)-C(44)-C(45)-C(46)	-10(5)
C(44)-C(45)-C(46)-C(47)	8(5)
C(43)-C(42)-C(47)-C(46)	4(5)
C(13)-C(42)-C(47)-C(46)	-178(3)
C(45)-C(46)-C(47)-C(42)	-6(5)
C(49)-O(1)-C(48)-O(2)	6(5)
C(49)-O(1)-C(48)-N(1)	-172(3)
C(8)-N(1)-C(48)-O(2)	3(5)
C(7)-N(1)-C(48)-O(2)	169(3)
C(8)-N(1)-C(48)-O(1)	-180(3)
C(7)-N(1)-C(48)-O(1)	-14(5)
C(48)-O(1)-C(49)-C(50)	62(7)
C(48)-O(1)-C(49)-C(52)	-179(3)
C(48)-O(1)-C(49)-C(51)	-60(6)

O(1)-C(49)-C(52)-Cl(3)	62(4)
C(50)-C(49)-C(52)-Cl(3)	178(2)
C(51)-C(49)-C(52)-Cl(3)	-53(6)
O(1)-C(49)-C(52)-Cl(1)	-173(2)
C(50)-C(49)-C(52)-Cl(1)	-57(4)
C(51)-C(49)-C(52)-Cl(1)	72(5)
O(1)-C(49)-C(52)-Cl(2)	-58(4)
C(50)-C(49)-C(52)-Cl(2)	58(7)
C(51)-C(49)-C(52)-Cl(2)	-173(2)
C(91)-C(86)-C(87)-C(88)	6(7)
C(91)-C(86)-C(87)-C(89)	-2(4)
C(86)-C(87)-C(88)-C(89)	-13(6)
C(87)-C(88)-C(89)-C(90)	14(6)
C(86)-C(87)-C(89)-C(88)	171(5)
C(88)-C(87)-C(89)-C(90)	-168(5)
C(86)-C(87)-C(89)-C(90)	3(3)
C(88)-C(89)-C(90)-C(91)	-14(7)
C(87)-C(89)-C(90)-C(91)	-5(5)
C(89)-C(90)-C(91)-C(86)	5(6)
C(89)-C(90)-C(91)-C(98)	-175(4)
C(87)-C(86)-C(91)-C(90)	0(5)
C(87)-C(86)-C(91)-C(98)	179(3)
C(99)-O(3)-C(92)-C(97)	11(4)
C(99)-O(3)-C(92)-C(93)	-166(4)
C(97)-C(92)-C(93)-C(94)	8(6)
O(3)-C(92)-C(93)-C(94)	-175(3)
C(99)-C(92)-C(93)-C(94)	167(6)
C(92)-C(93)-C(94)-C(95)	-7(6)
C(93)-C(94)-C(95)-C(96)	8(5)
C(94)-C(95)-C(96)-C(97)	-9(5)
O(3)-C(92)-C(97)-C(98)	1(4)
C(93)-C(92)-C(97)-C(98)	179(4)
C(99)-C(92)-C(97)-C(98)	8(3)

O(3)-C(92)-C(97)-C(96)	175(2)
C(93)-C(92)-C(97)-C(96)	-8(5)
C(99)-C(92)-C(97)-C(96)	-179(3)
C(95)-C(96)-C(97)-C(98)	-179(4)
C(95)-C(96)-C(97)-C(92)	9(5)
C(92)-C(97)-C(98)-C(91)	-161(4)
C(96)-C(97)-C(98)-C(91)	27(8)
C(92)-C(97)-C(98)-C(99)	-9(4)
C(96)-C(97)-C(98)-C(99)	179(4)
C(90)-C(91)-C(98)-C(97)	137(5)
C(86)-C(91)-C(98)-C(97)	-42(7)
C(90)-C(91)-C(98)-C(99)	-7(6)
C(86)-C(91)-C(98)-C(99)	174(4)
C(92)-O(3)-C(99)-O(4)	-176(4)
C(92)-O(3)-C(99)-C(98)	-18(5)
C(97)-C(98)-C(99)-O(3)	18(5)
C(91)-C(98)-C(99)-O(3)	174(4)
C(97)-C(98)-C(99)-O(4)	176(4)
C(91)-C(98)-C(99)-O(4)	-27(7)
C(97)-C(98)-C(99)-C(92)	6(3)
C(91)-C(98)-C(99)-C(92)	162(4)
C(97)-C(92)-C(99)-O(3)	-169(4)
C(93)-C(92)-C(99)-O(3)	28(8)
C(97)-C(92)-C(99)-O(4)	-157(13)
O(3)-C(92)-C(99)-O(4)	12(11)
C(93)-C(92)-C(99)-O(4)	39(17)
C(97)-C(92)-C(99)-C(98)	-6(2)
O(3)-C(92)-C(99)-C(98)	163(4)
C(93)-C(92)-C(99)-C(98)	-169(7)

02152MNS (Figure 2.2)

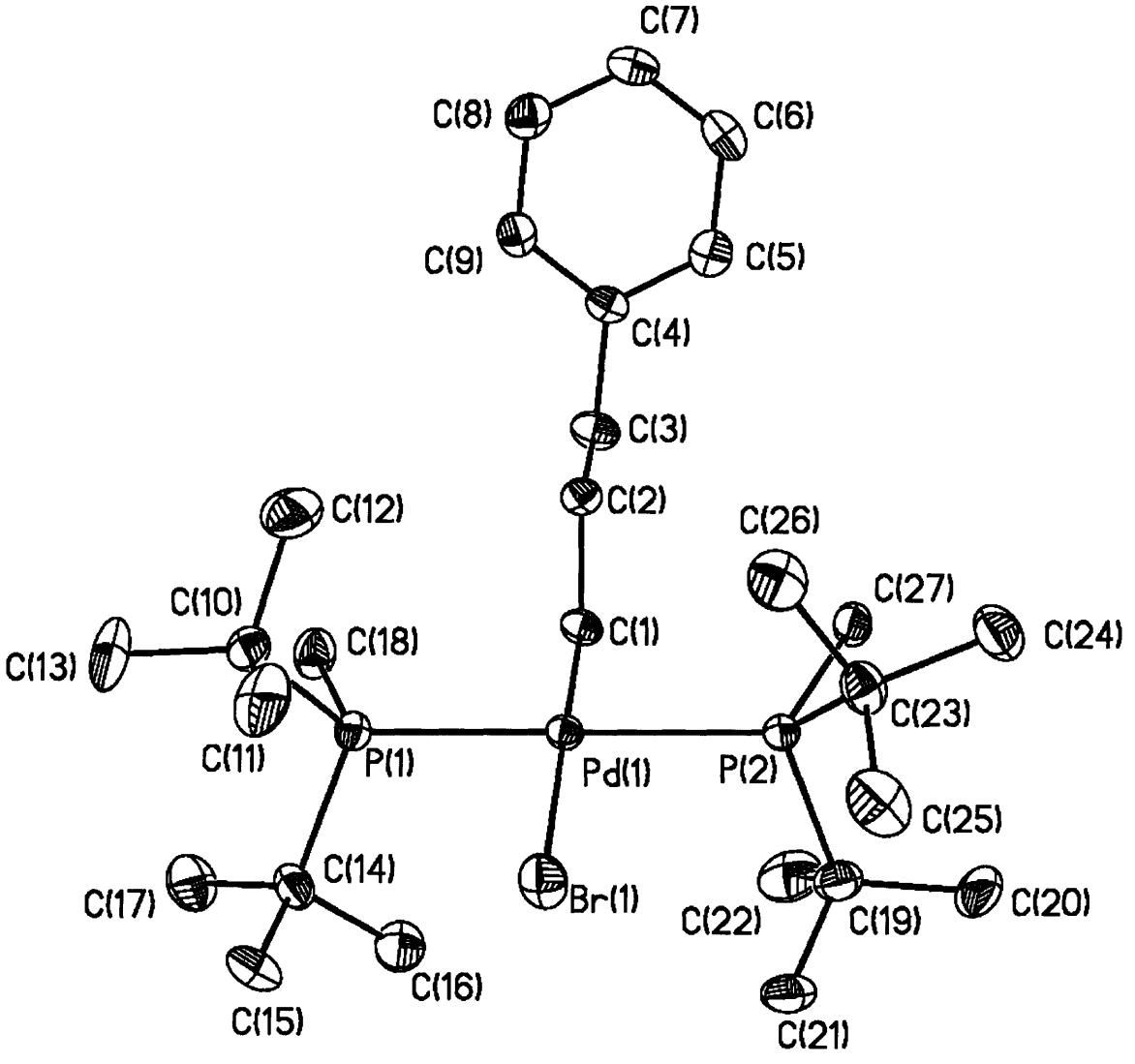

Table 1. Crystal data and structure refinement for 02152MNS.

Identification code	02152mns	
Empirical formula	C27 H53 Br P2 Pd	
Formula weight	625.94	
Temperature	193(2) K	
Wavelength	0.71073 Å	
Crystal system	Orthorhombic	
Space group	Pbca	
Unit cell dimensions	a = 11.1382(7) Å	α = 90°.
	b = 18.3329(11) Å	β = 90°.
	c = 29.5216(18) Å	γ = 90°.
Volume	6028.2(6) $Å^3$	
Z	8	
Density (calculated)	1.379 Mg/m^3	
Absorption coefficient	2.060 mm^{-1}	
F(000)	2608	
Crystal size	0.39 x 0.33 x 0.16 mm^3	
Theta range for data collection	2.25 to 23.27°.	
Index ranges	-10<=h<=12, -18<=k<=20, -32<=l<=32	
Reflections collected	22703	
Independent reflections	4332 [R(int) = 0.0660]	
Completeness to theta = 23.27°	99.8 %	
Absorption correction	Semi-empirical from equivalents	
Max. and min. transmission	0.783906 and 0.356572	
Refinement method	Full-matrix least-squares on F^2	
Data / restraints / parameters	4332 / 0 / 294	
Goodness-of-fit on F^2	1.287	
Final R indices [I>2sigma(I)]	R1 = 0.0613, wR2 = 0.1410	
R indices (all data)	R1 = 0.0631, wR2 = 0.1420	
Largest diff. peak and hole	0.994 and -0.982 $e.Å^{-3}$	

Table 2. Atomic coordinates (x 10^4) and equivalent isotropic displacement parameters ($Å^2$x 10^3) for 02152MNS. U(eq) is defined as one third of the trace of the orthogonalized U^{ij} tensor.

	x	y	z	U(eq)
Pd(1)	3508(1)	852(1)	6088(1)	23(1)
Br(1)	2467(1)	2098(1)	6187(1)	39(1)
P(1)	5255(2)	1400(1)	5768(1)	26(1)
P(2)	1798(2)	205(1)	6357(1)	24(1)
C(1)	4324(6)	-155(3)	6001(2)	28(2)
C(2)	5013(6)	-393(3)	6420(2)	27(2)
C(3)	5591(7)	-1141(4)	6358(2)	36(2)
C(4)	6176(6)	-1429(3)	6782(2)	28(2)
C(5)	5631(7)	-1965(4)	7036(3)	38(2)
C(6)	6159(8)	-2235(4)	7429(3)	44(2)
C(7)	7241(7)	-1974(4)	7570(2)	38(2)
C(8)	7795(7)	-1441(4)	7319(3)	40(2)
C(9)	7265(6)	-1175(4)	6935(2)	35(2)
C(10)	6168(7)	1985(4)	6166(2)	33(2)
C(11)	5396(8)	2576(5)	6382(3)	59(3)
C(12)	6590(9)	1491(5)	6545(3)	65(3)
C(13)	7268(8)	2342(6)	5939(3)	61(3)
C(14)	4919(7)	1883(4)	5216(2)	35(2)
C(15)	4468(8)	2668(4)	5286(3)	47(2)
C(16)	3897(8)	1444(5)	4998(3)	49(2)
C(17)	5979(8)	1912(5)	4889(3)	53(2)
C(18)	6409(7)	752(4)	5573(3)	43(2)
C(19)	618(7)	169(4)	5896(3)	40(2)
C(20)	-553(7)	-219(5)	6050(4)	59(3)
C(21)	300(8)	913(4)	5724(3)	49(2)
C(22)	1205(9)	-272(5)	5511(3)	60(2)

C(23)	1178(7)	522(4)	6920(2)	37(2)
C(24)	482(8)	-64(5)	7180(3)	51(2)
C(25)	349(9)	1181(5)	6882(3)	57(2)
C(26)	2281(8)	723(5)	7197(3)	51(2)
C(27)	2007(6)	-761(4)	6486(3)	36(2)

Table 3. Bond lengths [Å] and angles [°] for 02152MNS.

Pd(1)-C(1)	2.074(6)
Pd(1)-P(2)	2.3799(18)
Pd(1)-P(1)	2.3855(18)
Pd(1)-Br(1)	2.5783(9)
P(1)-C(18)	1.843(7)
P(1)-C(10)	1.888(7)
P(1)-C(14)	1.891(7)
P(2)-C(27)	1.826(7)
P(2)-C(23)	1.891(7)
P(2)-C(19)	1.894(7)
C(1)-C(2)	1.520(9)
C(2)-C(3)	1.526(9)
C(3)-C(4)	1.505(9)
C(4)-C(9)	1.376(10)
C(4)-C(5)	1.379(10)
C(5)-C(6)	1.391(11)
C(6)-C(7)	1.361(11)
C(7)-C(8)	1.374(11)
C(8)-C(9)	1.369(11)
C(10)-C(12)	1.515(11)
C(10)-C(11)	1.521(12)
C(10)-C(13)	1.542(11)
C(14)-C(17)	1.526(11)
C(14)-C(16)	1.536(11)
C(14)-C(15)	1.539(11)
C(19)-C(21)	1.499(11)
C(19)-C(22)	1.541(12)
C(19)-C(20)	1.553(11)
C(23)-C(26)	1.521(12)
C(23)-C(25)	1.525(11)
C(23)-C(24)	1.530(11)

C(1)-Pd(1)-P(2)	87.0(2)
C(1)-Pd(1)-P(1)	88.2(2)
P(2)-Pd(1)-P(1)	174.28(6)
C(1)-Pd(1)-Br(1)	179.1(2)
P(2)-Pd(1)-Br(1)	92.54(5)
P(1)-Pd(1)-Br(1)	92.18(5)
C(18)-P(1)-C(10)	100.7(4)
C(18)-P(1)-C(14)	99.8(4)
C(10)-P(1)-C(14)	112.2(3)
C(18)-P(1)-Pd(1)	114.9(3)
C(10)-P(1)-Pd(1)	115.6(2)
C(14)-P(1)-Pd(1)	112.1(2)
C(27)-P(2)-C(23)	99.3(3)
C(27)-P(2)-C(19)	101.7(3)
C(23)-P(2)-C(19)	112.9(4)
C(27)-P(2)-Pd(1)	116.8(2)
C(23)-P(2)-Pd(1)	115.7(2)
C(19)-P(2)-Pd(1)	109.4(3)
C(2)-C(1)-Pd(1)	112.1(4)
C(1)-C(2)-C(3)	111.9(5)
C(4)-C(3)-C(2)	113.4(6)
C(9)-C(4)-C(5)	116.7(6)
C(9)-C(4)-C(3)	122.4(6)
C(5)-C(4)-C(3)	120.9(7)
C(4)-C(5)-C(6)	121.5(7)
C(7)-C(6)-C(5)	120.3(7)
C(6)-C(7)-C(8)	118.8(7)
C(9)-C(8)-C(7)	120.5(7)
C(8)-C(9)-C(4)	122.1(7)
C(12)-C(10)-C(11)	107.0(7)
C(12)-C(10)-C(13)	109.1(7)
C(11)-C(10)-C(13)	109.2(7)

C(12)-C(10)-P(1)	106.7(5)
C(11)-C(10)-P(1)	111.1(5)
C(13)-C(10)-P(1)	113.4(5)
C(17)-C(14)-C(16)	109.1(6)
C(17)-C(14)-C(15)	107.7(6)
C(16)-C(14)-C(15)	107.7(7)
C(17)-C(14)-P(1)	114.1(6)
C(16)-C(14)-P(1)	105.2(5)
C(15)-C(14)-P(1)	112.7(5)
C(21)-C(19)-C(22)	109.1(7)
C(21)-C(19)-C(20)	108.5(7)
C(22)-C(19)-C(20)	109.4(7)
C(21)-C(19)-P(2)	112.1(5)
C(22)-C(19)-P(2)	104.7(5)
C(20)-C(19)-P(2)	113.0(6)
C(26)-C(23)-C(25)	109.7(7)
C(26)-C(23)-C(24)	108.1(7)
C(25)-C(23)-C(24)	106.6(6)
C(26)-C(23)-P(2)	104.5(5)
C(25)-C(23)-P(2)	113.6(5)
C(24)-C(23)-P(2)	114.2(5)

Table 4. Anisotropic displacement parameters ($Å^2 x\ 10^3$) for 02152MNS. The anisotropic displacement factor exponent takes the form: $-2p^2[\ h^2\ a^{*2}U^{11} + ... + 2\ h\ k\ a^*\ b^*\ U^{12}\ ]$

	U^{11}	U^{22}	U^{33}	U^{23}	U^{13}	U^{12}
Pd(1)	25(1)	21(1)	22(1)	0(1)	-1(1)	1(1)
Br(1)	42(1)	24(1)	52(1)	-1(1)	8(1)	4(1)
P(1)	25(1)	26(1)	26(1)	-1(1)	0(1)	-2(1)
P(2)	22(1)	24(1)	27(1)	3(1)	0(1)	1(1)
C(1)	35(4)	22(3)	27(3)	0(3)	-1(3)	5(3)
C(2)	28(4)	21(3)	33(4)	-1(3)	-1(3)	7(3)
C(3)	48(4)	27(4)	34(4)	0(3)	-3(4)	10(3)
C(4)	33(4)	22(3)	28(3)	-1(3)	4(3)	12(3)
C(5)	38(4)	32(4)	45(4)	-5(3)	2(4)	2(3)
C(6)	57(5)	36(4)	39(4)	7(3)	11(4)	-2(4)
C(7)	53(5)	33(4)	29(4)	-1(3)	-4(3)	11(4)
C(8)	33(4)	43(4)	43(4)	-2(4)	1(3)	7(4)
C(9)	31(4)	30(4)	43(4)	3(3)	7(3)	4(3)
C(10)	35(4)	35(4)	28(4)	-4(3)	-6(3)	-7(3)
C(11)	60(6)	63(6)	54(5)	-28(5)	-7(5)	-25(5)
C(12)	70(6)	65(6)	59(6)	4(5)	-32(5)	-14(5)
C(13)	43(5)	76(7)	64(6)	-16(5)	11(4)	-33(5)
C(14)	45(4)	33(4)	28(4)	5(3)	0(3)	-9(3)
C(15)	61(5)	40(5)	40(4)	16(4)	0(4)	5(4)
C(16)	53(5)	68(6)	27(4)	1(4)	-6(4)	-13(5)
C(17)	58(5)	62(6)	38(4)	4(4)	14(4)	-3(5)
C(18)	34(4)	37(4)	58(5)	0(4)	8(4)	1(3)
C(19)	38(4)	37(4)	45(4)	5(3)	-13(4)	-1(3)
C(20)	34(5)	49(5)	93(7)	18(5)	-18(5)	-15(4)
C(21)	46(5)	50(5)	53(5)	15(4)	-21(4)	0(4)
C(22)	64(6)	61(6)	55(5)	-15(5)	-23(5)	0(5)

C(23)	41(4)	36(4)	36(4)	-1(3)	11(3)	1(3)
C(24)	51(5)	53(5)	49(5)	17(4)	17(4)	8(4)
C(25)	71(6)	47(5)	52(5)	-1(4)	28(5)	19(5)
C(26)	59(5)	66(6)	28(4)	-9(4)	7(4)	-2(5)
C(27)	27(4)	28(4)	53(5)	9(3)	3(3)	2(3)

Table 5. Hydrogen coordinates (x 10^4) and isotropic displacement parameters ($Å^2$x 10^3) for 02152MNS.

	x	y	z	U(eq)
H(1A)	3703	-524	5930	33
H(1B)	4883	-129	5741	33
H(2A)	4458	-410	6682	33
H(2B)	5645	-29	6488	33
H(3A)	4969	-1491	6258	43
H(3B)	6203	-1108	6116	43
H(5)	4879	-2155	6942	46
H(6)	5763	-2602	7600	52
H(7)	7606	-2158	7838	46
H(8)	8551	-1255	7413	48
H(9)	7662	-803	6768	42
H(11A)	4679	2354	6516	89
H(11B)	5155	2929	6150	89
H(11C)	5858	2825	6618	89
H(12A)	6953	1786	6786	97
H(12B)	7187	1147	6427	97
H(12C)	5905	1220	6668	97
H(13A)	7747	2595	6168	92
H(13B)	6997	2692	5710	92
H(13C)	7758	1964	5794	92
H(15A)	5117	2967	5413	70
H(15B)	3787	2666	5496	70
H(15C)	4215	2872	4995	70
H(16A)	3207	1431	5204	74
H(16B)	4171	945	4938	74
H(16C)	3660	1676	4712	74

H(17A)	5742	2175	4614	79
H(17B)	6223	1415	4810	79
H(17C)	6652	2166	5033	79
H(18A)	7129	1021	5481	64
H(18B)	6100	474	5315	64
H(18C)	6612	417	5820	64
H(20A)	-929	62	6294	88
H(20B)	-362	-710	6158	88
H(20C)	-1108	-252	5793	88
H(21A)	1002	1131	5576	74
H(21B)	47	1222	5977	74
H(21C)	-357	873	5504	74
H(22A)	691	-256	5242	90
H(22B)	1307	-780	5608	90
H(22C)	1991	-62	5439	90
H(24A)	1019	-470	7252	77
H(24B)	-184	-241	6992	77
H(24C)	163	145	7461	77
H(25A)	184	1374	7185	85
H(25B)	-406	1034	6739	85
H(25C)	737	1558	6698	85
H(26A)	2723	1113	7044	77
H(26B)	2801	294	7228	77
H(26C)	2032	890	7498	77
H(27A)	2502	-811	6758	54
H(27B)	2407	-1000	6230	54
H(27C)	1223	-989	6537	54

Table 6. Torsion angles [°] for 02152MNS.

C(1)-Pd(1)-P(1)-C(18)	3.1(4)
P(2)-Pd(1)-P(1)-C(18)	-30.5(7)
Br(1)-Pd(1)-P(1)-C(18)	-176.0(3)
C(1)-Pd(1)-P(1)-C(10)	-113.5(3)
P(2)-Pd(1)-P(1)-C(10)	-147.1(6)
Br(1)-Pd(1)-P(1)-C(10)	67.3(3)
C(1)-Pd(1)-P(1)-C(14)	116.2(3)
P(2)-Pd(1)-P(1)-C(14)	82.6(7)
Br(1)-Pd(1)-P(1)-C(14)	-63.0(3)
C(1)-Pd(1)-P(2)-C(27)	12.4(3)
P(1)-Pd(1)-P(2)-C(27)	46.1(7)
Br(1)-Pd(1)-P(2)-C(27)	-168.3(3)
C(1)-Pd(1)-P(2)-C(23)	128.8(3)
P(1)-Pd(1)-P(2)-C(23)	162.5(6)
Br(1)-Pd(1)-P(2)-C(23)	-52.0(3)
C(1)-Pd(1)-P(2)-C(19)	-102.4(3)
P(1)-Pd(1)-P(2)-C(19)	-68.7(7)
Br(1)-Pd(1)-P(2)-C(19)	76.8(3)
P(2)-Pd(1)-C(1)-C(2)	-90.5(5)
P(1)-Pd(1)-C(1)-C(2)	92.7(5)
Br(1)-Pd(1)-C(1)-C(2)	-152(13)
Pd(1)-C(1)-C(2)-C(3)	178.9(5)
C(1)-C(2)-C(3)-C(4)	-174.2(6)
C(2)-C(3)-C(4)-C(9)	-76.2(9)
C(2)-C(3)-C(4)-C(5)	103.6(8)
C(9)-C(4)-C(5)-C(6)	0.1(10)
C(3)-C(4)-C(5)-C(6)	-179.8(7)
C(4)-C(5)-C(6)-C(7)	-0.4(11)
C(5)-C(6)-C(7)-C(8)	0.2(11)
C(6)-C(7)-C(8)-C(9)	0.3(11)
C(7)-C(8)-C(9)-C(4)	-0.6(11)

C(5)-C(4)-C(9)-C(8)	0.4(10)
C(3)-C(4)-C(9)-C(8)	-179.7(7)
C(18)-P(1)-C(10)-C(12)	-63.1(6)
C(14)-P(1)-C(10)-C(12)	-168.5(6)
Pd(1)-P(1)-C(10)-C(12)	61.3(6)
C(18)-P(1)-C(10)-C(11)	-179.5(6)
C(14)-P(1)-C(10)-C(11)	75.2(6)
Pd(1)-P(1)-C(10)-C(11)	-55.1(6)
C(18)-P(1)-C(10)-C(13)	57.1(7)
C(14)-P(1)-C(10)-C(13)	-48.3(7)
Pd(1)-P(1)-C(10)-C(13)	-178.5(5)
C(18)-P(1)-C(14)-C(17)	-29.3(6)
C(10)-P(1)-C(14)-C(17)	76.6(6)
Pd(1)-P(1)-C(14)-C(17)	-151.4(5)
C(18)-P(1)-C(14)-C(16)	90.2(6)
C(10)-P(1)-C(14)-C(16)	-163.9(5)
Pd(1)-P(1)-C(14)-C(16)	-31.9(6)
C(18)-P(1)-C(14)-C(15)	-152.6(6)
C(10)-P(1)-C(14)-C(15)	-46.8(7)
Pd(1)-P(1)-C(14)-C(15)	85.2(5)
C(27)-P(2)-C(19)-C(21)	-179.0(6)
C(23)-P(2)-C(19)-C(21)	75.5(7)
Pd(1)-P(2)-C(19)-C(21)	-54.8(6)
C(27)-P(2)-C(19)-C(22)	-60.8(6)
C(23)-P(2)-C(19)-C(22)	-166.3(5)
Pd(1)-P(2)-C(19)-C(22)	63.3(6)
C(27)-P(2)-C(19)-C(20)	58.1(7)
C(23)-P(2)-C(19)-C(20)	-47.4(7)
Pd(1)-P(2)-C(19)-C(20)	-177.7(5)
C(27)-P(2)-C(23)-C(26)	88.8(6)
C(19)-P(2)-C(23)-C(26)	-164.2(5)
Pd(1)-P(2)-C(23)-C(26)	-37.1(6)
C(27)-P(2)-C(23)-C(25)	-151.7(6)

C(19)-P(2)-C(23)-C(25)	-44.6(7)
Pd(1)-P(2)-C(23)-C(25)	82.5(6)
C(27)-P(2)-C(23)-C(24)	-29.1(6)
C(19)-P(2)-C(23)-C(24)	77.9(6)
Pd(1)-P(2)-C(23)-C(24)	-155.0(5)

02110MNS (Figure 2.2)

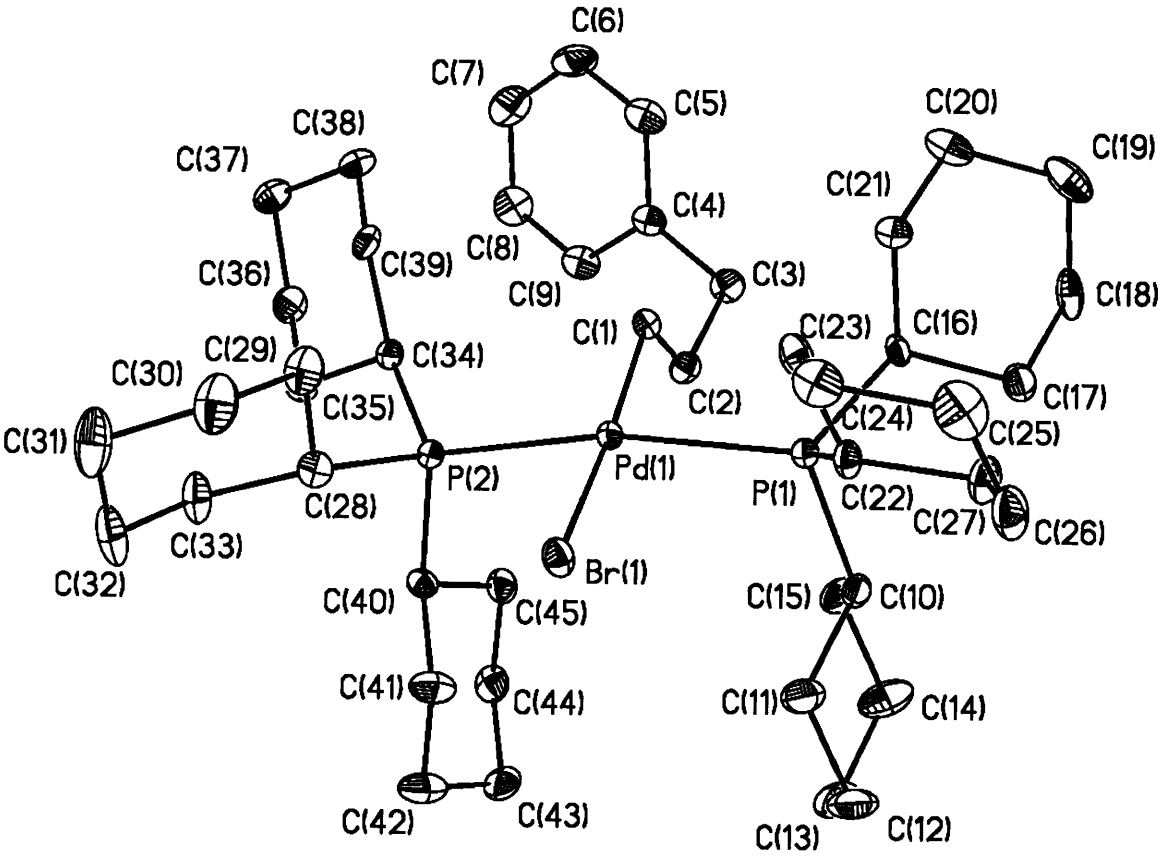

Table 1. Crystal data and structure refinement for 02110MNS.

Identification code	02110mns	
Empirical formula	C49 H87 Br O P2 Pd	
Formula weight	940.44	
Temperature	183(2) K	
Wavelength	0.71073 Å	
Crystal system	Monoclinic	
Space group	P21/n	
Unit cell dimensions	a = 13.7755(9) Å	α = 90°.
	b = 17.0727(11) Å	β = 98.5560(10)°.
	c = 21.0506(14) Å	γ = 90°.
Volume	4895.7(6) $Å^3$	
Z	4	
Density (calculated)	1.276 Mg/m^3	
Absorption coefficient	1.293 mm^{-1}	
F(000)	2000	
Crystal size	0.27 x 0.18 x 0.1 mm^3	
Theta range for data collection	2.25 to 23.27°.	
Index ranges	-15<=h<=10, -18<=k<=18, -23<=l<=23	
Reflections collected	19303	
Independent reflections	7017 [R(int) = 0.0328]	
Completeness to theta = 23.27°	99.6 %	
Absorption correction	Semi-empirical from equivalents	
Max. and min. transmission	0.908328 and 0.662613	
Refinement method	Full-matrix least-squares on F^2	
Data / restraints / parameters	7017 / 0 / 489	
Goodness-of-fit on F^2	1.502	
Final R indices [I>2sigma(I)]	R1 = 0.0686, wR2 = 0.1139	
R indices (all data)	R1 = 0.0722, wR2 = 0.1149	
Largest diff. peak and hole	0.626 and -1.096 $e.Å^{-3}$	

Table 2. Atomic coordinates (x 10^4) and equivalent isotropic displacement parameters ($Å^2$x 10^3) for 02110MNS. U(eq) is defined as one third of the trace of the orthogonalized U^{ij} tensor.

	x	y	z	U(eq)
Pd(1)	8569(1)	564(1)	1992(1)	16(1)
Br(1)	8299(1)	1874(1)	2533(1)	24(1)
P(1)	10283(1)	815(1)	2174(1)	18(1)
P(2)	6934(1)	188(1)	2037(1)	18(1)
O(1)	1596(6)	6681(5)	574(4)	92(2)
C(1)	8776(4)	-390(3)	1421(3)	16(1)
C(2)	9111(4)	-1162(3)	1742(3)	23(1)
C(3)	9442(5)	-1776(4)	1287(3)	27(2)
C(4)	8624(4)	-2148(3)	838(3)	23(1)
C(5)	8537(5)	-2051(4)	176(3)	35(2)
C(6)	7781(6)	-2400(4)	-226(3)	43(2)
C(7)	7099(6)	-2852(4)	15(4)	41(2)
C(8)	7173(5)	-2955(4)	671(3)	35(2)
C(9)	7929(5)	-2606(4)	1075(3)	30(2)
C(10)	10798(4)	536(4)	3010(3)	22(1)
C(11)	10388(5)	1011(4)	3523(3)	38(2)
C(12)	10873(6)	781(4)	4198(3)	42(2)
C(13)	10754(6)	-90(4)	4319(3)	43(2)
C(14)	11153(6)	-565(4)	3809(3)	45(2)
C(15)	10671(5)	-339(4)	3133(3)	32(2)
C(16)	11038(4)	241(3)	1675(3)	18(1)
C(17)	12128(4)	108(4)	1929(3)	29(2)
C(18)	12575(4)	-438(4)	1473(3)	33(2)
C(19)	12465(5)	-129(4)	796(3)	41(2)
C(20)	11384(5)	17(4)	543(3)	36(2)
C(21)	10927(5)	575(4)	989(3)	25(1)

C(22)	10633(4)	1864(3)	2143(3)	21(1)
C(23)	10170(5)	2311(4)	1542(3)	26(2)
C(24)	10349(5)	3190(4)	1639(3)	34(2)
C(25)	11427(5)	3395(4)	1823(4)	43(2)
C(26)	11887(5)	2926(4)	2397(4)	38(2)
C(27)	11739(4)	2051(4)	2299(3)	31(2)
C(28)	6073(4)	1023(4)	2004(3)	24(1)
C(29)	6048(5)	1560(4)	1419(3)	31(2)
C(30)	5505(5)	2321(4)	1517(4)	44(2)
C(31)	4461(5)	2158(4)	1670(4)	51(2)
C(32)	4488(5)	1598(4)	2226(4)	43(2)
C(33)	5012(4)	840(4)	2119(4)	33(2)
C(34)	6392(4)	-588(4)	1469(3)	20(1)
C(35)	5498(5)	-1036(4)	1628(3)	29(2)
C(36)	5211(5)	-1690(4)	1149(3)	30(2)
C(37)	5057(5)	-1409(4)	456(3)	32(2)
C(38)	5939(5)	-946(4)	306(3)	26(2)
C(39)	6185(4)	-274(4)	781(3)	23(1)
C(40)	6850(4)	-242(3)	2835(3)	20(1)
C(41)	7077(5)	347(4)	3387(3)	34(2)
C(42)	6977(6)	-31(4)	4034(3)	39(2)
C(43)	7621(5)	-748(4)	4161(3)	38(2)
C(44)	7404(5)	-1327(4)	3622(3)	30(2)
C(45)	7497(5)	-966(4)	2970(3)	27(2)
C(46)	1457(11)	7331(9)	190(8)	124(5)
C(47)	2359(12)	7744(7)	136(8)	138(6)
C(48)	772(9)	6238(10)	648(8)	132(6)
C(49)	1013(10)	5563(12)	1038(10)	190(9)

Table 3. Bond lengths [Å] and angles [°] for 02110MNS.

Pd(1)-C(1)	2.069(5)
Pd(1)-P(2)	2.3579(16)
Pd(1)-P(1)	2.3747(16)
Pd(1)-Br(1)	2.5610(7)
P(1)-C(22)	1.857(6)
P(1)-C(10)	1.861(6)
P(1)-C(16)	1.863(6)
P(2)-C(28)	1.849(6)
P(2)-C(40)	1.853(6)
P(2)-C(34)	1.864(6)
O(1)-C(46)	1.369(15)
O(1)-C(48)	1.392(15)
C(1)-C(2)	1.521(8)
C(2)-C(3)	1.535(8)
C(3)-C(4)	1.500(9)
C(4)-C(9)	1.386(9)
C(4)-C(5)	1.390(9)
C(5)-C(6)	1.376(10)
C(6)-C(7)	1.371(10)
C(7)-C(8)	1.380(10)
C(8)-C(9)	1.379(9)
C(10)-C(11)	1.524(9)
C(10)-C(15)	1.532(9)
C(11)-C(12)	1.530(9)
C(12)-C(13)	1.521(10)
C(13)-C(14)	1.512(10)
C(14)-C(15)	1.526(9)
C(16)-C(17)	1.534(8)
C(16)-C(21)	1.537(8)
C(17)-C(18)	1.531(9)
C(18)-C(19)	1.506(10)

C(19)-C(20)	1.526(10)
C(20)-C(21)	1.536(9)
C(22)-C(23)	1.532(8)
C(22)-C(27)	1.545(8)
C(23)-C(24)	1.530(9)
C(24)-C(25)	1.519(10)
C(25)-C(26)	1.508(10)
C(26)-C(27)	1.518(9)
C(28)-C(29)	1.533(9)
C(28)-C(33)	1.548(8)
C(29)-C(30)	1.529(9)
C(30)-C(31)	1.545(10)
C(31)-C(32)	1.507(11)
C(32)-C(33)	1.515(9)
C(34)-C(35)	1.529(8)
C(34)-C(39)	1.530(8)
C(35)-C(36)	1.518(9)
C(36)-C(37)	1.521(9)
C(37)-C(38)	1.520(9)
C(38)-C(39)	1.527(8)
C(40)-C(45)	1.525(8)
C(40)-C(41)	1.533(8)
C(41)-C(42)	1.534(9)
C(42)-C(43)	1.511(10)
C(43)-C(44)	1.501(9)
C(44)-C(45)	1.528(9)
C(46)-C(47)	1.448(18)
C(48)-C(49)	1.425(18)

C(1)-Pd(1)-P(2)	91.36(16)
C(1)-Pd(1)-P(1)	90.91(16)
P(2)-Pd(1)-P(1)	167.37(6)
C(1)-Pd(1)-Br(1)	170.87(15)

P(2)-Pd(1)-Br(1)	91.00(4)
P(1)-Pd(1)-Br(1)	88.70(4)
C(22)-P(1)-C(10)	102.5(3)
C(22)-P(1)-C(16)	108.5(3)
C(10)-P(1)-C(16)	103.4(3)
C(22)-P(1)-Pd(1)	115.17(19)
C(10)-P(1)-Pd(1)	109.66(19)
C(16)-P(1)-Pd(1)	116.08(19)
C(28)-P(2)-C(40)	102.3(3)
C(28)-P(2)-C(34)	109.3(3)
C(40)-P(2)-C(34)	103.2(3)
C(28)-P(2)-Pd(1)	113.5(2)
C(40)-P(2)-Pd(1)	109.5(2)
C(34)-P(2)-Pd(1)	117.45(19)
C(46)-O(1)-C(48)	117.5(11)
C(2)-C(1)-Pd(1)	118.9(4)
C(1)-C(2)-C(3)	114.4(5)
C(4)-C(3)-C(2)	114.6(5)
C(9)-C(4)-C(5)	117.8(6)
C(9)-C(4)-C(3)	120.4(6)
C(5)-C(4)-C(3)	121.8(6)
C(6)-C(5)-C(4)	120.7(7)
C(7)-C(6)-C(5)	120.9(7)
C(6)-C(7)-C(8)	119.3(7)
C(9)-C(8)-C(7)	120.0(7)
C(8)-C(9)-C(4)	121.3(6)
C(11)-C(10)-C(15)	109.7(5)
C(11)-C(10)-P(1)	113.9(4)
C(15)-C(10)-P(1)	111.9(4)
C(10)-C(11)-C(12)	111.4(6)
C(13)-C(12)-C(11)	111.3(6)
C(14)-C(13)-C(12)	110.3(6)
C(13)-C(14)-C(15)	111.9(6)

C(14)-C(15)-C(10)	111.0(5)
C(17)-C(16)-C(21)	109.8(5)
C(17)-C(16)-P(1)	118.7(4)
C(21)-C(16)-P(1)	110.4(4)
C(18)-C(17)-C(16)	109.6(5)
C(19)-C(18)-C(17)	112.8(5)
C(18)-C(19)-C(20)	110.1(5)
C(19)-C(20)-C(21)	110.8(6)
C(20)-C(21)-C(16)	110.6(5)
C(23)-C(22)-C(27)	110.4(5)
C(23)-C(22)-P(1)	115.5(4)
C(27)-C(22)-P(1)	116.4(4)
C(24)-C(23)-C(22)	109.8(5)
C(25)-C(24)-C(23)	113.0(6)
C(26)-C(25)-C(24)	111.2(6)
C(25)-C(26)-C(27)	112.4(6)
C(26)-C(27)-C(22)	110.0(5)
C(29)-C(28)-C(33)	109.8(5)
C(29)-C(28)-P(2)	115.4(4)
C(33)-C(28)-P(2)	117.0(4)
C(30)-C(29)-C(28)	110.7(6)
C(29)-C(30)-C(31)	111.4(6)
C(32)-C(31)-C(30)	111.1(6)
C(31)-C(32)-C(33)	112.6(6)
C(32)-C(33)-C(28)	109.4(5)
C(35)-C(34)-C(39)	109.9(5)
C(35)-C(34)-P(2)	118.2(4)
C(39)-C(34)-P(2)	111.0(4)
C(36)-C(35)-C(34)	111.2(5)
C(35)-C(36)-C(37)	113.0(5)
C(38)-C(37)-C(36)	111.2(5)
C(37)-C(38)-C(39)	111.2(5)
C(38)-C(39)-C(34)	110.4(5)

C(45)-C(40)-C(41)	110.0(5)
C(45)-C(40)-P(2)	112.1(4)
C(41)-C(40)-P(2)	113.2(4)
C(40)-C(41)-C(42)	111.2(5)
C(43)-C(42)-C(41)	111.7(6)
C(44)-C(43)-C(42)	110.8(5)
C(43)-C(44)-C(45)	112.2(6)
C(40)-C(45)-C(44)	111.7(5)
O(1)-C(46)-C(47)	113.2(13)
O(1)-C(48)-C(49)	112.3(12)

Table 4. Anisotropic displacement parameters ($Å^2 x\ 10^3$) for 02110MNS. The anisotropic displacement factor exponent takes the form: $-2p^2[\ h^2\ a^{*2}U^{11} + ... + 2\ h\ k\ a^*\ b^*\ U^{12}\ ]$

	U^{11}	U^{22}	U^{33}	U^{23}	U^{13}	U^{12}
Pd(1)	14(1)	18(1)	17(1)	-1(1)	2(1)	0(1)
Br(1)	20(1)	22(1)	31(1)	-6(1)	6(1)	-1(1)
P(1)	15(1)	23(1)	17(1)	1(1)	3(1)	-1(1)
P(2)	15(1)	21(1)	17(1)	0(1)	2(1)	0(1)
O(1)	69(5)	97(6)	111(6)	-8(5)	17(4)	12(5)
C(1)	17(3)	11(3)	20(3)	-2(2)	5(2)	-2(2)
C(2)	23(3)	20(3)	24(3)	-2(3)	1(3)	-1(3)
C(3)	30(4)	22(3)	28(4)	-4(3)	4(3)	5(3)
C(4)	31(4)	14(3)	24(3)	-1(3)	7(3)	5(3)
C(5)	46(4)	27(4)	33(4)	1(3)	13(3)	1(3)
C(6)	57(5)	46(5)	24(4)	-12(3)	2(4)	1(4)
C(7)	47(5)	30(4)	42(5)	-14(3)	-5(4)	-3(4)
C(8)	42(4)	19(4)	43(4)	-1(3)	7(3)	-4(3)
C(9)	40(4)	20(3)	30(4)	3(3)	9(3)	1(3)
C(10)	17(3)	24(3)	24(3)	-1(3)	0(3)	0(3)
C(11)	39(4)	48(5)	24(4)	-4(3)	0(3)	8(4)
C(12)	54(5)	52(5)	20(4)	-10(3)	3(3)	3(4)
C(13)	47(5)	57(5)	22(4)	11(4)	-3(3)	-7(4)
C(14)	69(5)	32(4)	29(4)	6(3)	-9(4)	-6(4)
C(15)	34(4)	35(4)	26(4)	6(3)	-4(3)	-2(3)
C(16)	13(3)	22(3)	21(3)	0(3)	6(2)	2(3)
C(17)	24(4)	31(4)	32(4)	-5(3)	7(3)	-1(3)
C(18)	16(3)	23(4)	61(5)	-2(3)	10(3)	8(3)
C(19)	53(5)	29(4)	50(5)	-2(4)	33(4)	8(4)
C(20)	51(5)	32(4)	30(4)	4(3)	20(3)	1(3)
C(21)	28(3)	27(3)	21(3)	2(3)	5(3)	0(3)

C(22)	14(3)	20(3)	29(3)	-7(3)	4(3)	-3(3)
C(23)	22(3)	22(3)	36(4)	2(3)	11(3)	7(3)
C(24)	42(4)	24(4)	37(4)	1(3)	9(3)	4(3)
C(25)	49(5)	25(4)	58(5)	-7(4)	16(4)	-9(4)
C(26)	24(4)	39(4)	53(5)	-16(4)	9(3)	-10(3)
C(27)	19(3)	28(4)	43(4)	-5(3)	0(3)	-6(3)
C(28)	25(3)	20(3)	27(3)	0(3)	3(3)	-1(3)
C(29)	30(4)	19(3)	43(4)	5(3)	1(3)	3(3)
C(30)	36(4)	30(4)	64(5)	11(4)	2(4)	3(3)
C(31)	30(4)	30(4)	91(7)	2(4)	2(4)	9(3)
C(32)	20(4)	34(4)	78(6)	-9(4)	17(4)	-1(3)
C(33)	17(3)	24(4)	58(5)	-7(3)	5(3)	0(3)
C(34)	16(3)	24(3)	20(3)	-1(3)	2(2)	-3(3)
C(35)	25(4)	35(4)	28(4)	-2(3)	6(3)	-5(3)
C(36)	26(4)	30(4)	34(4)	-5(3)	2(3)	-8(3)
C(37)	33(4)	34(4)	27(4)	-5(3)	-4(3)	-4(3)
C(38)	30(4)	27(4)	18(3)	-1(3)	-2(3)	-3(3)
C(39)	16(3)	26(3)	25(3)	7(3)	-3(3)	0(3)
C(40)	22(3)	18(3)	19(3)	2(3)	6(3)	1(3)
C(41)	48(4)	30(4)	24(4)	-5(3)	9(3)	-9(3)
C(42)	54(5)	41(4)	21(4)	-2(3)	9(3)	-11(4)
C(43)	31(4)	62(5)	20(4)	12(3)	0(3)	-6(4)
C(44)	30(4)	29(4)	32(4)	8(3)	3(3)	7(3)
C(45)	21(3)	31(4)	31(4)	-2(3)	6(3)	-4(3)
C(46)	115(12)	119(12)	140(13)	-5(11)	29(10)	60(10)
C(47)	142(14)	65(8)	210(18)	-50(10)	35(13)	-7(9)
C(48)	68(9)	160(15)	177(16)	27(12)	45(9)	47(10)
C(49)	64(9)	210(20)	300(30)	108(19)	37(12)	19(11)

Table 5. Hydrogen coordinates (x 10^4) and isotropic displacement parameters ($Å^2$x 10^3) for 02110MNS.

	x	y	z	U(eq)
H(1A)	8149	-488	1136	19
H(1B)	9263	-238	1142	19
H(2A)	8564	-1383	1942	27
H(2B)	9661	-1056	2090	27
H(3A)	9901	-1524	1029	32
H(3B)	9809	-2193	1548	32
H(5)	9004	-1742	0	41
H(6)	7731	-2326	-677	51
H(7)	6581	-3093	-266	49
H(8)	6704	-3267	843	42
H(9)	7974	-2680	1526	36
H(10)	11520	641	3063	26
H(11A)	9671	925	3484	45
H(11B)	10500	1576	3453	45
H(12A)	11581	913	4251	51
H(12B)	10573	1085	4520	51
H(13A)	11109	-229	4747	51
H(13B)	10050	-213	4312	51
H(14A)	11037	-1128	3881	54
H(14B)	11870	-482	3847	54
H(15A)	9963	-468	3081	39
H(15B)	10971	-647	2814	39
H(16)	10735	-292	1632	22
H(17A)	12480	615	1962	34
H(17B)	12198	-128	2363	34
H(18A)	13282	-510	1635	39

H(18B)	12254	-957	1471	39
H(19A)	12735	-514	517	50
H(19B)	12838	365	787	50
H(20A)	11024	-487	511	44
H(20B)	11322	248	108	44
H(21A)	10222	650	824	30
H(21B)	11255	1091	997	30
H(22)	10340	2112	2501	25
H(23A)	10461	2130	1165	31
H(23B)	9456	2206	1458	31
H(24A)	10087	3469	1237	41
H(24B)	9983	3378	1980	41
H(25A)	11779	3287	1455	52
H(25B)	11491	3961	1924	52
H(26A)	11598	3091	2779	46
H(26B)	12600	3040	2481	46
H(27A)	12026	1769	2694	37
H(27B)	12079	1873	1943	37
H(28)	6347	1359	2377	29
H(29A)	6728	1682	1351	38
H(29B)	5716	1288	1031	38
H(30A)	5460	2644	1123	52
H(30B)	5880	2621	1875	52
H(31A)	4155	2657	1776	61
H(31B)	4053	1933	1286	61
H(32A)	3808	1478	2293	51
H(32B)	4824	1853	2620	51
H(33A)	4656	561	1742	40
H(33B)	5028	497	2500	40
H(34)	6920	-990	1466	24
H(35A)	5649	-1259	2066	35
H(35B)	4939	-670	1623	35
H(36A)	4597	-1937	1243	36

H(36B)	5731	-2095	1203	36
H(37A)	4949	-1866	164	39
H(37B)	4464	-1075	379	39
H(38A)	5795	-733	-136	31
H(38B)	6512	-1299	325	31
H(39A)	5628	98	743	28
H(39B)	6768	11	679	28
H(40)	6155	-416	2829	24
H(41A)	6621	796	3310	40
H(41B)	7754	547	3399	40
H(42A)	7161	355	4382	46
H(42B)	6284	-182	4038	46
H(43A)	8319	-591	4207	46
H(43B)	7506	-996	4568	46
H(44A)	6730	-1532	3613	36
H(44B)	7864	-1774	3703	36
H(45A)	8190	-819	2961	33
H(45B)	7308	-1359	2629	33
H(46A)	1001	7692	365	148
H(46B)	1144	7169	-244	148
H(47A)	2685	7891	566	207
H(47B)	2209	8217	-124	207
H(47C)	2794	7404	-69	207
H(48A)	442	6070	219	159
H(48B)	305	6567	844	159
H(49A)	1219	5139	775	284
H(49B)	436	5397	1225	284
H(49C)	1548	5691	1383	284

Table 6. Torsion angles [°] for 02110MNS.

C(1)-Pd(1)-P(1)-C(22)	138.0(3)
P(2)-Pd(1)-P(1)-C(22)	-121.6(3)
Br(1)-Pd(1)-P(1)-C(22)	-32.8(2)
C(1)-Pd(1)-P(1)-C(10)	-107.1(3)
P(2)-Pd(1)-P(1)-C(10)	-6.7(4)
Br(1)-Pd(1)-P(1)-C(10)	82.1(2)
C(1)-Pd(1)-P(1)-C(16)	9.7(3)
P(2)-Pd(1)-P(1)-C(16)	110.0(3)
Br(1)-Pd(1)-P(1)-C(16)	-161.2(2)
C(1)-Pd(1)-P(2)-C(28)	-141.7(3)
P(1)-Pd(1)-P(2)-C(28)	118.0(3)
Br(1)-Pd(1)-P(2)-C(28)	29.5(2)
C(1)-Pd(1)-P(2)-C(40)	104.7(2)
P(1)-Pd(1)-P(2)-C(40)	4.4(4)
Br(1)-Pd(1)-P(2)-C(40)	-84.1(2)
C(1)-Pd(1)-P(2)-C(34)	-12.4(3)
P(1)-Pd(1)-P(2)-C(34)	-112.7(3)
Br(1)-Pd(1)-P(2)-C(34)	158.7(2)
P(2)-Pd(1)-C(1)-C(2)	-87.6(4)
P(1)-Pd(1)-C(1)-C(2)	80.0(4)
Br(1)-Pd(1)-C(1)-C(2)	167.5(7)
Pd(1)-C(1)-C(2)-C(3)	-168.1(4)
C(1)-C(2)-C(3)-C(4)	-73.4(7)
C(2)-C(3)-C(4)-C(9)	-64.6(8)
C(2)-C(3)-C(4)-C(5)	115.7(7)
C(9)-C(4)-C(5)-C(6)	0.2(10)
C(3)-C(4)-C(5)-C(6)	179.9(6)
C(4)-C(5)-C(6)-C(7)	-0.3(11)
C(5)-C(6)-C(7)-C(8)	0.3(11)
C(6)-C(7)-C(8)-C(9)	-0.1(11)
C(7)-C(8)-C(9)-C(4)	0.0(10)

C(5)-C(4)-C(9)-C(8)	0.0(9)
C(3)-C(4)-C(9)-C(8)	-179.8(6)
C(22)-P(1)-C(10)-C(11)	59.7(5)
C(16)-P(1)-C(10)-C(11)	172.5(5)
Pd(1)-P(1)-C(10)-C(11)	-63.1(5)
C(22)-P(1)-C(10)-C(15)	-175.2(4)
C(16)-P(1)-C(10)-C(15)	-62.4(5)
Pd(1)-P(1)-C(10)-C(15)	62.0(5)
C(15)-C(10)-C(11)-C(12)	56.4(7)
P(1)-C(10)-C(11)-C(12)	-177.4(5)
C(10)-C(11)-C(12)-C(13)	-56.9(8)
C(11)-C(12)-C(13)-C(14)	55.7(8)
C(12)-C(13)-C(14)-C(15)	-55.9(8)
C(13)-C(14)-C(15)-C(10)	56.8(8)
C(11)-C(10)-C(15)-C(14)	-56.0(7)
P(1)-C(10)-C(15)-C(14)	176.6(5)
C(22)-P(1)-C(16)-C(17)	73.0(5)
C(10)-P(1)-C(16)-C(17)	-35.3(5)
Pd(1)-P(1)-C(16)-C(17)	-155.4(4)
C(22)-P(1)-C(16)-C(21)	-55.0(5)
C(10)-P(1)-C(16)-C(21)	-163.3(4)
Pd(1)-P(1)-C(16)-C(21)	76.6(4)
C(21)-C(16)-C(17)-C(18)	-57.0(7)
P(1)-C(16)-C(17)-C(18)	174.8(4)
C(16)-C(17)-C(18)-C(19)	57.4(7)
C(17)-C(18)-C(19)-C(20)	-56.6(8)
C(18)-C(19)-C(20)-C(21)	55.9(7)
C(19)-C(20)-C(21)-C(16)	-57.6(7)
C(17)-C(16)-C(21)-C(20)	58.1(7)
P(1)-C(16)-C(21)-C(20)	-169.2(4)
C(10)-P(1)-C(22)-C(23)	-170.5(4)
C(16)-P(1)-C(22)-C(23)	80.5(5)
Pd(1)-P(1)-C(22)-C(23)	-51.5(5)

C(10)-P(1)-C(22)-C(27)	57.4(5)
C(16)-P(1)-C(22)-C(27)	-51.5(5)
Pd(1)-P(1)-C(22)-C(27)	176.4(4)
C(27)-C(22)-C(23)-C(24)	-56.6(7)
P(1)-C(22)-C(23)-C(24)	168.6(4)
C(22)-C(23)-C(24)-C(25)	54.8(7)
C(23)-C(24)-C(25)-C(26)	-53.2(8)
C(24)-C(25)-C(26)-C(27)	54.1(8)
C(25)-C(26)-C(27)-C(22)	-56.8(8)
C(23)-C(22)-C(27)-C(26)	58.0(7)
P(1)-C(22)-C(27)-C(26)	-167.7(5)
C(40)-P(2)-C(28)-C(29)	174.1(5)
C(34)-P(2)-C(28)-C(29)	-77.0(5)
Pd(1)-P(2)-C(28)-C(29)	56.2(5)
C(40)-P(2)-C(28)-C(33)	-54.5(5)
C(34)-P(2)-C(28)-C(33)	54.4(5)
Pd(1)-P(2)-C(28)-C(33)	-172.3(4)
C(33)-C(28)-C(29)-C(30)	58.4(7)
P(2)-C(28)-C(29)-C(30)	-166.9(5)
C(28)-C(29)-C(30)-C(31)	-55.4(8)
C(29)-C(30)-C(31)-C(32)	53.1(9)
C(30)-C(31)-C(32)-C(33)	-55.0(8)
C(31)-C(32)-C(33)-C(28)	58.0(8)
C(29)-C(28)-C(33)-C(32)	-58.9(7)
P(2)-C(28)-C(33)-C(32)	167.2(5)
C(28)-P(2)-C(34)-C(35)	-69.2(5)
C(40)-P(2)-C(34)-C(35)	39.1(5)
Pd(1)-P(2)-C(34)-C(35)	159.6(4)
C(28)-P(2)-C(34)-C(39)	59.1(5)
C(40)-P(2)-C(34)-C(39)	167.4(4)
Pd(1)-P(2)-C(34)-C(39)	-72.1(4)
C(39)-C(34)-C(35)-C(36)	56.3(7)
P(2)-C(34)-C(35)-C(36)	-174.9(4)

C(34)-C(35)-C(36)-C(37)	-53.7(7)
C(35)-C(36)-C(37)-C(38)	52.5(7)
C(36)-C(37)-C(38)-C(39)	-54.3(7)
C(37)-C(38)-C(39)-C(34)	58.1(7)
C(35)-C(34)-C(39)-C(38)	-58.7(6)
P(2)-C(34)-C(39)-C(38)	168.7(4)
C(28)-P(2)-C(40)-C(45)	179.0(4)
C(34)-P(2)-C(40)-C(45)	65.5(5)
Pd(1)-P(2)-C(40)-C(45)	-60.3(4)
C(28)-P(2)-C(40)-C(41)	-55.9(5)
C(34)-P(2)-C(40)-C(41)	-169.4(5)
Pd(1)-P(2)-C(40)-C(41)	64.8(5)
C(45)-C(40)-C(41)-C(42)	-54.9(7)
P(2)-C(40)-C(41)-C(42)	178.8(5)
C(40)-C(41)-C(42)-C(43)	56.1(8)
C(41)-C(42)-C(43)-C(44)	-55.6(8)
C(42)-C(43)-C(44)-C(45)	55.1(7)
C(41)-C(40)-C(45)-C(44)	54.5(7)
P(2)-C(40)-C(45)-C(44)	-178.6(4)
C(43)-C(44)-C(45)-C(40)	-55.4(7)
C(48)-O(1)-C(46)-C(47)	-179.0(12)
C(46)-O(1)-C(48)-C(49)	177.8(15)

03068IHS (Footnote 52)

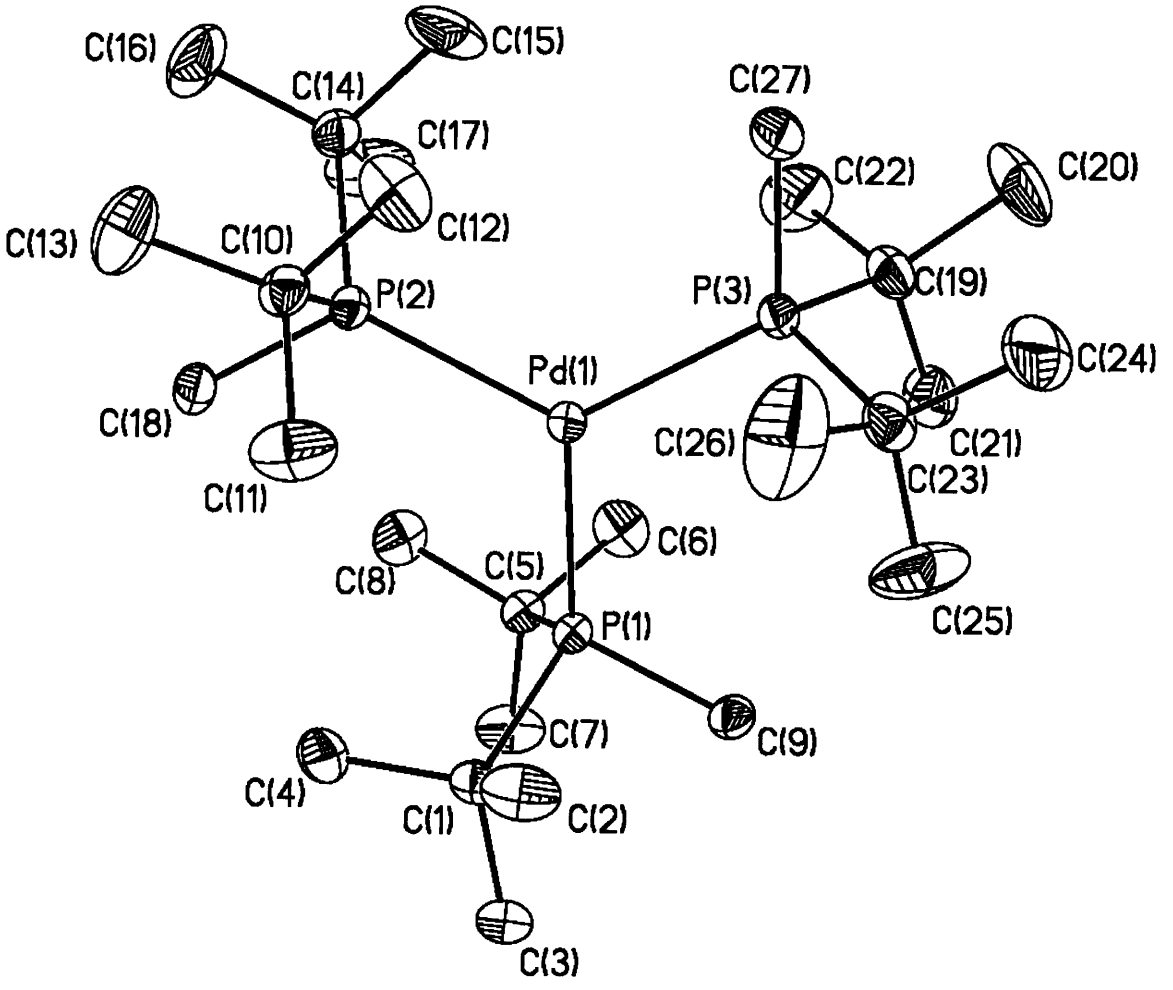

Table 1. Crystal data and structure refinement for 03068IHs.

Identification code	03068ihs	
Empirical formula	C27 H63 P3 Pd	
Formula weight	587.08	
Temperature	193(2) K	
Wavelength	0.71073 Å	
Crystal system	Monoclinic	
Space group	P2(1)/n	
Unit cell dimensions	a = 8.9087(11) Å	α = 90°.
	b = 31.057(4) Å	β = 94.481(2)°.
	c = 11.8390(14) Å	γ = 90°.
Volume	3265.6(7) $Å^3$	
Z	4	
Density (calculated)	1.194 Mg/m^3	
Absorption coefficient	0.728 mm^{-1}	
F(000)	1264	
Crystal size	0.43 x 0.19 x 0.19 mm^3	
Theta range for data collection	2.62 to 23.30°.	
Index ranges	-9<=h<=9, -29<=k<=34, -13<=l<=10	
Reflections collected	12788	
Independent reflections	4678 [R(int) = 0.0276]	
Completeness to theta = 23.30°	99.5 %	
Absorption correction	Bruker SADABS	
Max. and min. transmission	0.901164 and 0.659648	
Refinement method	Full-matrix least-squares on F^2	
Data / restraints / parameters	4678 / 0 / 301	
Goodness-of-fit on F^2	1.227	
Final R indices [I>2sigma(I)]	R1 = 0.0428, wR2 = 0.0900	
R indices (all data)	R1 = 0.0490, wR2 = 0.0921	
Largest diff. peak and hole	0.762 and -0.969 $e.Å^{-3}$	

Table 2. Atomic coordinates (x 10^4) and equivalent isotropic displacement parameters ($Å^2$x 10^3) for 03068IHs. U(eq) is defined as one third of the trace of the orthogonalized U^{ij} tensor.

	x	y	z	U(eq)
Pd(1)	2804(1)	1355(1)	1305(1)	22(1)
P(1)	2060(1)	2061(1)	1804(1)	23(1)
P(2)	2928(1)	1168(1)	-636(1)	24(1)
P(3)	3423(1)	840(1)	2744(1)	27(1)
C(1)	3303(4)	2516(1)	1348(4)	31(1)
C(2)	4913(5)	2373(2)	1728(5)	52(1)
C(3)	3074(5)	2963(1)	1874(4)	39(1)
C(4)	3168(6)	2564(2)	62(4)	49(1)
C(5)	18(4)	2176(1)	1322(4)	28(1)
C(6)	-919(5)	1870(2)	1991(5)	46(1)
C(7)	-526(5)	2636(2)	1481(5)	50(1)
C(8)	-277(5)	2051(2)	78(4)	43(1)
C(9)	2028(5)	2207(1)	3317(4)	33(1)
C(10)	4938(5)	1072(1)	-1007(4)	31(1)
C(11)	5802(6)	1470(2)	-586(5)	58(2)
C(12)	5618(5)	691(2)	-329(5)	53(1)
C(13)	5192(6)	1006(2)	-2250(5)	65(2)
C(14)	1672(5)	703(1)	-1177(4)	34(1)
C(15)	2029(7)	301(2)	-480(6)	69(2)
C(16)	1701(9)	592(2)	-2427(5)	88(2)
C(17)	78(6)	839(2)	-955(6)	71(2)
C(18)	2352(5)	1569(2)	-1744(4)	35(1)
C(19)	1797(5)	679(2)	3598(4)	39(1)
C(20)	2051(8)	301(2)	4419(6)	80(2)
C(21)	1225(7)	1058(2)	4244(5)	56(1)
C(22)	515(6)	563(2)	2700(5)	68(2)

C(23)	5126(5)	994(2)	3733(4)	39(1)
C(24)	5649(9)	669(2)	4635(6)	91(3)
C(25)	4866(7)	1417(2)	4298(7)	85(2)
C(26)	6396(7)	1050(3)	2952(6)	107(3)
C(27)	4032(6)	292(1)	2334(4)	42(1)

Table 3. Bond lengths [Å] and angles [°] for 03068IHs.

Pd(1)-P(3)	2.3707(11)
Pd(1)-P(1)	2.3774(11)
Pd(1)-P(2)	2.3814(11)
P(1)-C(9)	1.850(4)
P(1)-C(5)	1.898(4)
P(1)-C(1)	1.901(4)
P(2)-C(18)	1.852(4)
P(2)-C(10)	1.901(4)
P(2)-C(14)	1.907(4)
P(3)-C(27)	1.860(4)
P(3)-C(19)	1.896(5)
P(3)-C(23)	1.903(5)
C(1)-C(4)	1.526(6)
C(1)-C(2)	1.535(6)
C(1)-C(3)	1.540(6)
C(5)-C(7)	1.524(6)
C(5)-C(8)	1.526(6)
C(5)-C(6)	1.526(6)
C(10)-C(13)	1.520(7)
C(10)-C(11)	1.522(6)
C(10)-C(12)	1.528(6)
C(14)-C(15)	1.515(7)
C(14)-C(16)	1.522(7)
C(14)-C(17)	1.525(7)
C(19)-C(21)	1.514(7)
C(19)-C(20)	1.530(7)
C(19)-C(22)	1.542(7)
C(23)-C(25)	1.503(7)
C(23)-C(24)	1.515(7)
C(23)-C(26)	1.527(8)

P(3)-Pd(1)-P(1)	119.81(4)
P(3)-Pd(1)-P(2)	120.23(4)
P(1)-Pd(1)-P(2)	119.96(4)
C(9)-P(1)-C(5)	99.06(19)
C(9)-P(1)-C(1)	98.4(2)
C(5)-P(1)-C(1)	109.85(19)
C(9)-P(1)-Pd(1)	119.50(14)
C(5)-P(1)-Pd(1)	112.24(13)
C(1)-P(1)-Pd(1)	115.88(14)
C(18)-P(2)-C(10)	99.0(2)
C(18)-P(2)-C(14)	98.6(2)
C(10)-P(2)-C(14)	109.97(19)
C(18)-P(2)-Pd(1)	119.23(15)
C(10)-P(2)-Pd(1)	112.16(14)
C(14)-P(2)-Pd(1)	115.99(14)
C(27)-P(3)-C(19)	98.6(2)
C(27)-P(3)-C(23)	98.9(2)
C(19)-P(3)-C(23)	110.1(2)
C(27)-P(3)-Pd(1)	119.03(16)
C(19)-P(3)-Pd(1)	114.57(15)
C(23)-P(3)-Pd(1)	113.71(15)
C(4)-C(1)-C(2)	108.6(4)
C(4)-C(1)-C(3)	108.3(4)
C(2)-C(1)-C(3)	107.1(4)
C(4)-C(1)-P(1)	110.7(3)
C(2)-C(1)-P(1)	104.5(3)
C(3)-C(1)-P(1)	117.2(3)
C(7)-C(5)-C(8)	108.9(4)
C(7)-C(5)-C(6)	109.1(4)
C(8)-C(5)-C(6)	106.4(4)
C(7)-C(5)-P(1)	116.5(3)
C(8)-C(5)-P(1)	109.3(3)
C(6)-C(5)-P(1)	106.1(3)

C(13)-C(10)-C(11)	108.5(4)
C(13)-C(10)-C(12)	108.8(4)
C(11)-C(10)-C(12)	106.7(4)
C(13)-C(10)-P(2)	117.4(3)
C(11)-C(10)-P(2)	104.9(3)
C(12)-C(10)-P(2)	110.0(3)
C(15)-C(14)-C(16)	108.9(5)
C(15)-C(14)-C(17)	107.1(5)
C(16)-C(14)-C(17)	108.5(5)
C(15)-C(14)-P(2)	110.4(3)
C(16)-C(14)-P(2)	116.3(3)
C(17)-C(14)-P(2)	105.2(3)
C(21)-C(19)-C(20)	108.4(4)
C(21)-C(19)-C(22)	105.6(4)
C(20)-C(19)-C(22)	108.8(5)
C(21)-C(19)-P(3)	111.5(3)
C(20)-C(19)-P(3)	117.3(4)
C(22)-C(19)-P(3)	104.5(3)
C(25)-C(23)-C(24)	108.6(5)
C(25)-C(23)-C(26)	108.5(6)
C(24)-C(23)-C(26)	107.5(5)
C(25)-C(23)-P(3)	110.5(3)
C(24)-C(23)-P(3)	116.9(4)
C(26)-C(23)-P(3)	104.4(4)

Table 4. Anisotropic displacement parameters ($Å^2 x\ 10^3$) for 03068IHs. The anisotropic displacement factor exponent takes the form: $-2p^2[\ h^2\ a^{*2}U^{11} + ... + 2\ h\ k\ a^*\ b^*\ U^{12}\ ]$

	U^{11}	U^{22}	U^{33}	U^{23}	U^{13}	U^{12}
Pd(1)	21(1)	23(1)	22(1)	0(1)	2(1)	1(1)
P(1)	21(1)	24(1)	22(1)	-2(1)	1(1)	2(1)
P(2)	26(1)	26(1)	22(1)	-1(1)	4(1)	0(1)
P(3)	34(1)	25(1)	24(1)	2(1)	2(1)	4(1)
C(1)	23(2)	29(2)	41(3)	-3(2)	7(2)	-3(2)
C(2)	25(3)	44(3)	87(4)	-5(3)	5(3)	-3(2)
C(3)	39(3)	30(2)	48(3)	-3(2)	3(2)	-4(2)
C(4)	60(3)	46(3)	42(3)	0(2)	20(3)	-14(2)
C(5)	24(2)	29(2)	30(2)	-2(2)	-1(2)	5(2)
C(6)	27(2)	55(3)	58(3)	6(3)	2(2)	-3(2)
C(7)	30(3)	38(3)	82(4)	-7(3)	-4(3)	9(2)
C(8)	29(3)	51(3)	45(3)	0(2)	-12(2)	6(2)
C(9)	38(3)	29(2)	31(3)	-4(2)	2(2)	4(2)
C(10)	30(2)	33(2)	31(3)	-4(2)	9(2)	1(2)
C(11)	33(3)	54(3)	88(5)	-19(3)	14(3)	-10(2)
C(12)	35(3)	55(3)	71(4)	18(3)	15(3)	12(2)
C(13)	50(3)	98(5)	47(4)	-15(3)	15(3)	9(3)
C(14)	35(2)	34(2)	31(3)	-2(2)	1(2)	-6(2)
C(15)	77(4)	33(3)	93(5)	11(3)	-26(4)	-24(3)
C(16)	125(6)	100(5)	41(4)	-27(3)	13(4)	-68(5)
C(17)	30(3)	64(4)	119(6)	-28(4)	7(3)	-15(3)
C(18)	43(3)	38(3)	25(2)	0(2)	6(2)	2(2)
C(19)	44(3)	36(3)	39(3)	10(2)	9(2)	-1(2)
C(20)	103(5)	68(4)	77(5)	43(4)	50(4)	24(4)
C(21)	72(4)	55(3)	44(3)	5(3)	24(3)	3(3)
C(22)	50(3)	79(4)	75(5)	-9(3)	12(3)	-27(3)

C(23)	36(3)	40(3)	40(3)	8(2)	-7(2)	3(2)
C(24)	123(6)	60(4)	80(5)	21(4)	-60(5)	-5(4)
C(25)	69(4)	56(4)	121(6)	-36(4)	-50(4)	6(3)
C(26)	37(3)	203(10)	77(5)	5(6)	-14(3)	-26(5)
C(27)	57(3)	31(3)	38(3)	4(2)	3(2)	10(2)

Table 5. Hydrogen coordinates (x 10^4) and isotropic displacement parameters ($Å^2$x 10^3) for 03068IHs.

	x	y	z	U(eq)
H(2A)	5112	2092	1389	77
H(2B)	5022	2348	2556	77
H(2C)	5631	2585	1482	77
H(3A)	3851	3161	1644	58
H(3B)	3148	2938	2702	58
H(3C)	2078	3074	1611	58
H(4A)	2181	2685	-185	73
H(4B)	3273	2280	-289	73
H(4C)	3963	2755	-168	73
H(6A)	-1976	1886	1695	69
H(6B)	-833	1953	2792	69
H(6C)	-550	1575	1915	69
H(7A)	5	2830	997	76
H(7B)	-322	2721	2275	76
H(7C)	-1611	2652	1272	76
H(8A)	-1356	2076	-146	64
H(8B)	51	1754	-29	64
H(8C)	285	2244	-390	64
H(9A)	1491	2480	3382	49
H(9B)	3062	2237	3654	49
H(9C)	1514	1980	3715	49
H(11A)	6874	1432	-690	87
H(11B)	5668	1513	221	87
H(11C)	5419	1722	-1015	87
H(12A)	5174	422	-635	80
H(12B)	5406	721	467	80
H(12C)	6709	685	-385	80

H(13A)	6276	1004	-2344	97
H(13B)	4715	1241	-2699	97
H(13C)	4751	731	-2509	97
H(15A)	1296	75	-706	104
H(15B)	1976	367	325	104
H(15C)	3044	201	-609	104
H(16A)	2705	487	-2575	132
H(16B)	1463	849	-2885	132
H(16C)	954	367	-2627	132
H(17A)	-616	599	-1130	107
H(17B)	-223	1086	-1435	107
H(17C)	47	919	-156	107
H(18A)	2971	1828	-1630	53
H(18B)	1290	1644	-1696	53
H(18C)	2490	1447	-2493	53
H(20A)	2830	377	5016	120
H(20B)	2375	48	4006	120
H(20C)	1110	235	4760	120
H(21A)	267	982	4546	84
H(21B)	1073	1305	3733	84
H(21C)	1963	1133	4870	84
H(22A)	-407	505	3074	102
H(22B)	794	306	2283	102
H(22C)	342	804	2171	102
H(24A)	6523	784	5091	137
H(24B)	5930	400	4273	137
H(24C)	4833	613	5124	137
H(25A)	4124	1380	4860	127
H(25B)	4488	1628	3728	127
H(25C)	5815	1521	4676	127
H(26A)	6061	1241	2323	160
H(26B)	6668	769	2652	160
H(26C)	7275	1176	3379	160

H(27A)	4299	122	3018	63
H(27B)	4911	316	1889	63
H(27C)	3209	150	1880	63

Table 6. Torsion angles [°] for 03068IHs.

P(3)-Pd(1)-P(1)-C(9)	1.85(17)
P(2)-Pd(1)-P(1)-C(9)	-178.03(16)
P(3)-Pd(1)-P(1)-C(5)	-113.42(15)
P(2)-Pd(1)-P(1)-C(5)	66.69(15)
P(3)-Pd(1)-P(1)-C(1)	119.27(16)
P(2)-Pd(1)-P(1)-C(1)	-60.62(16)
P(3)-Pd(1)-P(2)-C(18)	177.16(17)
P(1)-Pd(1)-P(2)-C(18)	-2.95(18)
P(3)-Pd(1)-P(2)-C(10)	-67.93(15)
P(1)-Pd(1)-P(2)-C(10)	111.96(15)
P(3)-Pd(1)-P(2)-C(14)	59.56(16)
P(1)-Pd(1)-P(2)-C(14)	-120.55(16)
P(1)-Pd(1)-P(3)-C(27)	-178.97(19)
P(2)-Pd(1)-P(3)-C(27)	0.9(2)
P(1)-Pd(1)-P(3)-C(19)	64.80(17)
P(2)-Pd(1)-P(3)-C(19)	-115.31(17)
P(1)-Pd(1)-P(3)-C(23)	-63.03(18)
P(2)-Pd(1)-P(3)-C(23)	116.85(17)
C(9)-P(1)-C(1)-C(4)	-163.1(3)
C(5)-P(1)-C(1)-C(4)	-60.2(4)
Pd(1)-P(1)-C(1)-C(4)	68.3(3)
C(9)-P(1)-C(1)-C(2)	80.2(3)
C(5)-P(1)-C(1)-C(2)	-177.0(3)
Pd(1)-P(1)-C(1)-C(2)	-48.5(4)
C(9)-P(1)-C(1)-C(3)	-38.2(4)
C(5)-P(1)-C(1)-C(3)	64.6(4)
Pd(1)-P(1)-C(1)-C(3)	-166.9(3)
C(9)-P(1)-C(5)-C(7)	59.5(4)
C(1)-P(1)-C(5)-C(7)	-42.9(4)
Pd(1)-P(1)-C(5)-C(7)	-173.3(3)
C(9)-P(1)-C(5)-C(8)	-176.5(3)

C(1)-P(1)-C(5)-C(8)	81.1(3)
Pd(1)-P(1)-C(5)-C(8)	-49.3(3)
C(9)-P(1)-C(5)-C(6)	-62.1(3)
C(1)-P(1)-C(5)-C(6)	-164.5(3)
Pd(1)-P(1)-C(5)-C(6)	65.0(3)
C(18)-P(2)-C(10)-C(13)	-45.7(4)
C(14)-P(2)-C(10)-C(13)	56.9(4)
Pd(1)-P(2)-C(10)-C(13)	-172.4(4)
C(18)-P(2)-C(10)-C(11)	74.8(4)
C(14)-P(2)-C(10)-C(11)	177.4(3)
Pd(1)-P(2)-C(10)-C(11)	-51.9(4)
C(18)-P(2)-C(10)-C(12)	-170.7(3)
C(14)-P(2)-C(10)-C(12)	-68.1(4)
Pd(1)-P(2)-C(10)-C(12)	62.5(4)
C(18)-P(2)-C(14)-C(15)	174.1(4)
C(10)-P(2)-C(14)-C(15)	71.2(4)
Pd(1)-P(2)-C(14)-C(15)	-57.4(4)
C(18)-P(2)-C(14)-C(16)	49.3(5)
C(10)-P(2)-C(14)-C(16)	-53.6(5)
Pd(1)-P(2)-C(14)-C(16)	177.8(4)
C(18)-P(2)-C(14)-C(17)	-70.8(4)
C(10)-P(2)-C(14)-C(17)	-173.7(4)
Pd(1)-P(2)-C(14)-C(17)	57.8(4)
C(27)-P(3)-C(19)-C(21)	169.4(4)
C(23)-P(3)-C(19)-C(21)	66.5(4)
Pd(1)-P(3)-C(19)-C(21)	-63.1(4)
C(27)-P(3)-C(19)-C(20)	43.6(5)
C(23)-P(3)-C(19)-C(20)	-59.3(5)
Pd(1)-P(3)-C(19)-C(20)	171.1(4)
C(27)-P(3)-C(19)-C(22)	-77.0(4)
C(23)-P(3)-C(19)-C(22)	-179.8(3)
Pd(1)-P(3)-C(19)-C(22)	50.5(4)
C(27)-P(3)-C(23)-C(25)	-174.2(5)

C(19)-P(3)-C(23)-C(25)	-71.5(5)
Pd(1)-P(3)-C(23)-C(25)	58.6(5)
C(27)-P(3)-C(23)-C(24)	-49.3(5)
C(19)-P(3)-C(23)-C(24)	53.3(5)
Pd(1)-P(3)-C(23)-C(24)	-176.6(4)
C(27)-P(3)-C(23)-C(26)	69.4(5)
C(19)-P(3)-C(23)-C(26)	172.0(4)
Pd(1)-P(3)-C(23)-C(26)	-57.9(5)

P-1 (Figure 3.2)

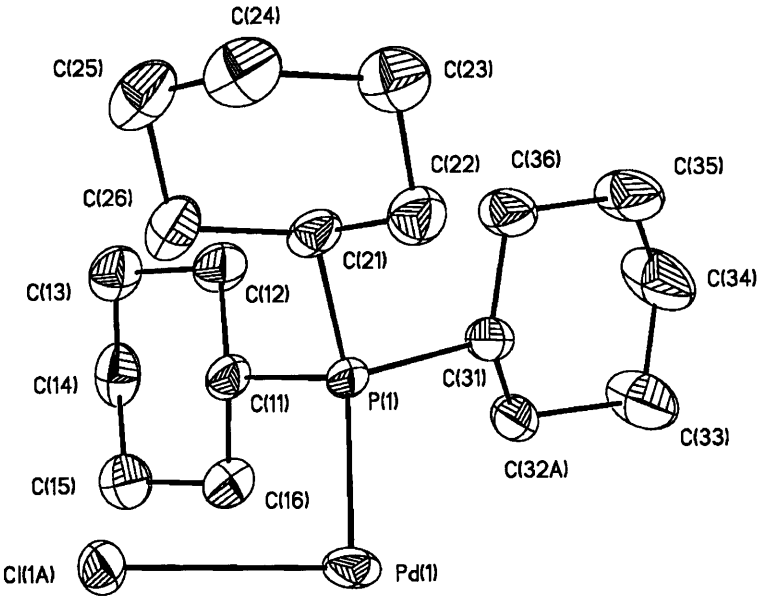
C(24)
C(25)
C(23)
C(22)
C(36)
C(35)
C(26)
C(21)
C(34)
C(13)
C(12)
C(14)
C(11)
P(1)
C(31)
C(33)
C(32A)
C(15)
C(16)
Cl(1A)
Pd(1)

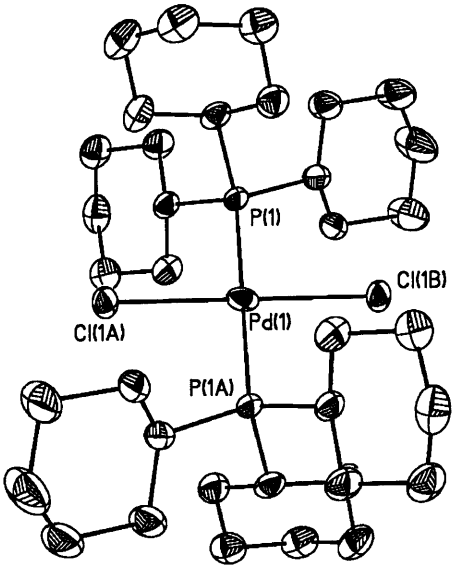
P(1)
Cl(1B)
Cl(1A)
Pd(1)
P(1A)

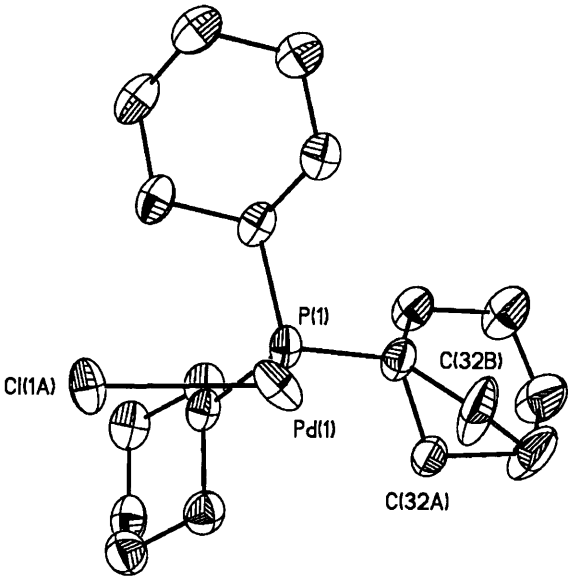
P(1)
C(32B)
Cl(1A)
Pd(1)
C(32A)

Tables 1-6 provide the full crystallographic data for the X-ray structure.

Table 1. Crystal data and structure refinement for 04014IH p-1.

Identification code	04014IH p-1	
Empirical formula	C36 H66 Cl P2 Pd	
Formula weight	702.68	
Temperature	193(2) K	
Wavelength	0.71073 Å	
Crystal system	Triclinic	
Space group	P-1	
Unit cell dimensions	a = 9.8843(5) Å	α = 66.6700(10)°.
	b = 10.2473(5) Å	β = 70.1810(10)°.
	c = 10.6255(6) Å	γ = 89.9180(10)°.
Volume	918.64(8) $Å^3$	
Z	1	
Density (calculated)	1.270 Mg/m^3	
Absorption coefficient	0.687 mm^{-1}	
F(000)	375	
Crystal size	0.28 x 0.19 x 0.16 mm^3	
Theta range for data collection	2.19 to 23.24°.	
Index ranges	-10<=h<=10, -10<=k<=11, -11<=l<=11	
Reflections collected	2596	
Independent reflections	2596 [R(int) = 0.0000]	
Completeness to theta = 23.24°	98.7 %	
Refinement method	Full-matrix least-squares on F^2	
Data / restraints / parameters	2596 / 242 / 197	
Goodness-of-fit on F^2	1.042	
Final R indices [I>2sigma(I)]	R1 = 0.0371, wR2 = 0.0884	
R indices (all data)	R1 = 0.0397, wR2 = 0.0905	
Largest diff. peak and hole	0.557 and -1.033 e.$Å^{-3}$	

Table 2. Atomic coordinates (x 10^4) and equivalent isotropic displacement parameters ($Å^2$x 10^3) for p-1. U(eq) is defined as one third of the trace of the orthogonalized U^{ij} tensor.

	x	y	z	U(eq)
Pd(1)	0	0	0	54(1)
P(1)	-2005(1)	-330(1)	2063(1)	41(1)
C(11)	-1649(4)	-1164(4)	3785(3)	43(1)
C(12)	-2903(4)	-1352(5)	5202(4)	56(1)
C(13)	-2371(5)	-1793(5)	6481(4)	63(1)
C(14)	-1717(5)	-3144(5)	6685(4)	65(1)
C(15)	-496(5)	-3010(5)	5285(5)	66(1)
C(16)	-994(4)	-2544(4)	3982(4)	58(1)
C(21)	-2546(4)	1418(4)	2014(4)	45(1)
C(22)	-2830(4)	2270(4)	602(4)	54(1)
C(23)	-3301(4)	3710(4)	535(5)	60(1)
C(24)	-2184(4)	4593(4)	691(4)	62(1)
C(25)	-1929(5)	3759(4)	2100(4)	65(1)
C(26)	-1442(4)	2325(4)	2174(4)	56(1)
C(31)	-3680(4)	-1331(4)	2260(5)	55(1)
C(32A)	-3672(5)	-2938(6)	2692(8)	66(2)
C(32B)	-3640(20)	-2170(30)	1380(30)	104(8)
C(33)	-4908(5)	-3500(7)	2327(9)	127(3)
C(34)	-6355(5)	-3283(6)	3245(9)	116(2)
C(35)	-6390(4)	-1799(6)	3028(7)	91(2)
C(36)	-5131(4)	-1129(5)	3198(5)	64(1)
Cl(1A)	1638(2)	797(2)	1035(2)	49(1)

Table 3. Bond lengths [Å] and angles [°] for 04014IH p-1.

Pd(1)-P(1)#1	2.3058(8)
Pd(1)-P(1)	2.3058(8)
Pd(1)-Cl(1A)#1	2.5337(16)
Pd(1)-Cl(1A)	2.5337(16)
P(1)-C(11)	1.844(3)
P(1)-C(31)	1.853(3)
P(1)-C(21)	1.854(3)
C(11)-C(16)	1.522(5)
C(11)-C(12)	1.532(4)
C(12)-C(13)	1.525(5)
C(13)-C(14)	1.496(6)
C(14)-C(15)	1.520(6)
C(15)-C(16)	1.525(5)
C(21)-C(26)	1.529(5)
C(21)-C(22)	1.529(5)
C(22)-C(23)	1.528(5)
C(23)-C(24)	1.520(5)
C(24)-C(25)	1.510(6)
C(25)-C(26)	1.526(5)
C(31)-C(32B)	1.492(13)
C(31)-C(36)	1.512(5)
C(31)-C(32A)	1.526(6)
C(32A)-C(33)	1.573(6)
C(32B)-C(33)	1.586(15)
C(33)-C(34)	1.507(7)
C(34)-C(35)	1.447(6)
C(35)-C(36)	1.519(6)
P(1)#1-Pd(1)-P(1)	180.00(6)
P(1)#1-Pd(1)-Cl(1A)#1	90.50(4)
P(1)-Pd(1)-Cl(1A)#1	89.50(4)
P(1)#1-Pd(1)-Cl(1A)	89.50(4)

P(1)-Pd(1)-Cl(1A)	90.50(4)
Cl(1A)#1-Pd(1)-Cl(1A)	180.00(8)
C(11)-P(1)-C(31)	109.42(18)
C(11)-P(1)-C(21)	104.15(15)
C(31)-P(1)-C(21)	103.56(15)
C(11)-P(1)-Pd(1)	112.80(11)
C(31)-P(1)-Pd(1)	114.93(12)
C(21)-P(1)-Pd(1)	111.06(11)
C(16)-C(11)-C(12)	110.8(3)
C(16)-C(11)-P(1)	114.2(2)
C(12)-C(11)-P(1)	116.2(2)
C(13)-C(12)-C(11)	110.2(3)
C(14)-C(13)-C(12)	110.8(3)
C(13)-C(14)-C(15)	112.1(3)
C(14)-C(15)-C(16)	111.7(3)
C(11)-C(16)-C(15)	110.3(3)
C(26)-C(21)-C(22)	110.3(3)
C(26)-C(21)-P(1)	113.4(3)
C(22)-C(21)-P(1)	110.3(2)
C(23)-C(22)-C(21)	111.8(3)
C(24)-C(23)-C(22)	110.9(3)
C(25)-C(24)-C(23)	110.6(3)
C(24)-C(25)-C(26)	111.6(3)
C(25)-C(26)-C(21)	111.2(3)
C(32B)-C(31)-C(36)	119.6(9)
C(32B)-C(31)-C(32A)	50.7(13)
C(36)-C(31)-C(32A)	108.3(4)
C(32B)-C(31)-P(1)	121.7(8)
C(36)-C(31)-P(1)	118.2(2)
C(32A)-C(31)-P(1)	115.1(3)
C(31)-C(32A)-C(33)	107.5(4)
C(31)-C(32B)-C(33)	108.5(10)
C(34)-C(33)-C(32A)	108.9(4)

C(34)-C(33)-C(32B)	118.4(9)
C(32A)-C(33)-C(32B)	48.3(12)
C(35)-C(34)-C(33)	112.3(5)
C(34)-C(35)-C(36)	114.4(4)
C(31)-C(36)-C(35)	111.6(3)

Symmetry transformations used to generate equivalent atoms:

#1 -x,-y,-z

Table 4. Anisotropic displacement parameters ($Å^2 x\ 10^3$) for 04014IH p-1. The Anisotropic displacement factor exponent takes the form: $-2p^2[\ h^2\ a^{*2}U^{11} + ... + 2\ h\ k\ a^*\ b^*\ U^{12}\ ]$

	U^{11}	U^{22}	U^{33}	U^{23}	U^{13}	U^{12}
Pd(1)	45(1)	97(1)	31(1)	-35(1)	-17(1)	37(1)
P(1)	29(1)	62(1)	43(1)	-37(1)	-9(1)	8(1)
C(11)	38(2)	56(2)	39(2)	-29(2)	-7(2)	1(2)
C(12)	50(2)	74(3)	38(2)	-29(2)	-3(2)	4(2)
C(13)	60(3)	81(3)	40(2)	-30(2)	-5(2)	-2(2)
C(14)	67(3)	71(3)	49(2)	-17(2)	-23(2)	-12(2)
C(15)	66(3)	73(3)	68(3)	-33(2)	-32(2)	17(2)
C(16)	60(2)	65(2)	56(2)	-35(2)	-20(2)	11(2)
C(21)	37(2)	53(2)	41(2)	-29(2)	1(2)	-2(2)
C(22)	47(2)	63(2)	54(2)	-32(2)	-12(2)	4(2)
C(23)	52(2)	57(2)	59(2)	-23(2)	-8(2)	1(2)
C(24)	58(2)	53(2)	56(2)	-22(2)	1(2)	-7(2)
C(25)	71(3)	59(2)	59(2)	-35(2)	-5(2)	-11(2)
C(26)	61(2)	60(2)	48(2)	-30(2)	-13(2)	-6(2)
C(31)	36(2)	66(2)	84(3)	-54(2)	-21(2)	13(2)
C(32A)	50(3)	73(3)	113(5)	-67(3)	-44(3)	26(2)
C(32B)	77(11)	151(15)	145(17)	-127(12)	-34(9)	10(10)
C(33)	65(3)	123(4)	278(8)	-155(5)	-77(4)	32(3)
C(34)	56(3)	95(4)	232(7)	-98(5)	-59(4)	14(3)
C(35)	36(2)	103(4)	153(5)	-87(4)	-17(3)	5(2)
C(36)	36(2)	68(3)	90(3)	-47(2)	-11(2)	3(2)
Cl(1A)	37(1)	82(1)	34(1)	-31(1)	-11(1)	3(1)

Table 5. Hydrogen coordinates (x 10^4) and isotropic displacement parameters ($Å^2$x 10^3) for 04014IH p-1.

	x	y	z	U(eq)
H(11)	-868	-463	3676	52
H(12A)	-3297	-438	5060	67
H(12B)	-3694	-2098	5431	67
H(13A)	-1636	-1011	6285	75
H(13B)	-3198	-1945	7397	75
H(14A)	-2483	-3947	6991	78
H(14B)	-1331	-3375	7484	78
H(15A)	-148	-3948	5449	79
H(15B)	328	-2297	5053	79
H(16A)	-154	-2386	3073	69
H(16B)	-1728	-3314	4153	69
H(21)	-3483	1207	2865	54
H(22A)	-1932	2445	-262	65
H(22B)	-3599	1695	553	65
H(23A)	-3419	4253	-417	72
H(23B)	-4253	3535	1337	72
H(24A)	-1257	4846	-162	75
H(24B)	-2534	5498	695	75
H(25A)	-2839	3580	2954	78
H(25B)	-1175	4338	2164	78
H(26A)	-1328	1789	3129	67
H(26B)	-485	2505	1377	67
H(31A)	-3697	-938	1242	66
H(31B)	-3625	-2198	3106	66
H(32A)	-3855	-3449	3757	79
H(32B)	-2715	-3108	2130	79
H(32C)	-2685	-2506	1124	125

H(32D)	-3766	-1549	448	125
H(33A)	-4736	-2965	1266	153
H(33B)	-4907	-4533	2548	153
H(33A)	-5080	-3855	1644	153
H(33B)	-4554	-4274	2997	153
H(34A)	-7130	-3594	2984	139
H(34B)	-6558	-3894	4299	139
H(35A)	-7313	-1743	3746	110
H(35B)	-6389	-1225	2027	110
H(36A)	-5165	-88	2909	76
H(36B)	-5231	-1574	4246	76

Table 6. Torsion angles [°] for 04014IH p-1.

P(1)#1-Pd(1)-P(1)-C(11)	-100(100)
Cl(1A)#1-Pd(1)-P(1)-C(11)	139.04(13)
Cl(1A)-Pd(1)-P(1)-C(11)	-40.96(13)
P(1)#1-Pd(1)-P(1)-C(31)	133(100)
Cl(1A)#1-Pd(1)-P(1)-C(31)	12.67(15)
Cl(1A)-Pd(1)-P(1)-C(31)	-167.33(15)
P(1)#1-Pd(1)-P(1)-C(21)	16(100)
Cl(1A)#1-Pd(1)-P(1)-C(21)	-104.47(13)
Cl(1A)-Pd(1)-P(1)-C(21)	75.53(13)
C(31)-P(1)-C(11)-C(16)	77.2(3)
C(21)-P(1)-C(11)-C(16)	-172.6(3)
Pd(1)-P(1)-C(11)-C(16)	-52.0(3)
C(31)-P(1)-C(11)-C(12)	-53.7(3)
C(21)-P(1)-C(11)-C(12)	56.5(3)
Pd(1)-P(1)-C(11)-C(12)	177.0(2)
C(16)-C(11)-C(12)-C(13)	57.8(4)
P(1)-C(11)-C(12)-C(13)	-169.7(3)
C(11)-C(12)-C(13)-C(14)	-57.1(4)
C(12)-C(13)-C(14)-C(15)	55.7(4)
C(13)-C(14)-C(15)-C(16)	-54.6(5)
C(12)-C(11)-C(16)-C(15)	-56.3(4)
P(1)-C(11)-C(16)-C(15)	170.2(3)
C(14)-C(15)-C(16)-C(11)	54.4(5)
C(11)-P(1)-C(21)-C(26)	53.7(3)
C(31)-P(1)-C(21)-C(26)	168.1(3)
Pd(1)-P(1)-C(21)-C(26)	-68.0(3)
C(11)-P(1)-C(21)-C(22)	178.0(2)
C(31)-P(1)-C(21)-C(22)	-67.6(3)
Pd(1)-P(1)-C(21)-C(22)	56.3(3)
C(26)-C(21)-C(22)-C(23)	-54.8(4)
P(1)-C(21)-C(22)-C(23)	179.1(2)

C(21)-C(22)-C(23)-C(24)	55.9(4)
C(22)-C(23)-C(24)-C(25)	-56.4(4)
C(23)-C(24)-C(25)-C(26)	57.0(4)
C(24)-C(25)-C(26)-C(21)	-56.6(4)
C(22)-C(21)-C(26)-C(25)	54.7(4)
P(1)-C(21)-C(26)-C(25)	179.0(2)
C(11)-P(1)-C(31)-C(32B)	-113.4(17)
C(21)-P(1)-C(31)-C(32B)	136.0(17)
Pd(1)-P(1)-C(31)-C(32B)	14.7(17)
C(11)-P(1)-C(31)-C(36)	74.4(4)
C(21)-P(1)-C(31)-C(36)	-36.2(4)
Pd(1)-P(1)-C(31)-C(36)	-157.5(3)
C(11)-P(1)-C(31)-C(32A)	-55.6(4)
C(21)-P(1)-C(31)-C(32A)	-166.2(4)
Pd(1)-P(1)-C(31)-C(32A)	72.5(4)
C(32B)-C(31)-C(32A)-C(33)	-51.1(11)
C(36)-C(31)-C(32A)-C(33)	62.7(6)
P(1)-C(31)-C(32A)-C(33)	-162.6(4)
C(36)-C(31)-C(32B)-C(33)	-39(3)
C(32A)-C(31)-C(32B)-C(33)	50.9(14)
P(1)-C(31)-C(32B)-C(33)	148.8(12)
C(31)-C(32A)-C(33)-C(34)	-62.2(7)
C(31)-C(32A)-C(33)-C(32B)	49.3(11)
C(31)-C(32B)-C(33)-C(34)	39(3)
C(31)-C(32B)-C(33)-C(32A)	-51.2(14)
C(32A)-C(33)-C(34)-C(35)	56.2(8)
C(32B)-C(33)-C(34)-C(35)	4.1(16)
C(33)-C(34)-C(35)-C(36)	-51.3(8)
C(32B)-C(31)-C(36)-C(35)	-2.6(16)
C(32A)-C(31)-C(36)-C(35)	-57.1(5)
P(1)-C(31)-C(36)-C(35)	169.7(4)
C(34)-C(35)-C(36)-C(31)	51.8(7)

Symmetry transformations used to generate equivalent atoms:

#1 -x,-y,-z

04006mih (Figure 3.2)

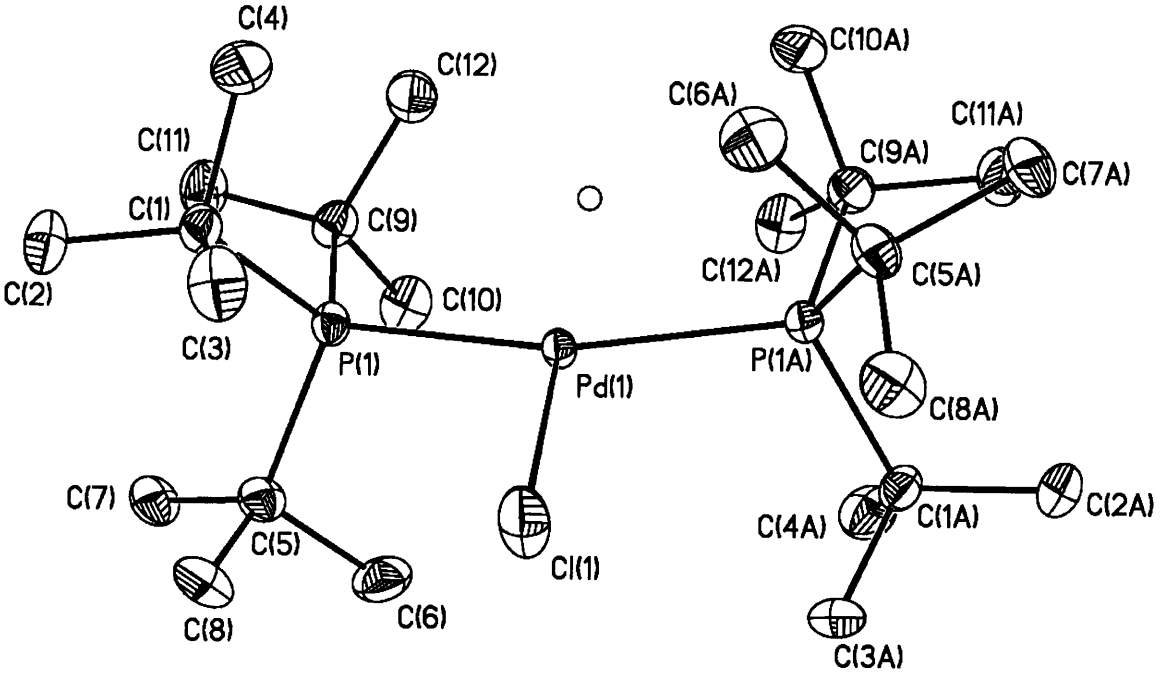

Table 1. Crystal data and structure refinement for 04006mih.

Identification code	04006mih	
Empirical formula	C24 H55 Cl P2 Pd	
Formula weight	547.47	
Temperature	193(2) K	
Wavelength	0.71073 Å	
Crystal system	Monoclinic	
Space group	P2/n	
Unit cell dimensions	a = 12.7692(12) Å	α = 90°.
	b = 8.7306(9) Å	β = 114.718(2)°.
	c = 13.8817(14) Å	γ = 90°.
Volume	1405.8(2) $Å^3$	
Z	2	
Density (calculated)	1.293 Mg/m^3	
Absorption coefficient	0.878 mm^{-1}	
F(000)	584	
Crystal size	0.27 x 0.26 x 0.07 mm^3	
Theta range for data collection	1.82 to 23.25°.	
Index ranges	-12<=h<=14, -9<=k<=7, -15<=l<=15	
Reflections collected	5946	
Independent reflections	2015 [R(int) = 0.0366]	
Completeness to theta = 23.25°	99.7 %	
Refinement method	Full-matrix least-squares on F^2	
Data / restraints / parameters	2015 / 0 / 140	
Goodness-of-fit on F^2	1.071	
Final R indices [I>2sigma(I)]	R1 = 0.0473, wR2 = 0.1195	
R indices (all data)	R1 = 0.0510, wR2 = 0.1234	
Largest diff. peak and hole	2.982 and -0.357 $e.Å^{-3}$	

Table 2. Atomic coordinates (x 10^4) and equivalent isotropic displacement parameters ($Å^2$x 10^3) for 04006mih. U(eq) is defined as one third of the trace of the orthogonalized U^{ij} tensor.

	x	y	z	U(eq)
Pd(1)	2500	7501(1)	2500	19(1)
P(1)	4191(1)	7955(1)	2249(1)	24(1)
Cl(1)	2500	4702(2)	2500	48(1)
C(1)	4088(4)	7299(5)	902(4)	29(1)
C(2)	5223(5)	7185(6)	795(4)	41(1)
C(3)	3495(4)	5714(6)	646(4)	43(1)
C(4)	3264(4)	8368(7)	33(3)	47(1)
C(5)	5446(3)	6931(6)	3344(3)	32(1)
C(6)	5235(5)	7044(7)	4365(4)	47(1)
C(7)	6662(4)	7552(5)	3602(4)	39(1)
C(8)	5444(4)	5215(5)	3090(4)	42(1)
C(9)	4538(4)	10132(5)	2352(3)	32(1)
C(10)	4841(4)	10635(5)	3502(4)	43(1)
C(11)	5536(4)	10617(6)	2069(4)	45(1)
C(12)	3475(4)	11085(5)	1642(4)	43(1)

Table 3. Bond lengths [Å] and angles [°] for 04006mih.

Pd(1)-P(1)	2.3608(11)
Pd(1)-P(1)#1	2.3608(11)
Pd(1)-Cl(1)	2.4436(18)
P(1)-C(1)	1.906(5)
P(1)-C(5)	1.907(4)
P(1)-C(9)	1.944(4)
C(1)-C(2)	1.521(8)
C(1)-C(4)	1.540(6)
C(1)-C(3)	1.546(6)
C(5)-C(8)	1.540(7)
C(5)-C(7)	1.540(7)
C(5)-C(6)	1.552(7)
C(9)-C(10)	1.541(6)
C(9)-C(11)	1.542(6)
C(9)-C(12)	1.545(6)
P(1)-Pd(1)-P(1)#1	160.68(6)
P(1)-Pd(1)-Cl(1)	99.66(3)
P(1)#1-Pd(1)-Cl(1)	99.66(3)
C(1)-P(1)-C(5)	109.4(2)
C(1)-P(1)-C(9)	106.61(18)
C(5)-P(1)-C(9)	108.1(2)
C(1)-P(1)-Pd(1)	113.71(15)
C(5)-P(1)-Pd(1)	108.59(14)
C(9)-P(1)-Pd(1)	110.33(14)
C(2)-C(1)-C(4)	109.3(4)
C(2)-C(1)-C(3)	108.3(4)
C(4)-C(1)-C(3)	104.7(4)
C(2)-C(1)-P(1)	116.0(3)
C(4)-C(1)-P(1)	109.3(3)
C(3)-C(1)-P(1)	108.7(3)

C(8)-C(5)-C(7)	107.5(4)
C(8)-C(5)-C(6)	106.7(4)
C(7)-C(5)-C(6)	108.0(4)
C(8)-C(5)-P(1)	110.7(3)
C(7)-C(5)-P(1)	116.7(3)
C(6)-C(5)-P(1)	106.8(3)
C(10)-C(9)-C(11)	108.0(4)
C(10)-C(9)-C(12)	106.3(4)
C(11)-C(9)-C(12)	106.8(4)
C(10)-C(9)-P(1)	107.8(3)
C(11)-C(9)-P(1)	115.9(3)
C(12)-C(9)-P(1)	111.6(3)

Symmetry transformations used to generate equivalent atoms:
#1 -x+1/2,y,-z+1/2

Table 4. Anisotropic displacement parameters ($Å^2 x\ 10^3$) for 04006mih. The anisotropic displacement factor exponent takes the form: $-2p^2[\ h^2\ a^{*2}U^{11} + ... + 2\ h\ k\ a^*\ b^*\ U^{12}\ ]$

	U^{11}	U^{22}	U^{33}	U^{23}	U^{13}	U^{12}
Pd(1)	18(1)	16(1)	25(1)	0	11(1)	0
P(1)	20(1)	29(1)	24(1)	-2(1)	10(1)	-1(1)
Cl(1)	51(1)	21(1)	91(2)	0	48(1)	0
C(1)	28(3)	38(3)	24(2)	-2(2)	13(2)	3(2)
C(2)	40(3)	52(3)	41(3)	-9(2)	26(2)	-2(2)
C(3)	41(3)	43(3)	45(3)	-24(2)	17(2)	-11(2)
C(4)	48(3)	59(4)	30(2)	1(2)	12(2)	6(3)
C(5)	22(2)	36(3)	32(2)	4(2)	7(2)	-1(2)
C(6)	49(3)	57(3)	29(2)	11(2)	12(2)	1(3)
C(7)	21(3)	47(4)	39(3)	3(2)	5(2)	2(2)
C(8)	35(3)	33(3)	51(3)	6(2)	10(2)	10(2)
C(9)	39(3)	24(2)	37(2)	-1(2)	20(2)	-6(2)
C(10)	51(3)	32(3)	49(3)	-12(2)	24(2)	-13(2)
C(11)	45(3)	38(3)	62(3)	-3(2)	31(2)	-6(2)
C(12)	51(3)	29(3)	58(3)	7(2)	31(2)	5(2)

Table 5. Hydrogen coordinates (x 10^4) and isotropic displacement parameters ($Å^2$x 10^3) for 04006mih.

	x	y	z	U(eq)
H(2A)	5073	6885	69	62
H(2B)	5715	6414	1292	62
H(2C)	5613	8180	956	62
H(3A)	3368	5410	-74	65
H(3B)	2753	5770	697	65
H(3C)	3989	4956	1154	65
H(4A)	3626	9374	93	70
H(4B)	2544	8479	119	70
H(4C)	3099	7930	-666	70
H(6A)	5859	6519	4948	70
H(6B)	4497	6560	4241	70
H(6C)	5217	8124	4551	70
H(7A)	6726	8603	3868	58
H(7B)	6800	7543	2958	58
H(7C)	7236	6904	4143	58
H(8A)	5677	5082	2505	63
H(8B)	4668	4797	2883	63
H(8C)	5987	4673	3718	63
H(10A)	5563	10145	3979	64
H(10B)	4220	10329	3702	64
H(10C)	4932	11750	3557	64
H(11A)	5319	10432	1313	68
H(11B)	6226	10018	2490	68
H(11C)	5699	11709	2223	68
H(12A)	3625	12173	1821	65
H(12B)	2803	10757	1759	65

H(12C)	3322	10930	896	65
H(99)	2500	310(50)	2500	0(11)

Table 6. Torsion angles [°] for 04006mih.

P(1)#1-Pd(1)-P(1)-C(1)	-114.04(15)
Cl(1)-Pd(1)-P(1)-C(1)	65.96(15)
P(1)#1-Pd(1)-P(1)-C(5)	123.95(16)
Cl(1)-Pd(1)-P(1)-C(5)	-56.05(16)
P(1)#1-Pd(1)-P(1)-C(9)	5.68(14)
Cl(1)-Pd(1)-P(1)-C(9)	-174.32(14)
C(5)-P(1)-C(1)-C(2)	-43.5(4)
C(9)-P(1)-C(1)-C(2)	73.1(4)
Pd(1)-P(1)-C(1)-C(2)	-165.1(3)
C(5)-P(1)-C(1)-C(4)	-167.6(3)
C(9)-P(1)-C(1)-C(4)	-51.0(4)
Pd(1)-P(1)-C(1)-C(4)	70.9(3)
C(5)-P(1)-C(1)-C(3)	78.7(3)
C(9)-P(1)-C(1)-C(3)	-164.7(3)
Pd(1)-P(1)-C(1)-C(3)	-42.9(3)
C(1)-P(1)-C(5)-C(8)	-44.7(4)
C(9)-P(1)-C(5)-C(8)	-160.4(3)
Pd(1)-P(1)-C(5)-C(8)	79.9(3)
C(1)-P(1)-C(5)-C(7)	78.6(4)
C(9)-P(1)-C(5)-C(7)	-37.1(4)
Pd(1)-P(1)-C(5)-C(7)	-156.8(3)
C(1)-P(1)-C(5)-C(6)	-160.5(3)
C(9)-P(1)-C(5)-C(6)	83.8(3)
Pd(1)-P(1)-C(5)-C(6)	-35.9(4)
C(1)-P(1)-C(9)-C(10)	-170.0(3)
C(5)-P(1)-C(9)-C(10)	-52.5(3)
Pd(1)-P(1)-C(9)-C(10)	66.1(3)
C(1)-P(1)-C(9)-C(11)	-48.9(4)
C(5)-P(1)-C(9)-C(11)	68.6(4)
Pd(1)-P(1)-C(9)-C(11)	-172.8(3)
C(1)-P(1)-C(9)-C(12)	73.7(3)

C(5)-P(1)-C(9)-C(12)	-168.9(3)
Pd(1)-P(1)-C(9)-C(12)	-50.3(3)

Symmetry transformations used to generate equivalent atoms:
#1 -x+1/2,y,-z+1/2

03268ih0 (Figure 5.5)

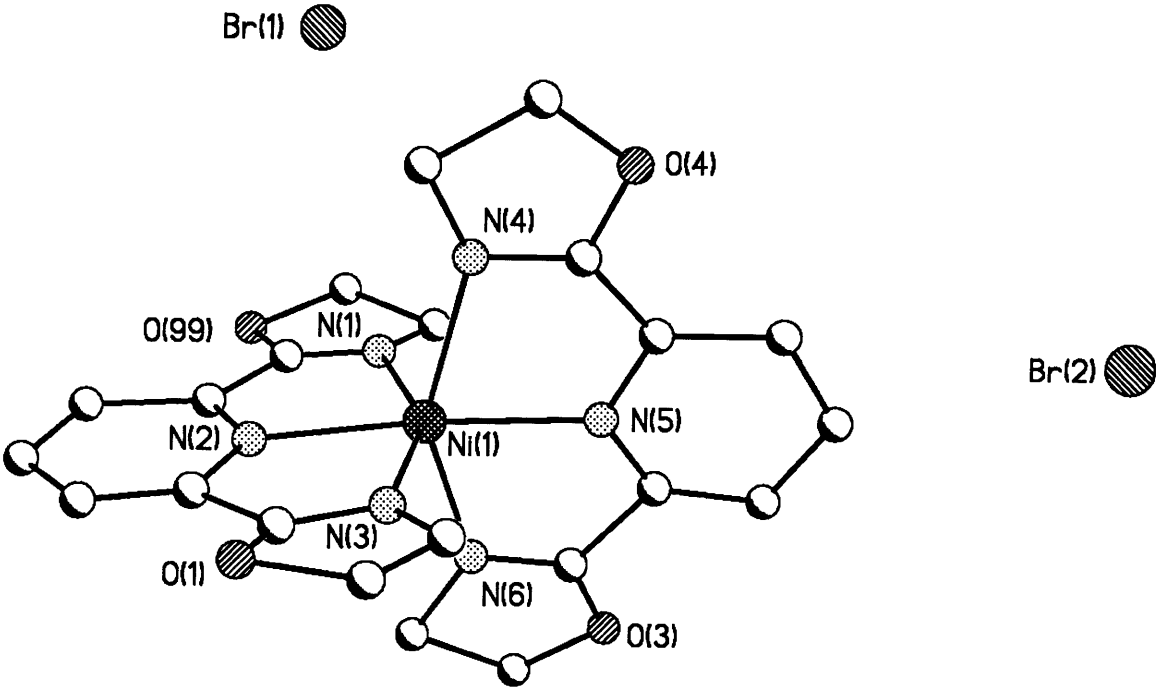

Table 1. Crystal data and structure refinement for 03268ih0.

Identification code	03268ih0	
Empirical formula	C38 H54 Br2 N6 Ni O4	
Formula weight	877.40	
Temperature	193(2) K	
Wavelength	0.71073 Å	
Crystal system	Triclinic	
Space group	P1	
Unit cell dimensions	a = 10.364(8) Å	α = 93.96(4)°.
	b = 10.634(15) Å	β = 110.533(17)°.
	c = 12.269(9) Å	γ = 109.46(4)°.
Volume	1167(2) $Å^3$	
Z	1	
Density (calculated)	1.248 Mg/m^3	
Absorption coefficient	2.167 mm^{-1}	
F(000)	454	
Theta range for data collection	1.81 to 23.24°.	
Index ranges	-11<=h<=11, -3<=k<=11, -10<=l<=10	
Reflections collected	2458	
Independent reflections	2458 [R(int) = 0.0000]	
Completeness to theta = 23.24°	72.9 %	
Refinement method	Full-matrix least-squares on F^2	
Data / restraints / parameters	2458 / 3 / 197	
Goodness-of-fit on F^2	2.338	
Final R indices [I>2sigma(I)]	R1 = 0.1775, wR2 = 0.4468	
R indices (all data)	R1 = 0.1815, wR2 = 0.4543	
Absolute structure parameter	0.13(6)	
Largest diff. peak and hole	5.492 and -1.856 $e.Å^{-3}$	

Table 2. Atomic coordinates (x 10^4) and equivalent isotropic displacement parameters ($Å^2$x 10^3) for 03268ih0. U(eq) is defined as one third of the trace of the orthogonalized U^{ij} tensor.

	x	y	z	U(eq)
Br(1)	8427(5)	2342(4)	8838(4)	57(1)
Br(2)	3082(3)	9687(3)	2975(3)	43(1)
N(1)	7610(30)	3490(20)	4090(20)	25(5)
N(2)	9160(30)	3610(20)	2800(30)	25(6)
N(3)	8970(30)	5600(20)	1670(30)	25(5)
N(4)	9650(30)	6890(30)	4160(30)	33(6)
N(5)	6640(30)	5930(30)	2800(30)	33(6)
N(6)	5800(30)	3460(30)	1730(30)	45(7)
Ni(1)	7964(3)	4789(3)	2884(3)	24(1)
O(1)	10510(40)	5460(30)	990(30)	63(8)
O(3)	3350(30)	3070(30)	1100(30)	45(6)
O(4)	9700(40)	9010(40)	4690(40)	76(10)
O(99)	7910(30)	1660(20)	4790(30)	42(6)
C(1)	8900(60)	9340(50)	370(50)	70(13)
C(2)	7990(40)	8050(40)	-310(40)	48(9)
C(3)	7680(40)	6820(30)	230(30)	34(7)
C(4)	6500(40)	5460(30)	-410(40)	40(8)
C(5)	9190(30)	6730(30)	1090(30)	24(6)
C(6)	9640(100)	6260(100)	700(90)	130(30)
C(7)	9770(40)	5030(30)	1490(30)	30(7)
C(8)	9910(30)	3830(30)	2100(30)	27(7)
C(9)	10600(30)	3010(30)	2090(30)	32(7)
C(10)	10680(30)	2000(30)	2760(30)	28(7)
C(11)	9990(30)	1900(30)	3500(30)	19(6)
C(12)	9040(30)	2680(30)	3480(30)	29(7)
C(13)	8180(30)	2700(30)	4140(30)	28(7)

C(15)	6560(40)	3100(30)	4660(40)	36(8)
C(16)	6830(50)	4310(40)	5450(50)	59(11)
C(17)	8410(40)	5090(40)	6490(40)	52(10)
C(18)	5660(60)	3810(50)	6200(50)	73(14)
C(19)	4230(50)	3160(50)	5600(50)	63(12)
C(21)	5450(40)	1520(30)	320(40)	40(8)
C(22)	4690(40)	1850(40)	-1080(40)	43(9)
C(23)	5070(40)	1970(30)	1100(30)	32(7)
C(24)	3300(50)	1740(40)	800(40)	53(10)
C(25)	4770(30)	3890(30)	1630(30)	26(6)
C(26)	5200(40)	5380(40)	2230(40)	44(9)
C(27)	4320(30)	6070(30)	2010(30)	30(7)
C(28)	4860(50)	7430(40)	2610(40)	52(10)
C(29)	6310(50)	7970(50)	3380(50)	64(12)
C(30)	7270(30)	7170(30)	3460(30)	20(6)
C(31)	8920(30)	7700(30)	4050(30)	31(7)
C(32)	11130(40)	9130(40)	5200(40)	44(9)
C(33)	11190(40)	7720(40)	4800(40)	38(9)
C(34)	12090(40)	7290(40)	5840(40)	46(9)
C(35)	13660(50)	8470(50)	6370(50)	62(11)
C(36)	12380(40)	5950(30)	5300(40)	40(8)
C(37)	12980(40)	5970(40)	4530(40)	48(9)
C(99)	6990(40)	2010(30)	5350(40)	36(8)

Table 3. Bond lengths [Å] and angles [°] for 03268ih0.

N(1)-C(13)	1.17(4)
N(1)-C(15)	1.45(5)
N(1)-Ni(1)	2.14(3)
N(2)-C(8)	1.34(5)
N(2)-C(12)	1.34(5)
N(2)-Ni(1)	2.06(3)
N(3)-C(7)	1.25(5)
N(3)-C(5)	1.43(5)
N(3)-C(6)	1.66(11)
N(3)-Ni(1)	2.17(3)
N(4)-C(31)	1.29(4)
N(4)-C(33)	1.42(5)
N(4)-Ni(1)	2.35(3)
N(5)-C(26)	1.30(5)
N(5)-C(30)	1.32(4)
N(5)-Ni(1)	2.10(3)
N(6)-C(25)	1.26(5)
N(6)-C(23)	1.52(5)
N(6)-Ni(1)	2.10(3)
O(1)-C(7)	1.14(5)
O(1)-C(6)	1.42(10)
O(3)-C(25)	1.33(4)
O(3)-C(24)	1.41(5)
O(4)-C(32)	1.35(5)
O(4)-C(31)	1.37(5)
O(99)-C(13)	1.42(5)
O(99)-C(99)	1.47(5)
C(1)-C(2)	1.38(6)
C(2)-C(3)	1.50(6)
C(3)-C(4)	1.48(5)
C(3)-C(5)	1.59(4)

C(5)-C(6)	0.98(10)
C(6)-C(7)	1.70(11)
C(7)-C(8)	1.54(5)
C(8)-C(9)	1.31(5)
C(9)-C(10)	1.40(5)
C(10)-C(11)	1.33(5)
C(11)-C(12)	1.48(4)
C(12)-C(13)	1.40(6)
C(15)-C(16)	1.44(6)
C(15)-C(99)	1.57(5)
C(16)-C(17)	1.58(6)
C(16)-C(18)	1.74(9)
C(18)-C(19)	1.30(7)
C(21)-C(23)	1.28(6)
C(21)-C(22)	1.74(6)
C(23)-C(24)	1.66(5)
C(25)-C(26)	1.54(5)
C(26)-C(27)	1.32(5)
C(27)-C(28)	1.41(5)
C(28)-C(29)	1.35(6)
C(29)-C(30)	1.49(6)
C(30)-C(31)	1.48(4)
C(32)-C(33)	1.58(5)
C(33)-C(34)	1.49(6)
C(34)-C(35)	1.56(6)
C(34)-C(36)	1.68(5)
C(36)-C(37)	1.31(6)

C(13)-N(1)-C(15)	109(3)
C(13)-N(1)-Ni(1)	113(3)
C(15)-N(1)-Ni(1)	136(2)
C(8)-N(2)-C(12)	129(3)
C(8)-N(2)-Ni(1)	118.2(19)

C(12)-N(2)-Ni(1)	113(3)
C(7)-N(3)-C(5)	105(3)
C(7)-N(3)-C(6)	70(4)
C(5)-N(3)-C(6)	36(3)
C(7)-N(3)-Ni(1)	114(3)
C(5)-N(3)-Ni(1)	141(2)
C(6)-N(3)-Ni(1)	176(3)
C(31)-N(4)-C(33)	107(3)
C(31)-N(4)-Ni(1)	106.8(19)
C(33)-N(4)-Ni(1)	144(2)
C(26)-N(5)-C(30)	120(3)
C(26)-N(5)-Ni(1)	121(2)
C(30)-N(5)-Ni(1)	118.6(19)
C(25)-N(6)-C(23)	108(3)
C(25)-N(6)-Ni(1)	116(2)
C(23)-N(6)-Ni(1)	136(2)
N(2)-Ni(1)-N(5)	175.0(12)
N(2)-Ni(1)-N(6)	100.9(11)
N(5)-Ni(1)-N(6)	75.4(11)
N(2)-Ni(1)-N(1)	76.7(11)
N(5)-Ni(1)-N(1)	106.0(12)
N(6)-Ni(1)-N(1)	83.9(12)
N(2)-Ni(1)-N(3)	77.2(11)
N(5)-Ni(1)-N(3)	100.3(12)
N(6)-Ni(1)-N(3)	103.1(13)
N(1)-Ni(1)-N(3)	153.8(9)
N(2)-Ni(1)-N(4)	107.7(9)
N(5)-Ni(1)-N(4)	76.0(10)
N(6)-Ni(1)-N(4)	151.4(11)
N(1)-Ni(1)-N(4)	103.0(10)
N(3)-Ni(1)-N(4)	83.0(11)
C(7)-O(1)-C(6)	83(5)
C(25)-O(3)-C(24)	107(3)

C(32)-O(4)-C(31)	105(3)
C(13)-O(99)-C(99)	103(3)
C(1)-C(2)-C(3)	122(4)
C(4)-C(3)-C(2)	124(3)
C(4)-C(3)-C(5)	113(3)
C(2)-C(3)-C(5)	111(3)
C(6)-C(5)-N(3)	85(7)
C(6)-C(5)-C(3)	116(6)
N(3)-C(5)-C(3)	114(3)
C(5)-C(6)-O(1)	138(10)
C(5)-C(6)-N(3)	59(6)
O(1)-C(6)-N(3)	85(5)
C(5)-C(6)-C(7)	101(9)
O(1)-C(6)-C(7)	42(3)
N(3)-C(6)-C(7)	44(3)
O(1)-C(7)-N(3)	121(3)
O(1)-C(7)-C(8)	120(3)
N(3)-C(7)-C(8)	119(4)
O(1)-C(7)-C(6)	56(4)
N(3)-C(7)-C(6)	67(4)
C(8)-C(7)-C(6)	174(5)
C(9)-C(8)-N(2)	113(3)
C(9)-C(8)-C(7)	135(4)
N(2)-C(8)-C(7)	112(3)
C(8)-C(9)-C(10)	127(4)
C(11)-C(10)-C(9)	116(3)
C(10)-C(11)-C(12)	121(3)
N(2)-C(12)-C(13)	116(3)
N(2)-C(12)-C(11)	112(3)
C(13)-C(12)-C(11)	131(3)
N(1)-C(13)-C(12)	122(3)
N(1)-C(13)-O(99)	120(4)
C(12)-C(13)-O(99)	118(3)

C(16)-C(15)-N(1)	107(3)
C(16)-C(15)-C(99)	112(4)
N(1)-C(15)-C(99)	103(3)
C(15)-C(16)-C(17)	120(4)
C(15)-C(16)-C(18)	107(4)
C(17)-C(16)-C(18)	103(4)
C(19)-C(18)-C(16)	119(5)
C(23)-C(21)-C(22)	115(3)
C(21)-C(23)-N(6)	122(4)
C(21)-C(23)-C(24)	121(3)
N(6)-C(23)-C(24)	99(3)
O(3)-C(24)-C(23)	104(3)
N(6)-C(25)-O(3)	122(3)
N(6)-C(25)-C(26)	119(3)
O(3)-C(25)-C(26)	120(3)
N(5)-C(26)-C(27)	124(3)
N(5)-C(26)-C(25)	109(3)
C(27)-C(26)-C(25)	126(3)
C(26)-C(27)-C(28)	120(3)
C(29)-C(28)-C(27)	116(4)
C(28)-C(29)-C(30)	120(4)
N(5)-C(30)-C(31)	115(3)
N(5)-C(30)-C(29)	118(3)
C(31)-C(30)-C(29)	127(3)
N(4)-C(31)-O(4)	117(3)
N(4)-C(31)-C(30)	122(3)
O(4)-C(31)-C(30)	119(3)
O(4)-C(32)-C(33)	108(3)
N(4)-C(33)-C(34)	120(3)
N(4)-C(33)-C(32)	102(3)
C(34)-C(33)-C(32)	111(3)
C(33)-C(34)-C(35)	105(4)
C(33)-C(34)-C(36)	107(3)

C(35)-C(34)-C(36)	104(3)
C(37)-C(36)-C(34)	124(4)
O(99)-C(99)-C(15)	102(3)

Table 4. Torsion angles [°] for 03268ih0.

C(8)-N(2)-Ni(1)-N(5)	59(15)
C(12)-N(2)-Ni(1)-N(5)	-120(14)
C(8)-N(2)-Ni(1)-N(6)	100(2)
C(12)-N(2)-Ni(1)-N(6)	-79(2)
C(8)-N(2)-Ni(1)-N(1)	-179(2)
C(12)-N(2)-Ni(1)-N(1)	2.0(19)
C(8)-N(2)-Ni(1)-N(3)	-1.2(19)
C(12)-N(2)-Ni(1)-N(3)	180(2)
C(8)-N(2)-Ni(1)-N(4)	-79(2)
C(12)-N(2)-Ni(1)-N(4)	102(2)
C(26)-N(5)-Ni(1)-N(2)	47(16)
C(30)-N(5)-Ni(1)-N(2)	-141(13)
C(26)-N(5)-Ni(1)-N(6)	5(3)
C(30)-N(5)-Ni(1)-N(6)	177(3)
C(26)-N(5)-Ni(1)-N(1)	-74(3)
C(30)-N(5)-Ni(1)-N(1)	98(3)
C(26)-N(5)-Ni(1)-N(3)	106(3)
C(30)-N(5)-Ni(1)-N(3)	-82(3)
C(26)-N(5)-Ni(1)-N(4)	-174(4)
C(30)-N(5)-Ni(1)-N(4)	-2(3)
C(25)-N(6)-Ni(1)-N(2)	177(3)
C(23)-N(6)-Ni(1)-N(2)	9(4)
C(25)-N(6)-Ni(1)-N(5)	-6(3)
C(23)-N(6)-Ni(1)-N(5)	-175(4)
C(25)-N(6)-Ni(1)-N(1)	102(3)
C(23)-N(6)-Ni(1)-N(1)	-66(4)
C(25)-N(6)-Ni(1)-N(3)	-103(3)
C(23)-N(6)-Ni(1)-N(3)	88(4)
C(25)-N(6)-Ni(1)-N(4)	-4(5)
C(23)-N(6)-Ni(1)-N(4)	-173(3)
C(13)-N(1)-Ni(1)-N(2)	-2(2)

C(15)-N(1)-Ni(1)-N(2)	-164(3)
C(13)-N(1)-Ni(1)-N(5)	173(2)
C(15)-N(1)-Ni(1)-N(5)	12(3)
C(13)-N(1)-Ni(1)-N(6)	101(2)
C(15)-N(1)-Ni(1)-N(6)	-61(3)
C(13)-N(1)-Ni(1)-N(3)	-7(3)
C(15)-N(1)-Ni(1)-N(3)	-168(2)
C(13)-N(1)-Ni(1)-N(4)	-108(2)
C(15)-N(1)-Ni(1)-N(4)	91(3)
C(7)-N(3)-Ni(1)-N(2)	0(2)
C(5)-N(3)-Ni(1)-N(2)	-169(3)
C(6)-N(3)-Ni(1)-N(2)	157(49)
C(7)-N(3)-Ni(1)-N(5)	-176(2)
C(5)-N(3)-Ni(1)-N(5)	15(3)
C(6)-N(3)-Ni(1)-N(5)	-19(49)
C(7)-N(3)-Ni(1)-N(6)	-99(2)
C(5)-N(3)-Ni(1)-N(6)	92(3)
C(6)-N(3)-Ni(1)-N(6)	58(48)
C(7)-N(3)-Ni(1)-N(1)	4(3)
C(5)-N(3)-Ni(1)-N(1)	-165(2)
C(6)-N(3)-Ni(1)-N(1)	161(48)
C(7)-N(3)-Ni(1)-N(4)	110(2)
C(5)-N(3)-Ni(1)-N(4)	-59(3)
C(6)-N(3)-Ni(1)-N(4)	-93(49)
C(31)-N(4)-Ni(1)-N(2)	170(3)
C(33)-N(4)-Ni(1)-N(2)	9(5)
C(31)-N(4)-Ni(1)-N(5)	-7(3)
C(33)-N(4)-Ni(1)-N(5)	-168(5)
C(31)-N(4)-Ni(1)-N(6)	-9(5)
C(33)-N(4)-Ni(1)-N(6)	-170(4)
C(31)-N(4)-Ni(1)-N(1)	-110(3)
C(33)-N(4)-Ni(1)-N(1)	89(5)
C(31)-N(4)-Ni(1)-N(3)	96(3)

C(33)-N(4)-Ni(1)-N(3)	-65(5)
C(1)-C(2)-C(3)-C(4)	168(4)
C(1)-C(2)-C(3)-C(5)	-53(5)
C(7)-N(3)-C(5)-C(6)	14(6)
Ni(1)-N(3)-C(5)-C(6)	-176(5)
C(7)-N(3)-C(5)-C(3)	130(3)
C(6)-N(3)-C(5)-C(3)	116(6)
Ni(1)-N(3)-C(5)-C(3)	-60(4)
C(4)-C(3)-C(5)-C(6)	58(9)
C(2)-C(3)-C(5)-C(6)	-86(8)
C(4)-C(3)-C(5)-N(3)	-38(5)
C(2)-C(3)-C(5)-N(3)	178(3)
N(3)-C(5)-C(6)-O(1)	-34(12)
C(3)-C(5)-C(6)-O(1)	-148(10)
C(3)-C(5)-C(6)-N(3)	-114(4)
N(3)-C(5)-C(6)-C(7)	-10(4)
C(3)-C(5)-C(6)-C(7)	-124(5)
C(7)-O(1)-C(6)-C(5)	37(13)
C(7)-O(1)-C(6)-N(3)	8(3)
C(7)-N(3)-C(6)-C(5)	-165(6)
Ni(1)-N(3)-C(6)-C(5)	37(51)
C(7)-N(3)-C(6)-O(1)	-8(3)
C(5)-N(3)-C(6)-O(1)	158(8)
Ni(1)-N(3)-C(6)-O(1)	-165(45)
C(5)-N(3)-C(6)-C(7)	165(6)
Ni(1)-N(3)-C(6)-C(7)	-158(48)
C(6)-O(1)-C(7)-N(3)	-13(5)
C(6)-O(1)-C(7)-C(8)	175(5)
C(5)-N(3)-C(7)-O(1)	2(4)
C(6)-N(3)-C(7)-O(1)	11(4)
Ni(1)-N(3)-C(7)-O(1)	-170(3)
C(5)-N(3)-C(7)-C(8)	175(2)
C(6)-N(3)-C(7)-C(8)	-177(4)

Ni(1)-N(3)-C(7)-C(8)	2(3)
C(5)-N(3)-C(7)-C(6)	-9(4)
Ni(1)-N(3)-C(7)-C(6)	178(4)
C(5)-C(6)-C(7)-O(1)	-155(8)
N(3)-C(6)-C(7)-O(1)	-168(5)
C(5)-C(6)-C(7)-N(3)	13(5)
O(1)-C(6)-C(7)-N(3)	168(5)
C(5)-C(6)-C(7)-C(8)	163(33)
O(1)-C(6)-C(7)-C(8)	-41(39)
N(3)-C(6)-C(7)-C(8)	150(37)
C(12)-N(2)-C(8)-C(9)	0(4)
Ni(1)-N(2)-C(8)-C(9)	-178(2)
C(12)-N(2)-C(8)-C(7)	-179(3)
Ni(1)-N(2)-C(8)-C(7)	2(3)
O(1)-C(7)-C(8)-C(9)	-10(5)
N(3)-C(7)-C(8)-C(9)	178(3)
C(6)-C(7)-C(8)-C(9)	29(39)
O(1)-C(7)-C(8)-N(2)	170(3)
N(3)-C(7)-C(8)-N(2)	-3(4)
C(6)-C(7)-C(8)-N(2)	-152(37)
N(2)-C(8)-C(9)-C(10)	-3(4)
C(7)-C(8)-C(9)-C(10)	176(3)
C(8)-C(9)-C(10)-C(11)	-1(5)
C(9)-C(10)-C(11)-C(12)	8(4)
C(8)-N(2)-C(12)-C(13)	179(3)
Ni(1)-N(2)-C(12)-C(13)	-2(3)
C(8)-N(2)-C(12)-C(11)	6(4)
Ni(1)-N(2)-C(12)-C(11)	-175.5(18)
C(10)-C(11)-C(12)-N(2)	-10(4)
C(10)-C(11)-C(12)-C(13)	178(3)
C(15)-N(1)-C(13)-C(12)	168(3)
Ni(1)-N(1)-C(13)-C(12)	2(4)
C(15)-N(1)-C(13)-O(99)	-6(4)

Ni(1)-N(1)-C(13)-O(99)	-173(2)
N(2)-C(12)-C(13)-N(1)	0(4)
C(11)-C(12)-C(13)-N(1)	172(3)
N(2)-C(12)-C(13)-O(99)	175(2)
C(11)-C(12)-C(13)-O(99)	-13(5)
C(99)-O(99)-C(13)-N(1)	-5(4)
C(99)-O(99)-C(13)-C(12)	-180(3)
C(13)-N(1)-C(15)-C(16)	132(3)
Ni(1)-N(1)-C(15)-C(16)	-66(4)
C(13)-N(1)-C(15)-C(99)	14(3)
Ni(1)-N(1)-C(15)-C(99)	176(2)
N(1)-C(15)-C(16)-C(17)	-59(5)
C(99)-C(15)-C(16)-C(17)	54(6)
N(1)-C(15)-C(16)-C(18)	-176(3)
C(99)-C(15)-C(16)-C(18)	-63(4)
C(15)-C(16)-C(18)-C(19)	-55(5)
C(17)-C(16)-C(18)-C(19)	178(4)
C(22)-C(21)-C(23)-N(6)	-79(4)
C(22)-C(21)-C(23)-C(24)	46(5)
C(25)-N(6)-C(23)-C(21)	128(4)
Ni(1)-N(6)-C(23)-C(21)	-62(5)
C(25)-N(6)-C(23)-C(24)	-7(4)
Ni(1)-N(6)-C(23)-C(24)	162(3)
C(25)-O(3)-C(24)-C(23)	-8(4)
C(21)-C(23)-C(24)-O(3)	-127(4)
N(6)-C(23)-C(24)-O(3)	9(4)
C(23)-N(6)-C(25)-O(3)	3(5)
Ni(1)-N(6)-C(25)-O(3)	-168(3)
C(23)-N(6)-C(25)-C(26)	178(3)
Ni(1)-N(6)-C(25)-C(26)	7(5)
C(24)-O(3)-C(25)-N(6)	4(5)
C(24)-O(3)-C(25)-C(26)	-171(4)
C(30)-N(5)-C(26)-C(27)	17(7)

Ni(1)-N(5)-C(26)-C(27)	-171(4)
C(30)-N(5)-C(26)-C(25)	-175(3)
Ni(1)-N(5)-C(26)-C(25)	-3(5)
N(6)-C(25)-C(26)-N(5)	-3(6)
O(3)-C(25)-C(26)-N(5)	173(4)
N(6)-C(25)-C(26)-C(27)	165(4)
O(3)-C(25)-C(26)-C(27)	-20(7)
N(5)-C(26)-C(27)-C(28)	-13(7)
C(25)-C(26)-C(27)-C(28)	-179(5)
C(26)-C(27)-C(28)-C(29)	2(7)
C(27)-C(28)-C(29)-C(30)	5(8)
C(26)-N(5)-C(30)-C(31)	-179(4)
Ni(1)-N(5)-C(30)-C(31)	9(4)
C(26)-N(5)-C(30)-C(29)	-8(6)
Ni(1)-N(5)-C(30)-C(29)	179(3)
C(28)-C(29)-C(30)-N(5)	-2(7)
C(28)-C(29)-C(30)-C(31)	167(5)
C(33)-N(4)-C(31)-O(4)	-10(5)
Ni(1)-N(4)-C(31)-O(4)	-178(3)
C(33)-N(4)-C(31)-C(30)	-177(4)
Ni(1)-N(4)-C(31)-C(30)	14(5)
C(32)-O(4)-C(31)-N(4)	6(6)
C(32)-O(4)-C(31)-C(30)	174(4)
N(5)-C(30)-C(31)-N(4)	-17(6)
C(29)-C(30)-C(31)-N(4)	174(4)
N(5)-C(30)-C(31)-O(4)	176(4)
C(29)-C(30)-C(31)-O(4)	7(6)
C(31)-O(4)-C(32)-C(33)	0(5)
C(31)-N(4)-C(33)-C(34)	131(4)
Ni(1)-N(4)-C(33)-C(34)	-68(6)
C(31)-N(4)-C(33)-C(32)	8(5)
Ni(1)-N(4)-C(33)-C(32)	169(3)
O(4)-C(32)-C(33)-N(4)	-5(5)

O(4)-C(32)-C(33)-C(34)	-133(4)
N(4)-C(33)-C(34)-C(35)	-176(4)
C(32)-C(33)-C(34)-C(35)	-58(5)
N(4)-C(33)-C(34)-C(36)	73(5)
C(32)-C(33)-C(34)-C(36)	-169(3)
C(33)-C(34)-C(36)-C(37)	56(5)
C(35)-C(34)-C(36)-C(37)	-56(5)
C(13)-O(99)-C(99)-C(15)	13(3)
C(16)-C(15)-C(99)-O(99)	-131(3)
N(1)-C(15)-C(99)-O(99)	-16(3)

03295IHm (Figure 5.7)

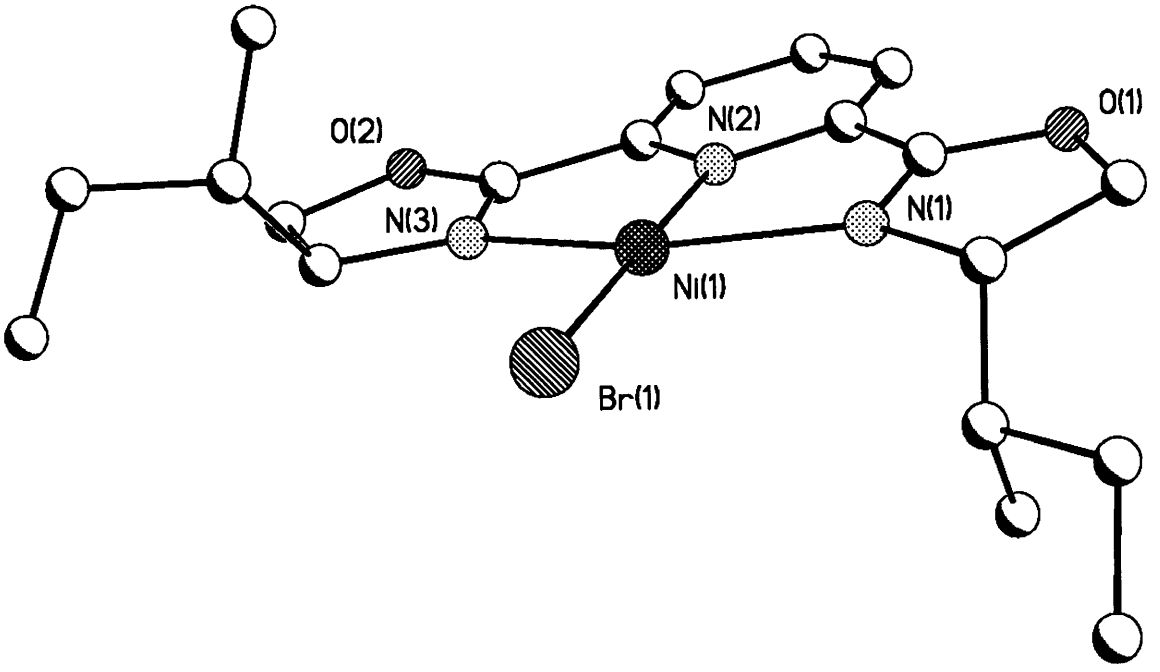

Table 1. Crystal data and structure refinement for 03295IHm.

Identification code	03295ihm	
Empirical formula	C25 H36 Br N3 Ni O2	
Formula weight	549.19	
Temperature	193(2) K	
Wavelength	0.71073 Å	
Crystal system	Monoclinic	
Unit cell dimensions	a = 5.9711(8) Å	α = 90°.
	b = 18.288(2) Å	β= 98.055(3)°.
	c = 11.7389(16) Å	γ = 90°.
Volume	1269.3(3) $Å^3$	
Z	2	
Density (calculated)	1.437 Mg/m^3	
Absorption coefficient	2.364 mm^{-1}	
F(000)	572	
Theta range for data collection	1.75 to 23.30°.	
Index ranges	-4<=h<=6, -17<=k<=20, -12<=l<=13	
Reflections collected	5847	
Independent reflections	3253 [R(int) = 0.0752]	
Completeness to theta = 23.30°	99.7 %	
Refinement method	Full-matrix least-squares on F^2	
Data / restraints / parameters	3253 / 1 / 121	
Goodness-of-fit on F^2	1.525	
Final R indices [I>2sigma(I)]	R1 = 0.1411, wR2 = 0.3551	
R indices (all data)	R1 = 0.1566, wR2 = 0.3696	
Absolute structure parameter	0.00	
Largest diff. peak and hole	4.150 and -2.352 $e.Å^{-3}$	

Table 2. Atomic coordinates (x 10^4) and equivalent isotropic displacement parameters ($Å^2$x 10^3) for 03295IHm. U(eq) is defined as one third of the trace of the orthogonalized U^{ij} tensor.

	x	y	z	U(eq)
Br(1)	7200(4)	7403(1)	8982(2)	49(1)
Ni(1)	7479(4)	8641(1)	9553(2)	30(1)
N(2)	7630(30)	9632(11)	10018(16)	41(4)
N(1)	4990(20)	8700(11)	10678(13)	30(3)
C(2)	4540(30)	7597(12)	11794(17)	34(5)
O(1)	3160(30)	9467(9)	11689(14)	48(4)
C(4)	3390(30)	8217(13)	11184(18)	35(5)
O(2)	12090(30)	10044(9)	8338(14)	51(4)
C(7)	6150(30)	9911(12)	10671(17)	33(4)
N(3)	10110(30)	9024(10)	8682(15)	37(4)
C(14)	11550(40)	8780(13)	7853(19)	42(5)
C(9)	7800(40)	11093(17)	10680(20)	57(7)
C(6)	4750(30)	9364(13)	10994(17)	36(5)
C(12)	10430(30)	9692(11)	8853(16)	29(5)
C(11)	9160(30)	10139(11)	9692(16)	28(4)
C(8)	6220(40)	10616(14)	11020(20)	46(6)
C(3)	2700(40)	7107(14)	12240(20)	46(6)
C(15)	10160(50)	8494(18)	6690(20)	67(8)
C(13)	12980(40)	9467(15)	7660(20)	52(6)
C(5)	2060(40)	8770(14)	11834(19)	44(6)
C(10)	9380(40)	10868(14)	10020(20)	48(6)
C(1)	6320(50)	7845(17)	12810(30)	71(8)
C(16)	8480(50)	9001(19)	6150(30)	73(8)
C(98)	3620(70)	6390(20)	12720(30)	90(11)
C(99)	11340(70)	8260(20)	5710(30)	94(11)
C(78)	12880(120)	7690(50)	6100(70)	210(30)

C(83)	2190(60)	-60(20)	4330(30)	87(10)
C(84)	3960(90)	400(30)	4390(40)	130(16)
C(82)	280(100)	250(30)	3720(50)	139(16)
C(85)	2060(120)	1080(50)	3550(70)	220(30)

Table 3. Bond lengths [Å] and angles [°] for 03295IHm.

Br(1)-Ni(1)	2.361(3)
Ni(1)-N(2)	1.890(19)
Ni(1)-N(1)	2.125(15)
Ni(1)-N(3)	2.109(18)
N(2)-C(7)	1.35(3)
N(2)-C(11)	1.39(3)
N(1)-C(6)	1.28(3)
N(1)-C(4)	1.49(3)
C(2)-C(4)	1.46(3)
C(2)-C(3)	1.56(3)
C(2)-C(1)	1.55(4)
O(1)-C(6)	1.35(3)
O(1)-C(5)	1.45(3)
C(4)-C(5)	1.55(3)
O(2)-C(12)	1.39(3)
O(2)-C(13)	1.46(3)
C(7)-C(8)	1.35(3)
C(7)-C(6)	1.39(3)
N(3)-C(12)	1.25(3)
N(3)-C(14)	1.46(3)
C(14)-C(13)	1.55(3)
C(14)-C(15)	1.58(4)
C(9)-C(10)	1.37(4)
C(9)-C(8)	1.38(4)
C(12)-C(11)	1.55(3)
C(11)-C(10)	1.39(3)
C(3)-C(98)	1.50(5)
C(15)-C(16)	1.45(4)
C(15)-C(99)	1.50(5)
C(99)-C(78)	1.42(8)
C(83)-C(84)	1.34(6)

C(83)-C(82)	1.39(6)
C(84)-C(85)	1.87(9)
C(82)-C(85)	1.87(9)

N(2)-Ni(1)-N(1)	77.3(8)
N(2)-Ni(1)-N(3)	79.3(8)
N(1)-Ni(1)-N(3)	156.6(7)
N(2)-Ni(1)-Br(1)	178.6(6)
N(1)-Ni(1)-Br(1)	101.4(5)
N(3)-Ni(1)-Br(1)	102.0(5)
C(7)-N(2)-C(11)	114.3(18)
C(7)-N(2)-Ni(1)	121.3(15)
C(11)-N(2)-Ni(1)	124.4(15)
C(6)-N(1)-C(4)	110.0(17)
C(6)-N(1)-Ni(1)	110.1(14)
C(4)-N(1)-Ni(1)	139.8(15)
C(4)-C(2)-C(3)	107.6(17)
C(4)-C(2)-C(1)	112(2)
C(3)-C(2)-C(1)	110.4(19)
C(6)-O(1)-C(5)	108.4(17)
C(2)-C(4)-C(5)	120.3(19)
C(2)-C(4)-N(1)	111.8(17)
C(5)-C(4)-N(1)	102.1(18)
C(12)-O(2)-C(13)	103.8(17)
C(8)-C(7)-C(6)	127(2)
C(8)-C(7)-N(2)	123(2)
C(6)-C(7)-N(2)	110(2)
C(12)-N(3)-C(14)	108.4(19)
C(12)-N(3)-Ni(1)	110.7(15)
C(14)-N(3)-Ni(1)	140.5(16)
N(3)-C(14)-C(13)	103.8(19)
N(3)-C(14)-C(15)	112.9(19)
C(13)-C(14)-C(15)	112.0(19)

C(10)-C(9)-C(8)	122(3)
N(1)-C(6)-O(1)	115.1(19)
N(1)-C(6)-C(7)	120(2)
O(1)-C(6)-C(7)	124(2)
N(3)-C(12)-O(2)	119.0(19)
N(3)-C(12)-C(11)	122.7(19)
O(2)-C(12)-C(11)	118.2(17)
C(10)-C(11)-N(2)	127(2)
C(10)-C(11)-C(12)	130(2)
N(2)-C(11)-C(12)	102.7(16)
C(7)-C(8)-C(9)	121(2)
C(98)-C(3)-C(2)	113(2)
C(16)-C(15)-C(99)	102(3)
C(16)-C(15)-C(14)	115(3)
C(99)-C(15)-C(14)	121(3)
O(2)-C(13)-C(14)	104.8(19)
O(1)-C(5)-C(4)	104.2(18)
C(9)-C(10)-C(11)	114(2)
C(78)-C(99)-C(15)	108(4)
C(84)-C(83)-C(82)	110(5)
C(83)-C(84)-C(85)	89(4)
C(83)-C(82)-C(85)	87(4)
C(82)-C(85)-C(84)	74(4)

Table 4. Torsion angles [°] for 03295IHm.

N(1)-Ni(1)-N(2)-C(7)	-5.7(15)
N(3)-Ni(1)-N(2)-C(7)	176.0(17)
Br(1)-Ni(1)-N(2)-C(7)	20(25)
N(1)-Ni(1)-N(2)-C(11)	176.9(18)
N(3)-Ni(1)-N(2)-C(11)	-1.4(16)
Br(1)-Ni(1)-N(2)-C(11)	-158(23)
N(2)-Ni(1)-N(1)-C(6)	5.5(13)
N(3)-Ni(1)-N(1)-C(6)	10(2)
Br(1)-Ni(1)-N(1)-C(6)	-173.9(12)
N(2)-Ni(1)-N(1)-C(4)	-177.0(19)
N(3)-Ni(1)-N(1)-C(4)	-172.8(18)
Br(1)-Ni(1)-N(1)-C(4)	3.6(18)
C(3)-C(2)-C(4)-C(5)	63(3)
C(1)-C(2)-C(4)-C(5)	-59(3)
C(3)-C(2)-C(4)-N(1)	-177.3(17)
C(1)-C(2)-C(4)-N(1)	61(3)
C(6)-N(1)-C(4)-C(2)	-127.3(19)
Ni(1)-N(1)-C(4)-C(2)	55(3)
C(6)-N(1)-C(4)-C(5)	3(2)
Ni(1)-N(1)-C(4)-C(5)	-175.0(13)
C(11)-N(2)-C(7)-C(8)	-3(3)
Ni(1)-N(2)-C(7)-C(8)	179.8(17)
C(11)-N(2)-C(7)-C(6)	-177.6(17)
Ni(1)-N(2)-C(7)-C(6)	5(2)
N(2)-Ni(1)-N(3)-C(12)	-2.1(14)
N(1)-Ni(1)-N(3)-C(12)	-6(2)
Br(1)-Ni(1)-N(3)-C(12)	177.3(13)
N(2)-Ni(1)-N(3)-C(14)	-174(2)
N(1)-Ni(1)-N(3)-C(14)	-178.5(18)
Br(1)-Ni(1)-N(3)-C(14)	5(2)
C(12)-N(3)-C(14)-C(13)	5(2)

Ni(1)-N(3)-C(14)-C(13)	177.4(17)
C(12)-N(3)-C(14)-C(15)	-116(2)
Ni(1)-N(3)-C(14)-C(15)	56(3)
C(4)-N(1)-C(6)-O(1)	0(2)
Ni(1)-N(1)-C(6)-O(1)	178.4(13)
C(4)-N(1)-C(6)-C(7)	176.8(17)
Ni(1)-N(1)-C(6)-C(7)	-5(2)
C(5)-O(1)-C(6)-N(1)	-3(2)
C(5)-O(1)-C(6)-C(7)	-179.5(19)
C(8)-C(7)-C(6)-N(1)	-174(2)
N(2)-C(7)-C(6)-N(1)	1(3)
C(8)-C(7)-C(6)-O(1)	2(3)
N(2)-C(7)-C(6)-O(1)	177.1(18)
C(14)-N(3)-C(12)-O(2)	-5(2)
Ni(1)-N(3)-C(12)-O(2)	-179.6(13)
C(14)-N(3)-C(12)-C(11)	179.9(17)
Ni(1)-N(3)-C(12)-C(11)	5(2)
C(13)-O(2)-C(12)-N(3)	2(2)
C(13)-O(2)-C(12)-C(11)	177.6(16)
C(7)-N(2)-C(11)-C(10)	4(3)
Ni(1)-N(2)-C(11)-C(10)	-178.9(17)
C(7)-N(2)-C(11)-C(12)	-173.8(16)
Ni(1)-N(2)-C(11)-C(12)	4(2)
N(3)-C(12)-C(11)-C(10)	177(2)
O(2)-C(12)-C(11)-C(10)	2(3)
N(3)-C(12)-C(11)-N(2)	-6(2)
O(2)-C(12)-C(11)-N(2)	178.9(17)
C(6)-C(7)-C(8)-C(9)	176(2)
N(2)-C(7)-C(8)-C(9)	2(3)
C(10)-C(9)-C(8)-C(7)	-2(4)
C(4)-C(2)-C(3)-C(98)	171(2)
C(1)-C(2)-C(3)-C(98)	-66(3)
N(3)-C(14)-C(15)-C(16)	53(3)

C(13)-C(14)-C(15)-C(16)	-63(3)
N(3)-C(14)-C(15)-C(99)	177(3)
C(13)-C(14)-C(15)-C(99)	60(4)
C(12)-O(2)-C(13)-C(14)	1(2)
N(3)-C(14)-C(13)-O(2)	-4(2)
C(15)-C(14)-C(13)-O(2)	118(2)
C(6)-O(1)-C(5)-C(4)	4(2)
C(2)-C(4)-C(5)-O(1)	120(2)
N(1)-C(4)-C(5)-O(1)	-4.0(19)
C(8)-C(9)-C(10)-C(11)	2(3)
N(2)-C(11)-C(10)-C(9)	-3(3)
C(12)-C(11)-C(10)-C(9)	173(2)
C(16)-C(15)-C(99)-C(78)	-174(4)
C(14)-C(15)-C(99)-C(78)	58(5)
C(82)-C(83)-C(84)-C(85)	0(5)
C(84)-C(83)-C(82)-C(85)	0(5)
C(83)-C(82)-C(85)-C(84)	0(3)
C(83)-C(84)-C(85)-C(82)	0(4)

Appendix B

Selected ^{1}H NMR Spectra

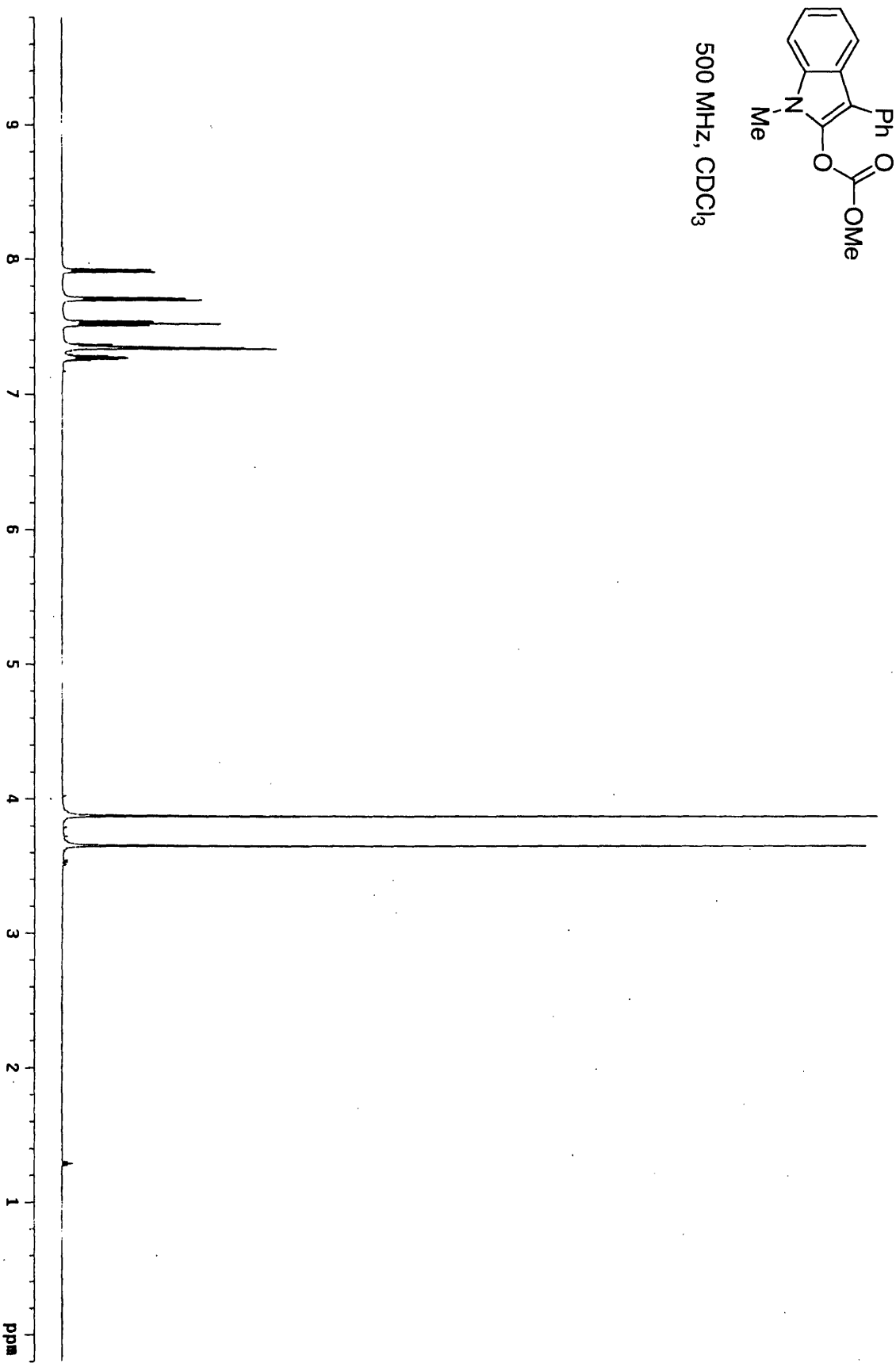
500 MHz, CDCl3
Ph
O
N
Me
O
OMe
9
8
7
6
5
4
3
2
1
ppm

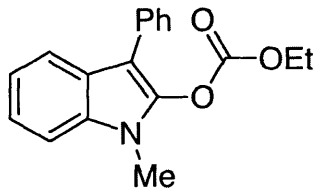

500 MHz, $CDCl_3$

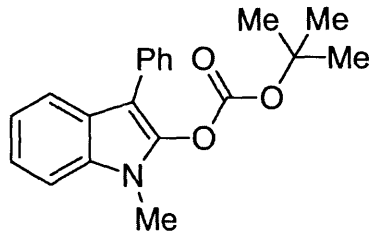

500 MHz, $CDCl_3$

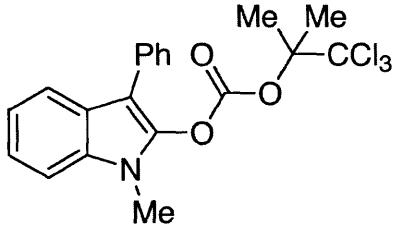

500 MHz, $CDCl_3$

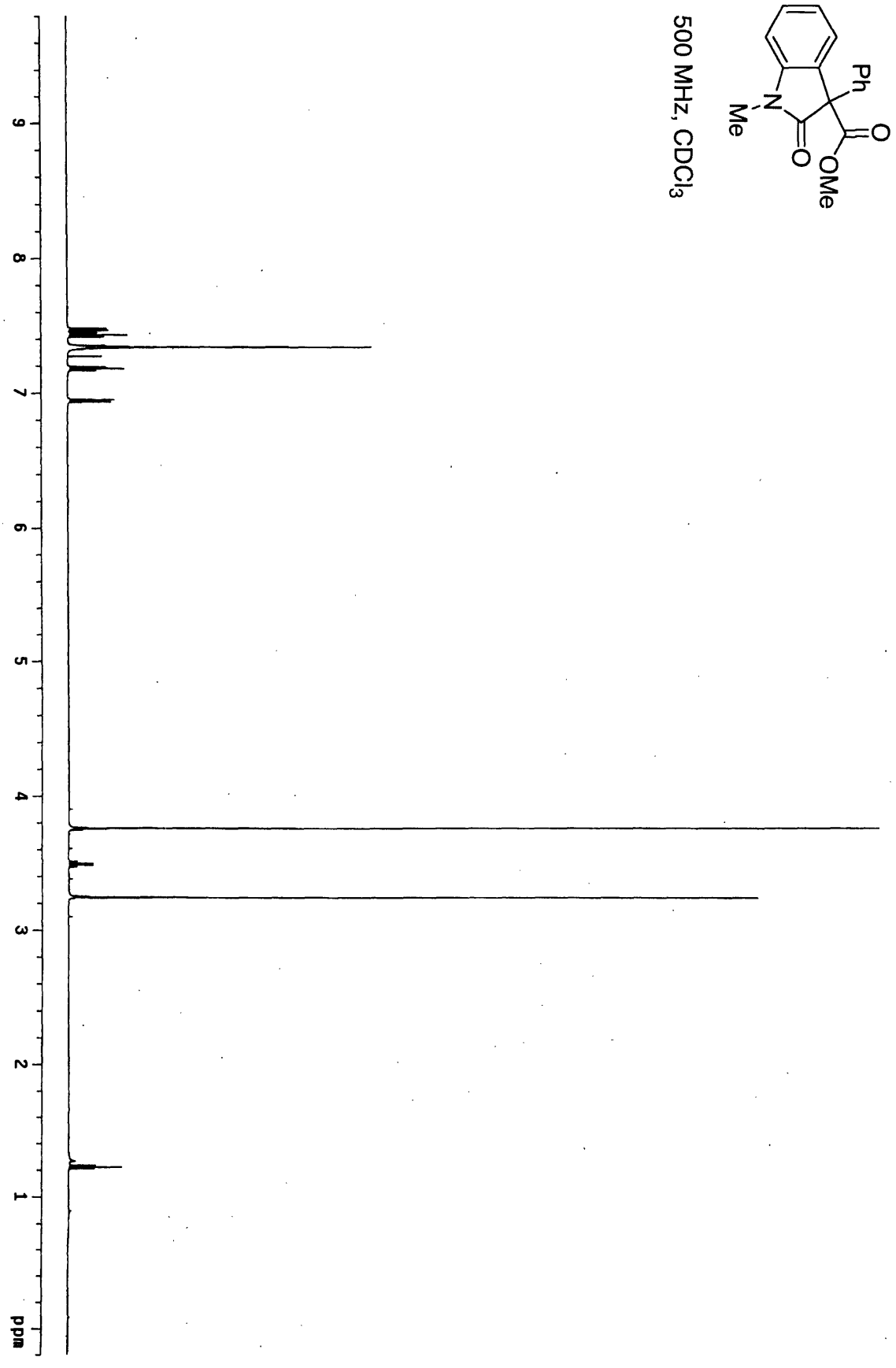
500 MHz, CDCl3
Ph
N
Me
O
O
OMe
9
8
7
6
5
4
3
2
1
ppm

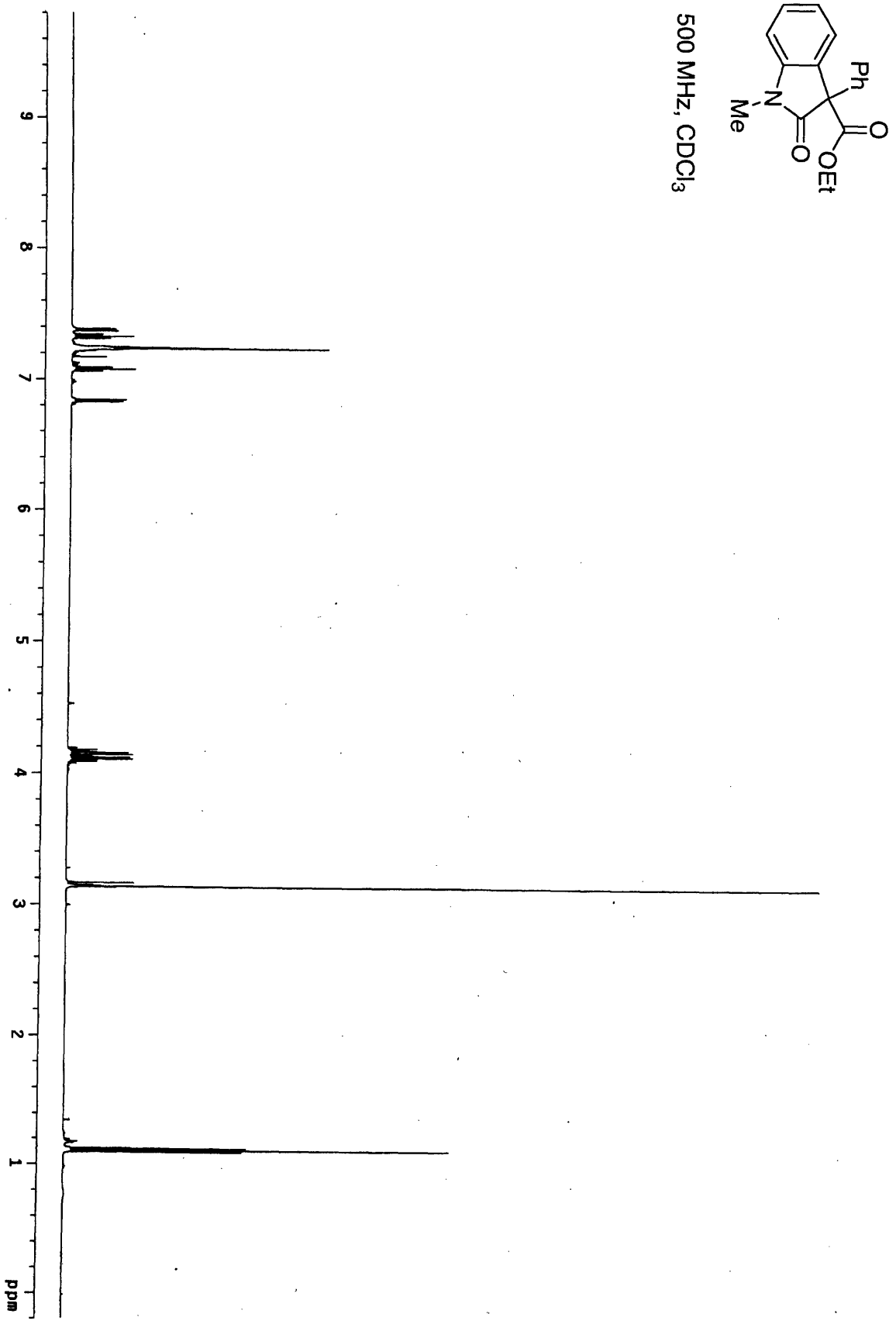
500 MHz, CDCl3
Ph
O
N
Me
O
OEt
9
8
7
6
5
4
3
2
1
ppm

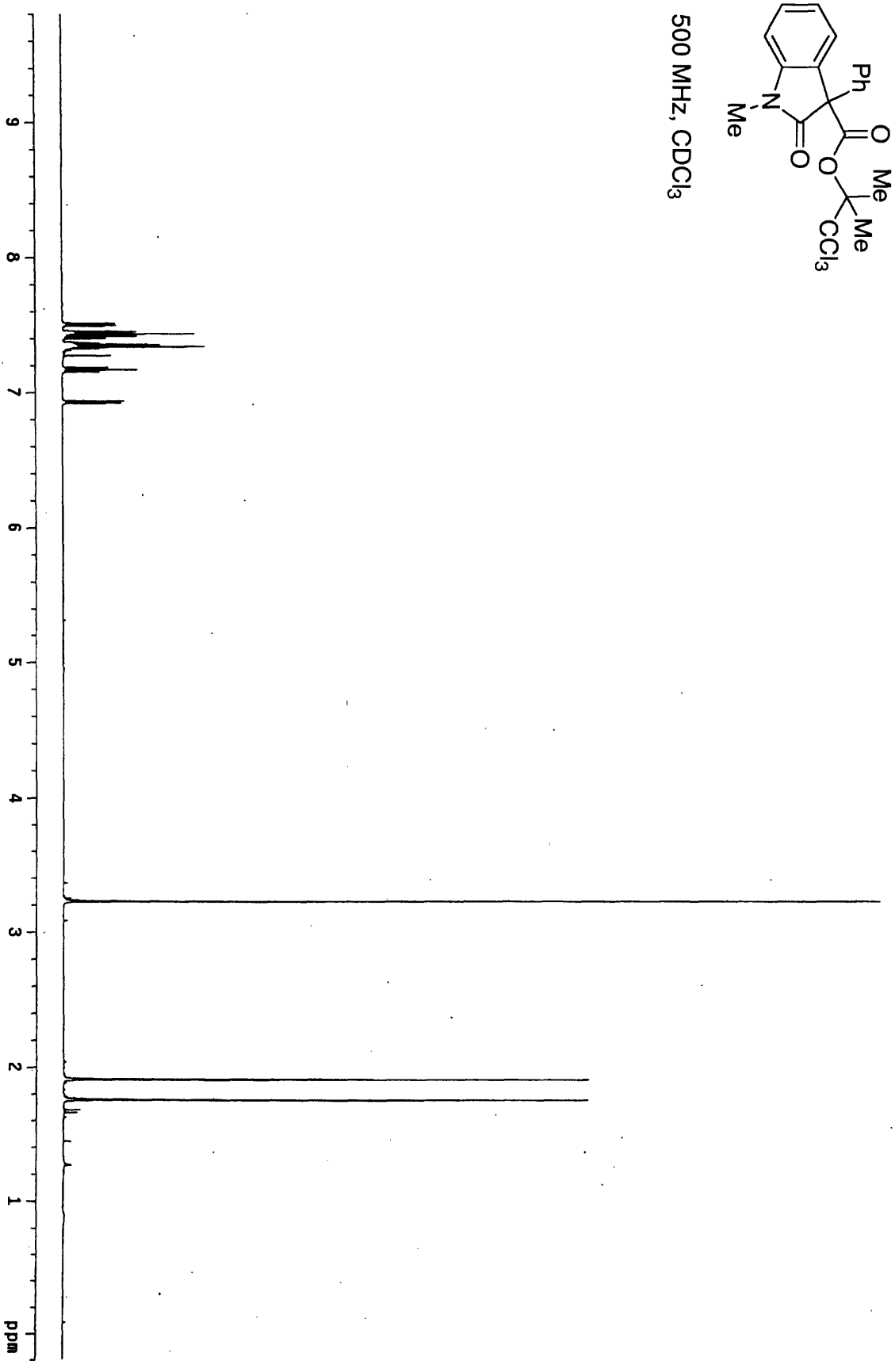
500 MHz, CDCl3
Ph
N
Me
O
O
O
Me
Me
CCl3
9
8
7
6
5
4
3
2
1
ppm

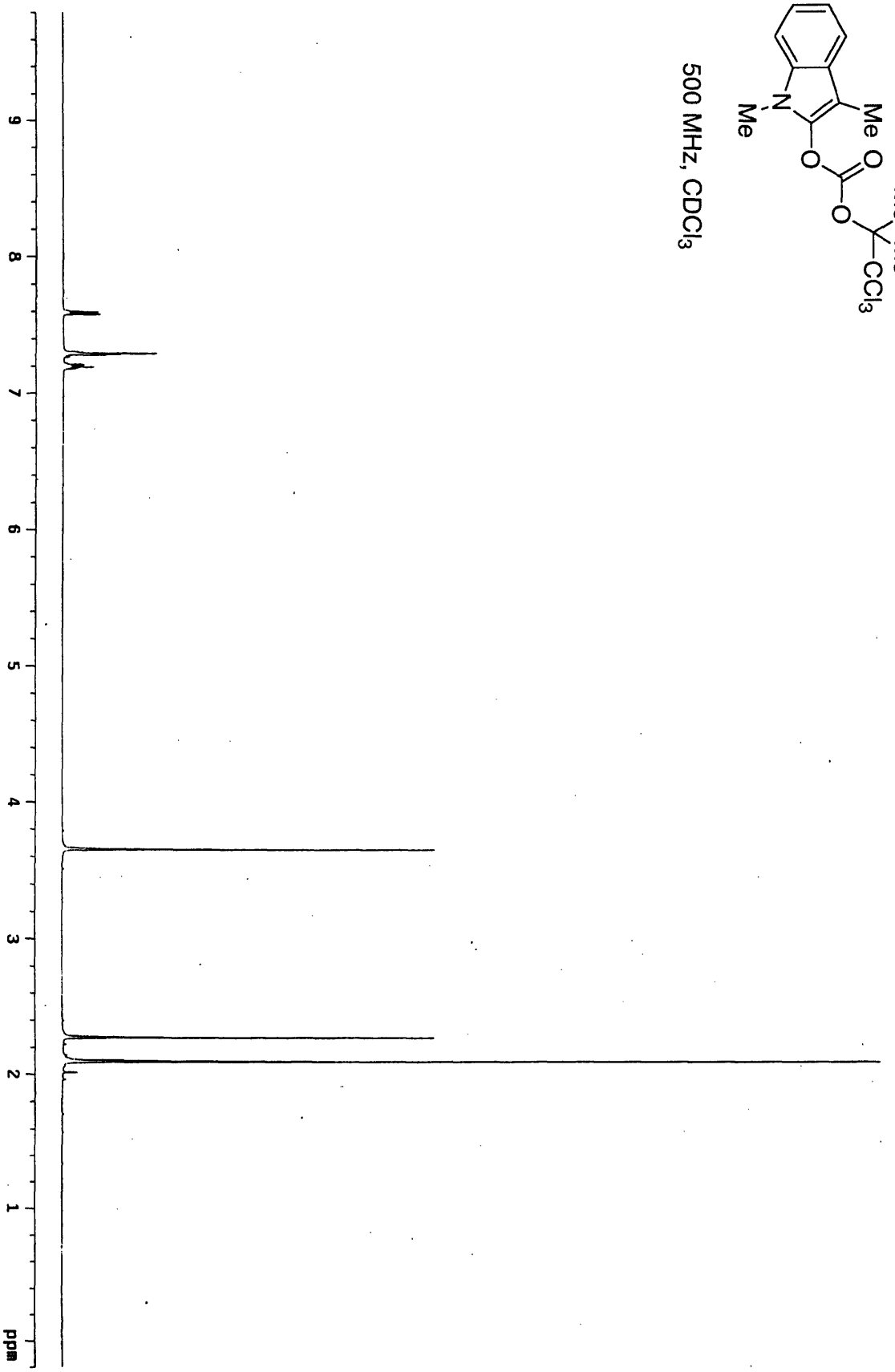
500 MHz, CDCl3
Me
N
Me
O
O
O
Me
Me
CCl3
9
8
7
6
5
4
3
2
1
ppm

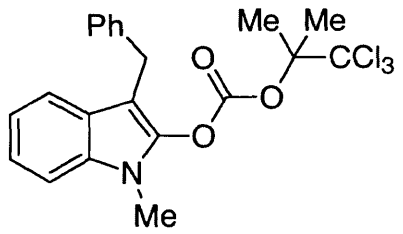

500 MHz, $CDCl_3$

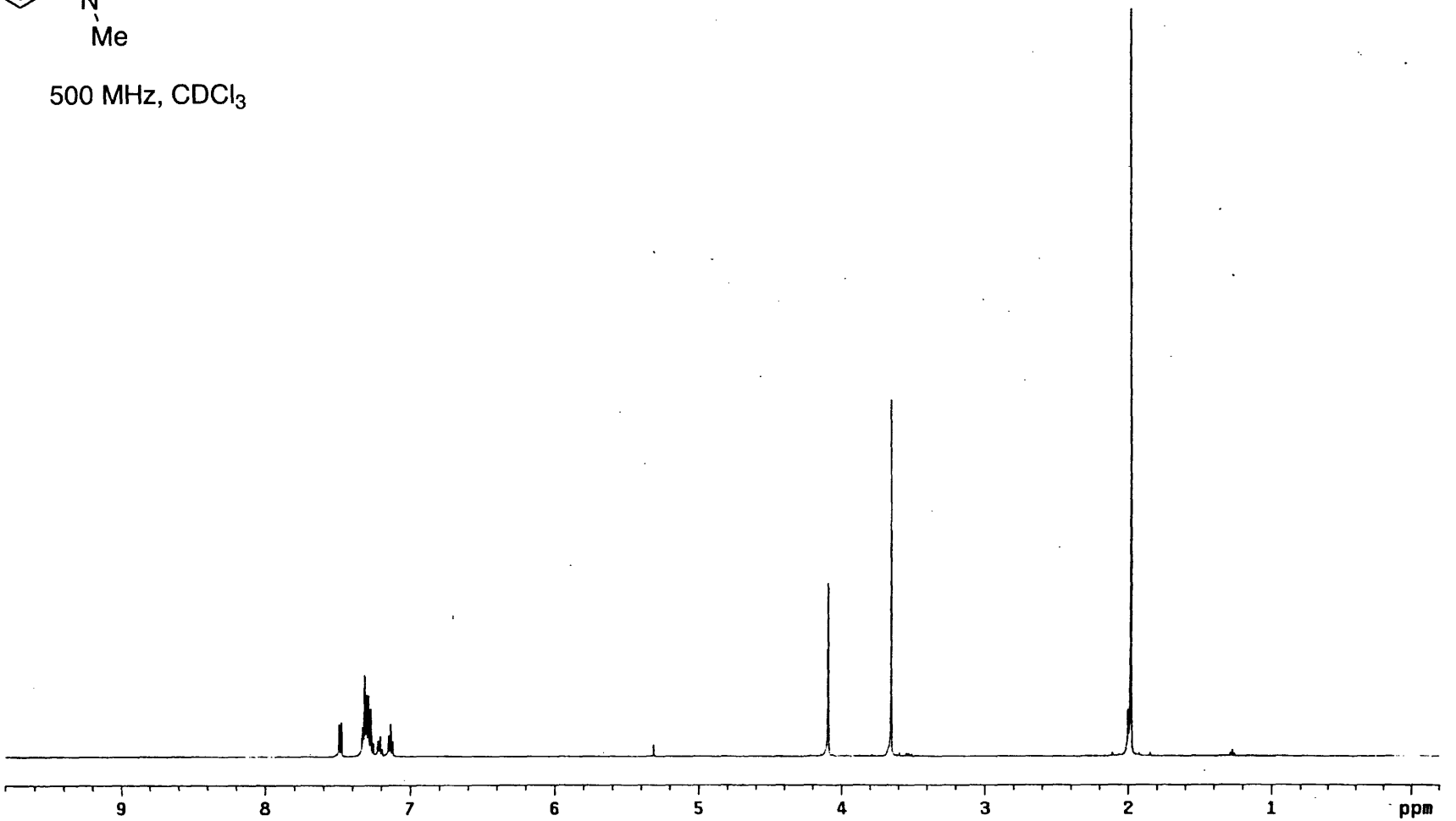

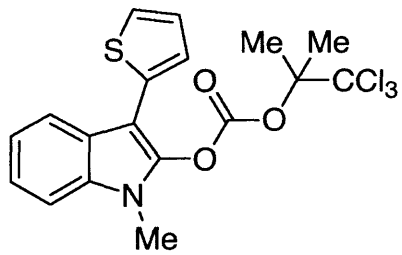

500 MHz, $CDCl_3$

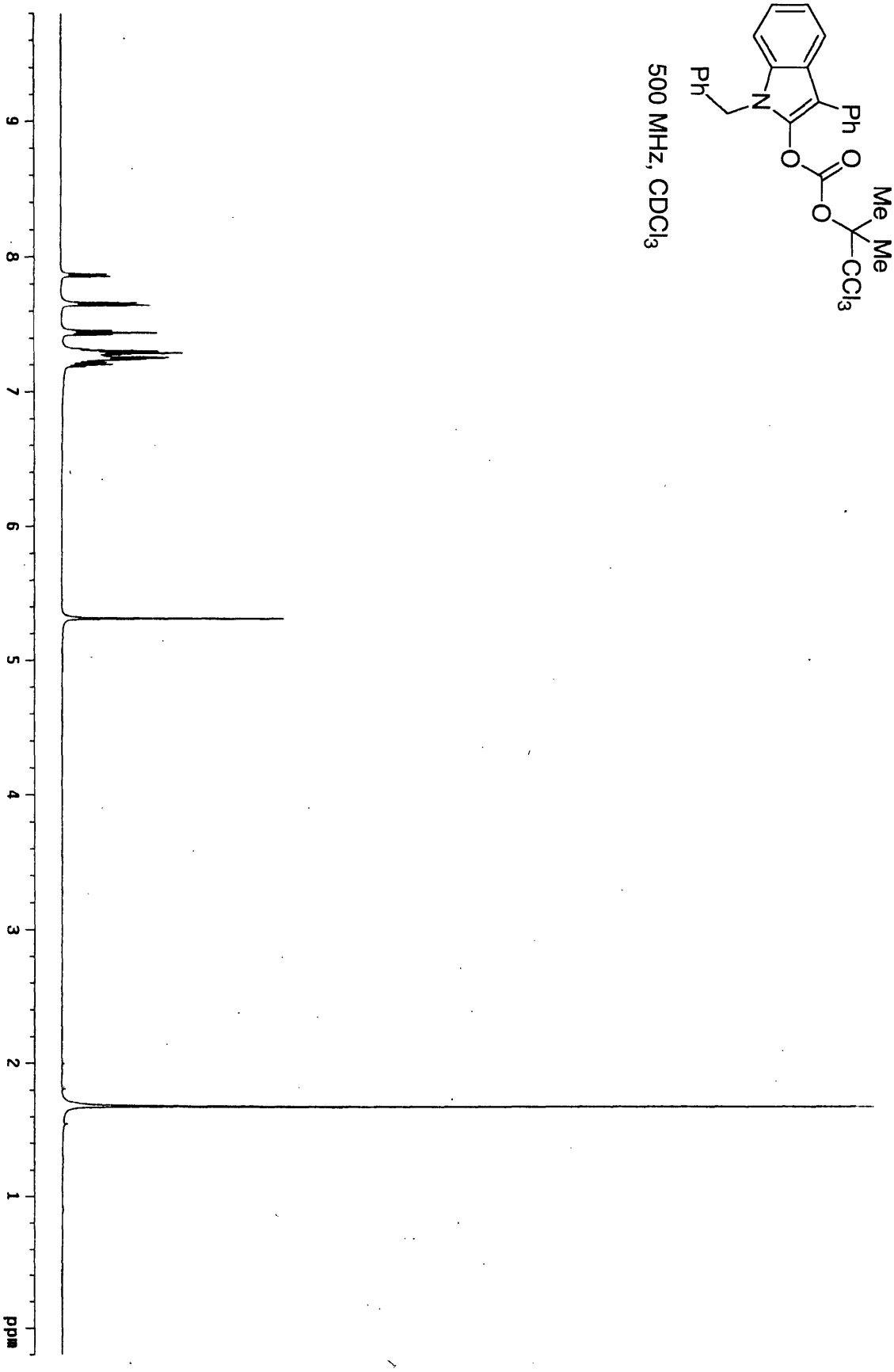
500 MHz, CDCl3
Ph
N
Ph
O
O
O
Me
Me
CCl3
9
8
7
6
5
4
3
2
1
ppm

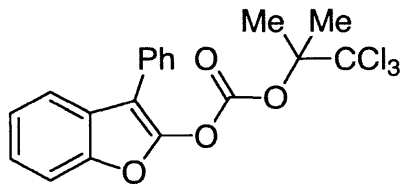

500 MHz, $CDCl_3$

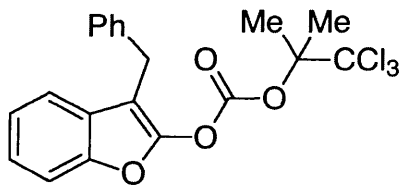

500 MHz, $CDCl_3$

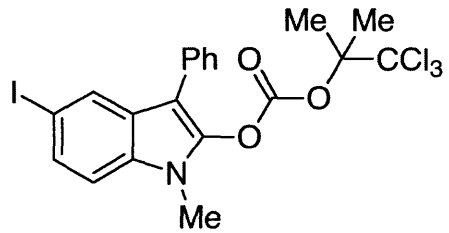

500 MHz, $CDCl_3$

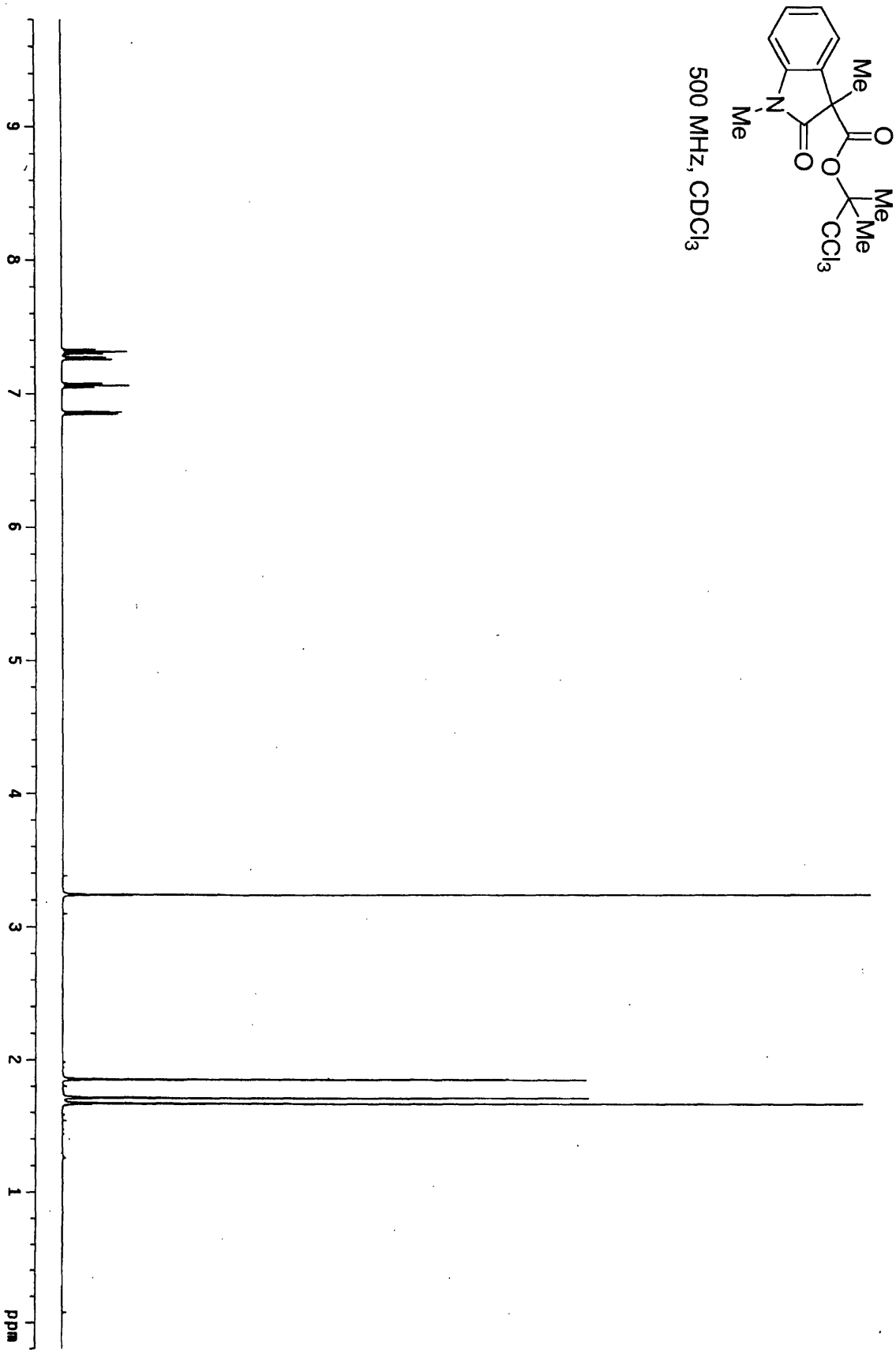
500 MHz, CDCl3
Me
N
Me
O
O
O
Me
Me
CCl3
9
8
7
6
5
4
3
2
1
ppm

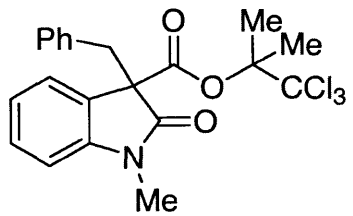

500 MHz, $CDCl_3$

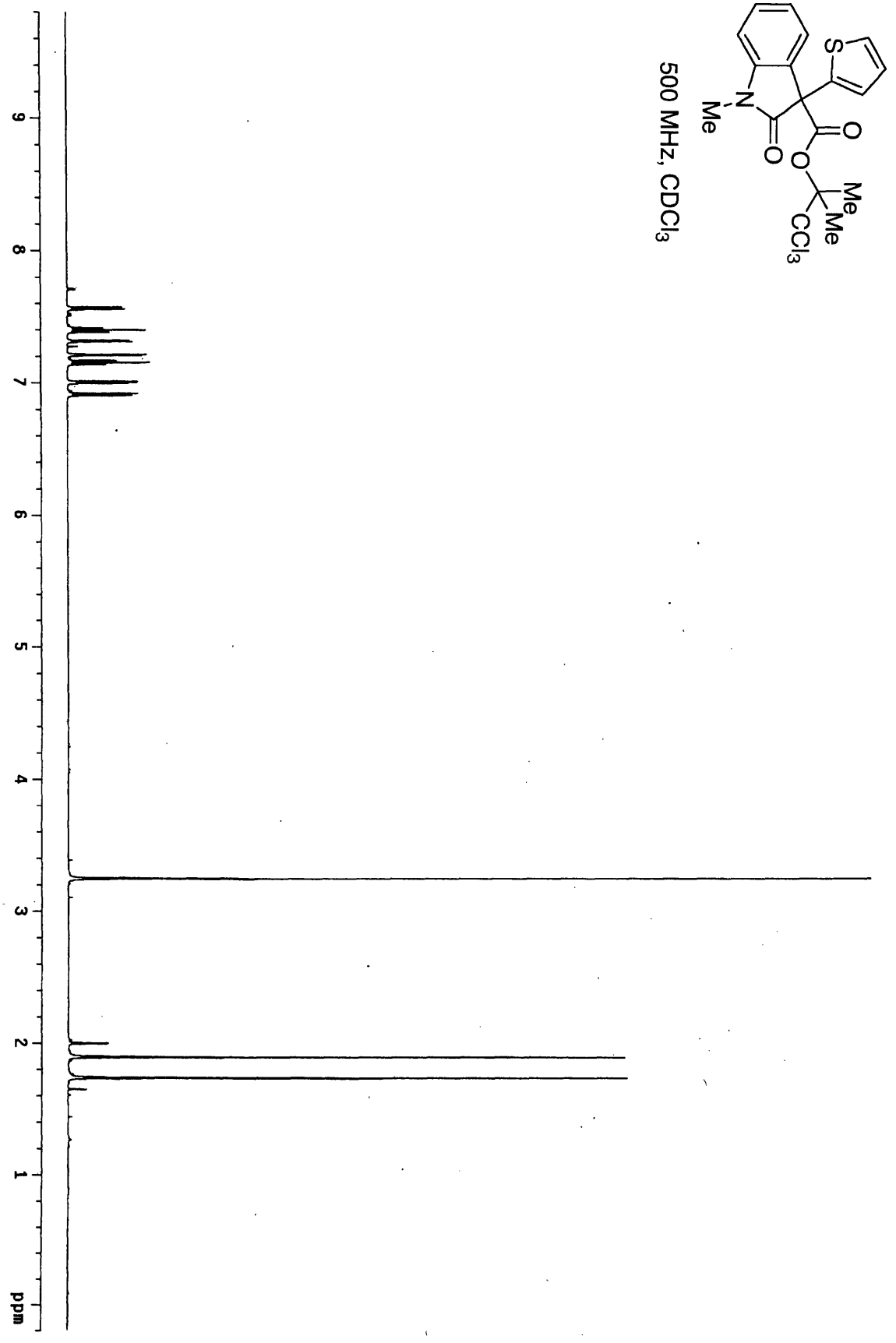
500 MHz, CDCl3
N
Me
S
O
O
O
Me
Me
CCl3
9
8
7
6
5
4
3
2
1
0
ppm

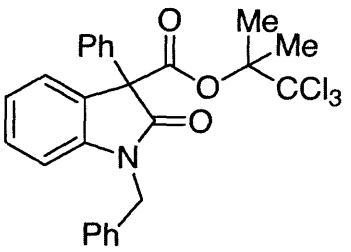

500 MHz, $CDCl_3$

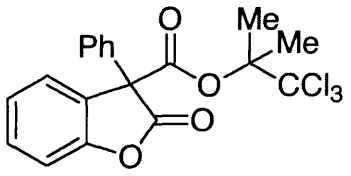

500 MHz, $CDCl_3$

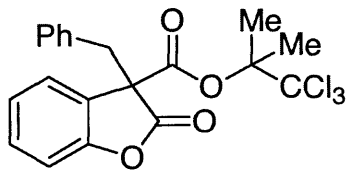

500 MHz, $CDCl_3$

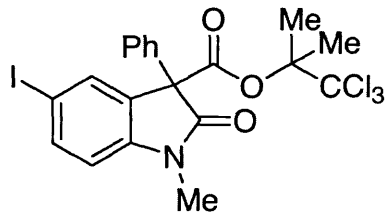

500 MHz, $CDCl_3$

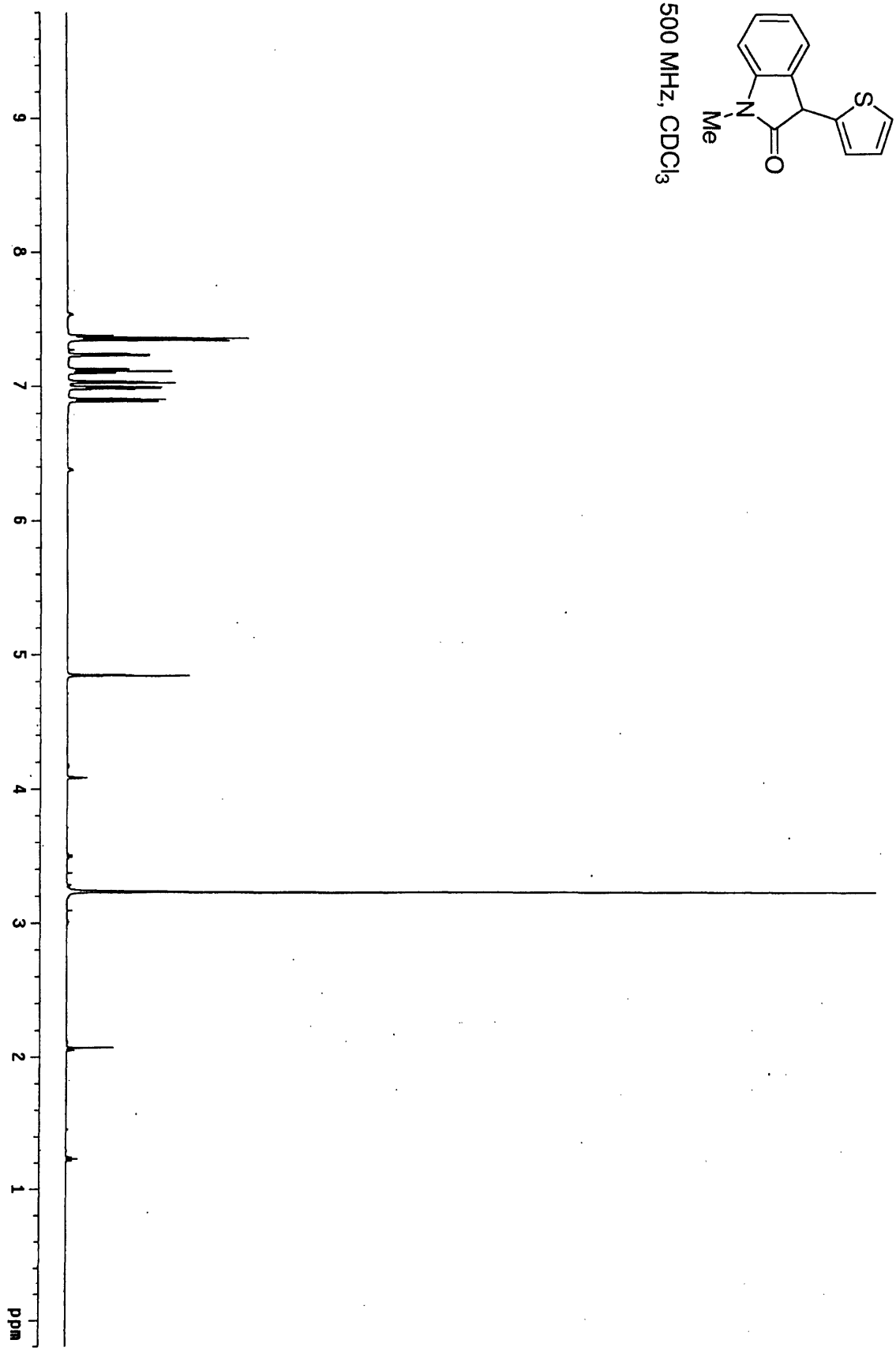
500 MHz, CDCl3
N
Me
O
S
9
8
7
6
5
4
3
2
1
ppm

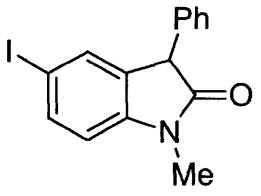

500 MHz, $CDCl_3$

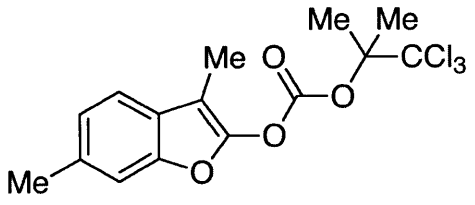

500 MHz, $CDCl_3$

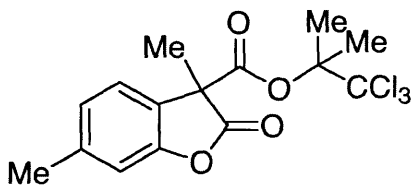

500 MHz, $CDCl_3$

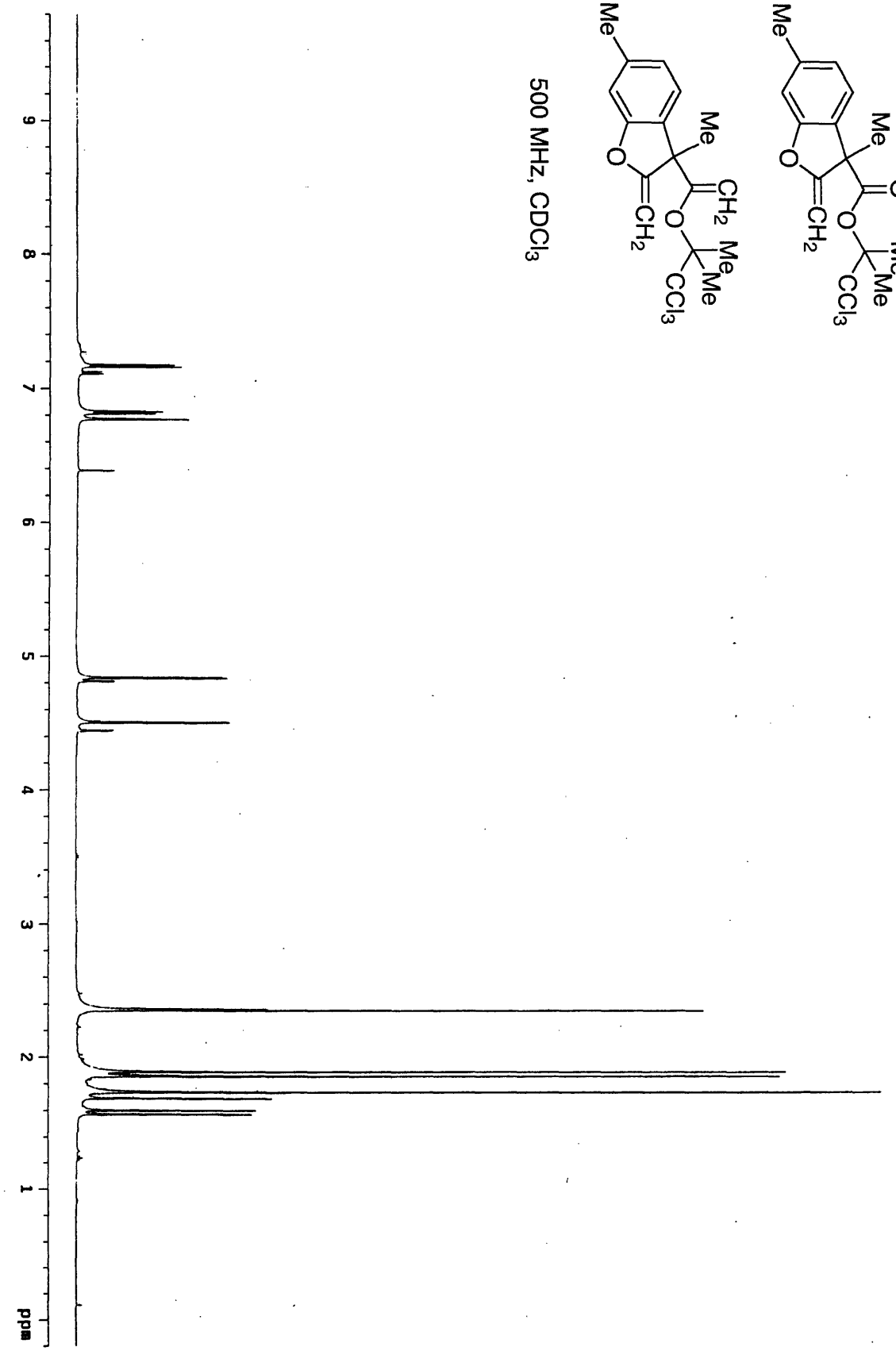
Me
O
Me
Me
CCl3
CH2
O
O
Me
CH2
Me
Me
CCl3
O
O
Me
CH2
500 MHz, CDCl3
9
8
7
6
5
4
3
2
1
ppm

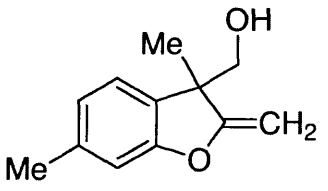

500 MHz, C_6D_6

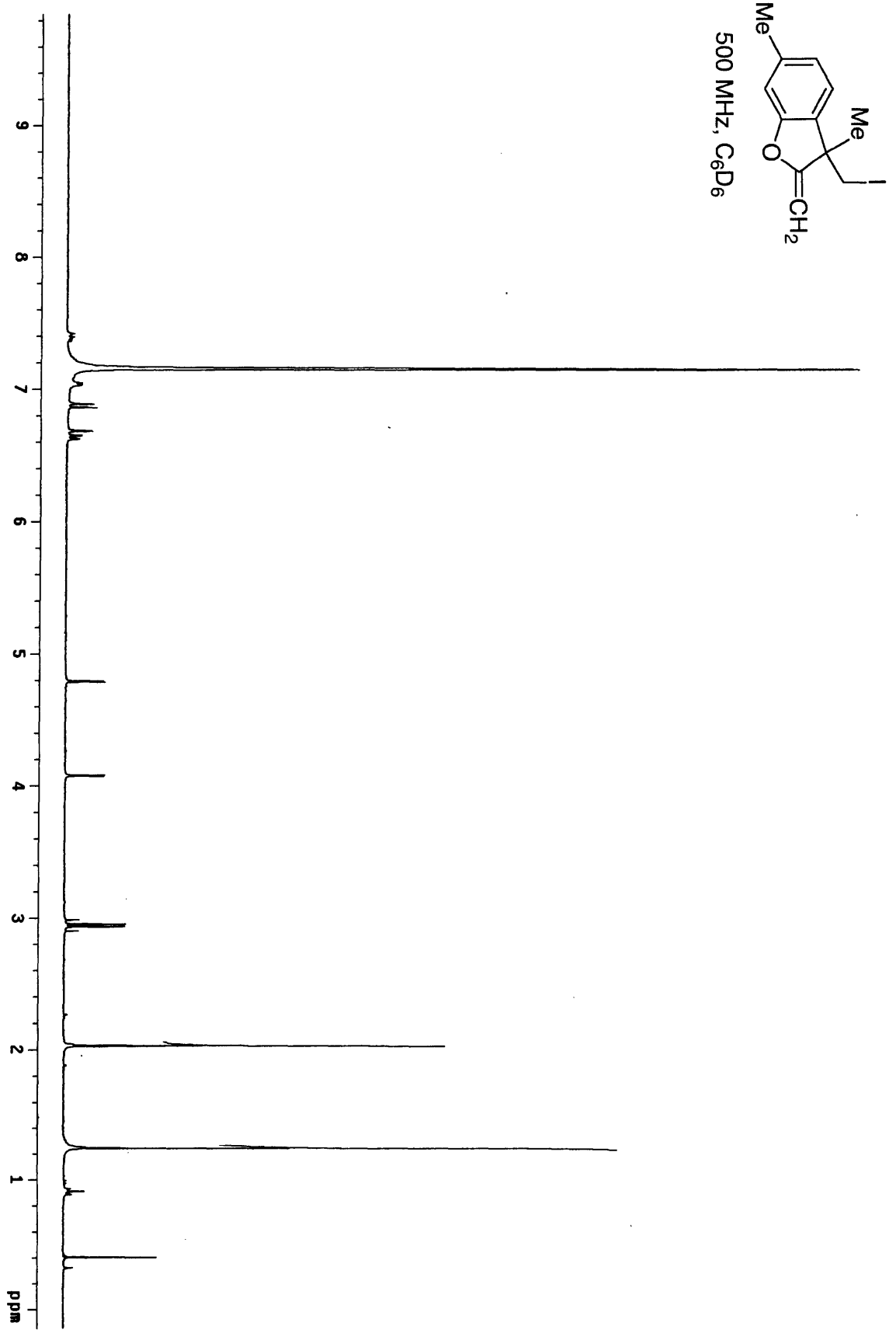
Me
Me
O
CH2
500 MHz, C6D6
9
8
7
6
5
4
3
2
1
ppm

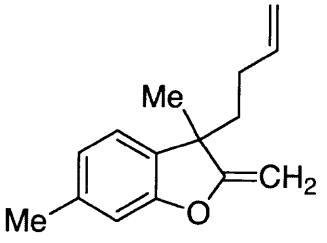

500 MHz, C_6D_6

$(P(t\text{-}Bu)_2Et)_2Pd$

500 MHz, $CDCl_3$